

Evaluation of Entrainers for the Dehydration of C₂ and C₃ Alcohols via Azeotropic Distillation

by

Cornelia Pienaar

Thesis presented in partial fulfillment

of the requirements for the Degree



**MASTER OF SCIENCE IN ENGINEERING
(CHEMICAL ENGINEERING)**

in the Faculty of Engineering

at Stellenbosch University

Supervised by

Prof. A.J. Burger and Prof. J.H. Knoetze

STELLENBOSCH

March 2012

DECLARATION

By submitting this thesis electronically, I declare that the entirety of the work contained therein is my own, original work, that I am the sole author thereof (save to the extent explicitly otherwise stated); that reproduction and publication thereof by Stellenbosch University will not infringe any third party rights and that I have not previously in its entirety or in part submitted it for obtaining any qualification.

Signature:

Date: 05/03/12

ABSTRACT

Distillation is the most widely used separation technique in the chemical process industry and typically accounts for approximately one-third of the total capital cost and more than half of the total energy consumption of a typical petrochemical-chemical plant. Therefore, the design and optimization of the distillation sequence are of critical importance to the economics of the entire process. Azeotropic mixtures cannot be separated into their pure components via normal distillation. Enhanced distillation techniques such as heterogeneous azeotropic distillation should be considered for these mixtures. Isobaric vapour-liquid-liquid equilibrium (VLLE) data are highly important for the design and analysis of heterogeneous distillation columns. However, limited VLLE data are available in literature due to the difficulties involved with measuring such data.

The objective of this work was to systematically evaluate and compare the performance of selected entrainers (including benzene, DIPE and cyclohexane) for the dehydration of C₂ and C₃ alcohols. To meet this objective, phase equilibrium data had to be measured. Isobaric VLLE at standard atmospheric conditions were measured with a dynamic Gillespie unit equipped with an ultrasonic homogenizer, which prevented liquid-liquid separation.

Vapour-liquid equilibrium (VLE) and VLLE data were measured for ethanol/water/di-isopropyl ether (DIPE), n-propanol/water/DIPE and n-propanol/water/isooctane. The VLE data were found to be thermodynamically consistent according to the L-W (Wisniak 1993) and McDermott-Ellis consistency tests. No thermodynamic consistency test, specifically for VLLE data, could be found in literature, but the LLE part of the data followed a regular profile according to the Othmer-Tobias correlation. The binary DIPE/water and isooctane/water azeotropes, as well as ternary ethanol/DIPE/water and n-propanol/isooctane/water azeotropes, as measured in this work, agree well with those found in literature.

Regressed parameters for the NRTL, UNIQUAC, and UNIFAC models, generally improved the model predictions compared with built-in Aspen parameters. This confirmed the importance of having actual measured VLLE data available for evaluation and improvement of estimations by thermodynamic models. NRTL predicted the ethanol/DIPE/water and n-propanol/DIPE/water VLLE most accurately. Despite the improved regressed parameters for n-propanol/isooctane/water predictions, the models are still considered unsuitable for accurate prediction of the VLLE behaviour of this system. Separation sequences were simulated in Aspen with built-in and regressed parameters, respectively, to illustrate the significant effect such inaccurate parameters have on these simulations.

Phase diagram (VLLE data) evaluation of ethanol and isopropanol (IPA) with various entrainers, as found in literature, indicated that DIPE might be a good entrainer for the dehydration of these alcohols. Benzene and cyclohexane are generally used as entrainers in industry for these processes. Benzene is however carcinogenic and therefore an alternative has to be found (United States Department of Labour - Occupational Safety & Health Administration 2011). Separation sequences were simulated for ethanol dehydration with benzene and DIPE as entrainers, respectively. Taking cost and safety into account, DIPE can be considered an acceptable replacement for benzene as entrainer for ethanol dehydration.

A separation sequence was also simulated for the dehydration of IPA with DIPE as entrainer and compared to a simulation with cyclohexane (Arifin, Chien 2007) as entrainer. DIPE was found to be a reasonable alternative to cyclohexane as entrainer for IPA dehydration. Two other separation sequences were simulated as practical

examples where DIPE could be used as entrainer for the recovery of ethanol or n-propanol from aqueous Fischer Tropsch waste streams.

DIPE is therefore found to be a feasible alternative entrainer to benzene and cyclohexane for the dehydration of ethanol and IPA via heterogeneous azeotropic distillation, based on pre-liminary cost considerations, separation ability and safety. Better entrainers than DIPE may exist, but from the data available in literature and the measurements made in this work DIPE appears to be superior to benzene, cyclohexane and isooctane.

OPSOMMING

Distillasie is die mees algemeen-gebruikte skeidings tegniek in die chemiese proses-industrie. Dit is tipies verantwoordelik vir 'n derde van die totale kapitaalkoste en meer as die helfte van die totale energie verbruik op 'n tipiese petrochemiese chemiese aanleg. Daarom is die ontwerp en optimalisering van 'n distillasie trein van kardinale belang vir die winsgewendheid van die proses. Azeotropiese mengsels kan nie slegs deur normale distillasie in suiwer komponente geskei word nie. Gevorderde distillasie tegnieke soos heterogene azeotropiese distillasie moet dus oorweeg word vir sulke mengsels. Isobariese damp-vloeistof-vloeistof ewewigsdata is een van die belangrikste fisiese eienskappe vir die ontwerp van heterogene distillasie kolomme. Die hoeveelheid damp-vloeistof-vloeistof ewewigsdata wat beskikbaar is in die literatuur is egter baie beperk omdat dit moeilik is om die data te meet.

In hierdie werk is isobariese damp-vloeistof-vloeistof ewewigsdata met 'n dinamiese Guillespie eenheid, by standaard atmosferiese druk gemeet. Die eenheid is toegerus met 'n ultrasoniese homogeniseerder om vloeistof-vloeistof skeiding te voorkom. Temperatuur is gemeet met 'n akkuraatheid van 0.03°C by 0°C . Die sisteem se druk is konstant gehou op 101.3 kPa met 'n akkuraatheid van 0.35 % VSU (Vol Skaal Uitset). Die ewewigsamestellings is met 'n relatiewe akkuraatheid van 2 % gemeet.

Daar is damp-vloeistof en damp-vloeistof-vloeistof ewewigsdata van etanol/water/di-isopropiel eter (DIPE), n-propanol/water/ DIPE en n-propanol/water/iso-oktaan gemeet. Die damp-vloeistof ewewigsdata is deur die L-W (Wisniak 1993) en McDermott-Ellis termodinamiese konsistensie toetse getoets en konsistent bevind. Geen termodinamiese konsistensie toets spesifiek vir damp-vloeistof-vloeistof ewewigsdata kon gevind word nie. Die Othmer-Tobias korrelasie dui egter aan dat die vloeistof-vloeistof ewewig gedeelte van die data 'n reëlmatige gang volg. Die binêre DIPE/water en iso-oktaan/water azeotrope en ternêre etanol/DIPE/water en n-propanol/iso-oktaan/water fase-ewewigte wat in hierdie werk gemeet is, stem ooreen met die wat in die literatuur te vind is.

Die parameters vir die modelle (NRTL, UNIQUAC en UNIFAC) wat in hierdie werk bestudeer is, is in die algemeen verbeter deur regressie van die eksperimentele data. Dit dui daarop dat dit belangrik is om eksperimentele damp-vloeistof-vloeistof ewewigsdata te hê om die voorspellings van termodinamiese modelle mee te evalueer en te verbeter. Die etanol/water/ DIPE en n-propanol/water/DIPE damp-vloeistof-vloeistof ewewigsdata is die akkuraatste deur NRTL voorspel. Ten spyte van die verbeteringe wat deur regressie behaal is met die NRTL en UNIQUAC parameters vir n-propanol/water/iso-oktaan, word hierdie modelle steeds nie as gepas vir die voorspelling van hierdie datastel beskou nie.

Skeidingsreekse is gesimuleer met die ingeboude Aspen parameters en regressie parameters, onderskeidelik, om te illustreer dat onakkurate parameters 'n beduidende effek op sulke simulaties het.

Die evaluasie van fase diagramme van etanol en IPA met verskeie skeidingsagente, wat in die literatuur te vind is, dui aan dat DIPE 'n goeie skeidingsagent kan wees vir die dehidrasie van hierdie alkohole. Skeidingsreekse vir die dehidrasie van etanol met benseen en DIPE, onderskeidelik, is gesimuleer. Met koste en veiligheid in ag geneem, is daar gevind dat DIPE 'n aanvaarbare plaasvervanger vir benseen as skeidingsagent vir etanol dehidrasie kan wees.

Daar is ook 'n skeidingsreeks vir die dehidrasie van IPA met DIPE as skeidingsagent gesimuleer en met 'n simulasie (Arifin, Chien 2007) wat sikloheksaan as skeidingsagent gebruik, vergelyk. Daar is bevind dat DIPE 'n redelike alternatief vir sikloheksaan kan wees as skeidingsagent vir IPA dehidrasie. Nog twee skeidingsreekse

is gesimuleer om as praktiese voorbeelde te dien van die gebruik van DIPE as skeidingsagent om etanol of n-propanol vanaf waterige Fischer-Tropsch afvalstrome te herwin.

Daarom is daar bevind dat DIPE 'n geldige alternatiewe skeidingsagent vir benseen en sikloheksaan is, gebaseer op koste, skeidingsvermoë en veiligheid. Daar kan beter skeidingsagente as DIPE bestaan, maar vanuit die data beskikbaar in literatuur en die metings geneem in hierdie werk, is DIPE die beste.

ACKNOWLEDGEMENTS

I would like to thank God for giving me the ability and opportunity to complete this degree; I give all the glory to Him.

Also my thanks go out to my mother and sister for their much needed support over the past two years.

To Prof A.J. Burger, Prof J.H. Knoetze and Dr. C.E. Schwarz for their insightful inputs and guidance in my project throughout the past two years and for the opportunity I received to learn more in the field of Separation Technology.

To Hanlie Botha, Jannie Barnard, Anton Cordier, Oliver Jooste, Alvin Petersen and Vincent Carolissen for their patience, willingness to help and assistance throughout my project.

And lastly, the financial assistance of Sasol Technology (Pty) Ltd and the Department of Trade and Industry (DTI) of South Africa through the Technology and Human Resources for Industry Programme (THRIP) towards this research is hereby acknowledged. Opinions expressed and conclusions arrived at are those of the authors and are not necessarily to be attributed to the sponsors.

TABLE OF CONTENTS

Declaration	i
Abstract.....	ii
Opsomming	iv
Acknowledgements	vi
Glossary.....	v
Nomenclature	viii
Tables	x
Figures	xvi
1 Introduction	1
1.1 Motivation and industrial relevance	1
1.2 Research Objectives	2
1.3 Thesis overview	4
I LITERATURE.....	6
2 Separation of Azeotropic Mixtures.....	6
2.1 Azeotropy.....	6
2.1.1 What is <i>azeotropy</i> ?.....	6
2.1.2 Vapour-liquid equilibrium, non-ideality and azeotropy.....	7
2.1.3 Non-ideality and separation by distillation	8
2.2 Alcohol/Water Azeotropes.....	9
2.3 Azeotropic Phase Equilibrium Diagrams	11
2.3.1 Vapour-liquid Equilibrium	11
2.3.2 Liquid-liquid Equilibrium.....	14
2.3.3 Vapour-liquid-liquid Equilibrium.....	16
2.3.4 Residue curves	18
2.3.5 Discussion.....	20
2.4 General separation processes	21
2.4.1 Membrane-distillation hybrids.....	21
2.4.2 Pressure-swing distillation	22
2.4.3 Entrainer-addition distillation methods.....	23
2.4.4 Discussion.....	24

2.5	Entrainer-addition distillation methods	25
2.5.1	Homogeneous azeotropic distillation.....	25
2.5.2	Heterogeneous azeotropic distillation.....	27
2.5.3	Extractive distillation.....	30
2.5.4	Entrainer selection	31
2.6	Summary	33
3	Thermodynamic basis.....	34
3.1	Criterion for phase equilibrium in a heterogeneous closed system	34
3.2	The Gibbs-Duhem Equation.....	35
3.3	The chemical potential	35
3.4	Fugacity and fugacity coefficient.....	36
3.5	Activity and activity coefficient.....	37
3.6	Evaluation of fugacities.....	37
3.7	NRTL (Non-random Two Liquid) Equation.....	39
3.8	UNIQUAC (Universal Quasi Chemical Theory) Equation.....	39
3.9	UNIFAC (Universal Functional Activity Coefficient) Equation.....	40
3.10	Thermodynamic Consistency Testing.....	42
3.10.1	VLE Consistency Testing.....	42
3.10.2	LLE Consistency Testing	44
3.10.3	VLLE Consistency Testing	45
4	Methods of Low-pressure VLE/VLLE Measurement	46
4.1	Purpose of Measuring VLLE	48
4.2	Problems with Measuring VLLE	49
4.3	Methods.....	51
4.3.1	Distillation Method	51
4.3.2	Dynamic Method	52
4.3.3	Flow method	53
4.4	Preferred Method and Equipment	54
4.4.1	Motivation for Ultrasound	55
4.4.2	Positioning of Ultrasonic Homogenizer.....	55
II	EXPERIMENTAL STUDIES ON TERNARY HETEROGENEOUS AZEOTROPIC SYSTEMS	57

5	Evaluation and Selection of Alcohol-Water-Entrainer Systems.....	57
5.1	Literature Data of Most Prominent Entrainers.....	57
5.2	Evaluation of Entrainers and Literature Data.....	57
5.2.1	Benzene.....	58
5.2.2	Cyclohexane.....	58
5.2.3	Hexane.....	59
5.2.4	Heptane.....	60
5.2.5	Isooctane.....	60
5.2.6	DIPE.....	61
5.2.7	DNPE.....	61
5.3	Selection of Entrainers for Experimental Work.....	61
6	Experimental Work.....	63
6.1	Materials.....	63
6.2	Apparatus.....	64
6.3	Procedure.....	67
6.4	Sampling and Analysis.....	68
6.5	Experimental Challenges and Rectifications.....	70
7	Data Regression and Simulation.....	70
7.1	Regression Method.....	70
7.2	Separation Sequence.....	72
8	Results and Discussions.....	75
8.1	Verification.....	75
8.1.1	Binary VLE: Ethanol/Isooctane.....	75
8.1.2	Ternary VLLE: IPA/Isooctane/Water.....	77
8.1.3	Ternary VLLE: IPA/DIPE/Water.....	77
8.1.4	Ternary VLLE: Ethanol/1-Butanol/Water.....	78
8.2	New Phase Equilibrium Data.....	87
8.2.1	Ethanol/DIPE/Water VLLE and VLE.....	87
8.2.2	n-Propanol/DIPE/Water VLLE and VLE.....	92
8.2.3	n-Propanol/Isooctane/Water VLLE and VLE.....	97
8.3	Entrainer comparison.....	102

8.4	Thermodynamic Modelling.....	108
8.4.1	Comparison of data with selected thermodynamic models.....	108
8.4.2	Regression of data.....	119
8.5	Separation Sequence Simulations	131
9	Conclusions and Recommendations	148
10	References	151
A.	MSDS Forms.....	160
B.	Calibration Certificates.....	167
C.	Experimental Data	174
D.	Thermodynamic Consistency Tests.....	183
E.	Othmer-Tobias Correlations	190
F.	Built-in Aspen Parameters	192
G.	Data from Literature for Regressions	195
H.	Regressed Parameters.....	197
I.	Detailed Simulation Results	200

GLOSSARY**A**

activity	
a measure of the effective concentration of a species in a real solution.....	34
antipyretic	
agent that reduces fever	10
azeotropes	
a mixture of two or more components in such a ratio that when it is boiled, the vapour and liquid phases have the same composition.....	1

B

bubble-point temperatures	
the temperature at which bubbles first appear when a liquid mixture is heated.....	29

C

chemical potential	
the potential a substance has to produce change in a system.....	34
Cottrell pump	
a narrow tube where the force of the boiling liquid pumps the two- phase vapour liquid mixture upwards.....	54

D

distillation boundary	
a residue curve that cannot be crossed via distillation alone.....	27

E

ebullition	
The state or process of boiling.....	54
entrainer	
an additive that forms an azeotrope with one or more components of a liquid mixture to aid in otherwise difficult separations by distillation, such as azeotropic distillation.....	4

F

Fischer Tropsch process	
a set of chemical reactions that convert a mixture of carbon monoxide and hydrogen to liquid hydrocarbons.....	10
the synthesis of hydrocarbons and, to a lesser extent, of aliphatic oxygenated compounds by the catalytic hydrogenation of carbon monoxide.....	10
fouling	
refers to the accumulation of unwanted material on solid surfaces	21

fugacity	
the effective pressure of a real gas that replaces the true mechanical pressure in accurate chemical equilibrium calculations	
.....	34

G

Gibbs-Duhem equation	
describes the relationship between changes in chemical potential for components in a thermodynamic system	34

H

heterogeneous mixture	
a mixture that lacks uniformity in character and/or composition.....	1
homogeneous	
a mixture that is uniform in composition or character	6
homogenizer mixture	
equipment used to blend (diverse elements) into a uniform mixture	54
hybrid	
to use of different methods together or in series, to obtain a certain product	21
hydrophilic substance	
a substance that is attracted to, and tends to be dissolved by water	29
hydrophobic substance	
a substance that is repelled by water.....	29

L

lipophilic	
refers to the ability of a compound to dissolve in fats and oils.....	10

O

oxygenates	
refers to compounds containing oxygen	10

P

permeability	
a measure of the ability of a membrane to allow certain molecules pass through it by diffusion	21
permeate	
a substance permeating through a solid or membrane	21
pervaporation	
a method using a membrane for the separation of mixtures of liquid via partial vaporization through a non-porous or porous membrane.....	6
phase envelope	
the region enclosed by the bubble point curve and dew point curve or the region on a ternary phase diagram enclosed by the LLE curve	15

plait point	
composition conditions at which the three coexisting phases of partially soluble components of a three-phase liquid system, approach each other in composition.....	15

R

raffinate	
a liquid stream that is left after the extraction with the immiscible liquid to remove solutes from the original liquid	26
retentate	
the substance unable to permeate through the membrane.....	21
rubefacient	
a substance for topical application that increase blood circulation in area of application.....	10

S

semiconductor	
a material with electrical conductivity due to electron flow intermediate in magnitude of that of a conductor and an insulator	10
solvent	
a substance in which another substance is dissolved	10

T

thermodynamic consistency	
wether a set of data conforms to the constraints posed by the Gibbs-Duhem equation	34
tie-lines	
a line on a phase diagram joining the two point which represents the composition of the phases in equilibrium	15

U

ultrasonic	
af or relating to acoustic frequencies above the range audible to the human ear	54

NOMENCLATURE

Symbol/Abbreviation	Description
A	Helmholtz energy
a	activity
AAD	average absolute deviation
AARD %	average absolute relative deviation percentage
B_i	bottoms of column i
B_{ij}	pure component Viral coefficient
C ₂ -alcohol	ethanol
C ₃ -alcohols	n-propanol and isopropanol
D	deviation in the McDermott-Ellis consistency test
D_i	distillate of column i
DIPE	diisopropyl ether
D_{max}	maximum allowable deviation in the McDermott-Ellis consistency test
DNPE	di-n-propyl ether
DRS	data regression system
EtOH	ethanol
f	fugacity
F_i	feed to column i
FID	flame ionization detector
FSO	full scale output
G	Gibbs energy
GC	gas chromatography
Δh	change in heat of vaporization
H	enthalpy
H ₂ O	water
IPA	isopropanol
KF	Karl Fischer
k_{OT}, c_{OT}	Othmer-Tobias constants
LLE	liquid-liquid equilibrium
MSDS	material safety data sheet
n	number of moles
P_i	pressure at state i or of component i
R	ideal gas constant
ΔS	change in vaporization entropy
S	entropy
SG	specific gravity
Temp	equilibrium temperature
T_i	temperature at state i or of component i
U	internal energy
UNIFAC LLE	UNIFAC with calculations based on LLE
UNIFAC VLE	UNIFAC with calculations based on VLE
V	volume
V_i^L	liquid molar volume of component i
VLE	vapour-liquid equilibrium
VLLE	vapour-liquid-liquid equilibrium

Symbol/Abbreviation	Description
wt %	weight percentage
x_i	liquid phase composition of component i
y_i	vapour phase composition of component i
μ_i	chemical potential
ϕ	fugacity coefficient
γ	activity coefficient
Φ	ratio of fugacity coefficients with the Poynting correction factor
δ	term relating second Viral coefficient
τ_{ij}	parameter in NRTL model
Φ_i	UNIQUAC segment fraction
θ	UNIQUAC area fraction
Γ_k	UNIFAC residual activity coefficient
Ψ	UNIFAC group interaction parameter

TABLES

Table 2-1: A typical Fischer Tropsch waste water stream (Carlson 1949).....	10
Table 4-1: Isobaric VLLE data at 101.3 kPa published to date (updated from Gomis et al. (2010)).....	47
Table 4-2: Classification of methods to determine VLE data by Hala et al. (1967).....	51
Table 5-1: Literature phase equilibrium data of possible entrainers for the dehydration of C ₂ and C ₃ alcohols via heterogeneous azeotropic distillation.....	57
Table 5-2: Simplified list of literature phase equilibrium data of possible entrainers for the dehydration of C ₂ and C ₃ alcohols via heterogeneous azeotropic distillation.....	62
Table 5-3: Bulk chemical prices of possible entrainers for the dehydration of C ₂ and C ₃ alcohols via heterogeneous azeotropic distillation.....	63
Table 6-1: List of chemicals with purities and suppliers	63
Table 8-1: AAD and AARD % values for VLE of Ethanol/Isooctane, measured in this work and found in literature, compared to activity coefficient model NRTL with built-in Aspen parameters at 101.325 kPa.....	76
Table 8-2: Temperature and composition of ternary and binary azeotropes measured for Ethanol/DIPE/Water at 101.325 kPa	88
Table 8-3: Temperature and composition of ternary and binary azeotropes measured for n-propanol/DIPE/water at 101.325 kPa	93
Table 8-4: Temperature and composition of ternary and binary azeotropes measured for n-propanol/isooctane/water at 101.325 kPa.....	98
Table 8-5: Ternary heterogeneous azeotropic compositions of the ethanol/entrainer/water systems at 101.3 kPa	102
Table 8-6: Ternary heterogeneous azeotropic compositions of the IPA/entrainer/water systems at 101.3 kPa ..	103
Table 8-7: Ternary heterogeneous azeotropic compositions of the n-propanol/entrainer/water systems at 101.3 kPa.....	103
Table 8-8: Azeotropes of the ethanol/DIPE/water system measured at 101.3 kPa, with those predicted by Aspen with built-in parameters.....	109
Table 8-9: Azeotropes of the n-propanol/DIPE/water system measured at 101.3 kPa, with those predicted by Aspen with built-in parameters.....	110
Table 8-10: Azeotropes of the n-propanol/isooctane/water system measured at 101.3 kPa, with those predicted by Aspen with built-in parameters.....	112
Table 8-11: AAD and AARD % values for VLLE of Ethanol/DIPE/Water by the NRTL, UNIQUAC, UNIFAC (VLE) and UNIFAC (LLE) models with built-in Aspen parameters at 101.325 kPa.....	114
Table 8-12: AAD and AARD % values for VLLE of n-Propanol/DIPE/Water by the NRTL, UNIQUAC, UNIFAC (VLE) and UNIFAC (LLE) models with built-in Aspen parameters at 101.325 kPa.....	116
Table 8-13: AAD and AARD % values for VLLE of n-Propanol/Isooctane/Water by the NRTL, UNIQUAC, UNIFAC (VLE) and UNIFAC (LLE) models with built-in Aspen parameters at 101.325 kPa.....	118
Table 8-14: Azeotropes of the ethanol/DIPE/water system measured at 101.3 kPa, with those predicted by Aspen with regressed parameters.	120
Table 8-15: Azeotropes of the n-propanol/DIPE/water system measured at 101.3 kPa, with those predicted by Aspen with regressed parameters.	122

Table 8-16: Azeotropes of the n-propanol/isooctane/water system measured at 101.3 kPa, with those predicted by Aspen with regressed parameters.	123
Table 8-17: AAD and AARD % values for VLLE of Ethanol/DIPE/Water by the NRTL, UNIQUAC, UNIFAC (VLE) and UNIFAC (LLE) models with regressed parameters at 101.325 kPa.....	126
Table 8-18: AAD and AARD % values for VLLE of n-Propanol/DIPE/Water by the NRTL, UNIQUAC, UNIFAC (VLE) and UNIFAC (LLE) models with regressed parameters at 101.325 kPa.....	128
Table 8-19: AAD and AARD % values for VLLE of n-Propanol/Isooctane/Water by the NRTL and UNIQUAC models with regressed parameters at 101.325 kPa.	130
Table 8-20: Flow sheet information for the azeotropic column (C1) of ethanol dehydration with DIPE as entrainer, comparing built-in Aspen parameters with regressed parameters.	132
Table 8-21: Flow sheet information for the recovery column (C2) of ethanol dehydration with DIPE as entrainer, comparing built-in Aspen parameters with regressed parameters.	133
Table 8-22: Flow sheet information for the azeotropic columns, C1, of ethanol dehydration with benzene and DIPE as entrainers respectively.	134
Table 8-23: Flow sheet information for the recovery columns, C2, of ethanol dehydration with benzene and DIPE as entrainers respectively.	135
Table 8-24: Flow sheet information for the azeotropic columns, C ₁ , of IPA dehydration with cyclohexane and DIPE as entrainers respectively.	136
Table 8-25: Flow sheet information for the recovery columns, C ₂ , of IPA dehydration with cyclohexane and DIPE as entrainers respectively.	137
Table 8-26: Flow sheet information for the azeotropic column, C ₁ , of n-propanol dehydration from a Fischer Tropsch waste stream with DIPE as entrainer.	138
Table 8-27: Flow sheet information for the second column (producing nearly pure water) of n-propanol dehydration from a Fischer Tropsch waste stream with DIPE as entrainer.	138
Table 8-28: Bottoms from the azeotropic column of Carlson's (1945) example compared to the simulation in this work.	139
Table 8-29: Flow sheet information for the azeotropic column, C1, of ethanol dehydration from a Fischer Tropsch waste stream with DIPE as entrainer.	139
Table 8-30: Flow sheet information for the second column (producing nearly pure water) of ethanol dehydration from a Fischer Tropsch waste stream with DIPE as entrainer.	140
Table A-1: Benzene MSDS	160
Table A-2: Cyclohexane MSDS	161
Table A-3: Hexane MSDS.....	162
Table A-4: Heptane MSDS.....	163
Table A-5: Isooctane MSDS.....	164
Table A-6: DIPE MSDS	165
Table A-7: DNPE MSDS	166
Table C-1: Binary VLE data (mole fraction) of Ethanol/Isooctane at 101.325 kPa	177
Table C-2: Ternary VLLE data (mole fraction) of IPA/Isooctane/Water at 101.325 kPa	177
Table C-3: Ternary VLLE data (mole fraction) of IPA/DIPE/Water at 101.325 kPa.....	178

Table C-4: Ternary VLLE data (mole fraction) of Ethanol/n-Butanol/Water at 101.325 kPa.....	178
Table C-5: Ternary VLLE data (mole fraction) of Ethanol/DIPE/Water at 101.325 kPa.....	179
Table C-6: Ternary VLE data (mole fraction) of Ethanol/DIPE/Water at 101.325 kPa.....	179
Table C-7: Ternary VLLE data (mole fraction) of n-Propanol/DIPE/Water at 101.325 kPa	180
Table C-8: Ternary VLE data (mole fraction) of n-Propanol/DIPE/Water at 101.325 kPa.....	180
Table C-9: Ternary VLLE data (mole fraction) of n-Propanol/Isooctane/Water at 101.325 kPa.....	181
Table C-10: Ternary VLE data (mole fraction) of n-Propanol/Isooctane/Water at 101.325 kPa	182
Table D-1: Herington consistency test results for ethanol/isooctane VLE measured by Hiaki et al. (1994).	183
Table D-2: Herington consistency test results for ethanol/isooctane VLE measured by Ku and Tu (2005).	183
Table D-3: Parameter input for PRO-VLE 2.0 software	186
Table D-4: L-W consistency test results for Ethanol/DIPE/Water VLE	187
Table D-5: McDermott-Ellis consistency test results for Ethanol/DIPE/Water VLE.....	187
Table D-6: L-W consistency test results for n-Propanol/DIPE/Water VLE	188
Table D-7: McDermott-Ellis consistency test results for n-Propanol/DIPE/Water VLE.....	188
Table D-8: L-W consistency test results for n-Propanol/Isooctane/Water VLE.....	189
Table D-9: McDermott-Ellis consistency test results for n-Propanol/Isooctane/Water VLE	189
Table F-1: Aspen Plus NIST Wagner 25 Liquid Vapour Pressure Equation Parameters.	192
Table F-2: Aspen UNIFAC groups used in this work.	192
Table F-3: Built-in Aspen parameters for NRTL.	193
Table F-4: Built-in Aspen parameters for UNIQUAC.....	194
Table G-1: Isobaric phase equilibrium data at 101.3 kPa, used from literature and this work, for parameter regressions.	195
Table G-2: Weighting of data from Table G-1, used in parameter regressions.	196
Table H-1: NRTL Model Parameters of the Water (1) + DIPE (2) + Ethanol (3) ternary mixture.....	197
Table H-2: UNIQUAC Model Parameters of the Water (1) + DIPE (2) + Ethanol (3) ternary mixture.....	197
Table H-3: UNIFAC (vapour-liquid equilibrium calculations) Model Parameters of the Water (1) + DIPE (2) + Ethanol (3) ternary mixture.	197
Table H-4: UNIFAC (liquid-liquid equilibrium calculations) Model Parameters of the Water (1) + DIPE (2) + Ethanol (3) ternary mixture.	197
Table H-5: NRTL Model Parameters of the Water (1) + DIPE (2) + n-Propanol (3) ternary mixture.	198
Table H-6: UNIQUAC Model Parameters of the Water (1) + DIPE (2) + n-Propanol (3) ternary mixture.	198
Table H-7: UNIFAC (vapour-liquid equilibrium calculations) Model Parameters of the Water (1) + DIPE (2) + n-Propanol (3) ternary mixture.	198
Table H-8: UNIFAC (liquid-liquid equilibrium calculations) Model Parameters of the Water (1) + DIPE (2) + n-Propanol (3) ternary mixture.	198
Table H-9: NRTL Model Parameters of the Water (1) + Isooctane (2) + n-Propanol (3) ternary mixture.	199
Table H-10: UNIQUAC Model Parameters of the Water (1) + Isooctane (2) + n-Propanol (3) ternary mixture.	199
Table H-11: NRTL Model Parameters of the Water + Ethanol + Benzene mixture, regressed by Christo Crause (2011).	199

Table I-1: Stream results for the dehydration of ethanol via heterogeneous azeotropic distillation with DIPE as entrainer. The simulation was performed with Aspen using NRTL with built-in Aspen parameters.	200
Table I-2: Azeotropic column information for the dehydration of ethanol via heterogeneous azeotropic distillation with DIPE as entrainer. The simulation was performed with Aspen using NRTL with built-in Aspen parameters.....	201
Table I-3: Azeotropic column information (continued) for the dehydration of ethanol via heterogeneous azeotropic distillation with DIPE as entrainer. The simulation was performed with Aspen using NRTL with built-in Aspen parameters.....	202
Table I-4: Recovery column information for the dehydration of ethanol via heterogeneous azeotropic distillation with DIPE as entrainer. The simulation was performed with Aspen using NRTL with built-in Aspen parameters.....	203
Table I-5: Stream results for the dehydration of ethanol via heterogeneous azeotropic distillation with DIPE as entrainer. The simulation was performed with Aspen using NRTL with parameters regressed in this work.	204
Table I-6: Azeotropic column information for the dehydration of ethanol via heterogeneous azeotropic distillation with DIPE as entrainer. The simulation was performed with Aspen using NRTL with parameters regressed in this work.	205
Table I-7: Azeotropic column information (continued) for the dehydration of ethanol via heterogeneous azeotropic distillation with DIPE as entrainer. The simulation was performed with Aspen using NRTL with parameters regressed in this work.....	206
Table I-8: Recovery column information for the dehydration of ethanol via heterogeneous azeotropic distillation with DIPE as entrainer. The simulation was performed with Aspen using NRTL with parameters regressed in this work.....	207
Table I-9: Stream results for the dehydration of ethanol via heterogeneous azeotropic distillation with benzene as entrainer. The simulation was performed with Aspen using NRTL with parameters supplied by Christo Crause (2011).	208
Table I-10: Azeotropic column information for the dehydration of ethanol via heterogeneous azeotropic distillation with benzene as entrainer. The simulation was performed with Aspen using NRTL with parameters supplied by Christo Crause (2011).	209
Table I-11: Azeotropic column information (continued) for the dehydration of ethanol via heterogeneous azeotropic distillation with benzene as entrainer. The simulation was performed with Aspen using NRTL with parameters supplied by Christo Crause (2011).....	210
Table I-12: Recovery column information for the dehydration of ethanol via heterogeneous azeotropic distillation with benzene as entrainer. The simulation was performed with Aspen using NRTL with parameters supplied by Christo Crause (2011).	211
Table I-13: Stream results for the dehydration of IPA via heterogeneous azeotropic distillation with DIPE as entrainer. The simulation was performed with Aspen using NRTL with built-in Aspen parameters.	212
Table I-14: Azeotropic column information for the dehydration of IPA via heterogeneous azeotropic distillation with DIPE as entrainer. The simulation was performed with Aspen using NRTL with built-in Aspen parameters.....	213

Table I-15: Recovery column information for the dehydration of IPA via heterogeneous azeotropic distillation with DIPE as entrainer. The simulation was performed with Aspen using NRTL with built-in Aspen parameters.....	214
Table I-16: Stream results for the recovery of n-propanol from a Fischer-Tropsch waste water stream via heterogeneous azeotropic distillation with DIPE as entrainer. The simulation was performed with Aspen using NRTL.....	215
Table I-17: Stream results (continued) for the recovery of n-propanol from a Fischer-Tropsch waste water stream via heterogeneous azeotropic distillation with DIPE as entrainer. The simulation was performed with Aspen using NRTL.....	216
Table I-18: Azeotropic column information for the vapour phase for the recovery of n-propanol from a Fischer-Tropsch waste water stream via heterogeneous azeotropic distillation with DIPE as entrainer. The simulation was performed with Aspen using NRTL.....	217
Table I-19: Azeotropic column information (continued) for the vapour phase for the recovery of n-propanol from a Fischer-Tropsch waste water stream via heterogeneous azeotropic distillation with DIPE as entrainer. The simulation was performed with Aspen using NRTL.....	218
Table I-20: Azeotropic column information for the 1 st liquid phase phase for the recovery of n-propanol from a Fischer-Tropsch waste water stream via heterogeneous azeotropic distillation with DIPE as entrainer. The simulation was performed with Aspen using NRTL.....	219
Table I-21: Azeotropic column information (continued) for the 1 st liquid phase phase for the recovery of n-propanol from a Fischer-Tropsch waste water stream via heterogeneous azeotropic distillation with DIPE as entrainer. The simulation was performed with Aspen using NRTL.....	220
Table I-22: Azeotropic column information for the 2 nd liquid phase phase for the recovery of n-propanol from a Fischer-Tropsch waste water stream via heterogeneous azeotropic distillation with DIPE as entrainer. The simulation was performed with Aspen using NRTL.....	221
Table I-23: Azeotropic column information (continued) for the 2 nd liquid phase phase for the recovery of n-propanol from a Fischer-Tropsch waste water stream via heterogeneous azeotropic distillation with DIPE as entrainer. The simulation was performed with Aspen using NRTL.....	222
Table I-24: Recovery column information for the vapour phase phase for the recovery of n-propanol from a Fischer-Tropsch waste water stream via heterogeneous azeotropic distillation with DIPE as entrainer. The simulation was performed with Aspen using NRTL.....	223
Table I-25: Recovery column information for the liquid phase phase for the recovery of n-propanol from a Fischer-Tropsch waste water stream via heterogeneous azeotropic distillation with DIPE as entrainer. The simulation was performed with Aspen using NRTL.....	224
Table I-26: Stream results for the recovery of ethanol from a Fischer-Tropsch waste water stream via heterogeneous azeotropic distillation with DIPE as entrainer. The simulation was performed with Aspen using NRTL.....	225
Table I-27: Stream results (continued) for the recovery of ethanol from a Fischer-Tropsch waste water stream via heterogeneous azeotropic distillation with DIPE as entrainer. The simulation was performed with Aspen using NRTL.....	226

Table I-28: Azeotropic column information for the vapour phase for the recovery of ethanol from a Fischer-Tropsch waste water stream via heterogeneous azeotropic distillation with DIPE as entrainer. The simulation was performed with Aspen using NRTL.	227
Table I-29: Azeotropic column information (continued) for the vapour phase for the recovery of ethanol from a Fischer-Tropsch waste water stream via heterogeneous azeotropic distillation with DIPE as entrainer. The simulation was performed with Aspen using NRTL.	228
Table I-30: Azeotropic column information for the 1 st liquid phase phase for the recovery of ethanol from a Fischer-Tropsch waste water stream via heterogeneous azeotropic distillation with DIPE as entrainer. The simulation was performed with Aspen using NRTL.	229
Table I-31: Azeotropic column information (continued) for the 1 st liquid phase phase for the recovery of ethanol from a Fischer-Tropsch waste water stream via heterogeneous azeotropic distillation with DIPE as entrainer. The simulation was performed with Aspen using NRTL.	230
Table I-32: Azeotropic column information for the 2 nd liquid phase phase for the recovery of ethanol from a Fischer-Tropsch waste water stream via heterogeneous azeotropic distillation with DIPE as entrainer. The simulation was performed with Aspen using NRTL.	231
Table I-33: Azeotropic column information (continued) for the 2 nd liquid phase phase for the recovery of ethanol from a Fischer-Tropsch waste water stream via heterogeneous azeotropic distillation with DIPE as entrainer. The simulation was performed with Aspen using NRTL.	232
Table I-34: Recovery column information for the vapour phase phase for the recovery of ethanol from a Fischer-Tropsch waste water stream via heterogeneous azeotropic distillation with DIPE as entrainer. The simulation was performed with Aspen using NRTL.	233
Table I-35: Recovery column information for the liquid phase phase for the recovery of ethanol from a Fischer-Tropsch waste water stream via heterogeneous azeotropic distillation with DIPE as entrainer. The simulation was performed with Aspen using NRTL.	234

FIGURES

Figure 1-1: Preliminary comparison of benzene and DIPE as entrainers for the dehydration of ethanol via heterogeneous azeotropic distillation.....	3
Figure 1-2: Illustration of this thesis layout	5
Figure 2-1: a) Phase diagram exhibiting both partial miscibility and an azeotrope, b) phase diagram exhibiting VLLE. According to Koretsky (2004).....	8
Figure 2-2: Vapour-liquid equilibrium T-x-y phase diagram for an ideal binary mixture of a and b. According to Koretsky (2004).....	11
Figure 2-3: Vapour-liquid equilibrium x-y phase diagram for an ideal binary mixture.	12
Figure 2-4: Vapour-liquid equilibrium x-y phase diagram for a binary mixture that forms an azeotrope. According to Seader and Henley (2006).....	12
Figure 2-5: Vapour-liquid equilibrium T-x-y phase diagram for a binary mixture that forms an azeotrope. According to Seader and Henley (2006).....	13
Figure 2-6: Vapour-liquid equilibrium compositions of ternary mixtures of A-B-C at 1atm. The dashed lines y_A and the solid lines are labeled y_B . According to Walas (1985).....	14
Figure 2-7: Binary liquid-liquid phase equilibrium diagram. According to Koretsky (2004).	15
Figure 2-8: Ternary liquid-liquid phase equilibrium diagram. According to Seader and Henley (2006).....	16
Figure 2-9: a) Phase diagram exhibiting both partial miscibility and an azeotrope, b) phase diagram exhibiting VLLE. According to Koretsky (2004).....	17
Figure 2-10: Ternary vapour-liquid-liquid phase equilibrium diagram.	18
Figure 2-11: Typical residue curve map with projected VLLE data. Simulated in Aspen with NRTL.....	20
Figure 2-12: Schematic illustration of the mechanism upon which membrane distillation functions	22
Figure 2-13: (a) Illustration of the function of pressure-swing distillation on a phase diagram; (b) Typical separation sequence for pressure-swing distillation. According to Seader and Henley (2006).	23
Figure 2-14: Residue curve map of the benzene-acetone-cyclohexane system. Simulated in Aspen with NRTL.	26
Figure 2-15: Hybrid separation sequence involving homogeneous azeotropic distillation.	27
Figure 2-16: Ternary phase diagram with liquid-liquid equilibrium phase envelope, vapour line and distillation boundaries of the ethanol-water-benzene system. Simulated in Aspen with NRTL.....	28
Figure 2-17: Typical separation sequence for heterogeneous azeotropic distillation of ethanol/benzene/water. According to Seader and Henley (2006).....	29
Figure 2-18: Residue curve map of the water-acetone-methanol system. The residue curves were calculated in Aspen using the NRTL thermodynamic model.	30
Figure 2-19: Typical separation sequence for extractive distillation. According to Seader and Henley (2006)...	31
Figure 4-1: Comparison of entrainers for the dehydration of ethanol via heterogeneous azeotropic distillation according to Gomis et al. (2007)	49
Figure 4-2: Temperature-composition diagram in a binary partially miscible system: L, liquid; V, vapour. According to Gomis et al. (2010)	50
Figure 4-3: Experimental apparatus of Hands and Norman (1945).....	52

<i>Figure 4-4: Schematic illustration of the mechanism upon which the dynamic method functions. According to Gomis et al. (2010)</i>	52
Figure 4-5: Experimental apparatus of Newsham and Vahdat (1977).....	54
Figure 4-6: Optimum positioning of the ultrasonic homogenizer as suggested by Gomis et al. (2000).....	56
Figure 6-1: Schematic representation of experimental set-up. Apparatus redrawn and edited from the Pilodist VLE 100 D user manual.	65
Figure 7-1: Typical ternary phase diagram with liquid-liquid equilibrium phase envelope, vapour line and distillation boundaries of an alcohol-water-entrainer system.	73
Figure 7-2: Typical separation sequence for heterogeneous azeotropic distillation	73
Figure 8-1: Binary T-x-y phase diagram of measured Ethanol/Isooctane VLE data at 101.325 kPa, compared to data published by Haiki et al. (1994) and Ku and Tu (2005) and to the thermodynamic model NRTL.....	75
Figure 8-2: Binary x-y phase diagram of measured Ethanol/Isooctane VLE data at 101.325 kPa, compared to data published by Haiki et al. (1994) and Ku and Tu (2005) and to the thermodynamic model NRTL.....	76
Figure 8-3: Illustration of repeatability and accuracy	79
Figure 8-4: Ternary phase diagram of measured IPA/Isooctane/Water VLLE data at 101.325 kPa, compared with data published by Font et al. (2004) and the thermodynamic model UNIFAC (parameters based on LLE).80	
Figure 8-5: Ternary phase diagram of measured IPA/Isooctane/Water tie lines at 101.325 kPa, compared with data published by Font et al. (2004) and the thermodynamic model UNIFAC (parameters based on LLE).	81
Figure 8-6: Ternary phase diagram of measured IPA/Isooctane/Water tie lines (with corrected aqueous liquid phase compositions) at 101.325 kPa, compared with data published by Font et al. (2004) and the thermodynamic model UNIFAC (parameters based on LLE).	82
Figure 8-7: Ternary phase diagram of measured IPA/DIPE/Water VLLE data at 101.325 kPa, compared with data published by Lladosa et al. (2008) and the liquid phases of thermodynamic models NRTL and UNIQUAC.	83
Figure 8-8: Ternary phase diagram of measured IPA/DIPE/Water tie lines at 101.325 kPa, compared with data published by Lladosa et al. (2008) and the thermodynamic model UNIFAC (parameters based on LLE).	84
Figure 8-9: Ternary phase diagram of measured IPA/DIPE/Water VLLE data at 101.325 kPa, compared with data published by Lladosa et al. (2008) and the vapour phase of thermodynamic models NRTL and UNIQUAC.	85
Figure 8-10: Ternary phase diagram of measured Ethanol/n-Butanol/Water VLLE data at 101.325 kPa, compared with data published by Newsham and Vahdat (1977) and Gomis et al. (2000).	86
Figure 8-11: Ternary phase diagram of measured Ethanol/DIPE/Water VLLE data at 101.325 kPa.....	89
Figure 8-12: Ternary phase diagram of measured Ethanol/DIPE/Water VLE data at 101.325 kPa.....	90
Figure 8-13: Ternary phase diagram for the calculation of the heterogeneous ternary azeotrope from measured Ethanol/DIPE/Water VLLE data at 101.325 kPa	91
Figure 8-14: Ternary phase diagram of measured n-Propanol/DIPE/Water VLLE data at 101.325 kPa	94
Figure 8-15: Ternary phase diagram of measured n-Propanol/DIPE/Water VLE data at 101.325 kPa.....	95
Figure 8-16: Ternary phase diagram for the calculation of the heterogeneous ternary azeotrope from measured n-Propanol/DIPE/Water VLLE data at 101.325 kPa	96
Figure 8-17: Ternary phase diagram of measured n-Propanol/Isooctane/Water VLLE data at 101.325 kPa.....	99

Figure 8-18: Ternary phase diagram of measured n-Propanol/Isooctane/Water VLE data at 101.325 kPa	100
Figure 8-19: Ternary phase diagram for the calculation of the heterogeneous ternary azeotrope from measured n-Propanol/Isooctane/Water VLLE data at 101.325 kPa	101
Figure 8-20: Entrainer comparison for ethanol dehydration via heterogeneous azeotropic distillation at 101.325 kPa. Each phase envelope is plotted with its azeotropic tie-line.....	105
Figure 8-21: Entrainer comparison for IPA dehydration via heterogeneous azeotropic distillation at 101.325 kPa. Each phase envelope is plotted with its azeotropic tie-line.	106
Figure 8-22: Entrainer comparison for n-Propanol dehydration via heterogeneous azeotropic distillation at 101.325 kPa. Each phase envelope is plotted with its azeotropic tie-line.....	107
Figure 8-23: Ternary phase diagram of measured Ethanol/DIPE/Water VLLE data at 101.325 kPa and thermodynamic models (with tie lines and azeotropes) with built-in Aspen parameters.....	113
Figure 8-24: Ternary phase diagram of measured n-Propanol/DIPE/Water VLLE data at 101.325 kPa and thermodynamic models (with tie lines and azeotropes) with built-in Aspen parameters.....	115
Figure 8-25: Ternary phase diagram of measured n-Propanol/Isooctane/Water VLLE data at 101.325 kPa and thermodynamic models (with tie lines and azeotropes) with built-in Aspen parameters.....	117
Figure 8-26: Ternary phase diagram of measured Ethanol/DIPE/Water VLLE data at 101.325 kPa and thermodynamic models (with tie lines and azeotropes) with regressed parameters.	125
Figure 8-27: Ternary phase diagram of measured n-Propanol/DIPE/Water VLLE data at 101.325 kPa and thermodynamic models (with tie lines and azeotropes) with regressed parameters.	127
Figure 8-28: Ternary phase diagram of measured n-Propanol/Isooctane/Water VLLE data at 101.325 kPa and thermodynamic models (with tie lines and azeotropes) with regressed parameters.	129
Figure 8-29: Flow sheet of the dehydration of ethanol via heterogeneous azeotropic distillation with DIPE as entrainer. All compositions are in mole fractions. The simulation was performed with Aspen using NRTL and its built-in parameters.	141
Figure 8-30: Flow sheet of the dehydration of ethanol via heterogeneous azeotropic distillation with DIPE as entrainer. All compositions are in mole fractions. The simulation was performed with Aspen using NRTL with parameters regressed in this work.....	142
Figure 8-31: Flow sheet of the dehydration of ethanol via heterogeneous azeotropic distillation with benzene as entrainer. All compositions are in mole fractions. The simulation was performed with Aspen using NRTL with parameters supplied by Christo Crause (2011).....	143
Figure 8-32: Flow sheet of the dehydration of IPA via heterogeneous azeotropic distillation with cyclohexane as entrainer. All compositions are in mole fractions. The simulation was performed by Arifin and Chien (2007).	144
Figure 8-33: Flow sheet of the dehydration of IPA via heterogeneous azeotropic distillation with DIPE as entrainer. All compositions are in mole fractions. The simulation was performed with Aspen using NRTL and its built-in parameters.	145
Figure 8-34: Flow sheet of the recovery of n-propanol from a typical aqueous Fischer Tropsch stream, contaminated with other close-boiling oxygenated components (Carlson 1949). DIPE is used as entrainer. All compositions are in mole fractions. The simulation was performed with Aspen using NRTL.	146

Figure 8-35: Flow sheet of the recovery of ethanol from a typical aqueous Fischer Tropsch stream, contaminated with other close-boiling oxygenated components (Nel, de Klerk 2007). DIPE is used as entrainer. All compositions are in mole fractions. The simulation was performed with Aspen using NRTL.	147
Figure C-1: Water vapour pressure curve.	174
Figure C-2: Ethanol vapour pressure curve.	174
Figure C-3: n-Propanol vapour pressure curve.	175
Figure C-4: DIPE vapour pressure curve.	175
Figure C-5: Isooctane vapour pressure curve.	176
Figure D-1: Graphical Herington consistency test results for ethanol/isooctane VLE measured by Hiaki et al. (1994).	184
Figure D-2: Graphical Herington consistency test results for ethanol/isooctane VLE measured by Ku and Tu (2005).	185
Figure E-1: Othmer-Tobias Correlation for Ethanol/DIPE/Water liquid phases.	190
Figure E-2: Othmer-Tobias Correlation for n-Propanol/DIPE/Water liquid phases.	190
Figure E-3: Othmer-Tobias Correlation for n-Propanol/Isooctane/Water liquid phases.	191

1 INTRODUCTION

When deciding on a separation method for a certain mixture, the most important factor to consider is the nature of this mixture. A mixture rarely behaves ideally and the complexities that occur are usually obstacles for its separation. One such an obstacle is the formation of azeotropes. This phenomena can however be used to enhance separation as well. In this thesis the dehydration of C₂- and C₃-alcohols are studied. Various separation techniques are briefly discussed whereafter the focus is directed to heterogeneous azeotropic distillation.

1.1 MOTIVATION AND INDUSTRIAL RELEVANCE

Purification and recovery of products, by-products and unreacted raw materials are vital steps in the industrial production of chemicals. Distillation is the most widely used separation technique in the chemical process industry. Practically every chemical plant has a separation unit to recover products, by-products and excess raw materials. Separation is commonly accomplished in multistage processes of which distillation is the most significant. Typically, distillation accounts for approximately one-third of the total capital cost and more than half of the total energy consumption of a petro-chemical plant (Julka, Chiplunkar & O'Young 2009).

Liquid mixtures are in the liquid phase, rather than the gaseous phase, due to forces of intermolecular attraction. When two or more components are mixed, these interactions may lead to the formation of an inseparable mixture. Such a mixture, characterized by equal vapour and liquid compositions at equilibrium at certain temperature and pressures is called an azeotrope. Azeotropy is similar to eutectics and peritectics in liquid-solid systems. And it plays an important role in vapour-liquid equilibrium separation processes such as distillation. Insight into the fundamental features of azeotropic phase behaviour at equilibrium is imperative to the development of separation processes for azeotropic mixtures. The feasible operating region, in which any real distillation process must operate, is defined by the vapour-liquid envelope at the equilibrium temperature surface. When azeotropes occur in the mixture, it complicates the layout of this operating region and the consequential distillation behaviour of multi-component azeotropic mixtures may be very complex. Azeotropic phase equilibrium diagrams unveil the physical and chemical restrictions on the separation process resulting from the nature of the mixture. Diagram analysis serves as the first step toward determining which separation method to use and designing the separation sequence. It is therefore of utmost importance to have accurate azeotropic phase equilibrium diagrams constructed with accurate phase equilibrium data.

This work is focussed on the separation of alcohol/water azeotropes, specifically the ethanol/water, n-propanol/water and isopropanol/water azeotropes. These azeotropes frequently occur in the chemical process industry (Nel, de Klerk 2007, Lin, Wang 2004). More information on the azeotropes is provided in Section 2.2. Common industrial entrainers for the separation of these azeotropes through heterogeneous azeotropic distillation are benzene and cyclohexane (Lin, Wang 2004, Gomis et al. 2007). These and other entrainers are discussed in more detail in Chapter 5.

1.2 RESEARCH OBJECTIVES

The aim of the project was to systematically evaluate and compare the performance of selected entrainers (including benzene, DIPE and cyclohexane) for the dehydration of C₂ and C₃ alcohols. As such, the research was performed while targeting the following objectives:

- To become familiarized with literature pertaining to heterogeneous azeotropic distillation of alcohol/water azeotropes and entrainer selection for such operations.
- To commission and verify equipment that can measure VLE and VLLE data.
- To measure VLE and VLLE data of three ternary systems (ethanol/water/DIPE, n-propanol/water/DIPE, n-propanol/water/isooctane).
- To compare entrainers for the dehydration of ethanol, n-propanol and IPA via heterogeneous azeotropic distillation.
- To compare the data experimentally obtained with thermodynamic model predictions (NRTL, UNIFAC, UNIQUAC) with built-in Aspen parameters.
- To regress thermodynamic model parameters for the measured data.
- To construct and simulate separation sequences for the dehydration of ethanol, IPA and n-propanol.

It is anticipated that DIPE will be a more effective entrainer than cyclohexane (or any other alkanes considered in this study) for the dehydration of C₂ and C₃ alcohol. This hypothesis is based on the performance of these entrainers with the dehydration of IPA (Verhoeve 1968, Font et al. 2004, Lladosa et al. 2008). For ethanol dehydration specifically, DIPE is anticipated to enable similar separation as benzene. This hypothesis is founded on the comparison of VLLE data of ethanol/benzene/water found in literature, with VLLE data of ethanol/DIPE/water predicted thermodynamically (Figure 1-1). Based on separation, benzene is currently the best entrainer for ethanol dehydration (Webb 1937, Guinot, Clark 1938, Rovaglio et al. 1992).

It is expected that, of the models available in Aspen, the NRTL thermodynamic model will predict the VLLE measured data most accurately. This prediction is made based on the results previously obtained by Lee and Shen (2003) and Gomis et al. (2005). Although the NRTL model is expected to yield the most accurate prediction of equilibrium data, it is also anticipated that it will still portray a larger heterogeneous region than what is found from experimental data. This may prove the importance of obtaining accurate experimental data to effectively design and simulate separation sequences.

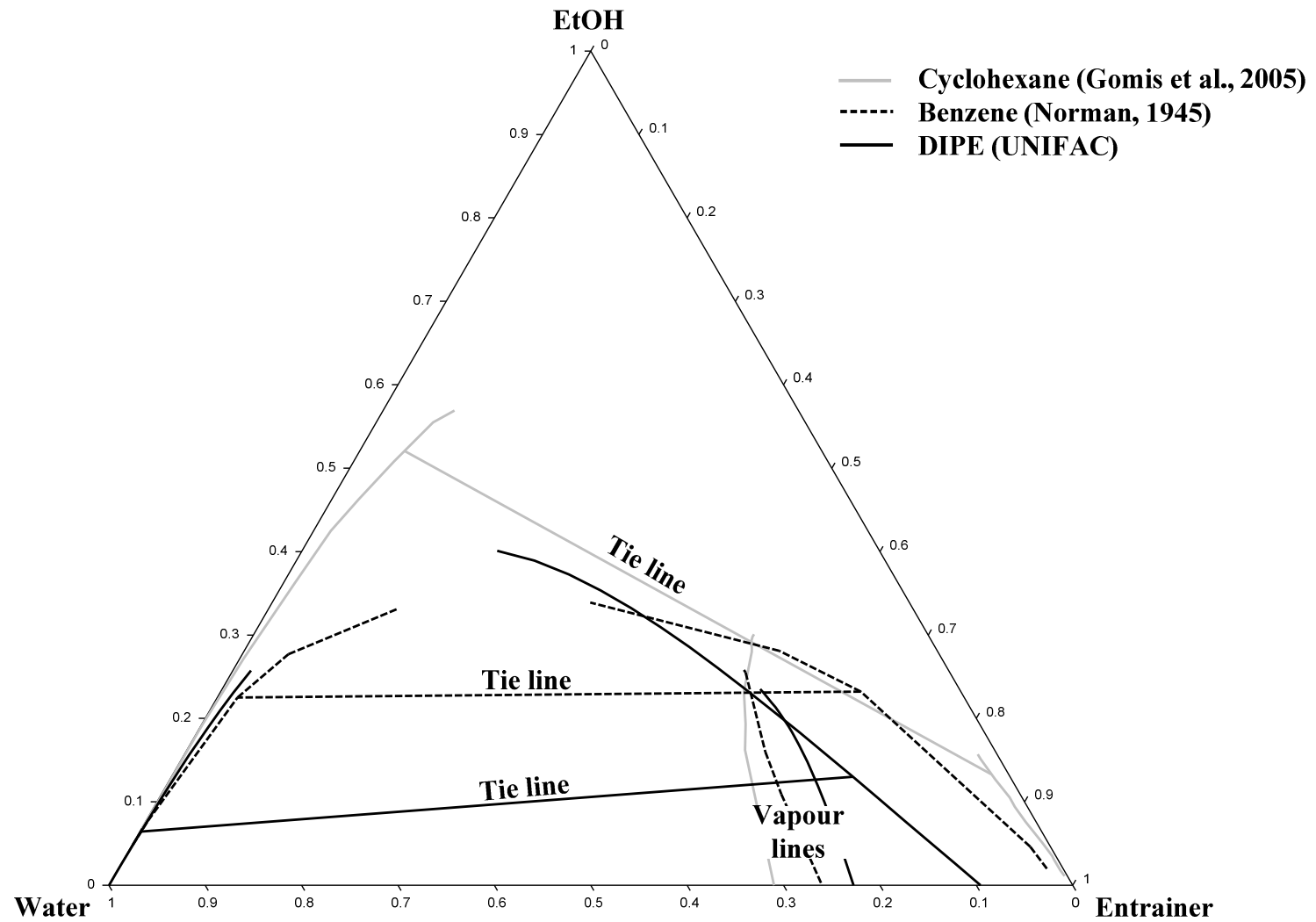


Figure 1-1: Preliminary comparison of benzene and DIPE as entrainers for the dehydration of ethanol via heterogeneous azeotropic distillation.

1.3 THESIS OVERVIEW

This report entails the study of vapour-liquid equilibrium and vapour-liquid-liquid equilibrium of three alcohol-water-entrainer systems. Figure 1-2 provides an illustrative layout of this thesis.

Chapter 2 of this thesis is focused on what azeotropy is, common alcohol/water azeotropes are discussed and the methods by which it can be separated. It also entails the classification of different phase equilibrium diagrams and the azeotropic form of those diagrams. The chapter concludes with a motivation for the use of heterogeneous azeotropic distillation as method of choice in this work. In **Chapter 3** an account is given of the thermodynamic basis of both vapour-liquid and vapour-liquid-liquid equilibrium. The criteria for equilibrium are specified and the Gibbs-Duhem Equation, chemical potential, fugacity, fugacity coefficient, activity and activity coefficient are defined. The thermodynamic models NRTL, UNIQUAC and UNIFAC are also discussed. The chapter concludes with a discussion of thermodynamic consistency testing methods. **Chapter 4** highlights the purpose of and problems with measuring VLLE data. The equipment used to measure VLLE data is also discussed. In **Chapter 5** the available alcohol/entrainer/water VLLE data is discussed and possible entrainers are identified. This chapter also reports which alcohol/entrainer/water systems are to be measured in this work. **Chapter 6** deals with the experimental stage of this project. The materials, apparatus and procedures, as well as the experimental challenges, are discussed. **Chapter 7** reports on the method used for data regression and the simulation of separation sequences. **Chapter 8** contains the equipment verification results, new phase equilibrium data measured in this work, a comparison of entrainers, thermodynamic modelling and separation sequence simulations. All of the results are also discussed in this chapter. The essential findings of the work are concluded in **Chapter 9**.

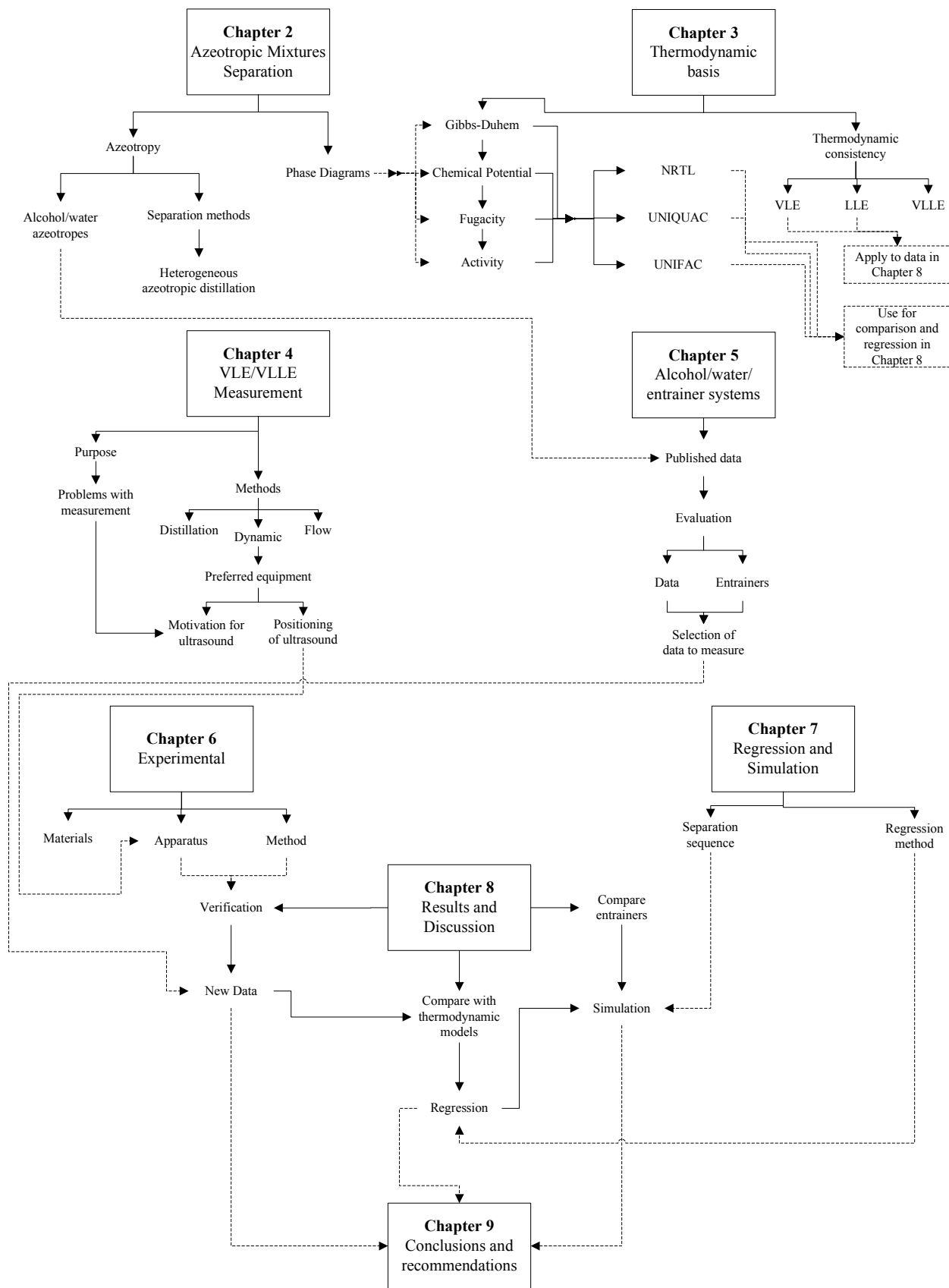


Figure 1-2: Illustration of this thesis layout.

I LITERATURE

2 SEPARATION OF AZEOTROPIC MIXTURES

Separation of homogeneous liquid mixtures commonly requires the formation of another phase within the system. Distillation is the most frequently used method for this purpose. It entails repeated vapourization and condensation in order to enrich the vapour phase with the more volatile component. Therefore, the successful execution of distillation depends on the fact that equilibrium compositions of the vapour and liquid phases differ. The desired degree of separation is then achieved by segregating the phases and repeating partial vapourization. Ordinary distillation cannot separate azeotropes since no enrichment of the vapour phase can occur beyond this point. Special methods utilizing a separating agent other than energy need to be employed to separate these azeotrope-forming components. This agent may be a membrane for pervaporation or an entrainer for extractive or azeotropic distillation. This chapter introduces azeotropy, distinguishes between various methods to separate homogeneous azeotropic mixtures and takes a closer look at extractive and heterogeneous azeotropic distillation.

2.1 AZEOTROPY

2.1.1 What is *azeotropy*?

The word azeotrope means “constant boiling” derived from the Greek words *a-* (non), *zeo-* (boil) and *tropos-* (change). This indicates that the vapour and liquid phase compositions of a mixture of two or more components are equal at equilibrium at a given temperature and pressure. Azeotropes have even been mistaken for pure components since they boil at a constant temperature, other than the pure components’ boiling temperature. Azeotropes can however easily be distinguished from a pure component due to a change in composition with a change in pressure. Azeotropy was first identified by Wade and Merriman in 1911 as the phenomenon when mixtures exhibit a maximum or minimum in the boiling temperature under isobaric conditions, or with an extreme point in the vapour pressure under isothermal conditions (Malesinski 1965). The composition in a mixture that corresponds to such an extreme point is called an azeotrope. If the liquid mixture is homogeneous at the equilibrium temperature, the azeotrope is called a homogeneous azeotrope. If the vapour phase coexists with two liquid phases, it is called a heterogeneous azeotrope. Mixtures that do not display any azeotropes are called zeotropic (Swietoslowski 1963). In the next sections the conditions of an azeotropic mixture and the physical traits leading to non-ideality and azeotropy are addressed in more detail.

2.1.2 Vapour-liquid equilibrium, non-ideality and azeotropy

Vapour-liquid-phase non-ideality is quantified as:

$$y_i \phi_i P = x_i \gamma_i f_i^o, \quad i = 1, 2, \dots, n \quad 2-1$$

Where, y_i = vapour composition of component i

x_i = liquid composition of component i

P = system pressure

ϕ_i = fugacity coefficient of component i in the vapour phase

γ_i = activity coefficient of component i in the liquid phase

f_i^o = fugacity of component i in the liquid phase

The vapour-liquid phase equilibrium at low to moderate pressures and temperatures far from the critical point are expressed as:

$$y_i P = x_i \gamma_i P_i^{sat}, \quad i = 1, 2, \dots, n \quad 2-2$$

Where, P_i^{sat} = saturated vapour pressure of component i

The non-ideality of a mixture is measured by the activity coefficient and changes with both temperature and composition. The mixture is considered ideal when the activity coefficient is equal to one. Equation 2-2 then simplifies to Raoult's law.

$$y_i P = x_i P_i^{sat}(T), \quad i = 1, 2, \dots, n \quad 2-3$$

For non-ideal mixtures the activity coefficient will exhibit positive (greater than one) or negative (less than one) deviations from Raoult's law. A mixture is azeotropic when these deviations become large enough for the boiling temperature to exhibit an extreme point at constant pressure, or the vapour pressure to exhibit an extreme point at constant temperature. At this point the vapour and liquid equilibrium phases have the same composition. This azeotropic behaviour is illustrated in Figure 2-1a by the tangential condensation and boiling temperature curves with zero slopes. Sufficiently large positive deviations (typically larger than 4) result in the occurrence of phase splitting and the formation of a heterogeneous azeotrope (Figure 2-1b). At the heterogeneous azeotropic point (y_a) the overall liquid composition is equal to the equilibrium vapour composition, but the three individual coexisting phases have different compositions. This phenomenon will be discussed in more detail in Section 2.3.

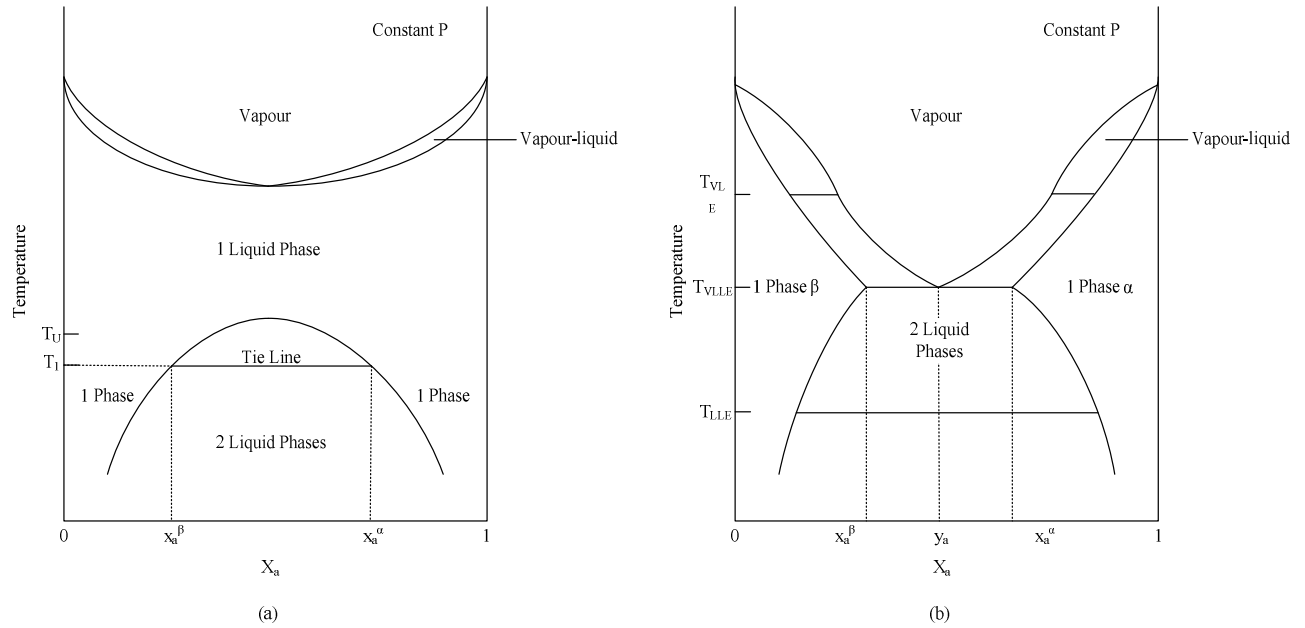


Figure 2-1: a) Phase diagram exhibiting both partial miscibility and an azeotrope, b) phase diagram exhibiting VLE. According to Koretsky (2004).

2.1.3 Non-ideality and separation by distillation

Ease of separation or degree of enrichment is measured by the relative volatility between two components (Equation 2-4). Relative volatility (α_{ij}) generally changes with temperature, pressure and composition. When α_{ij} deviates significantly from unity, it is easy to separate the one component from the other. The relative volatility of azeotropic components is equal to one at the azeotropic point and therefore the vapour cannot be enriched any further. This is why it is impossible to separate azeotropes into pure components by conventional distillation.

$$\alpha_{ij} = \frac{y_i/x_i}{y_j/x_j} = \frac{\gamma_i P_i^{sat}}{\gamma_j P_j^{sat}} \quad 2-4$$

Ordinary distillation typically becomes uneconomical when $0.95 < \alpha_{ij} < 1.05$, due to the large number of theoretical stages and high reflux ratio required (Hilmen 2000, Van Winkle 1967). Close-boiling zeotropic mixtures may also be separated by the special methods applied to azeotropic mixtures.

2.2 ALCOHOL/WATER AZEOTROPES

Aqueous alcohol azeotropes are some of the most common azeotropes. This project focuses specifically on the ethanol/water, IPA/water and n-propanol/water azeotropes at standard atmospheric conditions. Ethanol and water forms an azeotrope with a composition of 89.5 mole % ethanol and 10.5 mole % water at 78.12°C. The IPA/water azeotrope boils at 80.18°C with a composition of 67.28 mole % IPA and 32.72 mole % water. n-Propanol and water forms an azeotrope with a composition of 43.17 mole % ethanol and 56.83 mole % water at 78.12°C (Gmehling et al. 1994).

Ethanol (ethyl alcohol) is a straight-chain alcohol with a molecular formula of C_2H_5OH . It is commonly abbreviated as EtOH. Ethanol has long been used as fuel for heat and light. Lately it is also used as motor fuel and fuel additive, which has become the largest single use of ethanol. Ethanol is the prime psychoactive ingredient of alcoholic beverages, in which its concentration may vary (Hanson, Venturelli & Fleckenstein 2011). It is also an essential solvent and feedstock for the synthesis of other products in chemistry. Ethanol has a widespread medicinal use due to its antibacterial properties. It has extensive use as a solvent in substances intended for human consumption or contact, such as flavourings, colourings and perfumes. It is mainly produced via two processes, the hydration of ethylene and the fermentation of sugars. The raw material for dehydration of ethylene is derived from natural gas or petroleum. The fermentation raw materials are agricultural products. Ethylene hydration can be performed via two routes, directly and indirectly. There has been a shift away from the indirect route due to better yields, less by-products, and reduced quantities of pollutants produced by the direct route. In the primary chemical reaction for the direct hydration process, water vapour and ethylene are mixed at an elevated pressure and temperature and passed over a catalyst impregnated with phosphoric acid. The reaction produces a dilute crude alcohol. Ethanol produced via fermentation refers to the conversion of sugars (glucose, fructose and sucrose) to ethanol by yeast. The conversion is performed in the absence of oxygen and is therefore classified as anaerobic. One of the by-products in this process is water and therefore it yields an aqueous ethanol product (Nexant Chem Systems 2006).

n-Propanol is a colourless liquid with an average volatility and characteristic alcoholic odour. It is less inclined to absorb water than lower alcohols and has a significantly milder and more pleasant odour than higher alcohols. n-Propanol is mainly used as a solvent in flexographic and other printing inks. It is also used in the coatings industry to improve the drying characteristics of alkyd resins, electro-deposition paints, baking finishes, etc. n-propanol is present in floor polishes, metal degreasing fluids and de-icing fluids. It is also used in the manufacturing of adhesives and is a feedstock in the manufacturing of insecticides, herbicides and pharmaceuticals (BASF 2011). n-Propanol is manufactured by the hydrogenation of propionaldehyde. Depending on the catalyst, the product stream may contain a substantial amount of water in order to prevent the formation of other impurities (Unruh, Ryan & Dugan 1999). n-Propanol can also be recovered as a by-product of the high pressure synthesis of methanol from carbon monoxide and hydrogen. Water is also a product of this reaction and the n-propanol recovered could therefore be aqueous (Frolich, Lewis 1928). During the amination of n-propanol a mixture of mono-, di- and tri-n-propylamines, n-propanol and water is formed. The mono-n-propylamines can be removed via distillation and the di- and tri-n-propylamines via fractional distillation. The aqueous n-propanol subsequently needs to be purified past the n-propanol/water azeotrope (Challis 1954).

Isopropanol (2-propanol) is an organic compound with the molecular formula C_3H_8O . This compound is also known as propan-2-ol, 2-propanol or abbreviated as IPA. It is a flammable, colourless chemical compound with a strong odor. IPA is structural isomer of propanol. It is a low-cost solvent with various consumer and industrial applications. It is mainly used for this purpose, especially for dissolving lipophilic contaminants such as oil. Apart from solvent properties, IPA also possesses cooling, antipyretic, rubefacient, cleansing and antiseptic properties. IPA is also a major ingredient in “gas dryer” fuel additives. A significant quantity of water in fuel tanks poses a problem as it separates from the gasoline. This can cause freezing in the supply lines at cold temperatures. Since water is soluble in IPA, the addition of IPA to fuel can prevent water from accumulating and freezing in the supply lines (International Programme on Chemical Safety 1990). Large amounts of IPA are also used as cleaning and dehydrating agent in the electronic and precision machinery industries. IPA is used extensively in various stages of water surface washing and cleaning in the semiconductor manufacturing process. Thousands of tons of high-purity IPA is consumed each year by this process and after washing and cleaning, ends up as waste solvent. Incineration might be used to dispose of this waste solvent due to its sufficient organic content. However, incineration would lead to loss of recoverable IPA (Lin, Wang 2004). The above to show that there exists due motivation to study the recovery or dehydration of ethanol, n-propanol and IPA from waste streams.

The Fischer Tropsch process is an example of an industrial process that produces a waste stream containing all of the abovementioned alcohols in aqueous form. It produces hydrocarbons from synthesis gas which is accompanied by the production of water and oxygenates, such as alcohols (Table 2-1). Most of the polar oxygenates, formed during the stepwise condensation of the Fischer Tropsch product, dissolves in the water to form an aqueous solution commonly referred to as reaction water. Since a significant amount of Fischer Tropsch product often ends up in the reaction water, there exists an economic incentive to recover these components (Nel, de Klerk 2007).

Table 2-1: A typical Fischer Tropsch waste water stream (Carlson 1949).

Component	Composition (wt %)
Aldehydes	2-6
Esters	0.2-3
Water	28-29
Alcohols (EtOH, n-propanol, IPA, sec. BuOH, i-BuOH)	62-69.8
Ketones	Trace

2.3 AZEOTROPIC PHASE EQUILIBRIUM DIAGRAMS

To gain a fundamental understanding of the highly non-ideal thermodynamic behaviour of azeotropic mixtures, one has to analyse the structural properties of VL(L)E diagrams. This analysis is also imperative for the conceptual design of an azeotropic distillation process.

2.3.1 Vapour-liquid Equilibrium

When chemical engineers encounter phase equilibrium problems, it most frequently involves vapour-liquid equilibrium (VLE). At vapour-liquid equilibrium there exist two phases, one vapour and the other liquid, in equilibrium with each other. Phase equilibrium diagrams are useful tools for solving problems involving phase equilibrium. They can be used for identifying the thermodynamic state of a mixture, indicate what phase/phases are present and the composition of the liquid and vapour phases as well as their relative amounts. These diagrams are typically constructed for either a constant pressure ($T - x$ diagram) or constant temperature ($P - x$ diagram). Figure 2-2 illustrates the vapour-liquid phase equilibrium of a binary mixture (component a and b) at constant pressure. By convention, the component that boils more easily (lighter component) is labelled a . At high temperatures the mixture will exist in the form of a superheated vapour, as indicated in the top of Figure 2-2. At very low temperatures the mixture will exist in the form of a sub-cooled liquid, as indicated in the bottom of Figure 2-2. Between these extremes the mixture exists in a two-phase region where it is in vapour-liquid equilibrium. The symbol z_a designates the feed composition. The equilibrium vapour and liquid compositions at the system temperature (T_{sys}) are labelled y_a^{eq} and x_a^{eq} respectively.

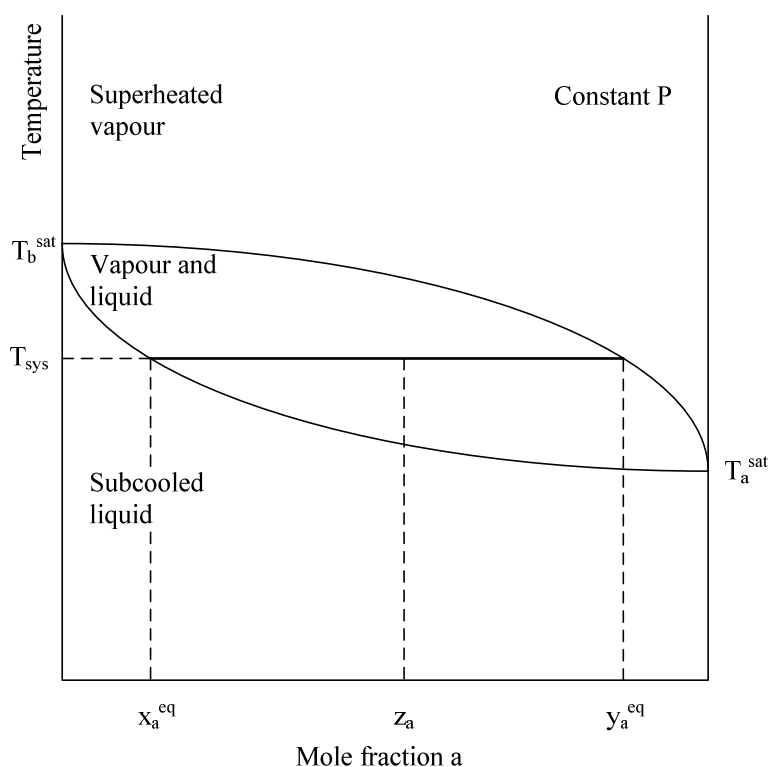


Figure 2-2: Vapour-liquid equilibrium T - x - y phase diagram for an ideal binary mixture of a and b . According to Koretsky (2004).

Alternatively, binary VLE data can be represented on a x - y diagram (Figure 2-3). On such a diagram, the curve of an azeotropic system crosses the 45° line (Figure 2-4).

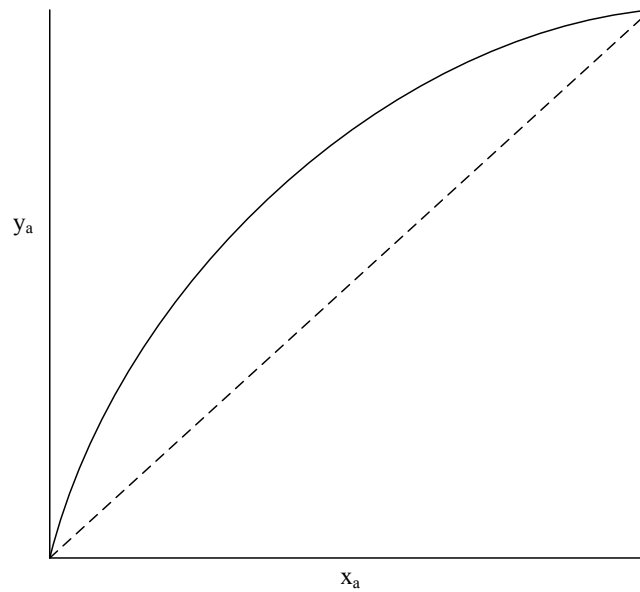


Figure 2-3: Vapour-liquid equilibrium x - y phase diagram for an ideal binary mixture.

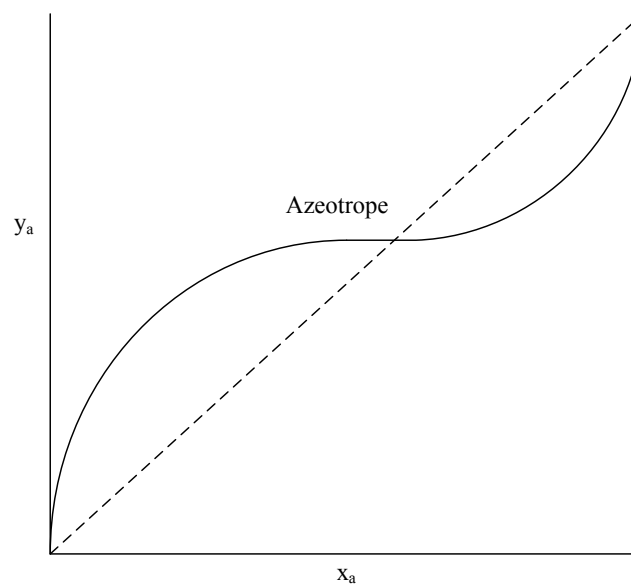


Figure 2-4: Vapour-liquid equilibrium x - y phase diagram for a binary mixture that forms an azeotrope.

According to Seader and Henley (2006).

On a T - x - y diagram, an azeotrope is illustrated as follow:

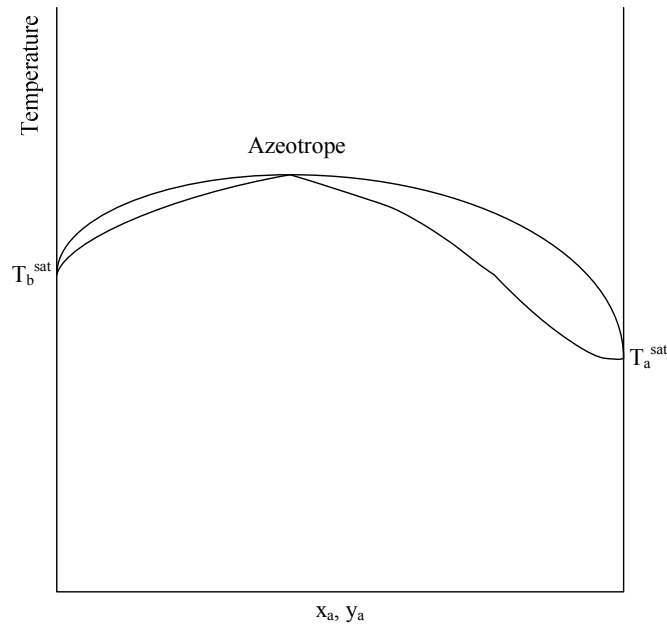


Figure 2-5: Vapour-liquid equilibrium T - x - y phase diagram for a binary mixture that forms an azeotrope.

According to Seader and Henley (2006).

One can plot ternary VLE data on an equilateral triangular phase diagram, as in Figure 2-6. The diagram shows that a liquid phase containing 30% A, 30% B and 40% C is in equilibrium with a vapour of $y_A = 0.4$ and $y_B = 0.08$. If at some point the composition of the liquid and vapour phases are exactly the same, a ternary homogeneous azeotrope occurs.

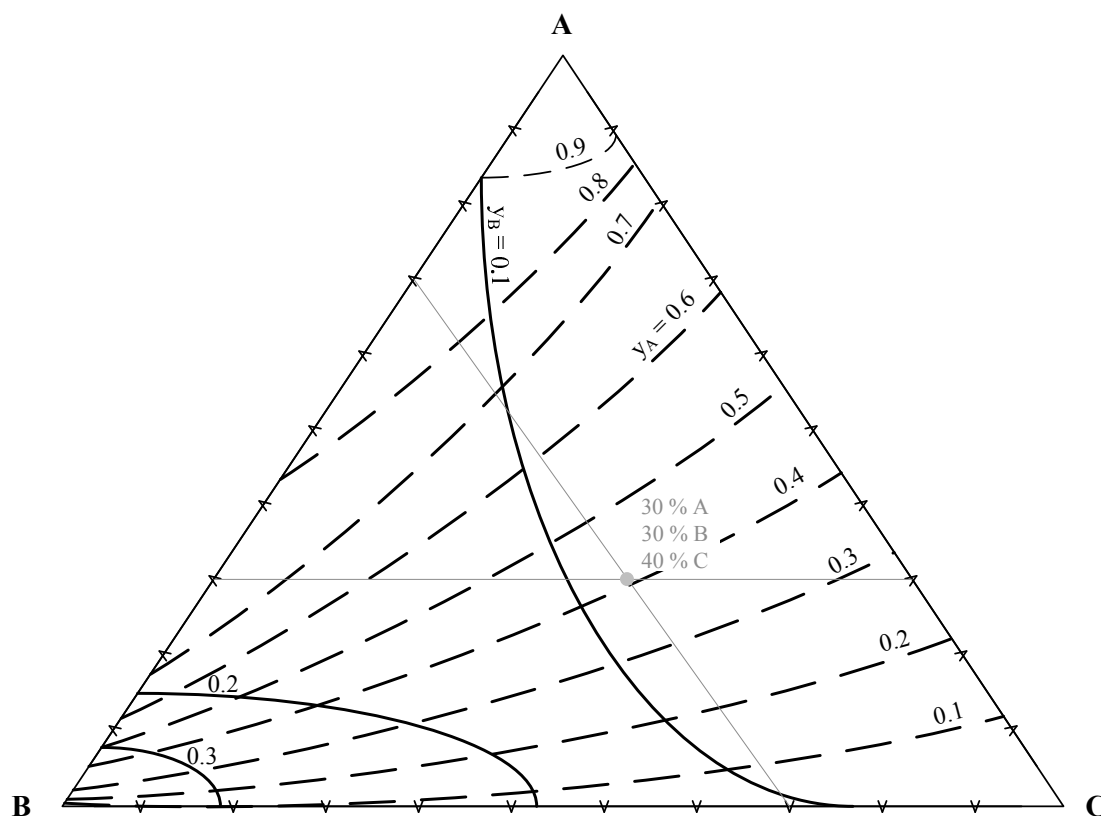


Figure 2-6: Vapour-liquid equilibrium compositions of ternary mixtures of A-B-C at 1 atm. The dashed lines y_A and the solid lines are labeled y_B . According to Walas (1985).

2.3.2 Liquid-liquid Equilibrium

When the like (a-a and b-b) interactions in a mixture are significantly stronger than the unlike (a-b) interactions, a liquid can split into two different partially miscible or immiscible phases. See labelled α and β . Separate phases are formed to lower the total Gibbs energy (see Section 3.2) of the system and this leads to liquid-liquid equilibrium. A typical liquid-liquid equilibrium phase diagram for a binary mixture is shown in Figure 2-7. The curve separating the single phase region from the two phase region is called the binodal curve. A tie-line drawn within this curve can be used to determine the compositions of the co-existing phases at any temperature (see Figure 2-7). The temperature above which the liquid mixture no longer separates into two phases at any composition is termed the upper consolute temperature (T_u). A lower consolute temperature will exist if the binodal curve exhibits a minimum temperature point rather than a maximum as in Figure 2-7. Phase diagrams of binary systems consisting of only liquid phases can exhibit either a convex, concave or closed form as a function of temperature. System *a-b* in Figure 2-7 exhibits a convex shape.

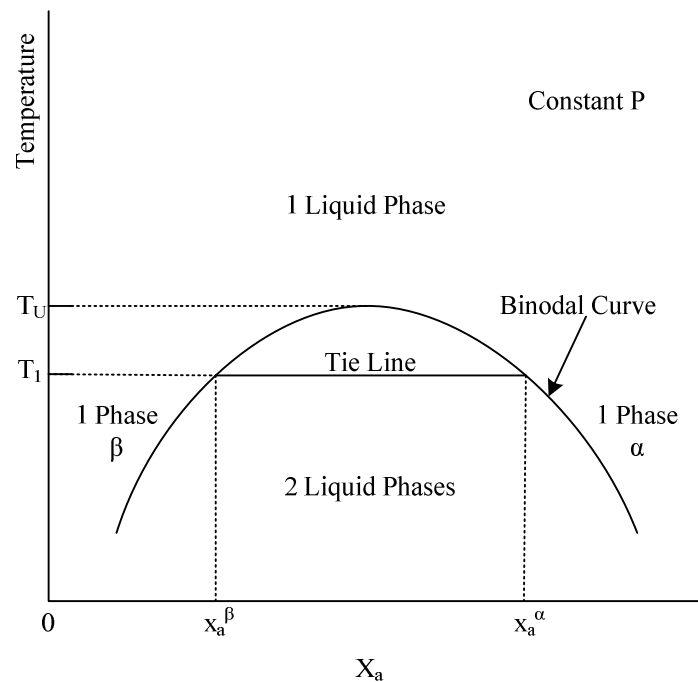


Figure 2-7: Binary liquid-liquid phase equilibrium diagram. According to Koretsky (2004).

Pressure changes only affect liquid phase equilibrium significantly at high pressures or near the critical point. The directional effect is predictable by Le Chatelier's principle.

A ternary liquid-liquid system can be plotted on a equilateral triangular phase diagram such as Figure 2-8. Components B and C are partially soluble in each other and component A distributes between the phases. The miscibility boundary between the 2 liquid phase and 1 liquid phase areas is known as the phase envelope. The dashed line represents the tie-lines that connect and indicate the two liquid phases in equilibrium with each other. At the plait point the two liquid phases have the exact same compositions. Consequently the tie lines converge to this point and the two liquid phases become one (Seader, Henley 2006). The ternary phase diagram can be constructed at constant temperature (from isothermal data), constant pressure (from isobaric data) or at both constant temperature and constant pressure.

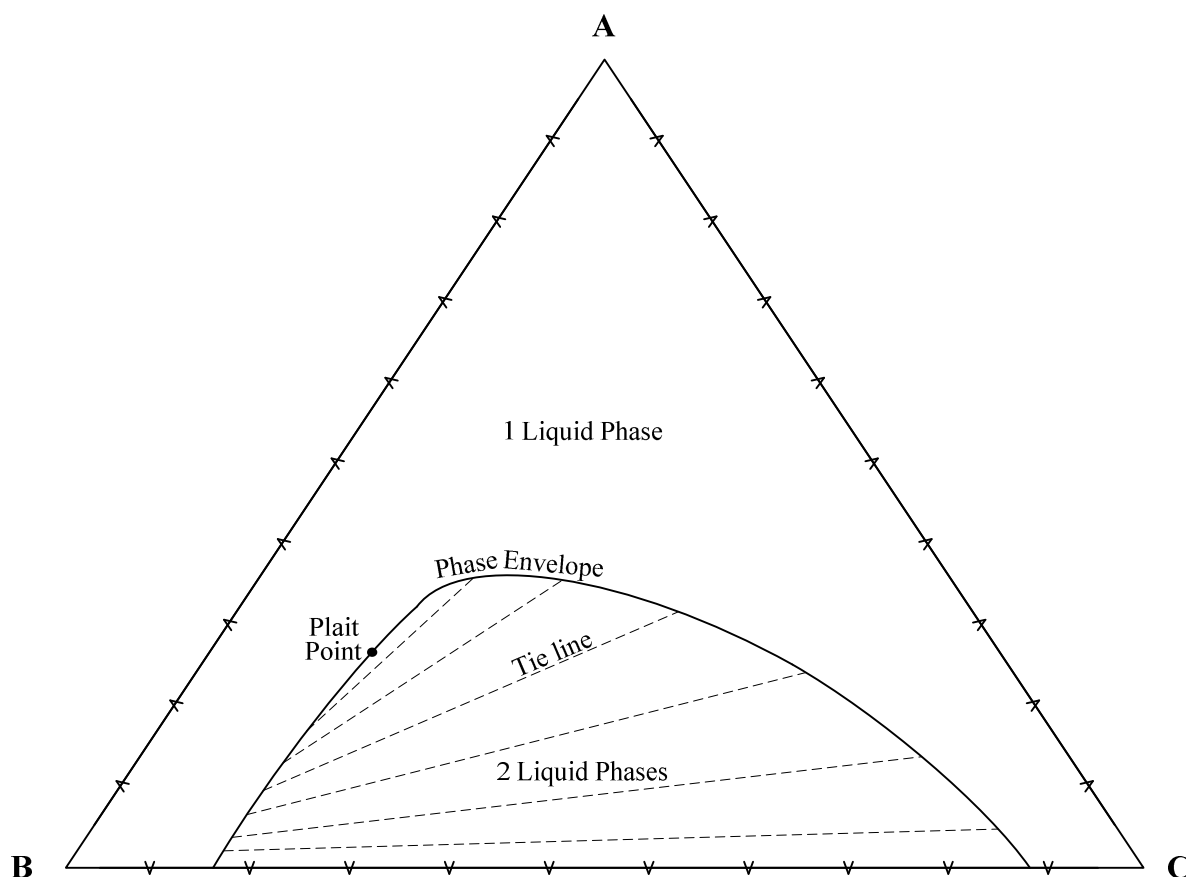


Figure 2-8: Ternary liquid-liquid phase equilibrium diagram. According to Seader and Henley (2006).

2.3.3 Vapour-liquid-liquid Equilibrium

Vapour-liquid-liquid equilibrium behaviour typically occurs once the pressure is decreased in a system with both liquid-liquid-equilibrium and an azeotrope in vapour-liquid equilibrium (Figure 2-9a). As the system pressure decreases, the constituents can become volatile before the upper consolute temperature is reached (Figure 2-9b). When this happens, the VLE and LLE curves intersect and it is possible for three phases (one vapour and two liquid) to exist at equilibrium (Koretsky 2004). At T_{LLE} , the lowest temperature, three different possibilities for phase behaviour exists. At low concentrations of component a only liquid phase β is present, while at high concentrations of component a only liquid phase α is present. At the intermediate composition of component a , the systems exhibits two liquid phases. The compositions of these phases are indicated by the position where tie-line in Figure 2-9b intersects with the phase envelope. Again at temperature T_{VLE} only liquid phase β is present at low concentrations of component a , while at high concentrations of component a only liquid phase α is present. As the concentration of x_a increases at T_{VLE} , a vapour phase in equilibrium with liquid β appears. This vapour-liquid phase is followed by a solitary vapour phase and then a vapour phase in equilibrium with liquid α . The compositions in the two phase regions are again given by the tie-lines indicated in Figure 2-9b. Yet again, at the intermediate temperature, T_{VLE} , only liquid phase β is present at low concentrations of component a , while at high concentrations of component a only liquid phase α is present. However, at concentrations of x_a between the two single-phase regions, both liquid α and β can exist along with a vapour phase. The compositions of these phases are given by the points on the tie-line at T_{VLE} , which

intersects with the dashed lines. Therefore, in the intermediate composition section at temperature T_{VLE} , this binary system exhibits VLE.

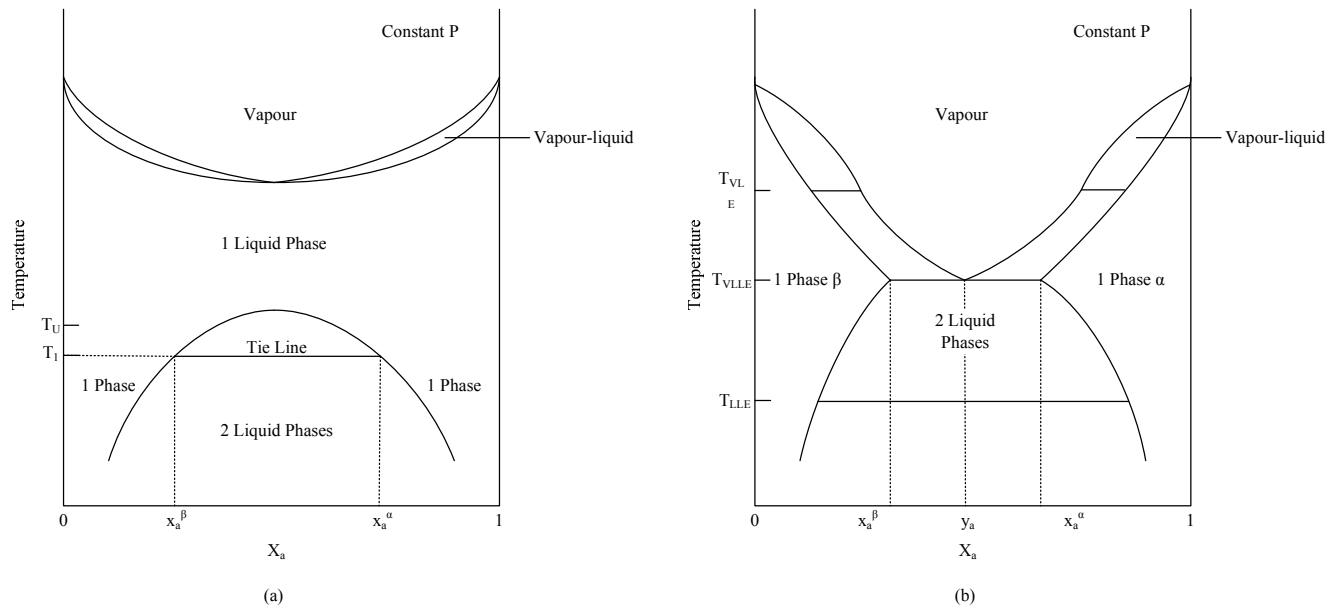


Figure 2-9: a) Phase diagram exhibiting both partial miscibility and an azeotrope, b) phase diagram exhibiting VLE. According to Koretsky (2004).

A ternary vapour-liquid-liquid system can be plotted on an equilateral triangular phase diagram as shown in Figure 2-10. This diagram has properties similar to that of the ternary liquid-liquid equilibrium phase diagram, such as the phase envelope, tie-lines and plait point. In addition to these properties, the vapour-liquid-liquid equilibrium phase diagram consists of a vapour phase indicated by a dashed line in Figure 2-10. A ternary heterogeneous azeotrope exists when the composition of the vapour phase lies on the tie line connecting the two liquid phases in equilibrium with the particular vapour phase. According to the mass balance rules of a ternary phase diagram, in such a case the vapour phase composition is the same as the overall liquid phase composition and therefore a ternary heterogeneous azeotrope exists at that point. In Figure 2-10 vapour point 4 exhibits such behaviour.

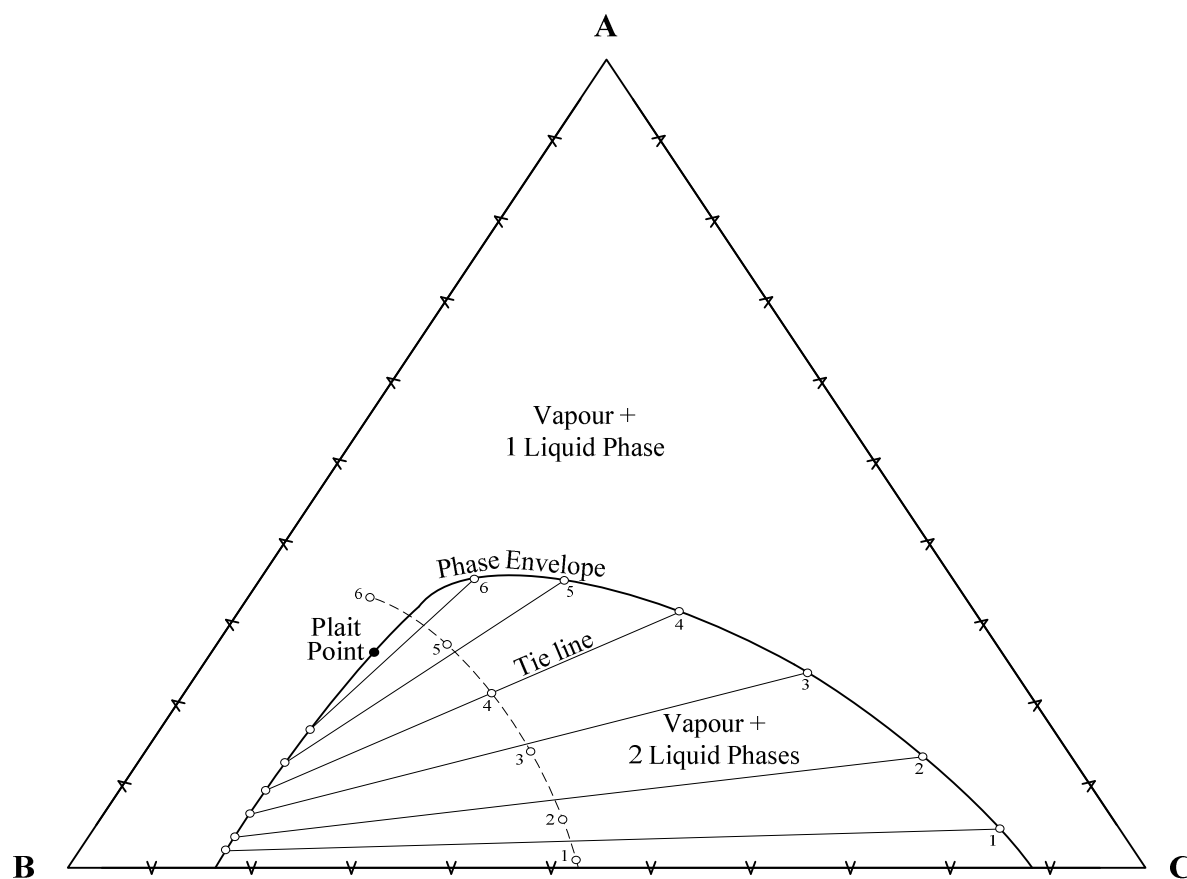


Figure 2-10: Ternary vapour-liquid-liquid phase equilibrium diagram.

2.3.4 Residue curves

Special techniques, such as azeotropic distillation must be applied to separate azeotropic mixtures. Generally, two types of azeotropic distillation are found. The first involves the separation of an azeotropic mixture without introducing any additional azeotropes. The second deals with the separation of an azeotropic mixture by deliberately adding an azeotrope-forming component (entrainer). In the first case, a separation sequence delivering the desired product specifications and recovery needs to be found. The second case additionally requires the selection of an entrainer that facilitates the desired separation and is easily recovered downstream. For both cases possible separation sequences need to be established before they are analyzed in detail. In order to do that, a tool to qualitatively predict the feasible separation of multi-component azeotropic mixtures is required. The analysis of RCMs is such a tool. It offers efficient preliminary analysis of non-ideal distillation problems and allows for the pre-synthesis of separation sequences (conceptual process design).

Conceptual process design is the fundamental process is to envisage, produce, compare and assess different design alternatives at an early stage of design when detailed information is not yet available. This process enables the systematic elimination of less favourable process alternatives and the subsequent detailed analysis of a reduced set of preferred alternatives. Residue curve maps (RCMs) are one of the most widely used conceptual design tools and are used for the conceptual design of non-ideal distillation separation sequences. It is the most mature conceptual design tool and forms part of almost every available design package (Aslam, Sunol 2006). The RCM methodology is extensively covered by Doherty and Malone (2001). The reliability of the

thermodynamic model representing the phase equilibrium and the algorithm used for prediction of thermodynamic markers such as azeotropes, determine the reliability of RCMs as a conceptual design tool.

When considering a wide variety of mixture types, it can be seen that there is a relatively simple and unique correspondence between the VLE characteristics of a mixture and the path of its equilibrium phase transformations (i.e. residue curves and distillation lines). The feasible separation sequences of a certain VLE diagram can be obtained from groups or classes of residue curve maps. Foucher et al. (1991) and Fien and Liu (1994) investigated and compiled such groups. The analysis of VLE diagrams therefore initializes the prediction of feasible separations by distillation. It can be used to determine the thermodynamic limitations and possibilities of the separation, caused by the nature of the mixture. Alternative separation sequences for further investigation and comparison can be constructed once a feasible separation is found. This method then allows for the consequent selection of the optimal separation sequence. Residue curve map analysis is particularly useful for the screening of entrainers for heterogeneous azeotropic and extractive distillation.

A RCM is a geometric representation of the VLE phase behaviour of multi-component mixtures. In particular, it highlights the properties that directly impact distillation and represent a collection of trajectories or residue curves of the liquid phase. A residue curve is a plot of the liquid-residue composition in the distillation still over a period of time. These curves can be determined either experimentally or by mathematical simulation of the experiment. To construct these diagrams, rules based on thermodynamic principles, material balances and distillation operation can be followed (Lee, Shen 2003). Procedures for calculating these curves are given by Doherty and Perkins (1978) and Bossen et al. (1993). Vapor-liquid-liquid equilibrium points can also be projected onto this graph and yield the liquid-liquid equilibrium curve and the composition line of the vapour phase (Figure 2-11). The thick solid lines in Figure 2-11 indicate distillation boundaries. These boundaries cannot be crossed by normal distillation. By projecting VLLE data onto the RCM, a distillation path can be found to obtain certain products by crossing the distillation boundaries through liquid-liquid split. This method is referred to as heterogeneous azeotropic distillation and is discussed in Section 2.5.2.

Literature indicates that RCM technology is one of the most common methodologies for determining entrainer feasibility with heterogeneous azeotropic distillation (Julka, Chiplunkar & O'Young 2009, Doherty, Malone 2001, de Villiers, French & Koplos 2002, Fien, Liu 1994, Ivonne, Vincent & Xavier 2001, Pham, Doherty 1990).

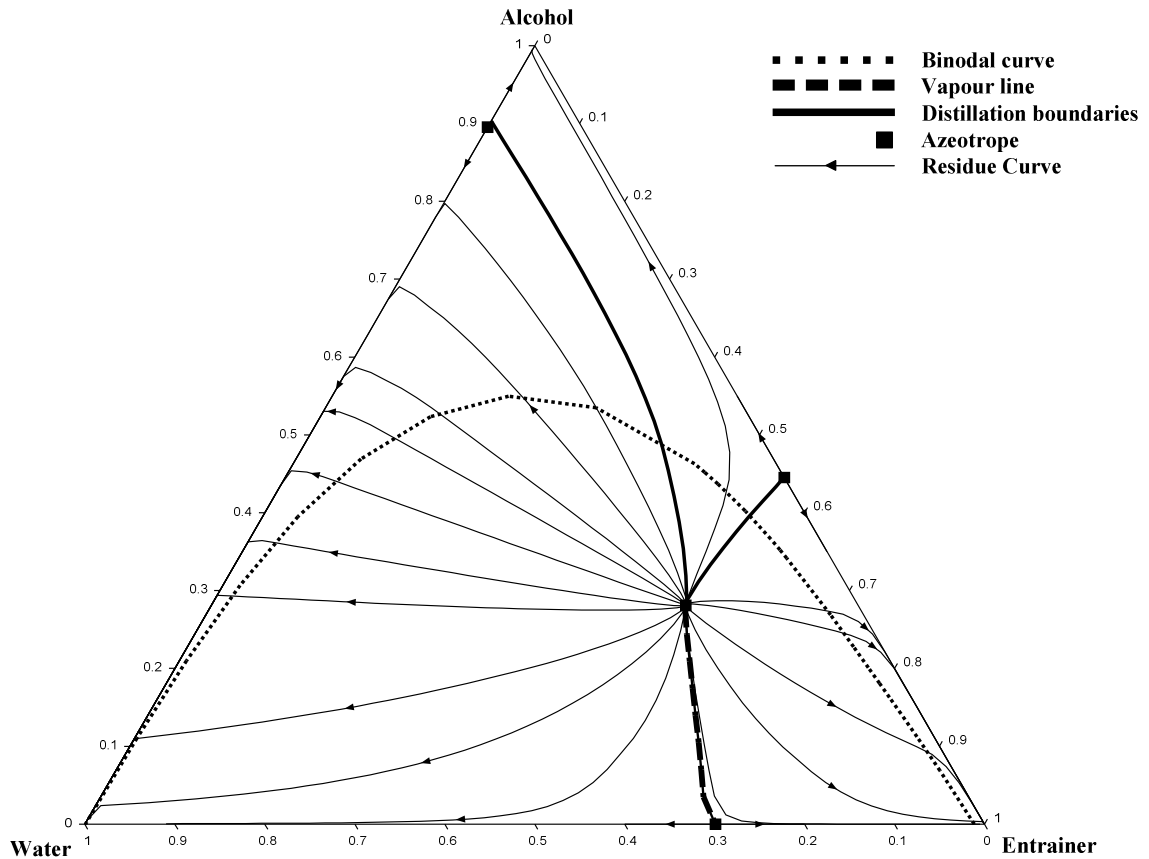


Figure 2-11: Typical residue curve map with projected VLE data. Simulated in Aspen with NRTL.

2.3.5 Discussion

This chapter presents the classification of a few types of equilibrium. This is done through various phase diagrams, each a record of the effects of temperature, pressure and composition on the kinds and numbers of phases that can exist in equilibrium with each other within a certain system. The kinds of phases that can exist at any given condition are characteristic of the chemical nature of the components. As opposed to numerical tabulation, graphical representation of phase equilibrium data clearly shows the interrelationships between all the variables and allows for easier inter- and extrapolation.

The choice of which diagram to use for a certain system is primarily based on the number of components, then the kinds and numbers of phases. The variables that could be represented on a phase diagram of a system of n substances are T , P and $n-1$ mol fractions. Ordinarily binary systems are represented on planar diagrams, which mean either a $T-x$ or $P-x$ diagram. To represent three variables (ternary systems), a spatial diagram would be required. The mole fractions of a ternary system can however also be represented on a planar triangular diagram (Walas 1985).

2.4 GENERAL SEPARATION PROCESSES

Homogenous azeotropes in liquid mixtures can be separated through various methods of which enhanced distillation is the oldest and most frequently used. Azeotropic distillation is performed either via pressure variation or the addition of a separating agent called an entrainer. The entrainer facilitates separation by altering the phase equilibrium of the mixture. Distillation is often complemented with other separation techniques, such as membrane separation. These separation sequences are referred to as hybrid distillation systems. Distillation systems employing a mass separating agent are categorized as enhanced distillation (Hilmen 2000, Seader, Henley 2006). In the following sections only the separation of homogeneous azeotropic mixtures will be considered, but heterogeneous azeotropes or multiple phases may be induced by the separation technique applied. Membrane-distillation hybrids, pressure-swing distillation and entrainer-addition methods are considered below in a collective discussion of the advantages and disadvantages of each method.

2.4.1 Membrane-distillation hybrids

The use of a membrane to separate liquid and vapour mixtures is an up-and-coming separation technique. Its industrial application increased greatly during the 1980's. The feed mixture is selectively separated by means of a membrane acting as a semi-permeable barrier. The part of the feed that does not pass through the membrane is called the retentate, and the part that does pass through is known as the permeate. The membrane preferentially absorbs and diffuses one of the components responsible for azeotrope formation (Seader, Henley 2006).

Pervaporation is the most commonly used membrane technology for the separation of azeotropic mixtures. With this membrane separation technique the phase state on the one side of the membrane is different from that on the other side, i.e. a liquid retentate side and a vapour permeate side. A composite membrane is used that is selective for one of the azeotrope-forming components (species A, Figure 2-12).

A membrane separation process can only be economic and efficient when the membrane has:

- Good permeability
- High selectivity
- Stability
- Low/no fouling
- Long lifetime (Seader, Henley 2006).

The "Membrane Handbook" (Fleming, Slater 1992) provides information on pervaporation membranes suitable for various mixtures. The phase change performed with pervaporation requires significantly more energy than for other pressure driven membrane processes such as reverse osmosis (Hilmen 2000). Major industrial applications of pervaporation include the dehydration of ethanol, dehydration of other organic alcohols, ketones and esters, removal of organics from water and the separation of organic mixtures. This process is applicable to separations over the entire composition range, but is best applied to feed mixtures dilute in the main permeate. With a permeate-rich feed, a number of membranes may be needed and only a small amount of permeate could be produced per stage. Re-heating of the retentate between stages may also be necessary (Seader, Henley 2006).

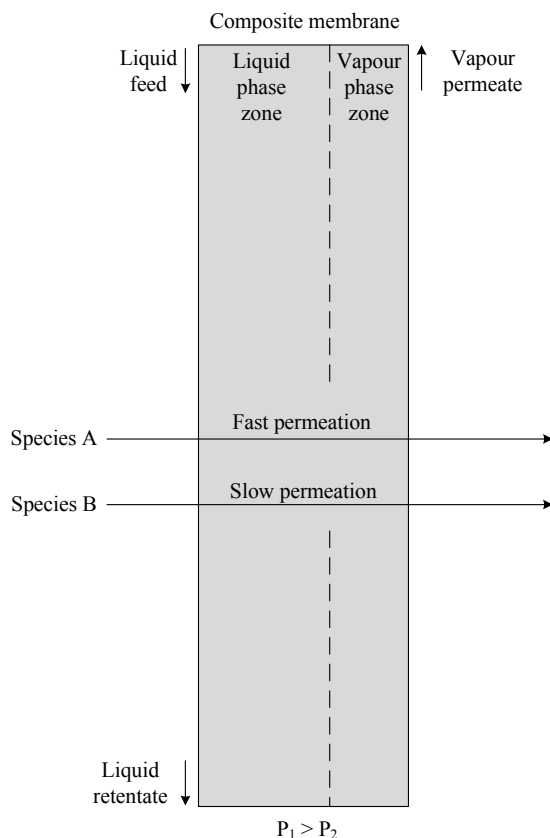


Figure 2-12: Schematic illustration of the mechanism upon which membrane distillation functions

According to Knauf et al. (1998), pervaporation accounts for 3.6% of all membrane applications in the chemical and pharmaceutical industries. The process is deemed expensive in both processing costs and investment. However, due to its high selectivity, pervaporation is considered in cases where conventional separation techniques perform inadequately. In this case, pervaporation is generally used in combination with normal distillation. The distillation column will then act as a pre-concentrator for the membrane. For ethanol dehydration the distillation column would have to produce the ethanol/water azeotrope as distillate and feed it to the pervaporation unit. Although such hybrid systems can have lower operating costs than azeotropic columns, the higher capital cost and lower maximal capacity are serious disadvantages (Szitkai et al. 2002).

2.4.2 Pressure-swing distillation

Azeotropes that disappear at some pressure, or changes composition by 5 mol% or more over a moderate pressure range, are good candidates for separation by pressure-swing distillation. The process is performed by operating two distillation columns in series, at different pressures. Figure 2-13 illustrates how a minimum-boiling azeotrope in mixture A-B can be separated via pressure-swing distillation. A binary homogeneous azeotropic mixture is introduced to the first column at a low pressure (P_1). The bottom product (B_1) from this column is nearly pure A while the overhead (D_1) is an azeotrope. The azeotrope (D_1) is fed to the second column, operating at a higher pressure. The high-pressure column produces nearly pure B in the bottoms (B_2) and another azeotrope in the overhead (D_2). D_2 is recycled as feed to the first column.

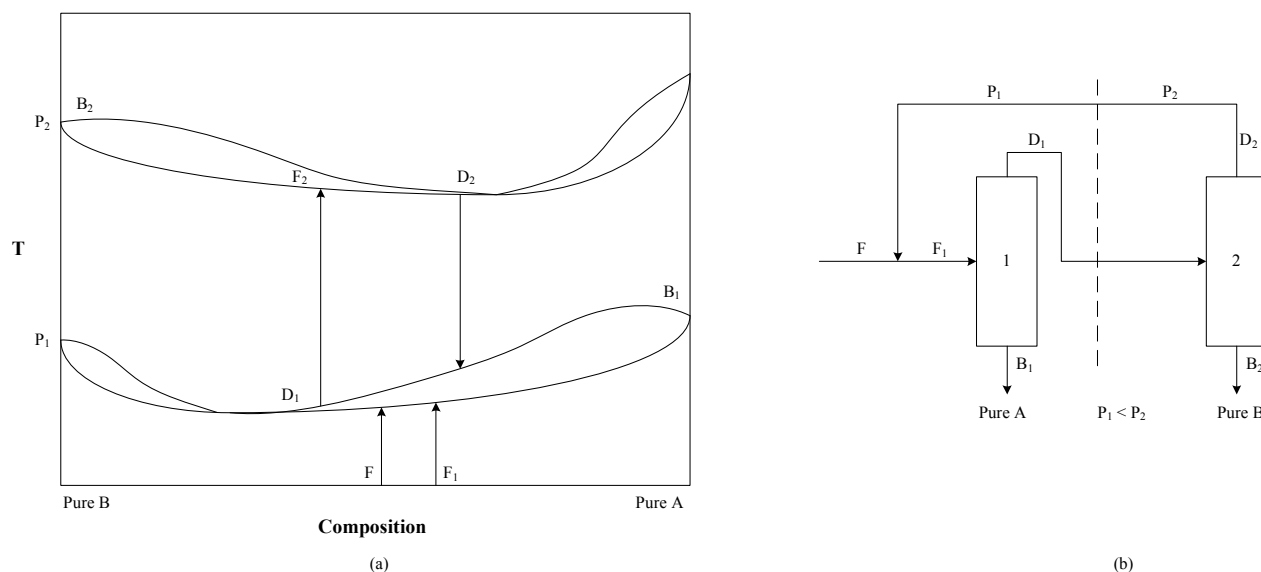


Figure 2-13: (a) Illustration of the function of pressure-swing distillation on a phase diagram; (b) Typical separation sequence for pressure-swing distillation. According to Seader and Henley (2006).

Unfortunately the ethanol-water azeotrope is not considered to be sufficiently pressure sensitive for the successful application of pressure-swing distillation (Hilmen 2000). The alteration of VLE properties of azeotropic mixtures by merely physical means may seem attractive, but it is usually not an option and often very uneconomical (Van Winkle 1967).

2.4.3 Entrainer-addition distillation methods

The modification of VLE behaviour of azeotropic mixtures, physically and chemically, via the addition of another liquid, offers various possibilities. The additional liquid introduced to the azeotropic mixture is called an entrainer. Entrainer-addition distillation methods are divided into three main groups based on the properties and role of the entrainer and the format of the process (Seader, Henley 2006):

- **Homogeneous azeotropic distillation** deals with an entrainer that is completely miscible with the components of the original mixture. The entrainer may form homogeneous azeotropes with the original mixture and distillation is carried out in a conventional single-feed column.
- **Heterogeneous azeotropic distillation** is carried out in a distillation column combined with a decanter. It involves the formation of a heterogeneous azeotrope between the entrainer and one or more of the components in the original mixture.
- **Extractive distillation** utilizes an entrainer with a boiling-point that is significantly higher than that of the original mixture components and it is selective to one of the components. This process is carried out in a two-feed column, the entrainer is introduced above the original mixture feed point and is largely removed as bottom product.

Other entrainer-addition distillation techniques also exist, such as:

- **Reactive distillation** in which the entrainer reacts selectively and reversibly with one or more of the components in the feed. The reaction product is distilled from the non-reacting components and the reaction is subsequently reversed to recover the entrainer and other reacting components.
- **Salt distillation**, a variation of extractive distillation, in which the relative volatility of the key components is altered by dissolving a salt (entrainer) in the top reflux. The dissolved salt stays in the liquid phase and passes down the column due to its non-volatility (Seader, Henley 2006).

All these methods mentioned may be combined to achieve desirable separation, depending on the nature of the components to be separated. The three main entrainer-addition distillation methods; homogeneous azeotropic distillation, heterogeneous azeotropic distillation and extractive distillation, are discussed in more detail in Section 2.5.

2.4.4 Discussion

According to Smith (1995) the basic advantages of distillation are the potential for high throughput, any feed concentration and high purity. These advantages, compared to other thermal separation techniques, are the grounds for the popularity of distillation as a separation process and this is why distillation is used in 90% of cases for the separation of binary and multi-component liquid mixtures (Hilmen 2000). Distillation is a mature technology. Its design, operation and control is well-developed, unlike other promising technologies such as membranes. Distillation does however have drawbacks such as a low thermodynamic efficiency and the introduction of an entrainer may result in complexities.

Hybrid-distillation systems, such as a combination of distillation and pervaporation, can simplify the overall process structure, reduce energy requirements and avoid the use of entrainers (Hömmereich, Rautenbach 1998). Membrane distillation methods exhibit a great advantage in that its selectivity is not dependant on the vapour-liquid equilibria. Augmenting distillation with pervaporation can allow a more flexible distillation column design, since the pervaporation unit can subsequently be used to separate the azeotrope only. Pervaporation and vapour permeation are however very expensive, due to relatively low permeate fluxes and low condensation temperatures (Hilmen 2000). The processing costs of pervaporation are even further increased by the required re-heating and integration of heat exchangers into the process. The high price of large capacity membrane modules also limits the industrial application of pervaporation to moderate volumes. The capital investment for distillation increases according to the “six-tenths power rule” as a function of capacity, while for membranes it increases linearly with capacity (Kunesh et al. 1995). Therefore, distillation has a great economic advantage at large throughput. This does not render other separation technologies, with lower throughput specifications, useless. Such technologies are best applied in the pharmaceutical and speciality chemical industries.

Membrane systems are not very flexible to feed composition variations. Distillation equipment, on the other hand, is robust and flexible in order to handle a wide range of compositions and frequent changes in feed mixture constituents. Another advantage of distillation, as previously mentioned, is the high degree of purity often achieved in the separation products. Many alternative separation techniques can only achieve partial

separation instead of pure end-products. Consequently, these methods have to be combined with distillation to achieve the desired product, whereas distillation can be used as a stand-alone operation.

It is essential to consider a separation process as a whole, including the restoration or recycle of the separating agent. Membrane materials often have to be regenerated with chemical solvents, which add similar complexities to the operation as for entrainer-addition distillation techniques. Utilizing pressure-sensitivity should generally be considered before the addition of an entrainer. When selecting an entrainer, one that forms a heterogeneous azeotrope is preferred above one that forms a homogeneous azeotrope. The former can be separated easily by decantation in combination with distillation. Sometimes a component that already exists in the process (or on the plant) can be used as an entrainer. This option should then be considered first.

Pharmaceutical products are commonly required to be absolutely entrainer-free. This may be impossible in entrainer-addition methods and therefore alternatives to conventional entrainer-addition distillation would have to be considered. Gmehling et al. (1994) compared extractive and heterogeneous azeotropic distillation and found the latter to be more favourable due to the high amount of energy required to vapourize the entrainer in extractive distillation. According to Tassios (1972), methods such as extractive and heterogeneous azeotropic distillation are under-utilized in industry. The reasons often used in defence of this trend are high investment and high operating costs, but in actual fact in the past the explanation were found in the time and money required to obtain a satisfactory process design. Nowadays, rapid methods are available for evaluating the techniques to separate a azeotropic mixtures, select a suitable separation method and predict the achievable product compositions. These methods are mostly based on the graphical analysis of vapour-liquid equilibrium diagrams. In combination with more advanced distillation synthesis tools and simulation software, the way distillation processes for non-ideal mixtures can be analyzed has been improved radically.

2.5 ENTRAINER-ADDITION DISTILLATION METHODS

2.5.1 Homogeneous azeotropic distillation

This separation method entails the ordinary distillation of ternary mixtures which contain at least one binary homogeneous azeotrope in the original mixture. The entrainer may form a new homogeneous azeotrope, but it is not a requirement for this separation technique. The only criterion is that the resulting ternary system should form a VLE diagram that shows the potential for separation. The thicker line on the triangular diagram (Figure 2-14) is known as a distillation boundary. It is important to note that with homogeneous azeotropic distillation alone, it is impossible to cross distillation boundaries. These lines are usually curvaceous in shape since they are related to the reflux ratio and stage number of the distillation column. Fien and Liu (1994) point out that a straight distillation boundary instead of curved one simplifies the conceptual design process and does not affect the accuracy to which the desired product specification is attained. Due to distillation boundaries it is often difficult to find a suitable entrainer for a separation sequence involving homogeneous azeotropic distillation. This method can however be incorporated into a hybrid sequence involving other separation operations. One such an example is the separation of the close-boiling system of benzene (normal boiling point 80.13°C) and cyclohexane (normal boiling point 80.64°C) which forms a minimum-boiling azeotrope at 1 atm and 77.4°C with a composition of 54.2 mol% benzene. Acetone can be used as entrainer for the azeotropic distillation section of this hybrid process.

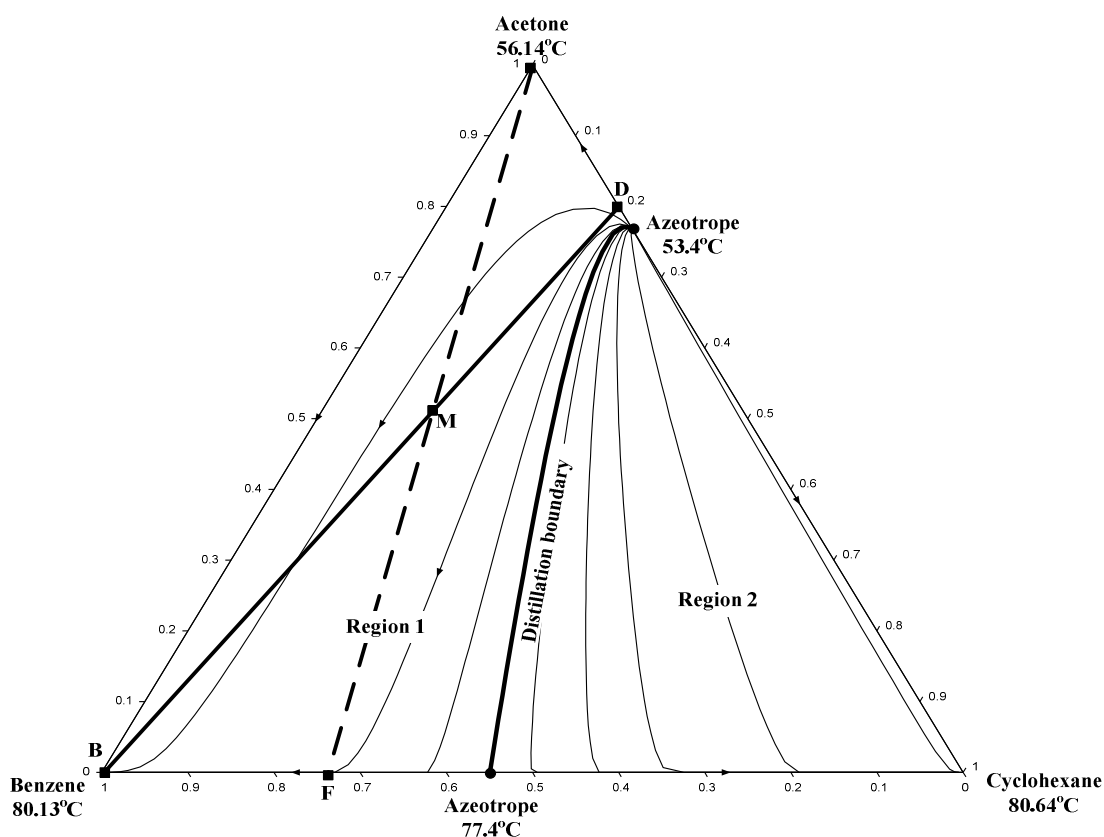


Figure 2-14: Residue curve map of the benzene-acetone-cyclohexane system. Simulated in Aspen with NRTL.

The separation sequence (Figure 2-15) involves three operations:

1. Homogeneous azeotropic distillation of the benzene-cyclohexane mixture using acetone as an entrainer. This operation produces nearly pure benzene (B) as bottom product and a distillate close in composition to the binary azeotrope of cyclohexane and acetone (D).
2. Liquid-liquid extraction of the distillate with water as separating agent. This operation produces a raffinate of nearly pure cyclohexane and an extract of acetone and water.
3. Ordinary distillation of the extract, producing a distillate of acetone and bottoms of water. The acetone can be recycled to the first operation and the water to the second.

Figure 2-14 shows the residue-curve map of the benzene/cyclohexane/acetone system at 1 atm. This diagram can be used to illustrate the distillation path in the first operation of the abovementioned hybrid separation sequence. The residue curves and azeotropes were calculated in Aspen using the NRTL thermodynamic model. A minimum-boiling azeotrope is formed between acetone and cyclohexane at 53.4°C and 1 atm with an acetone composition of 74.6 mol%. A distillation boundary connects the two azeotropes in the system and consequently divides the diagram into two distillation regions. The composition of a mixture of the fresh feed (F) and pure acetone entrainer (A) must lie somewhere in region 1, on the straight line connecting F and A. To obtain the acetone/cyclohexane azeotrope and pure benzene as the overhead and bottom products in the distillation of mixture M, these three points must also lie on a straight line. Therefore, a straight line can be drawn from the

azeotrope to pure benzene and the point at which it intersects with the F-A line denotes the composition of mixture M.

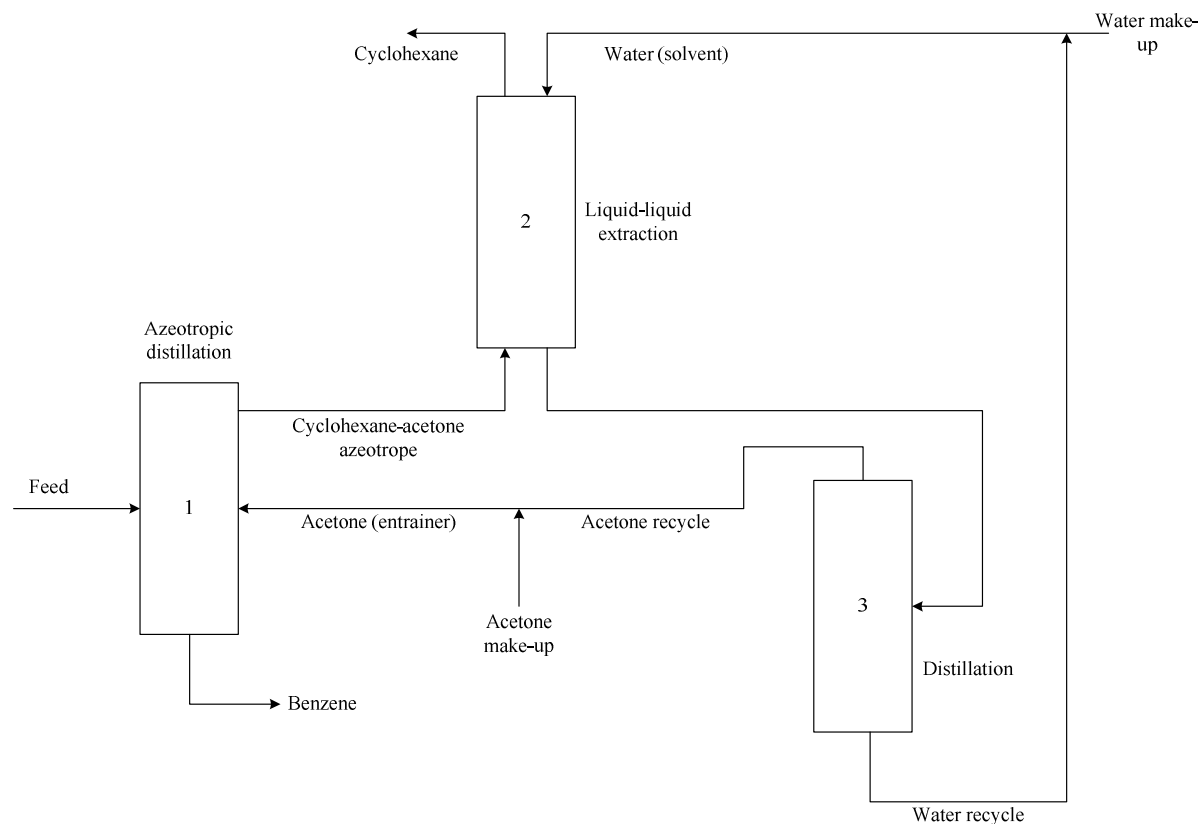


Figure 2-15: Hybrid separation sequence involving homogeneous azeotropic distillation.

2.5.2 Heterogeneous azeotropic distillation

This process refers to the formation of a heterogeneous azeotrope or the use of an existing one, to effect the desired separation. The main difference between the methods used for homogeneous and heterogeneous azeotropic distillation is that a heterogeneous azeotrope can be simply separated with a decanter.

The entrainer may be introduced to the column as a separate feed or it can be mixed with the original feed. It is usually added above the feed stage, if its volatility is below that of the feed. When the entrainer volatility is near that of the feed, it is typically mixed with the feed to form a single stream (Schweitzer 1997). A typical heterogeneous azeotropic separation process, the dehydration of ethanol with benzene as entrainer, is illustrated on a ternary phase diagram in Figure 2-16.

As in Figure 2-14, the thicker lines in Figure 2-16 also represent distillation boundaries. Liquid-liquid solubility is represented by a dashed, curved line (binodal curve). On the distillation boundary that separates distillation regions 2 and 3; thick dashes are superimposed to show the vapour composition in equilibrium with the two liquid phases.

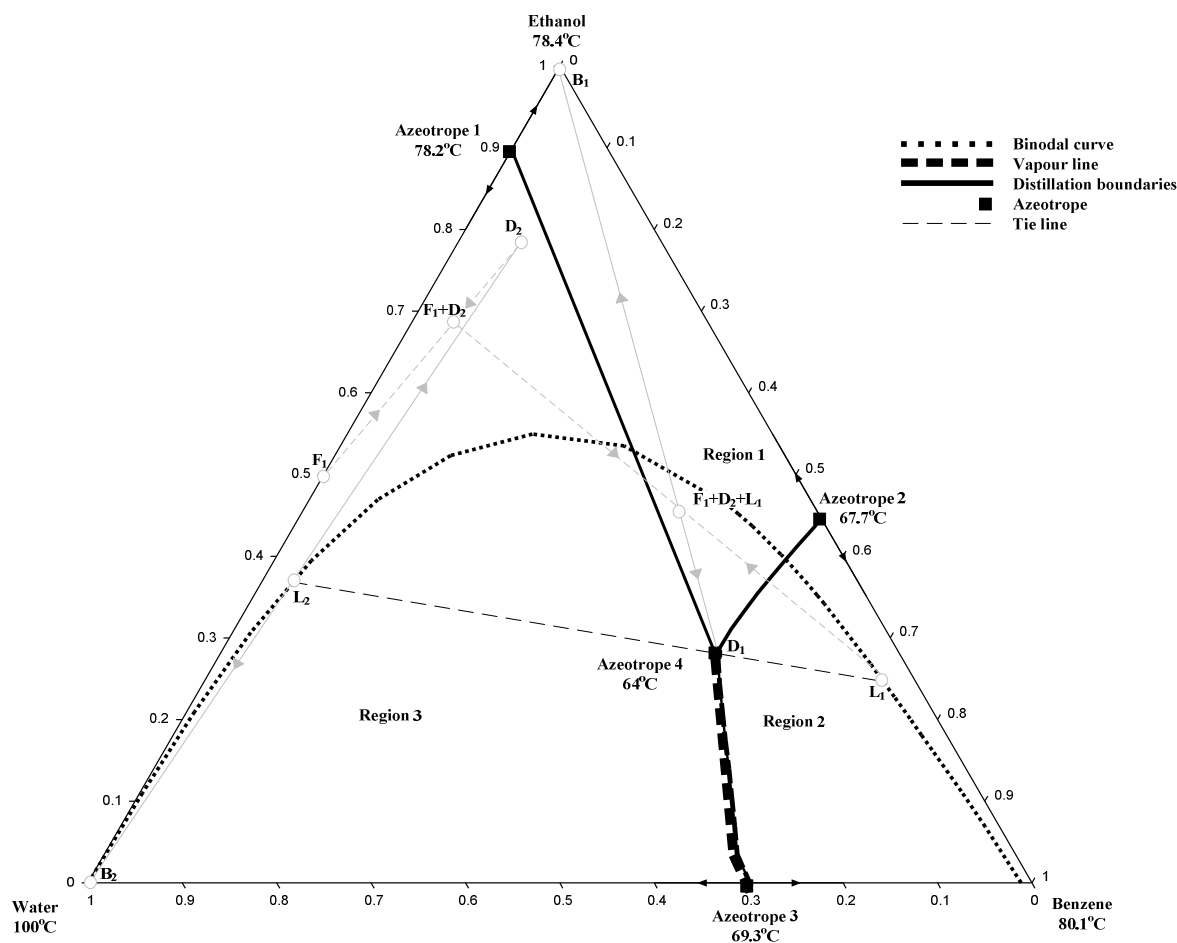


Figure 2-16: Ternary phase diagram with liquid-liquid equilibrium phase envelope, vapour line and distillation boundaries of the ethanol-water-benzene system. Simulated in Aspen with NRTL.

Consider the dehydration of ethanol via heterogeneous azeotropic distillation with benzene as entrainer as illustration of this entrainer-addition method. The thermodynamic model NRTL, in Aspen, was used to calculate the residue curves and azeotropes in Figure 2-16. The normal boiling points of ethanol, water and benzene are 78.4, 100 and 80.1 °C respectively. Ethanol and water forms a homogeneous minimum-boiling azeotrope at 78.2 °C and 10.5 mole % water. Ethanol and benzene also forms a homogeneous minimum-boiling azeotrope, but at 67.7 °C and 44.5 mole % ethanol. A heterogeneous minimum-boiling azeotrope is predicted to form between water and benzene at 69.4°C and 29.9 mole % water. A ternary heterogeneous minimum-boiling azeotrope is predicted to occur at 64°C and 19.1 mole % water, 28.2 mole % ethanol and 52.7 mole % benzene. This azeotrope enables the crossing of a distillation boundary. The overall composition of the two liquid phases is the same as that of the vapour phase. The thin dashed line (equilibrium tie-line) through azeotrope 4 in Figure 2-6, indicates the corresponding composition of each liquid phase on the phase envelope. The water-rich phase has a composition of 43.9 mole % ethanol, 6.3 mole % benzene and 49.8 mole % water. The benzene-rich phase has a composition of 18.4 mole % ethanol, 79.0 mole % benzene and 2.6 mole % water. This property allows for separation beyond the azeotropic point via decantation.

A typical separation sequence (Figure 2-17) can consist of two distillation columns (an azeotropic column and a recovery column) and a decanter. The first column is fed with an aqueous ethanol stream, organic reflux from

the decanter as well as the distillate of the recovery column. This column produces nearly pure ethanol as bottoms and a distillate close to the composition of azeotrope 4. The azeotropic distillate is subsequently separated into a water-rich and benzene-rich phase in the decanter. The benzene-rich phase is recycled to the first column and the water-rich phase is fed to the second column. Nearly pure water is produced as bottoms in this column and a distillate of ethanol, benzene and water. The distillate from the second column, supplemented with an entrainer make-up stream, is fed to the first column. Material balance lines of this separation sequence are also shown in grey in Figure 2-16.

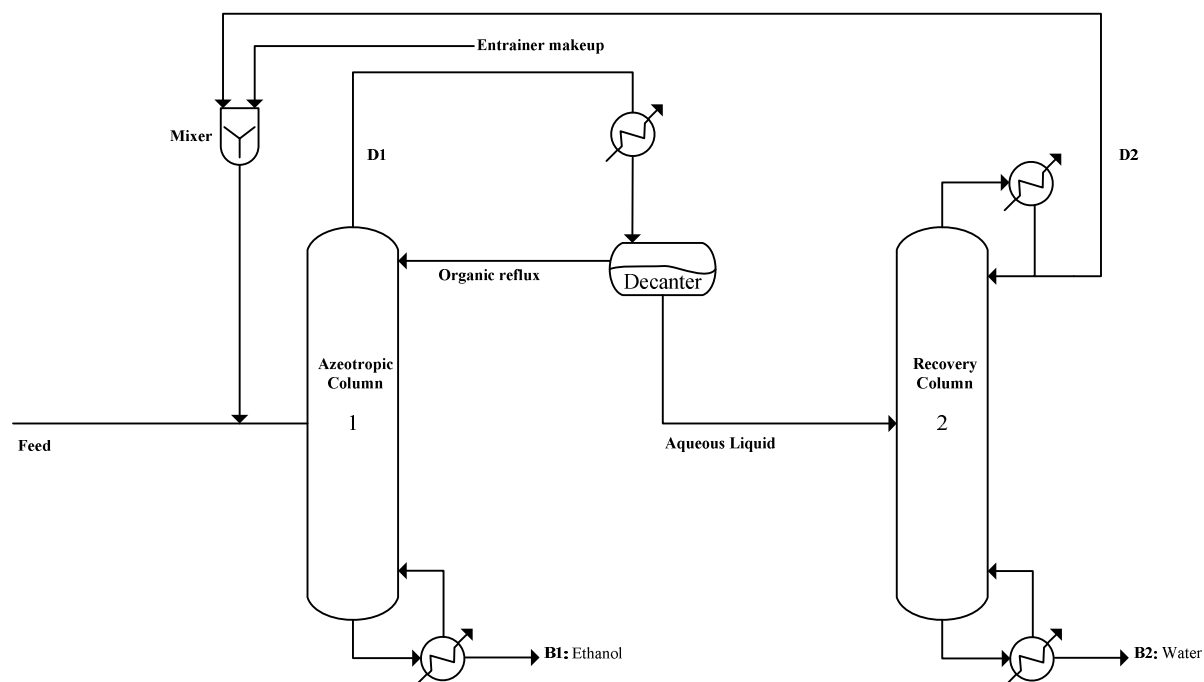


Figure 2-17: Typical separation sequence for heterogeneous azeotropic distillation of ethanol/benzene/water.

According to Seader and Henley (2006).

To construct diagrams such as Figure 2-16, full knowledge of the VLE data under isobaric conditions is required. This entails the determination of the boiling point temperature, the composition of both liquid phases and of the equilibrium vapour phase of numerous samples in the region at which the liquid mixtures are heterogeneous at their corresponding bubble-point temperatures (Julka, Chiplunkar & O'Young 2009, Gomis, Pequenín & Asensi 2010).

More information on heterogeneous azeotropic distillation in general can be found in the works of Pham and Doherty (1990a, 1990b, 1990c) and Widagdo and Seider (1992, 1996). The number of possible entrainers for heterogeneous azeotropic distillation is somewhat restricted, but heterogeneous azeotropic distillation is usually preferred compared to extractive distillation. When the original mixture consists of hydrophilic components and hydrophobic organic components (eg. water and ethanol), it is generally possible to find a heterogeneous azeotropic entrainer. When the mixture consists of only hydrophilic or hydrophobic components (eg. benzene and cyclohexane), it is much harder to find an entrainer (Hilmen 2000).

2.5.3 Extractive distillation

The name, extractive distillation, was coined by Dunn et al. (1945) in reference to the commercial separation of toluene from a paraffin-hydrocarbon mixture, using phenol as solvent. The basic principle of extractive distillation is that the entrainer interacts differently with each component in the original mixture and therefore alters their relative volatility. These interactions predominantly occur in the liquid phase and causes separation to become feasible and economical. The solvent should not form an azeotrope with any of the components in the feed. If a minimum-boiling azeotrope is fed to the column, the solvent (with a lower volatility than the key components of the feed mixture) is added to the tray above the feed stage and a few trays below the top of the column. This ensures that the solvent is present in the down-flowing liquid phase to the bottom of the column and minimal solvent is stripped and lost to the vapour overhead. If a maximum-boiling azeotrope is fed to the column, the solvent enters the column with the original mixture. Usually, a molar solvent-to-feed ratio of 1 is required to achieve the desirable separation. The bottoms from the extractive distillation column are treated to recover the solvent and recycle it to the feed (Seader, Henley 2006).

As illustration of this method, consider the acetone-methanol system. At 1 atm, acetone and methanol form a minimum-boiling azeotrope at a temperature of 55.7°C and composition of 77.75 mole % acetone. The NRTL thermodynamic model was used to predict the vapour-liquid equilibrium data for this system at 1 atm.

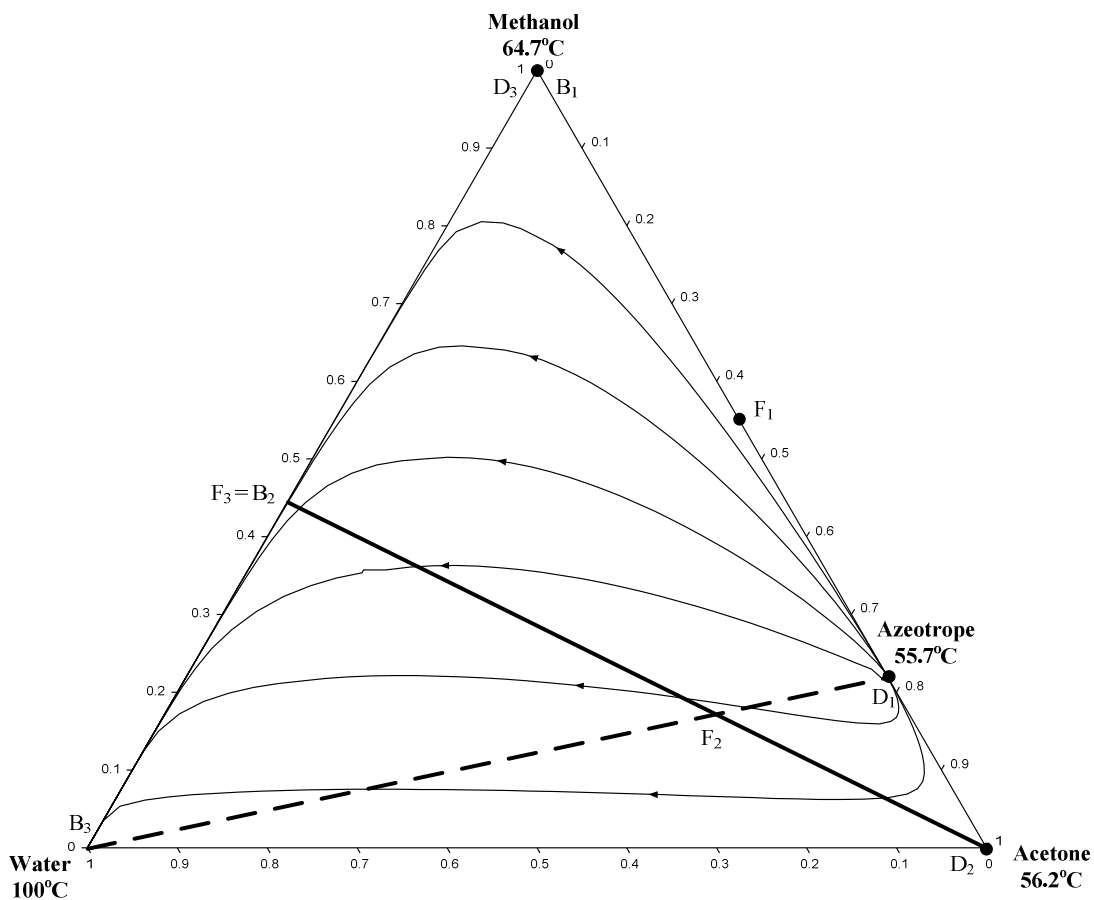


Figure 2-18: Residue curve map of the water-acetone-methanol system. The residue curves were calculated in Aspen using the NRTL thermodynamic model.

The model predicts a binary azeotrope at 55.2°C with 77.8 mole % acetone. When attempting to separate (Figure 2-19) a mixture (F_1) of acetone and methanol, only one component can be obtained in the pure form (B_1). The other product obtained would be the azeotrope (D_1). Water is a good candidate as solvent for extractive distillation for this system, because at 1 atm it does not form a binary or ternary azeotrope with acetone and/or methanol. It also has a boiling temperature of 100 °C, significantly higher than acetone and methanol. The subsequent residue curve map (Figure 2-18) was computed with Aspen Plus, also using the NRTL model. The arrows on the residue curves are directed away from the acetone-methanol azeotrope, towards pure water. No distillation boundaries exist within the system at these conditions. The presence of a substantial amount of water increases the liquid-phase activity coefficient of acetone and decreases that of methanol. Therefore, over the entire range of acetone and methanol, the relative volatility of acetone is increased. This allows the mixture to be separated by extractive distillation, resulting in a distillate of acetone (D_2) and bottoms of methanol and water (B_2). This mixture (B_2/F_3) can subsequently be separated by ordinary distillation into pure methanol and water (D_3 and B_3 respectively), since no azeotrope exists between these two components.

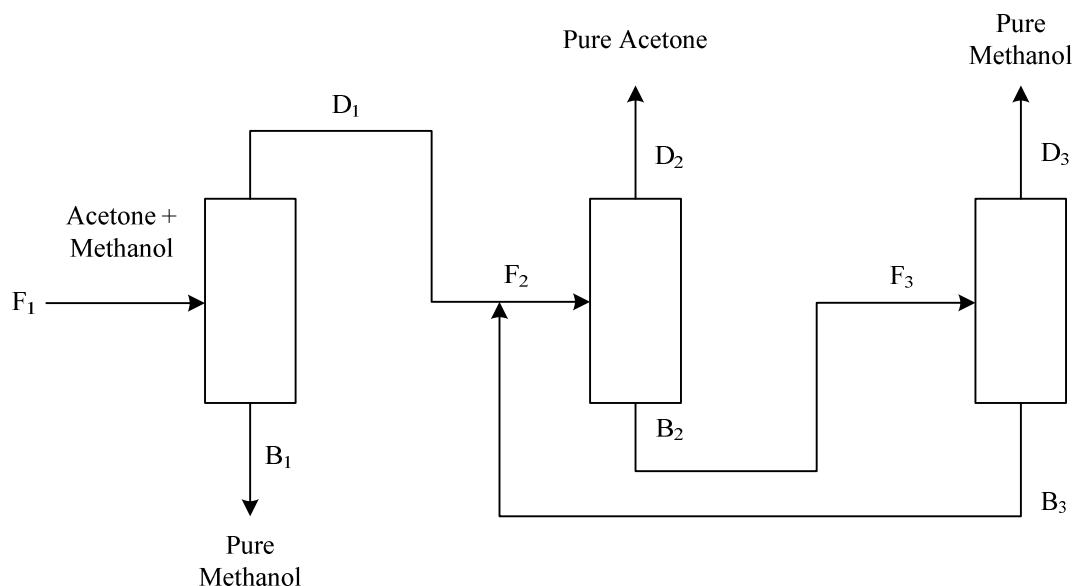


Figure 2-19: Typical separation sequence for extractive distillation. According to Seader and Henley (2006).

2.5.4 Entrainer selection

A variety of studies have been performed on entrainer selection for heterogeneous azeotropic distillation and valuable insight on this topic can be gained from literature. The task of entrainer selection should be based on a physical (knowledge of the intermolecular forces and VL(L)E diagram structure) and thermodynamic understanding of the component system in question. Entrainer effectiveness is evaluated based on its ability to alter the relative volatility of the original mixture.

Ewell et al. (1944) studied the relationship between azeotrope formation and hydrogen bonding. They determined that entrainers can be classified into 5 groups based on their hydrogen-bonding tendencies. From this a strategy was developed to identify chemical classes suitable as entrainers for heterogeneous azeotropic and extractive distillation. Berg (1969) discussed these guidelines and further developed a classification of

organic and inorganic mixtures. He used information on the molecular structure to identify promising entrainers for extractive and heterogeneous azeotropic distillation. According to Berg (1969), feasible entrainers for extractive distillation have high hydrogen-bonding tendencies (eg. water, amino alcohols, amides, phenol alcohols and organic acids).

Van Winkle (1967) calls attention to the fact that the whole process system must be considered in the selection of a feasible entrainer and that the recovery of the entrainer must be included in the evaluation. A candidate entrainer might have a high selectivity, but its recovery in the second column may be difficult. Consequently, the final selection must include an economic evaluation as well.

Brignole et al. (1986) developed and tested a strategy for computer-aided molecular design of entrainers. This strategy can be used to comment on the feasibility of an entrainer and analyze the effect of solvent mixtures as entrainers. Pham and Doherty (1990a) presented general principles for distinguishing between feasible and infeasible entrainers for the synthesis of continuous heterogeneous azeotropic distillation. If the resulting residue curve map provides a feasible column sequence, the entrainer is considered feasible. Furzer (1994) screened for entrainers using a UNIFAC group contribution method. Simple rules were developed to use in a knowledge database to limit the amount of molecules that could be used as entrainers. Rodriguez-Donis et al. (2001) developed entrainer selection rules specifically for batch columns, since heterogeneous azeotropic batch distillation is more flexible than its continuous counterpart and therefore more possible cases had to be included. They adopted Matsuyama and Nishimura's (1977) 113 classes of classification, which Foucher et al. (1991) later extended to 125. The complete set of rules for feasible entrainers was tabulated in their paper. Modla et al. (2003) also published results for heterogeneous azeotropic distillation in a batch rectifier and heterogeneous azeotropic distillation. The authors investigated the separation of a close-boiling mixture by using a heavy entrainer. Moussa and Jiménez (2006) presented a state task network to determine the separation sequence of heterogeneous azeotropic distillations. They used the residue curve maps reported by Kiva et al. (2003) for their investigation. In 2009 Julka et al. also presented a systematic methodology to identify and evaluate entrainers via residue curve map technology.

Typical entrainers for the dehydration of aqueous C_2 and C_3 alcohols through azeotropic distillation are discussed in Chapter 5.

2.6 SUMMARY

The separation of azeotropic mixtures is a topic of great practical and industrial interest. It is impossible to separate azeotropes, which are not pressure sensitive, with ordinary distillation. Separation of these components may however be achieved via membrane-distillation hybrids or entrainer-addition distillation methods. The use of membrane-distillation hybrids is limited due to its low maximal capacity and is therefore eliminated for this work.

Ternary VL(L)E diagrams are useful tools to efficiently predict feasible separation sequences for such distillation methods. One can distinguish between three different entrainer-addition methods depending on the entrainers properties and column sequence:

- *Homogeneous azeotropic distillation* is the ordinary distillation of homogeneous azeotropic mixtures with an entrainer. Separation can be achieved only for a limited number of VLE diagram structures. These separation schemes may be very complex, energy intensive or have multiplicities.
- *Heterogeneous azeotropic distillation* involves the use of decanter-distillation hybrids to separate heterogeneous azeotropic mixtures. Separation can be achieved for several VLLE diagram structures involving one or more heterogeneous azeotrope. The separation schemes are rather simple, but the range of feasible entrainers may be limited.
- *Extractive distillation* uses an entrainer which does not form another azeotrope with the original mixture, but rather alters the relative volatilities of its components. A wider range of feasible entrainers are available, but the process may be more energy intensive than heterogeneous azeotropic distillation.

Consequently this work focusses on heterogeneous azeotropic distillation as a method for the separation of selected alcohol/water azeotropes. Specific attention is given to the evaluation of possible entrainers (benzene, cyclohexane, hexane, heptane, isooctane, DIPE and DNPE) for alcohol/water azeotropic mixtures.

3 THERMODYNAMIC BASIS

Graphical representation of VL(L)E data and the use of this data in simulation software packages are vital to the prediction of a feasible operating space in which any real distillation process can take place. Experimental data are not always readily available and therefore it is of utmost importance to follow sound thermodynamic principles to predict VL(L)E data. The following section gives an account of the thermodynamic basis of both vapour-liquid and vapour-liquid-liquid equilibrium. In order to gain an understanding of the thermodynamic basis, the texts of Prausnitz (1999), Sandler (1999) and Smith and van Ness (2005) were studied and used throughout this chapter. The criteria for equilibrium are stipulated and the Gibbs-Duhem Equation, chemical potential, fugacity, fugacity coefficient, activity and activity coefficient are defined. The thermodynamic models applicable to VLE and VLLE data (in this work) are discussed. The selected models are all activity coefficient models i.e. NRTL, UNIQUAC and UNIFAC. Equations of state were also considered, but it is said that highly non-ideal liquid mixtures such as VLLE is best predicted by activity coefficient models (Aspen Technology 2009). Guidelines in Aspen suggest NRTL, UNIQUAC and UNIFAC for polar, non-electrolyte solutions at moderate pressures ($P < 10$ bar). Literature also indicates that NRTL, UNIQUAC and UNIFAC are generally used to predict alcohol/entrainer/water VLLE systems (Gomis et al. 2007, Lladosa et al. 2008, Lee, Shen 2003, Font et al. 2003, Gomis, Font & Saquete 2006, Gomis et al. 2005). The chapter concludes with a discussion of thermodynamic consistency testing methods. The interested reader is referred to the texts of Raal and Muhlbauer (1998), Walas (1985), Smith et al. (2001), Malanowski and Anderko (1992) and Prausnitz et al. (1986) for further reading.

3.1 CRITERION FOR PHASE EQUILIBRIUM IN A HETEROGENEOUS CLOSED SYSTEM

A heterogeneous, closed system consists of two or more phases with each phase considered as an open system within the overall closed system. The conditions under which this system is in a state of internal equilibrium regarding the three processes of heat transfer, boundary displacement and mass transfer are considered here. In terms of extensive thermodynamic potential, the following four criteria exist for equilibrium in a closed system (Prausnitz, Lichtenthaler & de Azevedo 1999):

$$dU_{S,V} = 0 \quad 3-1$$

$$dH_{S,P} = 0 \quad 3-2$$

$$dA_{T,V} = 0 \quad 3-3$$

$$dG_{T,P} = 0 \quad 3-4$$

Where U, H, A and G are internal energy, enthalpy, Helmholtz free energy and Gibbs free energy respectively. These variables cannot be measured directly and it is therefore more useful to define equilibrium in terms of intensive quantities T, P, and μ_i (temperature, pressure and chemical potential respectively). To attain thermal and mechanical equilibrium, the temperature and pressure must be uniform throughout the entire heterogeneous system. With μ_i as the intensive chemical potential governing mass transfer, it is also expected to have a uniform value throughout the system at equilibrium.

For a heterogeneous system consisting of π phases and m components, the following must be true at equilibrium:

$$T^{(1)} = T^{(2)} = \dots = T^{(\pi)} \quad 3-5$$

$$P^{(1)} = P^{(2)} = \dots = P^{(\pi)} \quad 3-6$$

$$\mu_1^{(1)} = \mu_1^{(2)} = \dots = \mu_1^{(\pi)} \quad 3-7$$

$$\mu_2^{(1)} = \mu_2^{(2)} = \dots = \mu_2^{(\pi)} \quad 3-8$$

$$\vdots \quad \quad \quad \vdots$$

$$\mu_m^{(1)} = \mu_m^{(2)} = \dots = \mu_m^{(\pi)} \quad 3-9$$

The superscript denotes the phase and the subscript denotes the component.

3.2 THE GIBBS-DUHEM EQUATION

The intensive state of each phase in a heterogeneous system at internal equilibrium can be characterized by its temperature and pressure, and the chemical potential for each component. These variables are however not all independently variable. The Gibbs-Duhem Equation illustrates how these variables are related and is a fundamental equation in the thermodynamics of solutions (Prausnitz, Lichtenthaler & de Azevedo 1999).

$$dG = \sum_i n_i d\mu_i = VdP - SdT \quad 3-10$$

where S , V and n are entropy, volume and number of moles respectively. The subscript i denotes the components in the system.

3.3 THE CHEMICAL POTENTIAL

The function of phase-equilibrium thermodynamics is to quantitatively describe the distribution of each component in a system, among all the phases present, at equilibrium. The chemical potential of a component in a particular phase in a certain system is used as a tool to evaluate phase equilibrium (Prausnitz, Lichtenthaler & de Azevedo 1999).

$$\mu_i \equiv \left(\frac{\partial G}{\partial n_i} \right)_{T,P,n_{j \neq i}} \quad 3-11$$

Chemical potential is an abstract concept and must be related to physically measurable quantities such as temperature, pressure and composition in order to be used.

$$d\mu_i = v_i dP - s_i dT \quad 3-12$$

where s_i is the molar entropy and v_i the molar volume.

One cannot compute an absolute value for chemical potential. Only a change in chemical potential due to any arbitrary change in the independent variables temperature, pressure and composition, can be calculated. Integrating Equation 3-12 and solving for μ_i at a certain temperature T and pressure P , gives:

$$\mu_i(T, P) = \mu_i(T^r, P^r) - \int_{T^r}^T s_i dT + \int_{P^r}^P v_i dP \quad 3-13$$

where subscript r refers to an arbitrary reference state.

In Equation 3-13 the two integrals on the right side can be determined from thermal and volumetric data over the temperature range of $T-T^r$ and the pressure range $P-P^r$. The chemical potential $\mu_i(T^r, P^r)$ is however unknown. Therefore, $\mu_i(T, P)$ can only be expressed relative to $\mu_i(T^r, P^r)$.

3.4 FUGACITY AND FUGACITY COEFFICIENT

Fugacity, f , is an auxiliary concept used to express an equivalent for chemical potential in the physical world. For an ideal gas, the change in chemical potential, under isothermal conditions from P^0 to P , is given by (Prausnitz, Lichtenthaler & de Azevedo 1999):

$$\mu_i - \mu_i^0 = RT \ln \frac{P}{P^0} \quad 3-14$$

Equation 3-14 is of value since it relates an abstract mathematical concept to a common, intensive property in the natural world. This equation is however only valid for pure, ideal gases. It can be generalized for an isothermal change for any component in any system (solid, liquid, or gas, pure or mixed, ideal or not) by defining a function f , called *fugacity*:

$$\mu_i - \mu_i^0 = RT \ln \frac{f_i}{f_i^0} \quad 3-15$$

The superscript 0, denotes the standard or reference state. Although μ_i^0 and f_i^0 are arbitrary, both may not be chosen independently. When one is chosen, the other is fixed.

For a pure, ideal gas, the fugacity is equal to the pressure. For component i in a mixture of ideal gases, the fugacity is equal to its partial pressure $y_i P$. Since all systems (pure or mixed) approach ideal-gas behaviour at very low pressures, the definition of fugacity is completed by the limit:

$$\frac{f_i}{y_i P} \rightarrow 1 \quad \text{as } P \rightarrow 0 \quad 3-16$$

where y_i is the mole fraction of i . The dimensionless ratio $f_i/y_i P$ is called the fugacity coefficient, designated by symbol ϕ_i . Therefore, for a mixture of ideal gases, $\phi_i = 1$. For a liquid phase the fugacity coefficient would be $f_i/x_i P$.

Since Equation 3-15 was formulated for an isothermal change, the temperature of the standard state must be the same as that of the state of interest. The pressure and compositions of the two states may, however, be different and usually are. Fugacity provides a convenient transformation of the fundamental equation of phase equilibrium, Equation 3-9.

From Equations 3-10 and 3-15, for phases α and β , the following needs to be true:

$$f_i^\alpha = f_i^\beta \quad 3-17$$

Equation 3-17 is very useful, because it conveys that the equilibrium condition in terms of chemical potentials can be replaced by an equation in terms of fugacities, without loss of generality.

3.5 ACTIVITY AND ACTIVITY COEFFICIENT

The activity (a_i) of component i at a temperature, pressure and composition of interest, is defined as the ratio of f_i at these conditions to the fugacity of i at the standard state (f_i^0). It provides a measure of how “active” the substance is relative to its standard state since it indicates the difference between the chemical potential of the substance at the state of interest and its standard state (Prausnitz, Lichtenthaler & de Azevedo 1999).

$$a_i(T, P, x) \equiv \frac{f_i(T, P, x)}{f_i(T, P^0, x^0)} \quad 3-18$$

where P^0 and x^0 are, respectively, an arbitrary but specified pressure and composition. For an ideal mixture the activity equals the mole fraction ($a_i = x_i$).

Departure from this ideal behaviour is accounted for by the activity coefficient (γ_i). It is the ratio of the activity of i to the concentration of i (x_i), usually in mole fraction:

$$\gamma_i \equiv \frac{a_i}{x_i} = \frac{f_i}{x_i f_i^0} \quad 3-19$$

Consequently for an ideal solution the activity coefficient is equal to one. Ideal solution behaviour can also be characterized by the Lewis/Randall rule:

$$f_i^{ideal} = x_i f_i^L \quad 3-20$$

This relation illustrates that the fugacity of component i in an ideal solution is proportional to its mole fraction. As x_i approaches unity, the fugacity of the ideal solution approaches the fugacity of the pure liquid at the solution temperature and pressure.

3.6 EVALUATION OF FUGACITIES

When determining the fugacity of a pure liquid at a pressure above the saturation pressure, the fugacity at saturation has to be considered first. At this point the liquid phase fugacity is equal to the vapour phase fugacity (Prausnitz, Lichtenthaler & de Azevedo 1999):

$$f_i^L = f_i^{sat} = \phi_i^{sat} P_i^{sat} \quad 3-21$$

Increasing the pressure above saturation at constant temperature, yields the following change in fugacity from Equations 3-11 and 3-15:

$$dG_i = V_i dP - S_i dT = RT d \ln f_i \quad 3-22$$

or written as:

$$d \ln f_i = \frac{V_i^L}{RT} dP \quad 3-23$$

Integration from P_i^{sat} to P gives:

$$f_i^L = f_i^{sat} \exp \left[\frac{1}{RT} \int_{P_i^{sat}}^P V_i^L dP \right] \quad 3-24$$

The exponential term in Equation 3-23 is called the *Poynting Correction*. It is small at low pressures, but increases with increasing pressure. The liquid molar volume (V_i^L) in Equation 3-23 is at a temperature well below the critical point and is a weak function of pressure. Therefore its dependence on pressure is negligible and one may directly integrate Equation 3-23. The saturation fugacity of component i (f_i^{sat}) in Equation 3-23 is eliminated in Equation 3-24 by incorporating the fugacity coefficient (φ_i^{sat}).

$$f_i^L = \varphi_i^{sat} P_i^{sat} \exp \left[\frac{V_i^L (P - P_i^{sat})}{RT} \right] \quad 3-25$$

According to Equation 3-17 the equilibrium requirement between a liquid (L) and a vapour (V), at the same temperature and pressure is:

$$f_i^L = f_i^V \quad 3-26$$

By incorporating the definition of the fugacity coefficient and the definition of the activity coefficient, Equation 3-26 transforms to:

$$y_i \varphi_i P = x_i \gamma_i f_i^L \quad 3-27$$

f_i^0 in the definition of the activity coefficient has been replaced by f_i^L following the convention used in the Lewis/Randall relation. This technique whereby the fugacity and activity coefficients are respectively used to describe non-idealities in the vapour and liquid phases is called the *combined method of VLE*.

Substituting f_i^L in Equation 3-27 with Equation 3-25 yields:

$$y_i \Phi_i P = x_i \gamma_i P_i^{sat} \quad 3-28$$

where,

$$\Phi_i = \frac{\varphi_i}{\varphi_i^{sat}} \exp \left[- \frac{V_i^L (P - P_i^{sat})}{RT} \right] \quad 3-29$$

Equation 3-27 is the fundamental relationship relating liquid and vapour phase in equilibrium.

3.7 NRTL (NON-RANDOM TWO LIQUID) EQUATION

The NRTL Equation, developed by Renon and Prausnitz (1968), represents an extension of the Wilson Equation. The NRTL Equation is valid for multi-component VLE, LLE and VLLE. For multi-component VLE only binary pair-constants from the corresponding binary-pair experimental data are required. The NRTL Equation for a multi-component mixture is as follows:

$$\frac{g^E}{RT} = \sum_i x_i \frac{\sum_j x_j \tau_{ji} G_{ji}}{\sum_k x_k G_{ki}} \quad 3-30$$

Where:

$$G_{ij} = \exp(-\alpha_{ji} \tau_{ji}) \quad 3-31$$

$$\tau_{ij} = a_{ij} + \frac{b_{ij}}{T} + e_{ij} \ln T + f_{ij} T \quad 3-32$$

The parameter α_{ji} characterizes the tendency of species j and species i to be distributed in a nonrandom manner.

Generally α_{ji} is independent of temperature and depends on molecular properties.

$$\alpha_{ij} = c_{ij} + d_{ij} T \quad 3-33$$

G_{ii} is equal to 1 and τ_{ii} to 0. a_{ij} , b_{ij} , e_{ij} and f_{ij} are unsymmetrical. Therefore a_{ij} may for example not be equal to a_{ji} .

Equation 3-1 combined with the equation of activity coefficients from Gibbs free energy, yields Equation 3-38. Therefore the activity coefficient for any component i is given by:

$$\ln \gamma_i = \frac{\sum_j x_j \tau_{ji} G_{ji}}{\sum_k x_k G_{ki}} + \sum_j \frac{x_j G_{ji}}{\sum_k x_k G_{kj}} \left(\tau_{ij} - \frac{\sum_m x_m \tau_{mj} G_{mj}}{\sum_k x_k G_{kj}} \right) \quad 3-34$$

3.8 UNIQUAC (UNIVERSAL QUASI CHEMICAL THEORY) EQUATION

In attempt to base the calculations of liquid-phase activity coefficients on simple, but more theoretical grounds, Abrams and Prausnitz (1975) used statistical mechanics to derive an expression for excess free energy. Their model, the UNIQUAC Equation, generalizes a previous analysis by Guggenheim and extends it to mixtures of molecules that differ significantly in shape and size. Similar to Wilson and NRTL, UNIQUAC also uses local concentrations. UNIQUAC however uses the local area fraction θ_{ij} as the primary concentration variable, rather than local volume fractions or local mole fractions. The local area fraction is determined by representing a molecule by a set of bonded segments. Each molecule is characterized by two structural parameters. These parameters are the relative number of segments per molecule, r (volume parameter), and the relative surface area of the molecule, q (surface parameter).

Excess free energy for a multi-component mixture, according to the UNIQUAC model is:

$$\frac{g^E}{RT} = \left(\frac{g^E}{RT}\right)_{\text{combinatorial}} + \left(\frac{g^E}{RT}\right)_{\text{residual}} \quad 3-35$$

$$\left(\frac{g^E}{RT}\right)_{\text{combinatorial}} = \sum_i x_i \ln \frac{\Phi_i}{x_i} + \frac{z}{2} \sum_i q_i x_i \ln \frac{\theta_i}{\Phi_i} \quad 3-36$$

$$\left(\frac{g^E}{RT}\right)_{\text{residual}} = - \sum_i q'_i x_i \ln [\sum_j \theta'_j \tau_{ji}] \quad 3-37$$

The combinatorial term accounts for effects due to differences in molecule size and shape. The residual term accounts for effects due to differences in intermolecular forces, where segment fraction Φ_i and area fractions θ_i and θ'_i are given by

$$\Phi_i = \frac{x_i r_i}{\sum_j x_j r_j} \quad 3-38$$

$$\theta_i = \frac{x_i q_i}{\sum_j x_j q_j} \quad 3-39$$

$$\theta'_i = \frac{x_i q'_i}{\sum_j x_j q'_j} \quad 3-40$$

and

$$\tau_{ij} = \exp \left[a_{ij} + \frac{b_{ij}}{T} + c_{ij} \ln T + d_{ij} T + e_{ij} T^2 \right] \quad 3-41$$

Binary parameters a_{ij} , b_{ij} , c_{ij} , d_{ij} , e_{ij} and f_{ij} are the only adjustable parameters.

Equation 4-6 combined with the equation of activity coefficients from Gibbs free energy, yields the following:

$$\ln \gamma_i = \ln \frac{\Phi_i}{x_i} + \frac{z}{2} q_i \ln \frac{\theta_i}{\Phi_i} + l_i - \frac{\Phi_i}{x_i} \sum_j x_j l_j - q'_i \ln (\sum_j \theta'_j \tau_{ji}) + q'_i - q'_i \sum_j \frac{\theta'_j \tau_{ij}}{\sum_k \theta'_k \tau_{kj}} \quad 3-42$$

where,

$$l_i = \frac{z}{2} (r_i - q_i) - (r_i - 1) \quad 3-43$$

where Z is the lattice coordination number and is set to 10 (Prausnitz, Lichtenthaler & de Azevedo 1999).

3.9 UNIFAC (UNIVERSAL FUNCTIONAL ACTIVITY COEFFICIENT) EQUATION

Liquid-phase activity coefficients have to be estimated for non-ideal mixtures, even when experimental phase equilibrium data is not available and when the assumption of regular solutions is not valid due to the presence of polar compounds. Wilson and Deal (1962) presented methods for treating a solution as a combination of functional groups rather than molecules, for such predictions. To estimate the partial molar excess free energies and subsequently the activity coefficients, the size parameters for each functional group as well as the binary

interaction parameters for each pair of functional groups are required. Size parameters can be calculated from theory while the interaction parameters need to be back-calculated from existing phase equilibrium data. These parameters are then used to predict phase equilibrium properties of mixtures for which no experimental data are available. The UNIFAC group-contribution method has several advantages over other group-contribution methods:

- It is theoretically based on the UNIQUAC method.
- The parameters are in essence independent of temperature.
- The size and interaction parameters are available for a wide range of functional groups.
- Predictions can be made for temperatures ranging between 275 and 425 K and for pressures up to a few atmospheres.
- Widespread comparisons with experimental data are available.

For the UNIFAC Equation, based on the UNIQUAC Equation, the volume and surface parameters in the combinatorial terms are replaced by:

$$r_i = \sum_k v_k^{(i)} R_k \quad 3-44$$

$$q_i = \sum_k v_k^{(i)} Q_k \quad 3-45$$

Where $v_k^{(i)}$ is the number of functional groups of type k in molecule i , and R_k and Q_k are the volume and area parameters, respectively, for the type- k functional group.

The residual term is replaced by Equation 3-46:

$$\ln \gamma_i(\text{residual}) = \sum_k v_k^{(i)} [\ln \Gamma_k - \ln \Gamma_k^{(i)}] \quad 3-46$$

Where Γ_k is the residual activity coefficient in the actual mixture and $\Gamma_k^{(i)}$ is the same quantity, but in a reference mixture that contains only molecules of type i .

$$\ln \Gamma_k = Q_k \left[1 - \ln(\sum_m \Theta_m \Psi_{mk}) - \sum_m \frac{\Theta_m \Psi_{km}}{\Theta_n \Psi_{nm}} \right] \quad 3-47$$

Where Θ_m is the area fraction of group m , given by:

$$\Theta_m = \left(\begin{array}{c} \text{surface area} \\ \text{fraction of} \\ \text{group m} \end{array} \right) = \frac{X_m Q_m}{\sum_n X_n Q_n} \quad 3-48$$

X_m = mole fraction of group m in mixture

And Ψ_{mn} is a group interaction parameter given by:

$$\Psi_{mn} = \exp \left[\frac{-(u_{mn} - u_{nn})}{kT} \right] = \exp \left[\frac{-a_{mn}}{T} \right] \quad 3-49$$

where u_{mn} is a measure of interaction energy between groups m and n, and a_{mn} is an adjustable group binary interaction parameter.

3.10 THERMODYNAMIC CONSISTENCY TESTING

Consistency tests are methods through which VLE data are analyzed and assessed. Wisniak et al. (1997) defined their significance as follows:

If the data satisfy the criteria of well-formulated consistency tests, then they are considered appropriate for design and modeling purposes and their reproducibility and matching with any thermodynamical relation is assumed.

It is therefore vital to critically analyze experimental phase equilibrium data. Numerous consistency tests (Wisniak, Apelblat & Segura 1997) exist (Wisniak, Apelblat & Segura 1997), but only those pertinent to this work are discussed below. Literature also indicates that these tests have generally been used to evaluate phase equilibrium data measured for alcohol/entrainer/water systems (Font et al. 2004, Lladosa et al. 2008, Font et al. 2003, Font et al. 2003, Gomis et al. 2007).

3.10.1 VLE Consistency Testing

One of the most basic thermodynamic consistency tests is the Area test, also referred to as the Herington test (Herington, 1951). The Herington test indicates compliance with Gibbs-Duhem relation (Equation 3-10) over the entire composition range. It is a simple method for testing binary VLE data for thermodynamic consistency.

Over composition x_1 , at constant pressure:

$$A^* = 100 \left(\int_0^1 \ln \frac{\gamma_1}{\gamma_2} dx + \int_0^1 \varepsilon dx \right) \quad 3-50$$

Where

$$\varepsilon = - \left(\frac{H^E}{RT^2} \right) \left(\frac{\partial T}{\partial x_1} \right)_p \quad 3-51$$

For the data to pass the Herington test, $|A^*| < 3$. However, the lack of reliability and availability of excess enthalpy data, H^E , causes these calculations to be difficult for isobaric systems. Therefore Wisniak (1994) proposed the following modification to the Herington test:

$$D = 100 \left| \frac{A-B}{A+B} \right| \quad 3-52$$

$$J = 150 \left| \frac{\Delta T_{max}}{T_{min}} \right| \quad 3-53$$

Where A is the area above the zero line on the plot of $\ln \frac{\gamma_1}{\gamma_2}$ against x , and B is the area below the zero line on this plot. If $D-J < 10$, the data pass the consistency test. This test is used in Aspen Plus for thermodynamic verification of internal data sets and experimental data sets imported into Aspen.

Wisniak and co-workers (Elly, Landa & Wisniak 2003) developed software (PRO-VLE 2.0) for binary and ternary VLE consistency testing. After personal communication with Wisniak, well-known for his work in this field, the software was acquired. The program performs two thermodynamic consistency tests on the VLE data it receives, only one of which is derived from the Gibbs-Duhem relation (Equation 3-10).

L/W consistency test

The L/W test (Wisniak 1993) is not derived from the Gibbs-Duhem relation and therefore a set of data proved consistent by this test, will not necessarily obey the Gibbs-Duhem Equation. The L/W test is beneficial in that no heat and/or volume of mixing information are required for the liquid phase, it is simultaneously a point-to-point and area test, and can be used for systems containing any number of components. It is however advised that the L/W test must be used in addition to a test derived from the Gibbs-Duhem relation, to more accurately qualify the data.

The L/W test consists of Equations 3-54 to 3-61:

$$L = \int_0^1 L_i dx_i \quad 3-54$$

$$W = \int_0^1 W_i dx_i \quad 3-55$$

$$L_i = \frac{\sum T_K^0 x_K \Delta S_K^0}{\Delta S} - T = \frac{G^E}{\Delta S} - \frac{RTW}{\Delta S} = W \quad 3-56$$

$$\Delta S \equiv \sum x_K \Delta S_K^0 \quad 3-57$$

$$\Delta S_K^0 = \frac{RT \ln \left(\frac{P}{P_K^0} \right)}{T_K^0 - T} = \frac{\Delta h_K^0}{T_K^0} \quad 3-58$$

$$G^E = RT \sum x_k \ln \gamma_k \quad 3-59$$

Where T_K^0 , ΔS_K^0 and Δh_K^0 are the boiling temperature, vaporization entropy and heat of vaporization of component k at pressure P , respectively.

$$W \equiv \sum x_k \ln \left(\frac{y_k}{x_k} \right) \quad 3-60$$

$$D \equiv 100 \cdot \frac{|L-W|}{L+W} \quad 3-61$$

For values of D smaller than 3 to 5, the L/W test proves that the VLE data are thermodynamically consistent. When the boiling temperatures of the various components differ significantly, Wisniak et al. (1997) recommend that the variation in heat of vaporization with temperature be taken into account.

McDermott-Ellis consistency test

The McDermott-Ellis consistency test (McDermott, Ellis 1965) is derived from the Gibbs-Duhem relation and is therefore used for a more reliable qualification of data. This test verifies the thermodynamic consistency of every two consecutive experimental points, taken in pairs.

The McDermott-Ellis test is given by Equations 3-62:

$$D = \sum_{i=1}^N (x_{ia} - x_{ib}) (\ln \gamma_{ib} - \ln \gamma_{ia}) \quad 3-62$$

McDermott and Ellis (1965) recommend that a maximum deviation of 0.01 be allowed if the accuracy of the measurement of vapour and liquid fractions is within ± 0.001 . Wisniak and Tamir (1977) propose that the local maximum deviation (D_{max}) due to experimental errors, should not be a constant value and that it should rather be calculated by Equation 3-63.

$$D_{max} = \sum_{i=1}^N (x_{ia} + x_{ib}) \left(\frac{1}{x_{ia}} + \frac{1}{x_{ib}} + \frac{1}{y_{ia}} + \frac{1}{y_{ib}} \right) \Delta x + 2 \sum_{i=1}^N |\ln \gamma_{ib} - \ln \gamma_{ia}| \Delta x + \sum_{i=1}^N (x_{ia} + x_{ib}) \frac{\Delta P}{P} + \sum_{i=1}^N (x_{ia} + x_{ib}) \beta_i \left(\frac{1}{|t_a + \delta_i|^2} + \frac{1}{|t_b + \delta_i|^2} \right) \Delta t \quad 3-63$$

Where Δx , ΔP and Δt are errors in measurement of concentrations, pressure and temperature, respectively. β_i and δ_i are the B_i and C_i Antoine constants of the particular component.

3.10.2 LLE Consistency Testing

As far as could be ascertained no consistency tests derived from the Gibbs-Duhem relation, for the qualification of experimental LLE data exists. Empirical correlations have however been proposed by Hand (1930) and by Othmer and Tobias (1942) for the evaluation of such data. Treybal (1963) considers these correlations as excellent tools for the evaluation of experimental LLE data. In a critical analysis of the Hand and Othmer-Tobias correlations, Carniti et al. (1978) concluded that these correlations are too insensitive to various types of errors to be adequate criticism of experimental data. It was however stated that the Othmer-Tobias correlation is slightly more sensitive than Hand's correlation and can be useful to check whether experimental data follows a steady course. Therefore it can be used to identify tie lines with high random errors.

The Othmer-Tobias correlation is given by Equation 3-64:

$$\log \frac{1-x_{22}}{x_{22}} = k_{OT} \log \frac{1-x_{11}}{x_{11}} + c_{OT} \quad 3-64$$

Where x_{ij} is the weight fraction of component i in the j -rich phase and k_{OT} and c_{OT} are constants. When employed into Equation 3-63, the experimental LLE data has to be tested for linearity by plotting $\log \frac{1-x_{22}}{x_{22}}$ versus $\log \frac{1-x_{11}}{x_{11}}$ and applying a least-squares regression. Carniti et al. (1978) set $r = 0.990$ as the lowest limit for a good linear fit.

3.10.3 VLLE Consistency Testing

No consistency test, explicitly for VLLE, could be found in literature. Personal communication with Prof. Jaime Wisniak (2011) and Prof. Hugo Segura (2010), both knowledgeable in the field of thermodynamic consistency testing, confirmed that they do not know of the existence of such a test. VLE consistency tests have been applied to VLLE, but these are not necessarily valid. Therefore the reliability of the VLLE data measured in this work relies on the thorough verification of the phase equilibrium equipment (Section 8.1) and the mass balances performed on the samples (Section 7.4).

4 METHODS OF LOW-PRESSURE VLE/VLLE MEASUREMENT

Equilibrium data, VLE, LLE and VLLE, are of great importance in the design and simulation of heterogeneous azeotropic distillation. When no equilibrium data are available, it is usually substituted by predictions using activity coefficient models calculated with group contribution methods such as UNIFAC, or by the UNIQUAC or NRTL model with parameters based on the correlation of binary VLE and LLE data (Gomis et al. 2007). The proper simulation of an azeotropic distillation column for the dehydration of alcohol with an entrainer, requires knowledge of the exact size and shape of the heterogeneous region and the gradient of the liquid-liquid tie lines. These features greatly influence the compositions obtained of the two liquids produced in the decanter from the condensed vapour that exit the top of the distillation column and can only be obtained accurately from accurate VLLE data.

There, however, exists an enormous lack of published VLLE data. See Table 4-1 for a list of all the published isobaric VLLE data measured at ambient pressure up to date. Many authors have already pointed out this scarcity of VLLE data, starting with Norman in 1945 up until Pham and Doherty (1990) and Younis et al. in 2007. The main reason why this data is hard to come by is due to the difficulty with which it is measured experimentally using commercially available equipment. Commercially available equipment is only designed to measure VLE data involving homogeneous liquids. For this reason some researchers have attempted to measure VLLE data with VLE equipment while others have modified VLE equipment to measure VLLE data more accurately (see Table 4-1).

Table 4-1: Isobaric VLLE data at 101.3 kPa published to date (updated from Gomis et al. (2010)).

System	Reference	Date	Method	Pressure (kPa)	No. of lines
(Water + ethanol + benzene)	Barbaudy	1927	Distillation	101.3	6
(Water + allylic alcohol + trichloroethylene)	Hands and Norman	1945	Distillation	101.3	6
(Water + allylic alcohol + carbon tetrachloride)	Hands and Norman	1945	Distillation	101.3	6
(Water + acetone + chloroform)	Reinders and De Minjer	1947	Distillation	101.3	22
(Water + acetonitrile + acrylonitrile)	Blackford and York	1965	Distillation	101.3	6
(Water + cyclohexanone oxime + nitrocyclohexane)	Lutugina and Soboleva	1967	Dynamic Othmer	101.3	11
(Water + acetonitrile + acrylonitrile)	Volpicelli	1968	Distillation	101.3	5
(Water + 2-propanol + cyclohexane)	Verhoeve	1968	Distillation	101.3	6
(Water + acetic acid + p-xylene)	Murogova et al.	1971	Dynamic Othmer	Atmospheric	13
(Water + methanol + ethyl acetate)	Van Zandijcke and Verhoeve	1974	Dynamic Othmer	101.3	6
(Water + ethanol + ethyl acetate)	Van Zandijcke and Verhoeve	1974	Dynamic Gulliespie	101.3	4
	Lee et al.	1996	Dynamic Othmer	Atmospheric	11
	Gomis et al.	2000	Dynamic Gulliespie	101.3	5
(Water + methanol + n-butanol)	Newsman and Vahdat	1977	Flow	99.2	10
(Water + ethanol + n-butanol)	Newsman and Vahdat	1977	Flow	102.2	7
(Water + n-propanol + n-butanol)	Newsman and Vahdat	1977	Flow	99.7	13
(Hexane + benzene + tetramethylene sulfone)	Rawat et al.	1980	Dynamic Othmer	101.3	5
(Water + 2-propanol + 1-butanol)	Aicher et al.	1995	Dynamic Gulliespie	Atmospheric	16
(Water + ethanol + 1-butanol)	Gomis et al.	2000	Dynamic Gulliespie	101.3	4
	Iwakabe and Kosogoe	2001	Dynamic Gulliespie	101.3	4
(Water + 2-propanone + 2-butanone)	Gomis et al.	2000	Dynamic Gulliespie	101.3	6
(Water + ethanol + diethyl ether)	Gomis et al.	2000	Dynamic Gulliespie	101.3	7
(Water + 1-butanol + n-butyl acetate)	Gomis et al.	2000	Dynamic Gulliespie	101.3	8
(Ethanol + 2-butanol + water)	Iwakabe and Kosogoe	2001	Dynamic Gulliespie	101.3	12
(Water + 1-propanol + 1-pentanol)	Asensi et al.	2002	Dynamic Gulliespie	101.3	7
(Water + n-propanol + cyclohexane)	Lee and Shen	2003	Dynamic Othmer	101.3	23
(Water + ethanol + isooctane)	Font et al.	2003	Dynamic Gulliespie	101.3	10
(Water + isopropanol + isooctane)	Font et al.	2004	Dynamic Gulliespie	101.3	8
(Water + ethanol + cyclohexane)	Gomis et al.	2005	Dynamic Gulliespie	101.3	11
(Water + ethanol + heptane)	Gomis et al.	2006	Dynamic Gulliespie	101.3	14
(Water + ethanol + hexane)	Gomis et al.	2007	Dynamic Gulliespie	101.3	21
(Water + ethanol + n-butyl acetate)	Younis et al.	2007	Dynamic Othmer	101.3	9
	Younis et al.	2007	Dynamic Othmer	80	7
	Younis et al.	2007	Dynamic Othmer	48	7
(Water + ethanol + methyl ethyl ketone)	Younis et al.	2007	Dynamic Othmer	101.3	6
(Water + acetone + methyl ethyl ketone)	Younis et al.	2007	Dynamic Othmer	101.3	8
(Water + acetone + n-butyl acetate)	Younis et al.	2007	Dynamic Othmer	101.3	11
	Younis et al.	2007	Dynamic Othmer	80	6
	Younis et al.	2007	Dynamic Othmer	48	6
(Water + ethanol + acetone + n-butyl acetate)	Younis et al.	2007	Dynamic Othmer	101.3	35
	Younis et al.	2007	Dynamic Othmer	80	30
	Younis et al.	2007	Dynamic Othmer	48	29
(Water + ethanol + acetone + methyl ethyl ketone)	Younis et al.	2007	Dynamic Othmer	101.3	25
(Water + ethanol + toluene)	Gomis et al.	2008	Dynamic Gulliespie	101.3	8
(Diisopropyl ether + isopropyl alcohol + water)	Lladosa et al.	2008	Dynamic Gulliespie	100	12
(Di-n-propyl ether + n-propyl alcohol + water)	Lladosa et al.	2008	Dynamic Gulliespie	100	11
(Water + acetic acid + methyl acetate + p-xylene)	Lee and Lin	2008	Dynamic Othmer	101.3	25
(Water + ethanol + p-xylene)	Gomis et al.	2009	Dynamic Gulliespie	101.3	11
(Water + cyclohexane + isooctane)	Pequenín et al.	2010	Dynamic Gulliespie	101.3	4
(Water + ethanol + cyclohexane + isooctane)	Pequenín et al.	2010	Dynamic Gulliespie	101.3	51
(Water + 2-butanone + 2-butanol)	Lladosa et al.	2011	Dynamic Gulliespie	101.3	12
(Water + 4-methyl-2-pentanone + 2-butanol)	Lladosa et al.	2011	Dynamic Gulliespie	101.3	14
(Water + hexane + toluene)	Pequenín et al.	2011	Dynamic Gulliespie	101.3	4
(Water + ethanol + hexane + toluene)	Pequenín et al.	2011	Dynamic Gulliespie	101.3	21

4.1 PURPOSE OF MEASURING VLLE

The VLE and VLLE of ternary systems are used to describe and solve problems regarding the design, analysis and control of separation sequences involving heterogeneous azeotropic distillation columns through RCMs and distillation lines (de Villiers, French & Koplos 2002).

Knowledge of the size and shape of the heterogeneous region and the slope of the liquid-liquid tie lines of a ternary system is of vital importance to properly simulate an azeotropic distillation column for the dehydration of alcohol. The compositions of the two liquids obtained in the decanter after condensation of the vapour from the top of the column, are greatly influenced by these characteristics. Gomis et al. (2005; 2007) found that the size of the heterogeneous region calculated by thermodynamic models is larger than the region determined experimentally. They found that the region with the highest concentrations of ethanol (in an ethanol-water-cyclohexane or ethanol-water-hexane system) reveals the greatest difference between experimental and calculated data. Some homogeneous points are even portrayed as heterogeneous by these thermodynamic models. The tie lines in these regions are those required for the calculations involving the decanter and consequently are very important to the simulation of the column. Therefore, it is imperative to evaluate the predictions of thermodynamic models by comparing it to experimental data. Otherwise, the simulations performed with these models may not at all portray the phase equilibrium that will exist in practice.

Experimental equilibrium data can also be used for comparison with other hydrocarbon systems commonly used as entrainers. When using an azeotropic distillation column to dehydrate ethanol with such a hydrocarbon system, the process efficiency is raised if the amount of water removed in the condenser-decanter section of the column is increased. In Figure 4-1 Gomis et al. (2007) compare the entrainers benzene, cyclohexane and n-hexane for the dehydration of ethanol. The composition of the vapour leaving the top of the column is close to that of the ternary heterogeneous azeotrope and therefore the composition of the aqueous phase from the tie-line (tie-line indicated on Figure 4-1) containing the azeotropic point reflects the amount of water that can be eliminated after condensation and decantation. Figure 4-1 illustrates that the aqueous phase has a larger water composition when using benzene than with cyclohexane or hexane. For the latter two systems, a larger stream will need to be re-circulated in order to remove the same amount of water. This will consequently increase equipment and production cost.

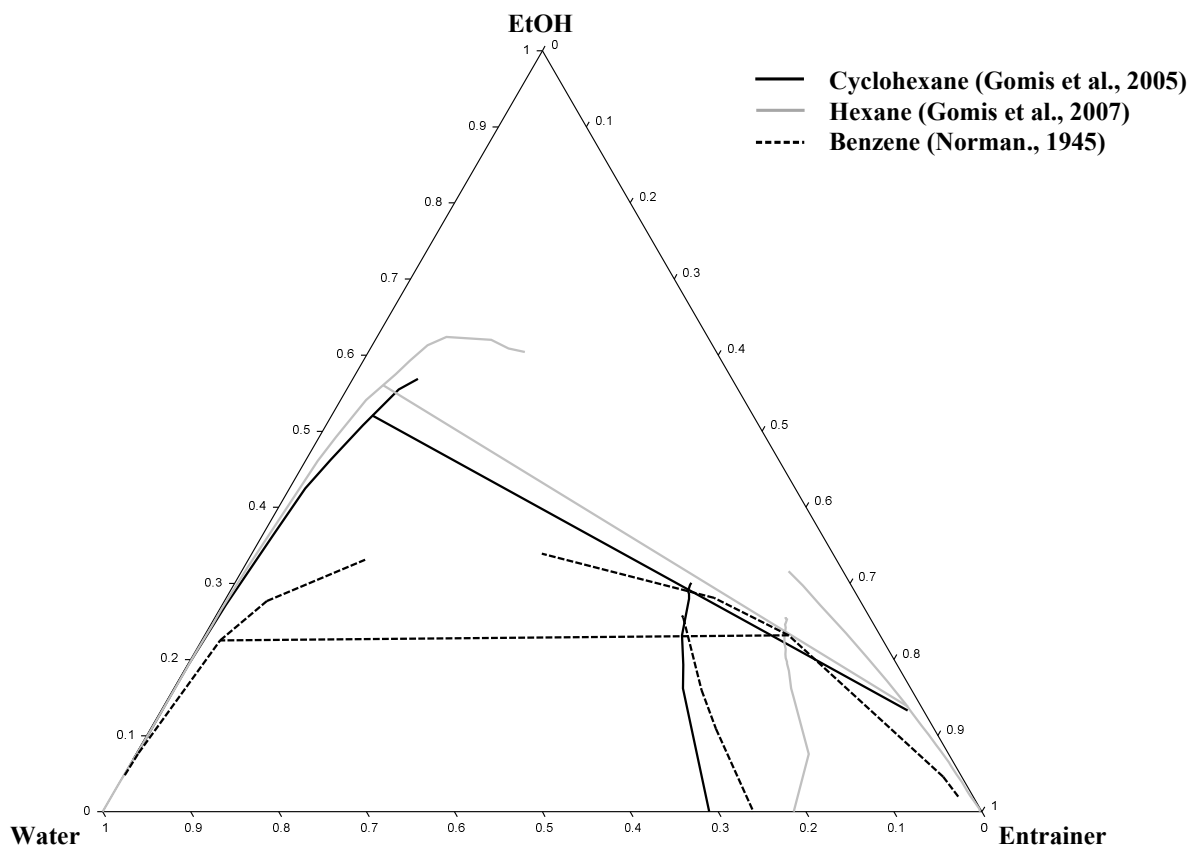


Figure 4-1: Comparison of entrainers for the dehydration of ethanol via heterogeneous azeotropic distillation according to Gomis et al. (2007)

4.2 PROBLEMS WITH MEASURING VLLE

When determining VLLE data for a heterogeneous liquid, the liquid mixture in the boiling flask divides into cleanly separated phases with a visible interface between them. Due to the clean separation, a small interfacial surface exists between the phases and only a limited mass transfer rate between the phases is possible. This phenomenon prevents the system from attaining stability and can be explained by means of the following example of a binary system containing a heterogeneous azeotrope (Figure 4-2). The system consists of two components, water (W) and an organic component (O). At equilibrium the heterogeneous binary mixture will consist of two liquid phases of compositions X_E and X_F , and a vapour phase of composition X_Z , at temperature T_Z . According to equilibrium conditions, neither the temperatures nor the compositions of the liquid phases will change as long as the overall composition of the liquid mixture stays between X_E and X_F . However, if the liquid phases are not sufficiently mixed, it might be near impossible to attain this equilibrium. When insufficient mixing occurs, the liquid phases may separate in the boiling chamber and two phases with different boiling points will then exist. Say for instance the aqueous phase (X_E) settles out below the organic phase (X_F) and has a higher boiling temperature. The organic phase might then start to boil and evaporate, while the aqueous phase cannot reach its boiling point. The vapour phase that is formed in that instance would lie somewhere between X_Z and X_F and would only be in equilibrium with the organic phase. The vapour phase is continuously condensed and recycled to the mixing chamber where it is supposed to be mixed with the recycled liquid phases.

However, if the organic phase is floating on top of the aqueous phase and is the only liquid phase that is boiling, only the organic liquid component would be recycled back to the mixing chamber. Therefore the mixing chamber would then contain a liquid with a very high organic content. If the content of the mixing chamber is fed to the bottom of the boiling chamber, instantaneous vaporization might occur, disrupting the mixture in the boiling chamber and rendering the system extremely unstable for a while until most of the organics have either evaporated or settled on top of the aqueous phase. Then the cycle would be repeated. If the content of the mixing chamber was fed to the top of the boiling chamber, it would just combine with the organic phase already floating on top of the aqueous phase and no mixing of the two phases would ever occur.

It is therefore clear that sufficient mixing of all the phases is of vital importance for accurate measurement of VLLE data. Adequate mixing, or even emulsification of the liquid phases, would create the appearance of a single liquid phase with a new boiling (equilibrium) temperature at which the system could attain stability.

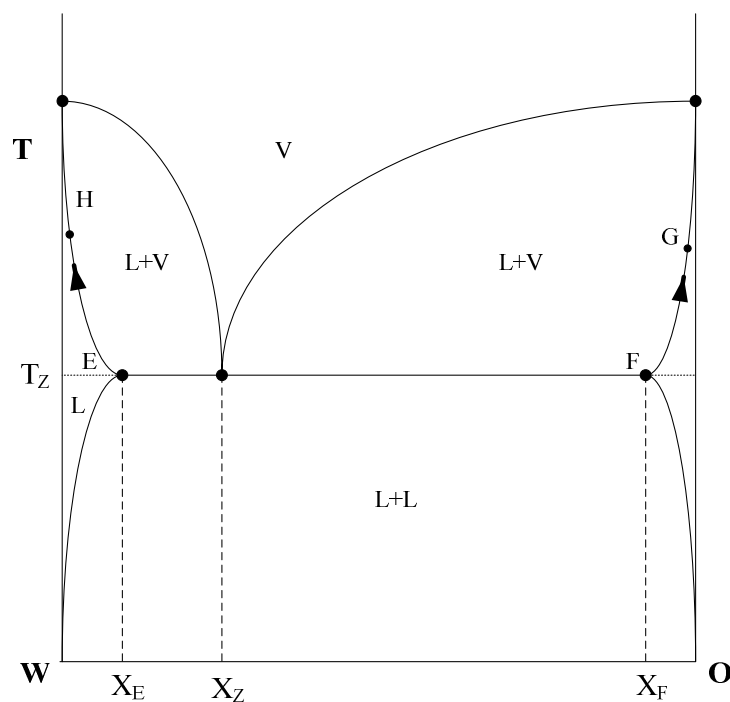


Figure 4-2: Temperature-composition diagram in a binary partially miscible system: L, liquid; V, vapour.

According to Gomis et al. (2010)

4.3 METHODS

In Table 4-2 the methods for the direct measurement of VLE data are classified into five groups (Hala et al. 1967). Only the first three of these methods have in the past been used to determine isobaric VLLE data.

Table 4-2: Classification of methods to determine VLE data by Hala et al. (1967).

Method	Type of Equilibrium Data
Distillation	
Dynamic/ Circulation	Isobaric
Flow	
Static	Isothermal
Dew- and bubble-point	

A method is chosen based upon the type of equilibrium data that needs to be obtained (isobaric or isothermal), the operating temperature and pressure and the nature of the system from which the data is to be obtained. The equipment used to measure isobaric data all operate in similar temperature ranges, but the flow equipment can operate over a wider range of pressures. The operating pressure of the equipment used to measure isothermal data is similar, but dew- and bubble-point method has a wider temperature range.

The design of the equipment previously used in literature to measure VLLE data is based on one of the following methods: distillation, dynamic or flow. These three methods will be briefly discussed below. More information on the static and dew- and bubble-point method is supplied by Weir and de Loos (2005) and Malanowski (1982) respectively for the reader interested in further details on the subject.

4.3.1 Distillation Method

Distillation was the first method used to obtain VLLE data, most probably since it was also the first method used to obtain VLE data with homogeneous liquid phases. This method is characterized by distilling a relatively small amount of liquid off in a boiling flask which contains a large liquid charge.

Distillation has the advantage of simplicity and played an important role in laying the foundation for the development and improvement of experimental techniques for measuring phase equilibrium data. This method does however have several shortcomings of which the inability to attain true thermodynamic equilibrium is one. Rectification due to the condensation of vapour against the cold sides of the flask during operation is another major drawback. Therefore, this method is rarely used even more (Hala et al. 1967).

Figure 4-3 is a schematic representation of one of the stills used by Hands and Norman in 1945. This equipment employed the distillation method and was used to measure phase equilibrium data of systems in which the liquids presented partial miscibility. These authors were of the first to propose equipment using the distillation principle to measure phase equilibrium data of systems with limited miscibility. Other authors incorporated stirrers in distilling flasks to facilitate the necessary mixing of the two liquid phases formed (Barbaudy 1926, Barbaudy 1926). Some authors also combined distillation and dynamic methods in order to take samples without affecting the conditions for equilibrium (Verhoeve 1968, Blackford, York 1965). These alterations to the distillation method reflect the great difficulty with which VLLE data is obtained.

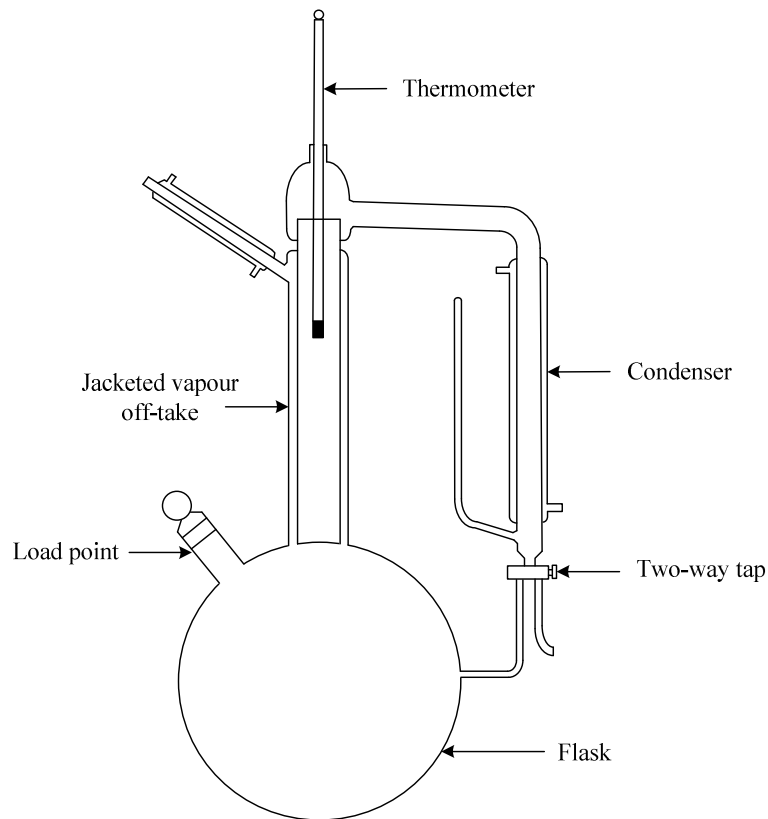


Figure 4-3: Experimental apparatus of Hands and Norman (1945).

4.3.2 Dynamic Method

The dynamic method is, up to now, the most frequently used frequently method for determining isobaric VLE data. Figure 4-4 schematically illustrates how circulation-based vapour-liquid equilibrium apparatus functions.

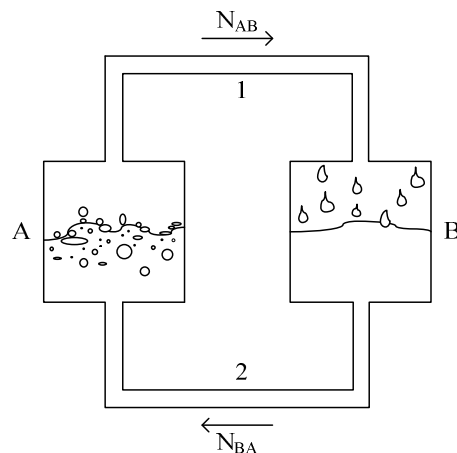


Figure 4-4: Schematic illustration of the mechanism upon which the dynamic method functions. According to Gomis et al. (2010)

The vapour formed from the mixture in distilling flask A is passed to flask B by means of channel where it collects after having been condensed. As flask B is filled, the condensate returns to distilling flask A through another channel. This process continuously repeats itself until equilibrium is reached, upon which the

compositions of the liquids in flasks A and B no longer change with time. The mass flow rate of vapour out of flask A then equals the mass flow rate of condensate into flask A. Laboratory equipment based on the circulation method usually either circulates only the vapour phase (Othmer's principle) or both the vapour and liquid phases simultaneously (Guillespie's principle).

Noteworthy modifications have been made to conventional equipment based on this method. Van Zandijcke and Verhoeve (1974) modified equipment that is based on the Gillespie principle. The equipment was modified by dividing the distilling flask into two sections to separate the liquid phases and heat each independently. Iwakabe and Kosuge (2001) found large temperature fluctuations inside the equilibrium chamber of the equipment used by Van Zandijcke and Verhoeve (1974). Poor thermodynamic consistency was also found for the VLLE data measured with this equipment. Therefore Iwakabe and Kosuge (2001) made another modification to the system by allowing both liquid phases to reach the Cottrell pump separately, unlike previously.

Gomis et al. (2000) made a completely different modification to the apparatus based on the Gillespie principle. An ultrasonic homogenizer was incorporated in the distilling flask in order to emulsify the two liquid phases. The emulsification allows rapid transfer between the two phases and brings about sufficient circulation of all phases through the apparatus. No collection of the liquid and vapour phases occurs unless sampling is initiated. Therefore de-mixing is not a concern in any intermediate stages of the apparatus. Other authors (Lladosa et al. 2008) have subsequently also employed this method and VLLE data from this procedure are still being published.

Another dynamic method of obtaining VLLE data is the modified Othmer principle with vapour condensation recirculation. This method was used by authors Lee and Shen (2003) and Younis et al. (2007). Lee and Lin (2008) also published data for which the Othmer principle was applied. Many difficulties, however, seem to arise when employing this principle. A rectification effect can occur in this type of equipment and difficulty with the keeping the liquid phases mixed may be experienced. The vapour phase obtained, splits into two phases upon condensation and difficulty is experienced with returning both phases correctly to the boiling flask. By directly re-circulating the condensed vapour phase to the boiling flask, without first undergoing separation, a sample of the vapour phase will have to be extracted before it could be allowed to be condensed (Gomis, Pequenín & Asensi 2010).

4.3.3 Flow method

The flow method (Figure 4-5) continuously feeds the equilibrium chamber a steady-state feed stream, as opposed to the dynamic method. This method was developed in the search for a method that will allow the system to reach equilibrium as soon as possible and to overcome the difficulties encountered with the dynamic flow method. One of the first flow stills was proposed by Colburn (1943). This still was fed by a stream consisting of vapour of a given composition. This method was also employed by Newsham and Vahdat (1977) and is discussed in more detail in their work. The still used by Newsham and Vahdat differs from the one used by Colburn in that it is fed with a liquid mixture instead of a vapour mixture. Equipment employing this method is however not widely used, mainly due to its complexity and the larger amount of material required (Gomis, Pequenín & Asensi 2010). The flow method is also said to be applicable only to systems in which the time needed to attain phase equilibrium is sufficiently short (Dohrn et al., 2010). Therefore in a highly non-ideal

system such as for VLLE determination, where extensive time may be required to obtain sufficient mixing, as well as chemical and thermal equilibrium, the flow method is deemed unsuitable.

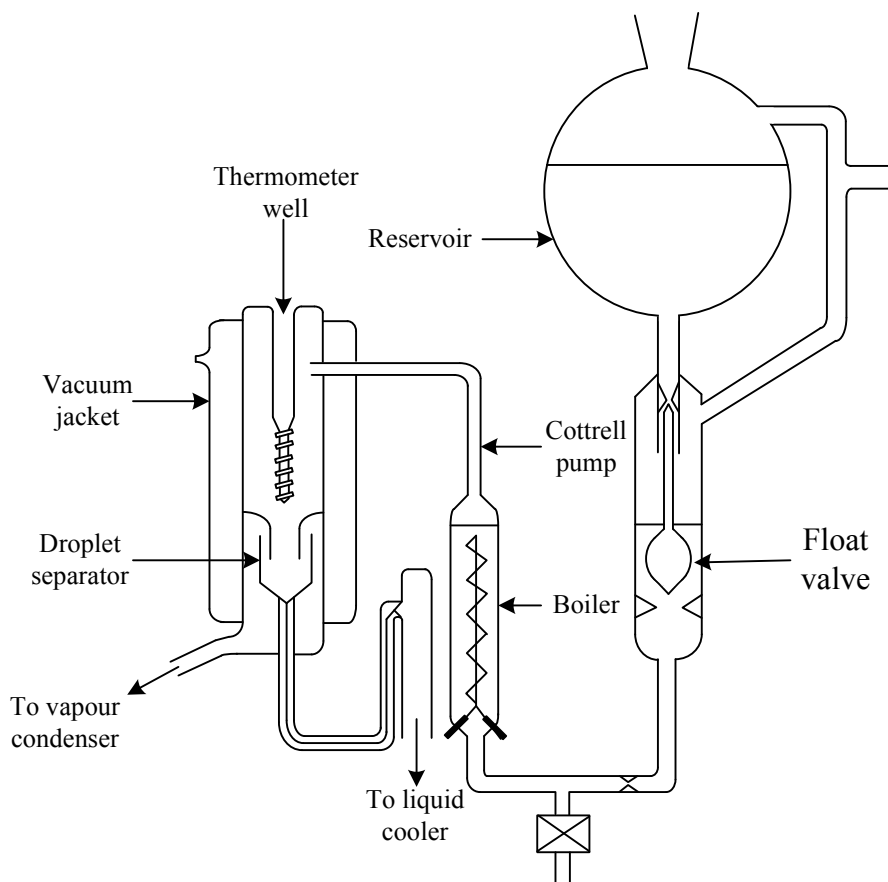


Figure 4-5: Experimental apparatus of Newsham and Vahdat (1977).

4.4 PREFERRED METHOD AND EQUIPMENT

Presently the dynamic method is most widely used to determine isobaric vapour-liquid equilibrium (VLE) for both homogeneous and heterogeneous mixtures and is therefore also chosen for this work. Commercially available equipment allows steady state to be reached relatively easily for homogeneous liquids, but this is not the case when the liquid is heterogeneous.

An issue that specifically arises when attempting to measure VLLE with the dynamic method, especially with equipment based on the Gillespie principle is a poor recirculation effect. This effect is caused by the well-defined separation of liquid phases formed in the boiling flask. The lower density phase floats on top of the higher density phase and is more likely to accumulate in the recirculation conduit. This could result in a situation where only the heavy liquid phase exists in the boiling flask, nowhere near equilibrium. When this phenomenon occurs, the phases only mix periodically. The lighter phase accumulates in the recirculation conduit, but occasionally flows back into the boiling flask, evaporates rapidly and causes a sudden temperature drop which is not sustainable. Again referring to Figure 4-2, the light and heavy phase can be represented by H and G respectively. If the two phases were to be mixed and the global composition of the mixture remains between X_E and X_F , the system would attempt to attain equilibrium, represented by point E, F and Z. Given that

equilibrium occurs at a much lower temperature than at which points G and H are, only sudden distillation (rapid evaporation) will allow the system to reach equilibrium, but steady mixing will sustain that equilibrium temperature and compositional state. Since this mixing process only occurs periodically, temperature will continuously oscillate and steady state will hardly ever be reached.

For equipment based on the Gillespie principle, which is the most widely used, two types of solutions for the aforementioned stability problems have been proposed. Firstly, to increase the extent to which the two phases in the boiling flask are mixed. This can be achieved either by mechanical stirring or by means of an ultrasonic homogenizer (Gomis, Ruiz & Asensi 2000). An ultrasonic homogenizer produces an ideal emulsion from the heterogeneous mixture which propagates throughout the system. Subsequently, the contact surface between phases and ultimately mass transfer is improved. This modification to equipment based on the Gillespie principle allows proper recirculation of the heterogeneous mixture since its sufficiently emulsified state cannot separate into two well-defined layers. Secondly, the equipment can be modified to keep the two liquid phases of the heterogeneous mixture completely separated between the outlet of the Cottrell pump and the boiling flask (through which it enters the Cottrell pump). This ensures that the two liquid phases only mix inside the Cottrell pump. The separation is accomplished by inserting a dividing element into the boiling flask and effectively partitioning it into two separate compartments. The mixed liquid phases exiting the Cottrell pump, passes through a separation unit and is circulated through separate conduits to their respective compartments in the boiling flask. The vapour phase leaving the Cottrell pump also pass through this separation unit after it is condensed and returns to the boiling flask along with the liquid phases. Consequently, the phases are re-circulated correctly, preventing the formation of an inconsistent mixture in the boiling flask which results in sudden distillation.

4.4.1 Motivation for Ultrasound

The application of ultrasonic sound is an efficient technique to emulsify partially miscible liquid phases. Therefore, it is a superb method for avoiding the problems arising from the use of VLE circulation instruments for liquids with limited miscibility. The sonic power applies extremely high acoustic pressures to the fluid in the two liquid phases, producing a sudden increase and decrease of shear pressure within the fluid as well as local shock heating. These effects cause cavitation to occur which results in the emulsification of the two liquid phases (Gomis, Ruiz & Asensi 2000). This method was successfully employed by Asensi et al. (2002), Gomis et al. (2005; 2006; 2007) and Lladosa (2008). It is also preferred above other methods since a dynamic Gillespie unit can be obtained commercially and modified to accommodate an ultrasonic homogenizer, upon special request. Therefore, the timely design and in-house manufacture of phase equilibrium measuring equipment is averted.

4.4.2 Positioning of Ultrasonic Homogenizer

Gomis et al. (2000) investigated and found the optimum position to place an ultrasonic homogenizer in an existing dynamic Gillespie still. Placement in the mixing chamber of the circulation instrument was considered, but was discarded due to the ebullition produced by the energy contribution of the homogenizer to a liquid at the bubble temperature. When this occurs, an unfavourable situation can arise in which the bubble produced by evaporation in the mixing chamber can obstruct the circulation of liquid phases. The homogenizer is optimally placed in the boiling flask, preferably vertically in the bottom of the boiling flask. This position is traditionally

occupied by the immersion heater which takes preference above the homogenizer. Alternatively the ultrasound can be applied as vertically as possible, next to the heater (see Figure 4-6). This optimally improves the mass transfer rate by immediately dispersing the incoming liquid and shifting it upwards. Gomis et al. (2000) validated and verified this modification to VLE equipment, based on the Gillespie principle to be as accurate and reliable by investigating 5 heterogeneous binary systems as well as 5 previously studied heterogeneous ternary systems.

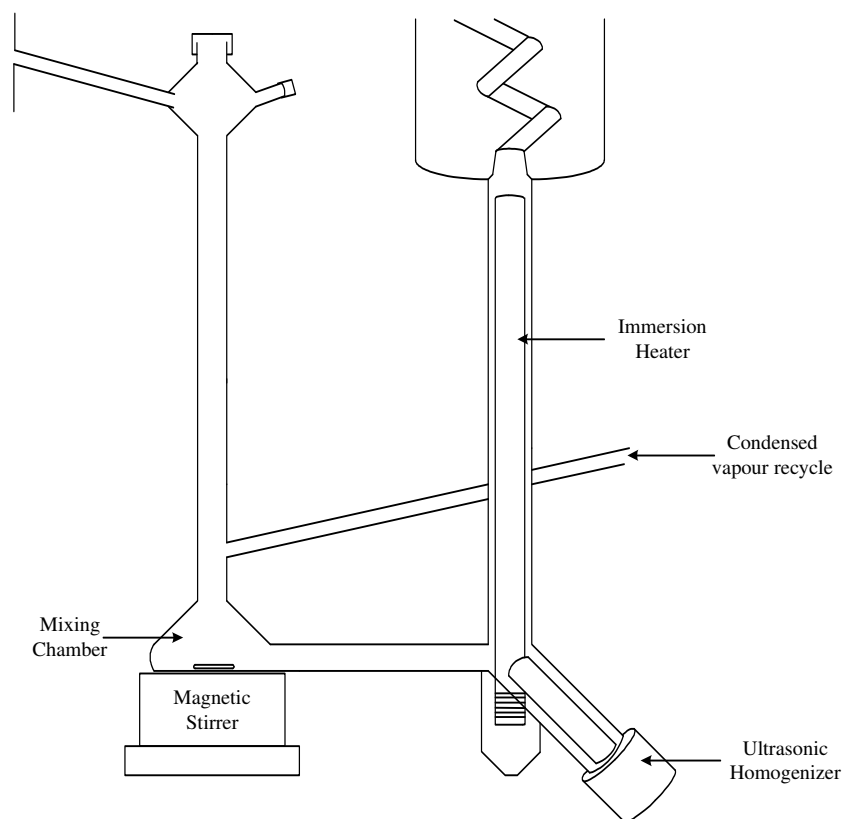


Figure 4-6: Optimum positioning of the ultrasonic homogenizer as suggested by Gomis et al. (2000).

II EXPERIMENTAL STUDIES ON TERNARY HETEROGENEOUS AZEOTROPIC SYSTEMS

5 EVALUATION AND SELECTION OF ALCOHOL-WATER-ENTRAINER SYSTEMS

5.1 LITERATURE DATA OF MOST PROMINENT ENTRAINERS

The phase equilibrium data available in literature of selected potential entrainers for the dehydration of ethanol, isopropanol and n-propanol via heterogeneous azeotropic distillation are extracted from Table 4-1 and listed in Table 5-1 below. These might not be the only entrainers for alcohol dehydration, but are the only ones for which isobaric VLLE data at atmospheric pressure could be found. These data served as basis for the identification of systems for measurement of new ternary VLLE data in this work. It is also used in Section 8.3 to compare the degree of separation that can be achieved with different entrainers, thus eliminating certain inefficient entrainers upfront and thereby reducing the number of entrainers studied in the separation sequence simulations in order to save time.

Table 5-1: Literature phase equilibrium data of possible entrainers for the dehydration of C₂ and C₃ alcohols via heterogeneous azeotropic distillation.

Entrainer	Aqueous Alcohol	Measurement Method	Quantity	Pressure (kPa)	Source
Benzene	Ethanol	Distillation	6 VLLE	101.3	Barbaudy (1927)
Cyclohexane	Ethanol	Dynamic Gulliespie	11 VLLE, 27 VLE	101.3	Gomis et al. (2005)
	n-Propanol	Dynamic Othmer	23 VLLE	101.3	Lee and Shen (2003)
Hexane	IPA	Distillation	6 VLLE, 40 VLE	101.3	Verhoeve (1968)
	Ethanol	Dynamic Gulliespie	21 VLLE, 49 VLE	101.3	Gomis et al. (2007)
Heptane	Ethanol	Dynamic Gulliespie	14 VLLE, 30 VLE	101.3	Gomis et al. (2006)
Isooctane	Ethanol	Dynamic Gulliespie	10 VLLE, 17 VLE	101.3	Font et al. (2003)
	IPA	Dynamic Gulliespie	8 VLLE, 22 VLE	101.3	Font et al. (2004)
DIPE	IPA	Dynamic Gulliespie	12 VLLE	100	Lladosa et al. (2008)
DNPE	n-Propanol	Dynamic Gulliespie	11 VLLE	100	Lladosa et al. (2008)

5.2 EVALUATION OF ENTRAINERS AND LITERATURE DATA

In this section the data available in literature for each entrainer, are discussed in detail. The characteristics and cost of each entrainer are also examined. Ternary diagrams in which these entrainers are compared for ethanol, IPA and n-propanol respectively in Section 8.3 in Figures 8-19 to 8-21. Detailed MSDS forms of the entrainers are available in Appendix A. Some of the literature discussed below, refer to thermodynamic consistency testing of VLLE. As explained in Section 3.10.3., it is evident that no such tests exist and that the application of VLE consistency tests to VLLE data is not necessarily valid.

5.2.1 Benzene

Benzene is an aromatic hydrocarbon and a constituent of products derived from coal and petroleum. It is used to produce detergents, plastics, pesticides, and other chemicals. Benzene is proven to be carcinogenic to humans. Individuals have likely developed and died from leukemia caused by exposures to benzene from 5-30 years. Short-term exposure to high levels of benzene may result in drowsiness, dizziness, unconsciousness, and death. Long-term exposure can adversely affect bone marrow and blood production (United States Department of Labour - Occupational Safety & Health Administration 2011).

The azeotropic distillation process was first established at the beginning of the 20th century, by Dr. Young (Norman 1945) using benzene as an entrainer to dehydrate ethanol. Various accounts of the commercial use of this process can be found in literature (Webb 1937, Guinot, Clark 1938, Rovaglio et al. 1992). Benzene has also been suggested for n-propanol dehydration (Challis 1954). However, due to the carcinogenic nature of benzene, the need for alternative entrainers have arisen (Gomis et al. 2007).

Norman (1945) reported 6 isobaric VLLE data points measured by Barbaudy (1926) at 101.3 kPa for the ethanol/benzene/water system. Mixtures of known composition were made up in a large copper still fitted with a stirrer, a jacketed line for vapour off take and a condenser. The mixture was distilled and numerous samples of the distillate were taken, weighed and analyzed. The composition of the remaining liquid in the still was determined from a mass balance. The composition of the liquid phase for a certain vapour phase sample was taken as the average of the compositions before and after each vapour phase sample was gathered. According to Norman, Barbaudy's results appear accurate and consistent.

5.2.2 Cyclohexane

Cyclohexane is a colourless, volatile liquid with a somewhat pungent smell similar to that of chloroform or benzene. It can be produced by the catalytic hydrogenation of benzene or from fractional distillation of petroleum. More than 90% of cyclohexane is used in the production of nylon fibre and nylon molding resin. The remainder used as solvents for paint, resins, oils, varnish, plasticisers or as an intermediate to produce other industrial chemicals (Harrison 2000).

Cyclohexane is known to be used extensively as entrainer for the dehydration of ethanol and IPA via heterogeneous azeotropic distillation (Lin, Wang 2004, Gomis et al. 2007, Gomis et al. 2007, Wang et al. 1998). Cyclohexane has also been suggested for n-propanol dehydration (Challis 1954).

Gomis et al. (2005) measured 11 isobaric VLLE and 27 isobaric VLE data points at 101.3 kPa for the ethanol/cyclohexane/water system. It is said in this work that cyclohexane is currently one of the most used entrainers for the dehydration of ethanol via heterogeneous azeotropic distillation and that numerous plants around the world are employing this chemical. The measurements were performed with a dynamic Gullispie unit with an ultrasonic homogenizer fitted to the boiling chamber of the unit (as described in Section 4.4). The uncertainty in the temperature measurements were reported to be 0.006°C. The pressure in the still is reported to be measured and controlled with an accuracy of 0.1 kPa. According to Gomis et al. (2005), the accuracy of the mole fraction measurements is estimated at ± 0.002 for all compounds except for the cyclohexane in the aqueous liquid phase and the water in the organic liquid phase, for which the accuracy is reported to be ± 0.005 .

The VLE and VLLE data is said to be tested by the point-to-point L/W Wisniak consistency test and found thermodynamically consistent. All the values of L/W are reportedly between 0.98 and 1.00. Gomis et al. (2005) compared the measured VLLE data to predictions from UNIFAC and NRTL using binary parameters from literature. It was found that the tie lines and vapour phase is predicted well by the models, but the shape of the phase envelope differs significantly.

Lee and Shen (2003) measured 23 isobaric VLLE data points at 101.3 kPa for the n-propanol/cyclohexane/water system. Lee and Shen (2003) also stated that benzene and cyclohexane are typically used as entrainers for the purification of azeotropic mixtures of aqueous alcohols. A dynamic Othmer unit with condensed vapour recirculation was used for this work. Premature condensation in the cell was prevented by the insulation of a vacuum jacket on the vapour path as well as another jacket with silicon oil. A liquid pump was added to the condensed vapour return line to ensure that both liquid phases return to the boiling chamber if phase separation occurs. The temperature measurements are reported to have an accuracy of 0.1 K. The accuracy of the pressure control at 760 mmHg is reported to be ± 1 mmHg. The authors determined UNIQUAC and NRTL binary interaction parameters for the n-propanol/cyclohexane/water mixture and found that NRTL correlated the data fairly well, whereas the UNIQUAC predictions were unsatisfactory.

Verhoeve (1968) measured 6 isobaric VLLE data points and 40 isobaric VLE data points at 101.3 kPa for the IPA/cyclohexane/water system. Measurements were actually conducted with a dynamic Othmer still in which the condensate receiver was replaced by a 3-way stopcock and therefore it referred to as a distillation method. VLE measurements were done and in the heterogeneous liquid region only the overall liquid composition was measured. The composition of each liquid phase is then determined by a LLE experiment at boiling point. The accuracy in composition of the VLE measurements is reported to be ± 0.1 mole % and 0.05 mole % for LLE measurements. The uncertainty of the temperature measurements is reported to be $\pm 0.1^\circ\text{C}$ for both the VLE and LLE data. The accuracy of the pressure control at 760 mmHg is reported to be ± 0.5 mmHg. Binary and ternary constants were determined for the Redlich-Kister Equations for the IPA/cyclohexane/water system.

5.2.3 Hexane

Hexane is a clear, colourless, highly flammable liquid with a distinctive petroleum-like smell. It is used as an alcohol denaturant, paint dilutant, component in petroleum and gasoline products, and as a cleaning agent in the textile, furniture and leather industries. It is also used in the extraction of vegetable oil from seeds such as soybean, flax, safflower and cotton (California Office of Environmental Health Hazard Assessment 2011).

Gomis et al. (2007) measured 21 isobaric VLLE and 49 isobaric VLE data points at 101.3 kPa for the ethanol/hexane/water system. The same equipment used by Gomis et al. (2005) for ethanol/cyclohexane/water measurements, was used for the work by Gomis et al. (2007). Although the uncertainty of the temperature measurements is stipulated to be 0.006°C according to the calibration certificates, the authors estimated the accuracy to be $\pm 0.05^\circ\text{C}$ instead. The VLE and VLLE data were tested by the point-to-point L/W Wisniak consistency test and found to be thermodynamically consistent. All the values of L/W are reportedly between 0.97 and 1.00. Binary parameters were determined for the NRTL and UNIQUAC models from the experimental data of the ethanol/hexane/water system. It is said in this work that hexane is a common component of gasoline and therefore a suitable entrainer for the azeotropic distillation of ethanol, since any traces of hexane in the

anhydrous ethanol product will not be problematic for subsequent fuel use. n-Hexane however has an octane number of ± 25 (Refining online 2011) and does therefore not have very good anti-knocking properties. If n-hexane undergoes structural isomerisation in the presence of a catalyst, it can form cyclohexane or benzene. Both of these compounds have excellent anti-knocking properties and are therefore suitable fuel additives (The Physical Sciences Initiative 2011).

5.2.4 Heptane

Heptane is a clear, colourless, straight-chain alkane with a gasoline-like odour. It is widely used in laboratories as a non-polar solvent. It is also used in paints and coatings, rubber cement solvent and as an outdoor stove fuel. Heptane is the zero point of the octane rating scale. Fuel-air mixtures in internal combustion engines have the tendency to ignite prematurely rather than burning smoothly. This phenomenon is referred to as engine knocking and causes a rattling sound in one or more of the cylinders. Octane rating of fuel is a measure of its resistance to knock. The octane rating is obtained by comparing the characteristics of the fuel to isooctane and heptanes. Pure isooctane is allocated an octane rating of 100, and pure heptane zero. Isooctane is a highly branched isomer and burns smoothly, with minimal knock. Heptane burns explosively, causing engine knocking and is therefore undesirable in fuel (Helmenstine 2011).

Gomis et al. (2006) measured 14 isobaric VLLE and 30 isobaric VLE data points at 101.3 kPa for the ethanol/heptane/water system. The same equipment used by Gomis et al. (2005) for ethanol/cyclohexane/water measurements, was again used for this work. According to Gomis et al. (2006) the point-to-point L/W Wisniak consistency test revealed that the VLE and VLLE data are thermodynamically consistent. All the values of L/W are reportedly between 0.97 and 0.98. Binary parameters were determined for the NRTL and UNIQUAC models from the experimental data of the ethanol/heptane/water system. The authors reported that systems of hydrocarbons, water and ethanol play a significant role in the fuel industry where ethanol-gasoline blends are used.

5.2.5 Isooctane

Isooctane (or 2,2,4-trimethylpentane) is a clear, colourless liquid with a mild hydrocarbon odour. It is manufactured on a large scale in the petroleum industry, generally as a mixture of related hydrocarbons. It can also be manufactured from isobutylene by dimerization using a catalyst. Isooctane defines the 100% point on the octane rating scale, as noted in Section 5.2.4 above.

Font et al. (2003) measured 10 isobaric VLLE and 17 isobaric VLE data points at 101.3 kPa for the ethanol/isooctane/water system. Font et al. (2004) also measured 8 isobaric VLLE and 22 isobaric VLE data points at 101.3 kPa for the IPA/isooctane/water system. These authors belong to the same research group as Gomis et al. (2005, 2006 and 2007) and therefore the same dynamic Gulespie unit equipped with an ultrasonic homogenizer was used for the phase equilibrium measurements. The VLE and VLLE data are said to be tested by the point-to-point L/W Wisniak consistency test and found to be thermodynamically consistent. All the values of L/W for the ethanol/isooctane/water system are reportedly between 0.97 and 1.00, and for the IPA/isooctane/water system between 0.94 and 1.00. The McDermott-Ellis consistency test was also performed on the IPA/isooctane/water data and reportedly found to be thermodynamically consistent with every calculated D lower than D_{\max} . Binary parameters were determined for the UNIQUAC models from the experimental data

of the ethanol/isooctane/water system. Font et al. (2003) reported several other works (Furzer 1985, Cairns, Furzer 1990a, Cairns, Furzer 1990b) in which isooctane is considered as entrainer for ethanol dehydration and found viable. In Font et al. (2004) it is said that isopropyl ether is generally used as entrainer for IPA dehydration.

5.2.6 DIPE

DIPE (diisopropyl ether) is a colourless liquid with an ethereal odour. It is only slightly soluble in water, but miscible with most organic solvents. DIPE is employed as oxygenate gasoline additive. It tends to form explosive peroxides upon prolonged periods of storage in air. This reaction occurs with even more ease for ethyl ether. Such a stored solvent should regularly be tested for the presence of peroxides.

Carlson (1949) proposed a method, based on azeotropic distillation, for recovering the alcohols from a crude aqueous n-propanol cut also containing ethanol and IPA. The proposed method employs DIPE as entrainer. Marples (1939) also suggested using DIPE as an entrainer for the dehydration of ethanol.

Lladosa et al. (2008) measured 12 isobaric VLLE data points at 100 kPa for the IPA/DIPE/water system. These measurements were also made with a dynamic Gillespie unit fitted with an ultrasonic homogenizer, similar to that of Gomis et al. (2005, 2006 and 2007) and Font et al. (2003 and 2004). The accuracy of the temperature measurements is estimated to be ± 0.01 K. The pressure in the still is reported to be measured and controlled with an accuracy of ± 0.1 kPa. According to Lladosa et al. (2008), the accuracy of the mole fraction measurements is estimated to be ± 0.001 . The point-to-point L/W Wisniak test was conducted on the experimental data and it was found that the data is thermodynamically consistent. The McDermott-Ellis consistency test was also performed and indicated thermodynamic consistency as well (all D values smaller than D_{\max}). This work also states that tertiary ethers (such as DIPE and DNPE) can be used as octane-enhancing compounds in fuel, improving combustion and reducing emissions.

5.2.7 DNPE

DNPE is also a colourless liquid, like DIPE, with an ethereal smell. In high concentrations, its vapour may be narcotic. It tends to form explosive peroxides as well, especially when anhydrous.

Along with the IPA/DIPE/water VLLE measurements, Lladosa et al. (2008) also measured 11 isobaric VLLE data points at 100 kPa for the n-propanol/DNPE/water system using the same equipment. All the data was reportedly also found thermodynamically consistent via the point-to-point L/W Wisniak and the McDermott-Ellis tests.

5.3 SELECTION OF ENTRAINERS FOR EXPERIMENTAL WORK

Table 5-2 contains a simplified list of the VLLE data available in literature, of possible alcohol/entrainer/water systems. Three alcohols/entrainer/water systems have been selected for experimental measurements. If one were to fill in the gaps on the list, n-propanol/benzene/water, IPA/benzene/water, n-propanol/hexane/water, IPA/hexane/water, n-propanol/heptane/water, IPA/heptane/water, n-propanol/isooctane/water, ethanol/DIPE/water, n-propanol/DIPE/water, ethanol/DNPE/water and IPA/DNPE/water are all options of data to be measured. Any benzene options are eliminated due to the carcinogenic nature of benzene. When

comparing the Aspen prediction of the ethanol/DIPE/water VLLE (Figure 1-1) to that of the ethanol/benzene/water VLLE found in literature, it seems as if DIPE might be a feasible alternative as entrainer to benzene. The basis upon which such a statement can be made, is discussed in Section 8.3. Therefore, ethanol/DIPE/water VLLE and VLE data measurements have been selected for this study. Since literature (Carlson 1949) suggests that DIPE can also be used to recover n-propanol from an aqueous n-propanol cut, it was decided to measure n-propanol/DIPE/water data as well.

Table 5-2: Simplified list of literature phase equilibrium data of possible entrainers for the dehydration of C₂ and C₃ alcohols via heterogeneous azeotropic distillation.

Entrainer	Aqueous Alcohol		
	Ethanol	n-Propanol	IPA
Benzene	√		
Cyclohexane	√	√	√
Hexane	√		
Heptane	√		
Isooctane	√		√
DIPE			√
DNPE		√	

Table 5-3 contains a list of static price indications of the possible entrainers for C₂ and C₃ alcohol dehydrations. The bulk chemical prices was obtained from ICIS.com and cost escalation to June 2011 was done with Equation 5-1 (Sinnott, Towler 2009). The Marshall and Swift index for chemicals was used from the *Chemical Engineering* magazine (Marshall 2006-2011).

$$Cost\ in\ year\ A = cost\ year\ B \times \frac{Cost\ index\ in\ year\ A}{Cost\ index\ in\ year\ B} \quad 5-1$$

Table 5-3 shows the bulk chemical price of DIPE is similar to that of benzene. For the third system n-propanol/isooctane/water was selected. Firstly since there is already data available for this entrainer with ethanol and IPA, and therefore this work will complete another set as for cyclohexane and DIPE. Secondly, Table 6-3 indicates that isooctane is the most economic choice of entrainer.

Table 5-3: Bulk chemical prices of possible entrainers for the dehydration of C_2 and C_3 alcohols via heterogeneous azeotropic distillation.

Chemical	Cost	Unit
Benzene	11,691.00	ZAR/tonne
Cyclohexane	6,141.95	ZAR/tonne
Hexane	3,807.62	ZAR/tonne
Heptane	4,476.08	ZAR/tonne
Isooctane *	2,745.78	ZAR/tonne
DIPE	11,278.74	ZAR/tonne
DNPE	11,278.74	ZAR/tonne

* Bulk cost estimated from laboratory scale

To summarize ethanol/DIPE/water n-propanol/DIPE/water and n-propanol/isooctane/water were selected for phase equilibrium measurements in this work. DIPE is selected since Aspen predicts phase equilibrium similar to that of benzene. Isooctane is selected for its low bulk chemical cost. The phase equilibrium of these entrainers with ethanol/water, IPA/water and n-propanol/water are compared and discussed in Section 8.3.

6 EXPERIMENTAL WORK

6.1 MATERIALS

All chemicals used, their purities and suppliers are listed in Table 6-1. Distilled water with a conductivity of $2 \mu\text{S}/\text{cm}$ was used. Before using them for experimental work, all chemicals were injected on a GC with FID. No impurities were identified on the resultant chromatograms. The chemicals were also tested with Karl Fischer titration and it was confirmed that the most prominent impurity listed by the suppliers was mainly water. The relevant vapour pressure data for the pure components used in this work are given in Appendix C, Figures C-1 to C-5. The parameters used to predict this data in Aspen Plus are provided in Appendix F, Table F-1.

Table 6-1: List of chemicals with purities and suppliers

Component	Purity	Supplier
Ethanol	$\geq 99.8 \%$	Sigma Aldrich
n-Propanol	$\geq 99.5 \%$	Sigma Aldrich
Isopropanol	$\geq 99.5 \%$	Sigma Aldrich
n-Butanol	$\geq 99.9 \%$	Sigma Aldrich
Isooctane	$\geq 99 \%$	Sigma Aldrich
Diisopropyl ether	$\geq 99 \%$	Merck
Acetone	$\geq 99.8 \%$	Sigma Aldrich
Acetonitrile	$\geq 99.9 \%$	Sigma Aldrich
2-Pentanol	$\geq 98 \%$	Sigma Aldrich

Technical grade nitrogen was used for pressure control in the phase equilibrium equipment. Ultra high purity helium and technical grade air was used for gas chromatography. All gas cylinders were supplied by Afrox.

6.2 APPARATUS

The all glass dynamic recirculating still used to experimentally determine VLE and VLLE data is shown in Figure 6-1. It is a commercial unit (VLE 100 D) manufactured in Germany by Pilodist and widely used to determine VLE data (Marrufo, Loras & Sanchotello 2009, Orchillés et al. 2009, Zhang, Bai & Zhang 2011, Torcal et al. 2010). The manufacturers modified the still and coupled an ultrasonic homogenizer (Braun Labsonic P) to its boiling flask (1.3) to enable VLLE data measurement. The still allows good mixing of the vapour and liquid phases and good separation of the phases once equilibrium is reached. The ultrasonic homogenizer ensures that the liquid phases are sufficiently emulsified when heterogeneous mixtures occur. An electrical immersion heater (10), which is concentrically installed into a flow heater (1.3), evaporates the liquid mixture. The vapour-liquid mixture passes through an extended contact line before entering the separation chamber (1.2). This facilitates intense phase exchange. Together, all the phases are sent forth onto the thermometer (7) which is used to measure the temperature of the bubble point. The gas and liquid phases are separated, condensed and returned to the mixing chamber (1.1). In the mixing chamber the phases are mixed with a magnetic stirrer and returned to the immersion heater (10). The separation chamber (1.2) is constructed in such a way that entrainment of liquid drops and partial condensation of the vapour phase is prevented. Equilibrium will be obtained swiftly due to regular circulation of vapour and liquid phases, simultaneous mixing of re-circulated streams in the mixing chamber (1.1) and emulsification by the ultrasonic homogenizer (17). The unit was installed within an extraction cabinet for safety reasons, as DIPE can form explosive peroxides and its vapour is volatile and flammable.

The unit can be operated in a pressure range of 2.5 mbar – 3 bar and up to a temperature of 250 °C. The equilibrium temperatures are measured with a Pt-100 probe connected to a digital Hart Scientific thermometer with an accuracy of 0.03°C at 0°C according to the certificate of calibration (Appendix B). The pressure and heating power are measured and controlled with a Pilodist M101 pressure control system. The pressure in the still is to be kept at 101.3 kPa, measured and controlled with an accuracy of 0.35% FSO (Full Scale Output).

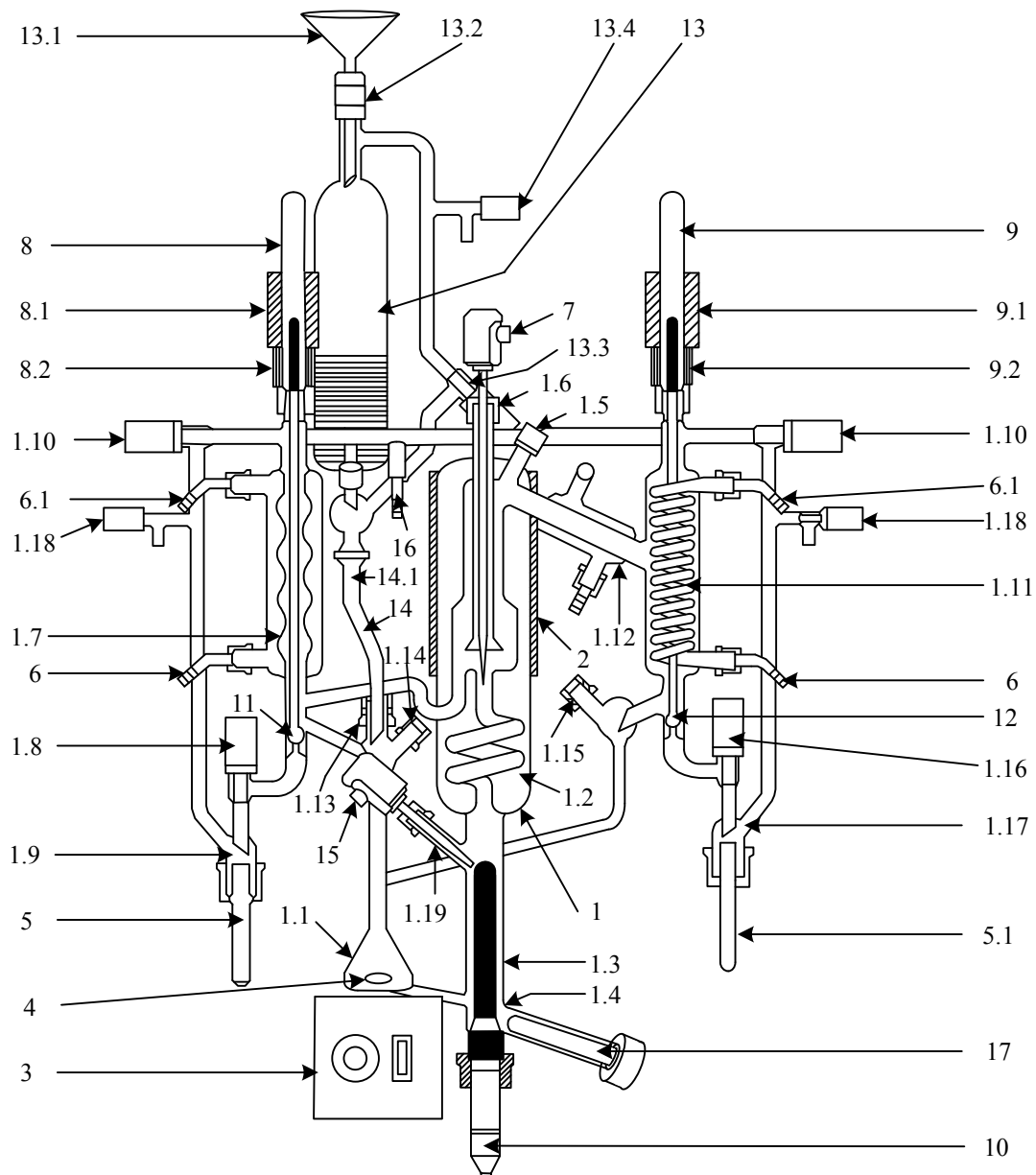


Figure 6-1: Schematic representation of experimental set-up. Apparatus redrawn and edited from the Pilodist VLE 100 D user manual.

1. Glass body of the phase equilibrium apparatus
- 1.1 Mixing chamber
- 1.2 Cottrell pump with silvered vacuum jacket
- 1.3 Flow heater (glass tube)
- 1.4 Discharge valve
- 1.5 Sampling nozzle (vapour phase)
- 1.6 Temperature probe nozzle
- 1.7 Cooler for liquid phase
- 1.8 Stop valve for receiver change under vacuum and positive pressure (liquid phase)
- 1.9 Sampling nozzle (liquid phase)

- 1.10 Stop valve
- 1.11 Condenser
- 1.12 Condenser
- 1.13 Filler nozzle (liquid phase)
- 1.14 Sampling nozzle (liquid phase)
- 1.15 Sampling nozzle (vapour phase)
- 1.16 Stop valve for receiver change under vacuum and positive pressure (vapour phase)
- 1.17 Sampling nozzle (vapour phase)
- 1.18 Aeration valves
- 1.19 Temperature probe nozzle

2. Compensation heating jacket

3. Magnetic stirrer

4. Stirring magnet

5. Glass receiver tube - liquid phase
- 5.1 Glass receiver tube - vapour phase

6. Hose connection olive with screw cap GL14 - inlet
- 6.1 Hose connection olive with screw cap GL14 - outlet

7. Temperature sensor

8. Valve caps
- 8.1 Solenoid coils - liquid phase
- 8.2 Spacer

9. Valve caps
- 9.1 Solenoid coils - vapour phase
- 9.2 Spacer

10. Immersion heater rod

11. Valve rod (liquid phase)

12. Valve rod (vapour phase)

13. Feed burette

- 13.1 Funnel
- 13.2 Filler nozzle for feed burette
- 13.3 Stop valve for feed burette
- 13.4 Aeration valve for feed burette

- 14. Inlet line
 - 14.1 Spherical ground joint

- 15. Temperature sensor

- 16. Glass connecting olive for vacuum or positive pressure

- 17. Ultrasonic homogenizer probe

6.3 PROCEDURE

The apparatus (Figure 6-1) is operated as follows:

- 1) Switch on apparatus
- 2) Open the stop valves (1.10) and aeration valves (1.19). The apparatus must be open to the outside.
- 3) Fill the feed burette via the filler nozzle (13.1) fitted with the screw cap and fill the substances to be measured (± 110 ml).
- 4) Open the precision control valve (13.5) on the feed burette. Close the valve as soon as the liquid just covers the immersion heater (1.3).
- 5) Switch on the control device.
- 6) Adjust the speed of the magnetic stirrer (3) in such a way that constant mixing of the substance is ensured.
- 7) Open the cooling water valve to allow for flow through the condensers (1.7, 1.11 and 1.12).
- 8) If the apparatus is operated at high temperatures (above 100 °C), the column must be heated by means of a heating jacket. This prevents partial condensation of the rising vapour. The heating jacket temperature is set on the set point controller of the control device and should be approx. 3 - 5 °C below the respective boiling temperature of the mixture.
- 9) In the case of substances with solidification points in the region of room temperature, the strip heater should be wrapped around the return lines from the coolers to the mixing chamber. The heating capacity can be adjusted via the power controller on the control device.
- 10) Select pressure conditions at which to operate (atmospheric, vacuum or over-pressure) on the control device. Due to lower pressure at atmospheric conditions, over-pressure is selected for this work to allow for operation at standard atmospheric pressure (101.325 kPa). Set at which pressure the set-up should be controlled on the control device. Set the pressure switch on the apparatus to "pressure" as well. Open the valve to the pressure compensation cylinder.
- 11) Set the heating capacity of the immersion heater (1.3) via the power controller on the control device.

When the heating capacity is correctly set, a continuous flow of condensate exists on the liquid side. The number of droplets at the droplet point on the vapour condensation side should still be readily observable. An optimum load can be achieved at a rate of ± 30 droplets per minute.

- 12) Select “start” on the control device. Once the mixture starts boiling, switch on the ultrasonic homogenizer (only for VLE measurements). The actual measurement of equilibrium can be started as soon as the boiling point of the pure substance is reached. The vapour temperature must remain constant, this indicates equilibrium is reached and occurs after ± 1 h of operation. The vapour temperature is displayed on the digital display of the control device.
- 13) Take samples of each phase once the boiling temperature has been recorded.
- 14) To perform another experiment, click “stop” on the control device. Switch off the ultrasonic homogenizer and magnetic stirrer. Add more feed to the mixing chamber, through the feed burette, to compensate for the volume lost through sampling. Repeat steps 12 and 13.

Cleaning procedure:

- 1) Click “stop” on the control device and switch off the ultrasonic homogenizer and magnetic stirrer.
- 2) Allow the mixture and immersion heater to cool down.
- 3) Drain all liquid from the mixing, equilibrium and boiling chamber through the valve at the base of the boiling chamber.
- 4) Remove the ultrasonic homogenizer probe.
- 5) Rinse the system with acetone.
- 6) Dry with high pressure air or allow to dry by itself.

6.4 SAMPLING AND ANALYSIS

Samples can be taken in three ways:

- A. If the sample is to be taken by means of the receivers (5 and 5.1), the stop valves (1.8 and 1.16) have to be opened first. Then briefly press the keys on the remote control device, until the sample quantity required for determining the concentration has flowed through the solenoid valve into the receivers. Then unscrew the receivers and replace them.
- B. Sampling can also be performed with a gas-tight syringe. Insert the syringe needle through the silicone seal of the screw caps on the sampling nozzles (1.14 and 1.15) and draw off the necessary quantity of sample substance from the dropping tips.
- C. In the case of mixtures which display a miscibility gap, a gaseous sample of the vapour phase must be taken at the sampling nozzle (1.5) using a gas-tight syringe. The sample is taken from the gaseous phase and condensed upon entering the syringe. It is assumed that no demixing occurs before condensation and that a representative vapour phase sample is captured. This is confirmed during the verification of the performance of the equipment (Section 8.1).

Before any sample is taken, the sample port is firstly rinsed by taking a “dummy” sample. This is done to prevent contamination of samples with any liquid that might have collected in the samples port while equilibrium was reached.

When measuring VLLE data, two liquid samples are taken. An over-all liquid sample is taken with a 1 ml gas tight syringe through sampling nozzle 1.14. A solvent (acetone or acetonitrile) is added to the over-all liquid sample to obtain a homogeneous liquid for analysis. The second liquid sample is taken by means of the liquid-side receiver (5 ml), through the solenoid valve. This sample is placed in a heating bath for two hours, at the boiling temperature of the sample, for the liquid phases to separate into two liquid layers. A sample of each layer is taken by means of a 1 ml gas tight syringe, through the silicon seal of the screw cap on the receiver and placed in a sample vial.

For VLLE systems displaying liquid-liquid immiscibility the vapour phase is sampled in the gaseous form via the sampling nozzle (6) with a 5 ml gas tight syringe fitted with a push-button valve. Gaseous samples are taken rather than condensed vapour samples, because of the heterogeneity of the condensed sample. When the vapour phase condenses, it may not be completely uniform in composition due to liquid-liquid separation and such a sample may not be representative of the actual vapour phase. Only once the condensed vapour phase is recycled to the boiling flask, the ultrasonic homogenizer can emulsify the mixture again for recirculation. Therefore it is best to sample the vapour phase in gaseous form. A solvent is also added to the vapour sample in order to obtain a homogeneous sample for analysis.

For VLE data measurement, both liquid and vapour samples can be taken by means of the receivers (5 and 5.1), through the solenoid valves (11 and 12). However, if the condensed vapour phase is heterogeneous, the abovementioned sampling procedure should be followed.

The analysis of all samples was carried out using a Hewlett Packard 5890 GC with a flame ionization detector (FID), coupled with a desktop computer using Delta 55 software. Separation of the components was achieved on a ZB-WAX-Plus capillary column of 30m x 0.53mm x 1.00µm. The column was operated at a temperature of 130°C and on a helium flow of 34.47 kPa. To obtain quantitative results an internal standard (2-pentanol) was used. To quantify the amount of water in each sample, Karl Fischer analysis was performed on a Metrohm 701 KF Titrino unit. The relative accuracy of the compositional measurements by the GC and Karl Fischer analysis is 2%. The response factor for each component against 2-propanol were determined via several injections of standards prepared with different known concentrations. The standards and samples were prepared on a weight basis and impurities in the 2-propanol (Section 6.1) were also accounted for on this basis. The repeatability of results for the GC injections with the experimental samples is shown in Table C-10 in the Appendix. Importantly, the results of the over-all liquid samples were used in a mass balance, to verify the results from each separate liquid phase. If the over-all liquid sample lies on the tieline connecting the respective organic and aqueous liquid points, it verifies the accuracy of liquid phase measurements and indicates that equilibrium was reached throughout the glass cell.

6.5 EXPERIMENTAL CHALLENGES AND RECTIFICATIONS

Most of the experimental challenges experienced in this study, occurred during the equipment commissioning stage of the project.

A standard Pilodist unit (VLE 100 D) was modified to measure VLLE in addition to VLE and measure the data more accurately. The standard unit is supplied with temperature sensors with an accuracy of 0.1 °C. These were replaced with temperature sensors with an accuracy of 0.03 °C. The controller module and computer software also had to be updated to accommodate the improved accuracy of temperature measurement.

All silicone seals had to be replaced with Viton or Kalrez ones in order to withstand the solvent quality of the materials used and the temperature of the ultrasonic probe during operation.

7 DATA REGRESSION AND SIMULATION

7.1 REGRESSION METHOD

The Aspen Plus Data Regression System (DRS) was used to fit the parameters of the activity coefficient models (discussed in Section 4), to measured phase equilibrium data and data obtained from literature. See Appendix G for a list of the data used from literature for each regression case. Different weights were allocated to the literature sets in each regression case (Appendix G, Table G-2). The weights were varied to determine parameters that would improve the fit of the model predictions on the data. The weights were also varied to obtain convergence of the regression cases in Aspen Plus DRS. Due to this variation in weightings, somewhat different simulation results could be obtained for NRTL and UNIQUAC on the same ternary mixture.

As described in Section 4, six binary interaction parameters (a_{ij} , b_{ij} , c_{ij} , d_{ij} , e_{ij} and f_{ij}) are specified for NRTL and five (a_{ij} , b_{ij} , c_{ij} , d_{ij} and e_{ij}) for UNIQUAC. For UNIFAC, one adjustable group binary parameter (a_{mn}) is specified. No parameters were fixed in any of the regression cases. In Table G-2 it is stipulated which data were used for which regression. For most of the cases VLE and LLE data were regressed simultaneously. The parameters (UNIFAC groups) of UNIFAC (VLE) in Aspen were determined from VLE data and similarly the parameters of UNIFAC (LLE) were determined from LLE data. For the regression of UNIFAC (VLE) and UNIFAC (LLE) parameters, the respective built-in Aspen groups were used as initial guesses. It should be noted that different UNIFAC groups were only modified specifically for the ternary systems in question and for the function of performing separation sequence simulations with model parameters that accurately predicted the data. The regressed UNIFAC groups should not be used for simulations in which other components are also present. These groups have been manipulated to fit a specific ternary system and the group numbers might not accurately predict other components belonging to that group, anymore.

Adjustable binary interaction parameters were determined by DRS using the maximum likelihood objective function with the Britt-Luecke algorithm (Aspen Technology 2009). In this maximum likelihood objective function, errors in all measured variables (T, P, x, and y) are considered. For phase equilibrium data, the maximum likelihood objective function is (Aspen Technology 2009):

$$Q = \sum_{x=1}^{NDG} w_n \sum_{i=1}^{NP} \left[\left(\frac{T_{e,j} - T_{m,j}}{\sigma_{T,j}} \right)^2 + \left(\frac{P_{e,j} - P_{m,i}}{\sigma_{P,i}} \right)^2 + \sum_{j=1}^{NC-1} \left(\frac{x_{e,i,j} - x_{m,i,j}}{\sigma_{x,i,j}} \right)^2 + \sum_{j=1}^{NC-1} \left(\frac{y_{e,i,j} - y_{m,i,j}}{\sigma_{y,i,j}} \right)^2 \right] \quad 7-1$$

Where:

Q	=	Objective function to be minimized by data regression
NDG	=	Number of data groups in the regression case
w_n	=	Weight of data group n
NP	=	Number of points in data group n
NC	=	Number of components present in the data group
T, P, x, y	=	Temperature, pressure, liquid and vapour mole fractions
e	=	Estimated data
m	=	Measured data
i	=	Data for data point i
j	=	Fraction data for component j
σ	=	Standard deviation of the indicated data

The objective function, Q, is minimized by manipulating the physical property parameters selected for the regression case and consequently manipulating the estimated value corresponding to each measurement. Different phase equilibrium data sets can be assigned different weights in the data regression case in order to highlight the importance of certain characteristics of the component system in question.

To assess the ability of the models to predict experimental data with these regressed parameters, the predicted phase equilibrium data needs to be compared to the experimental data. This can either be done visually by means of a ternary phase diagram or mathematically by means of descriptive statistics. In this work both these methods are used. The accuracy of the models (utilizing the regressed parameters) is quantified statistically by the average absolute deviation (AAD) and the average absolute relative deviation (AARD %) from the experimental data. Equations 7-2 and 7-3 present the formulas of AAD and AARD respectively (Lee, Shen 2003).

$$AAD = \frac{1}{N_T} \sum_{i=1}^{N_T} |x_{calculated} - x_{measured}| \quad 7-2$$

$$AARD \% = \frac{100}{N_T} \sum_{i=1}^{N_T} \left| \frac{x_{calculated} - x_{measured}}{x_{measured}} \right| \quad 7-3$$

Unlike variance and standard deviation, AAD does not square the distance from the mean and is therefore less affected by extreme observations. AARD is similar to AAD, but it also takes the relative size of each data point into account.

To summarize, the adjustable binary interaction parameters of selected thermodynamic models were determined with Aspen DRS using the maximum likelihood objective function. The predictability of these parameters was evaluated with AAD and AARD % from experimental data.

7.2 SEPARATION SEQUENCE

This section explains the approach to simulating a heterogeneous azeotropic distillation separation sequence, as discussed in Section 2.5.2. The aforementioned sequence pertained to ethanol dehydration utilizing benzene as entrainer. A more generalized sequence is used as a basis for all the simulations performed in this work.

The typical ternary phase diagram (Figure 7-1) for heterogeneous azeotropic distillation consists of homogeneous minimum-boiling azeotropes between the alcohol and water, and the alcohol and entrainer. A ternary heterogeneous minimum-boiling azeotrope is also formed and enables crossing of the distillation boundaries.

A typical separation sequence is shown in Figure 7-2. This sequence was chosen for its simplicity as the goal is only to illustrate how heterogeneous azeotropic distillation can be performed in practice, not to find the optimum separation sequence. The interested reader may be referred to other texts (Luyben, Chien 2010, Wang et al. 2008) pertaining to more complex sequences and determining an optimum flow sheet.

The separation sequence considered in this work consists of two distillation columns (an azeotropic column and a recovery column) and a decanter. The material balance lines of this separation sequence are shown by grey dashed lines in Figure 7-1 and the distillation lines by grey solid lines. These can be used to follow the conceptual design of the sequence. The first column is fed with an aqueous ethanol feed stream, organic reflux from the decanter as well as the distillate of the recovery column. This column produces nearly pure ethanol as bottoms and if a mass balance is performed over the system, essentially all alcohol fed in the feed stream needs to be removed through the bottoms of the first column. This can be used as column specification in Aspen Plus. The desired purity of the alcohol stream depends on downstream specifications. For the purpose of this work a purity of 98% is assumed.

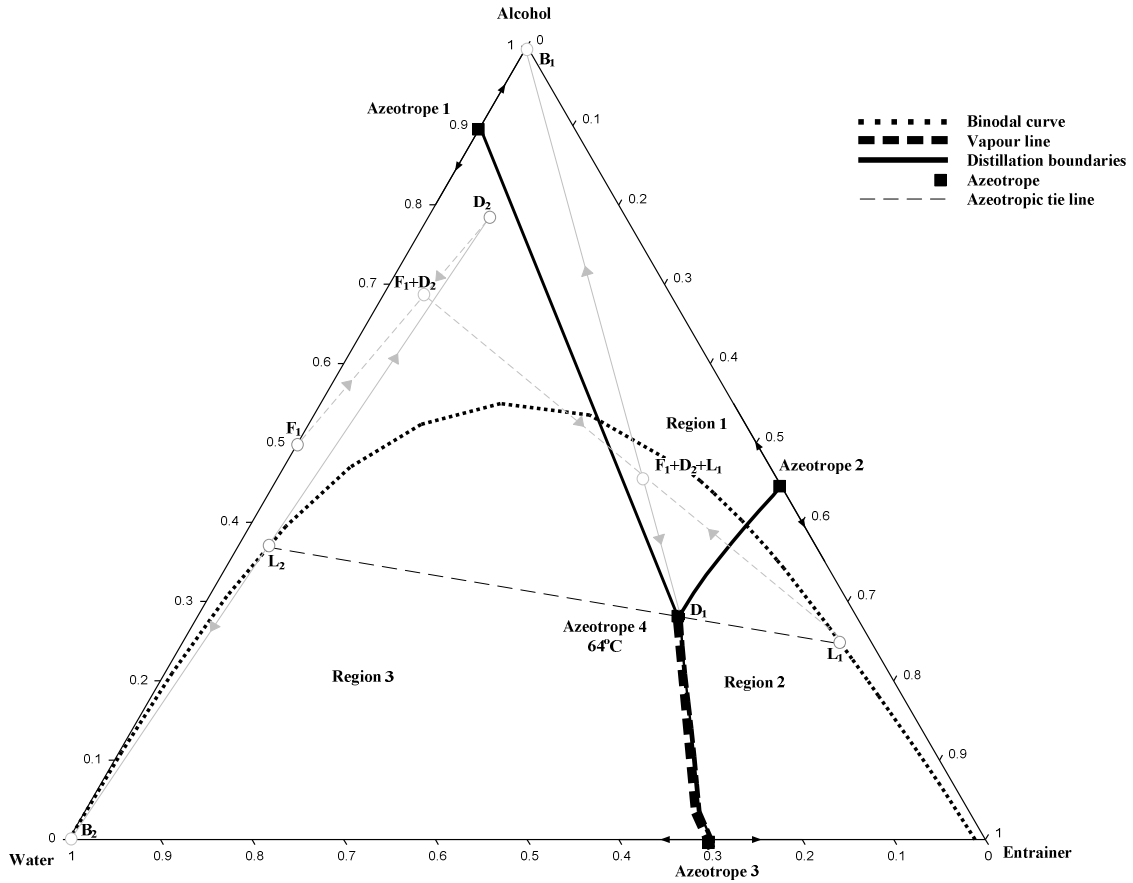


Figure 7-1: Typical ternary phase diagram with liquid-liquid equilibrium phase envelope, vapour line and distillation boundaries of an alcohol-water-entrainer system.

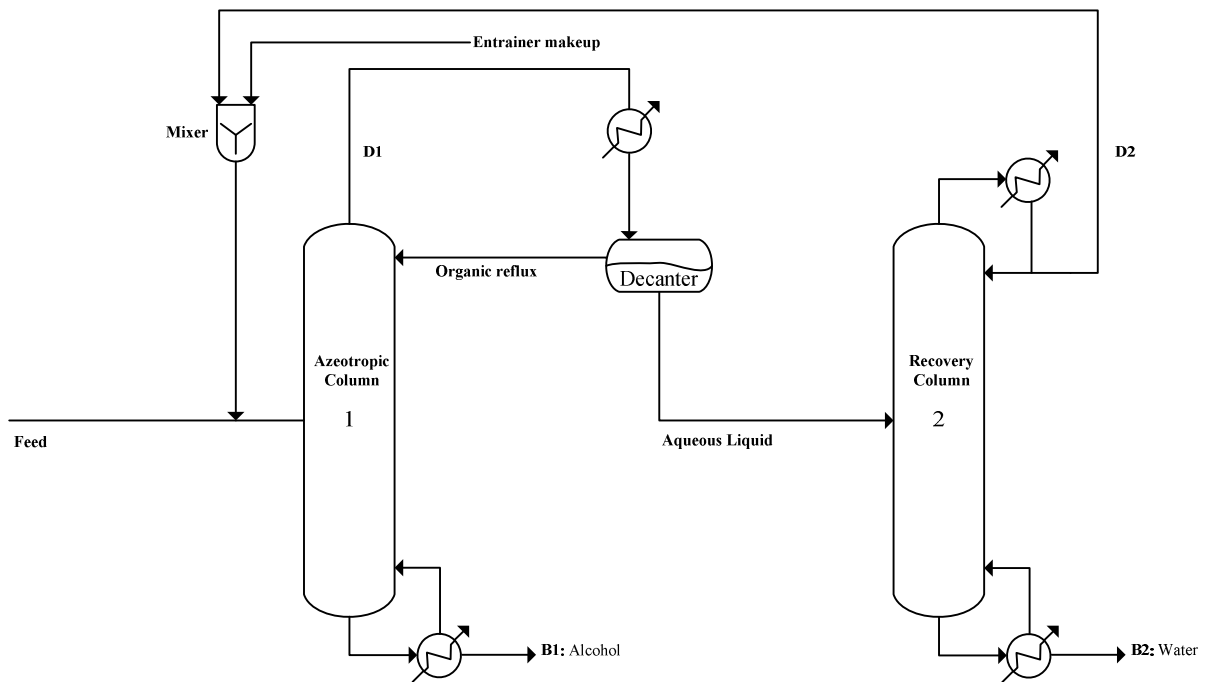


Figure 7-2: Typical separation sequence for heterogeneous azeotropic distillation

The composition of the distillate of the first column will be close to that of the ternary heterogeneous azeotrope (D_1). The azeotropic distillate is subsequently separated into an organic-rich (L_1) and water-rich (L_2) phase in the decanter. The compositions of these phases can be obtained from the phase equilibrium data of the ternary system. The organic-rich phase is refluxed to the first column, and fed together with fresh feed stream and recycled distillate from the second column ($L_1 + F_1 + D_2$). The composition of the organic reflux stream can be used as specification in Aspen when simulating this separation sequence. The water-rich phase is fed to the second column. Considering the recovery column, nearly pure water is produced as bottoms (B_2) and a distillate of ethanol, benzene and water (D_2). Adhering to mass balance rules, essentially all the water fed to the azeotropic column has to be removed as bottoms in the recovery column. This can be used as column specification for the second column in Aspen Plus.

When constructing the flow sheet the following design variables need to be selected:

- Number of column stages
- Feed stages of each column
- Alcohol composition of stream D_2

The number of column stages and feed stage of each column are selected and fixed for the simulation. A mass balance, as indicated in grey on Figure 7-1, is performed to initially guess the composition of D_2 . The composition of D_1 , L_1 and L_2 are known from phase equilibrium. The feed composition (F_1) is specified to be 50% alcohol and 50% water. Streams B_1 and B_2 are assumed to be nearly pure alcohol and water respectively. With all these variables known or estimated, an initial value for the composition of D_2 can be determined. The bottoms flow rates of both columns are then manipulated to achieve an alcohol purity of 98 mole % and a water purity of 99.99 mole % in B_1 and B_2 respectively, by manipulating the compositions and flowrates of streams L_1 and D_2 .

The purpose of simulating this separation sequence in Aspen for different alcohols and entrainers is to compare the efficiency of entrainers. By performing two simulations with the same alcohol, entrainer and thermodynamic model, but with different binary parameters, it can also be shown how the regression of parameters on experimental phase equilibrium data influences the results obtained in the separation sequence. These simulations are therefore not performed to find an optimum flow sheet, but merely used as a tool to evaluate entrainers and the binary interaction parameters regressed from experimental VLLE data.

8 RESULTS AND DISCUSSIONS

8.1 VERIFICATION

In order to verify the experimental set-up and method, measured data were compared to published results. Verification was done on one binary VLE system (ethanol/isooctane) and three ternary VLLE systems (Isopropanol/Isooctane/Water, Isopropanol/DIPE/Water and Ethanol/n-Butanol/Water). The marker size of each data point on the diagrams in this chapter is specifically selected through a sensitivity analysis to account for the accuracy of the phase equilibrium equipment. The vapour pressures of the pure components used were also measured in the apparatus. The results can be seen in Appendix C, Figures C-1 to C-5. From these figures it is clear that the measured vapour pressures agree with various literature data available in the NIST data bank in Aspen Plus and the NIST Wagner 25 Liquid Vapour Pressure Equation. Parameters fitted to these data (Appendix F, Table F-1), predict the vapour pressures well.

8.1.1 Binary VLE: Ethanol/Isooctane

The Ethanol/Isooctane system was selected for the verification of binary VLE measurement. A non-aqueous system was selected to simplify the analysis, i.e. only GC analysis was required (not Karl Fischer as well). Two sets of reliable published data (Hiaki et al. 1994, Ku, Tu 2005) are available for Ethanol/Isooctane and the activity coefficient model, NRTL adequately predicts the published data. The data measured in this work compares well visually, with published data and the NRTL prediction (Figures 8-1 and 8-2).

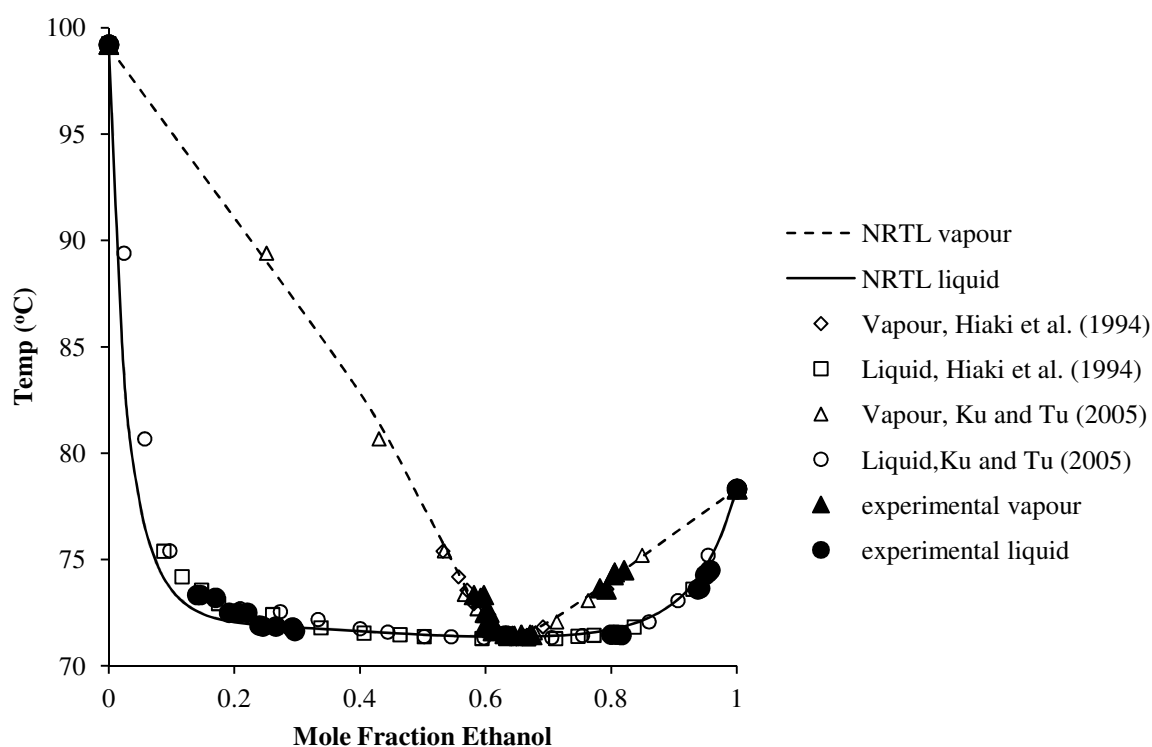


Figure 8-1: Binary T-x-y phase diagram of measured Ethanol/Isooctane VLE data at 101.325 kPa, compared to data published by Haiki et al. (1994) and Ku and Tu (2005) and to the thermodynamic model NRTL.

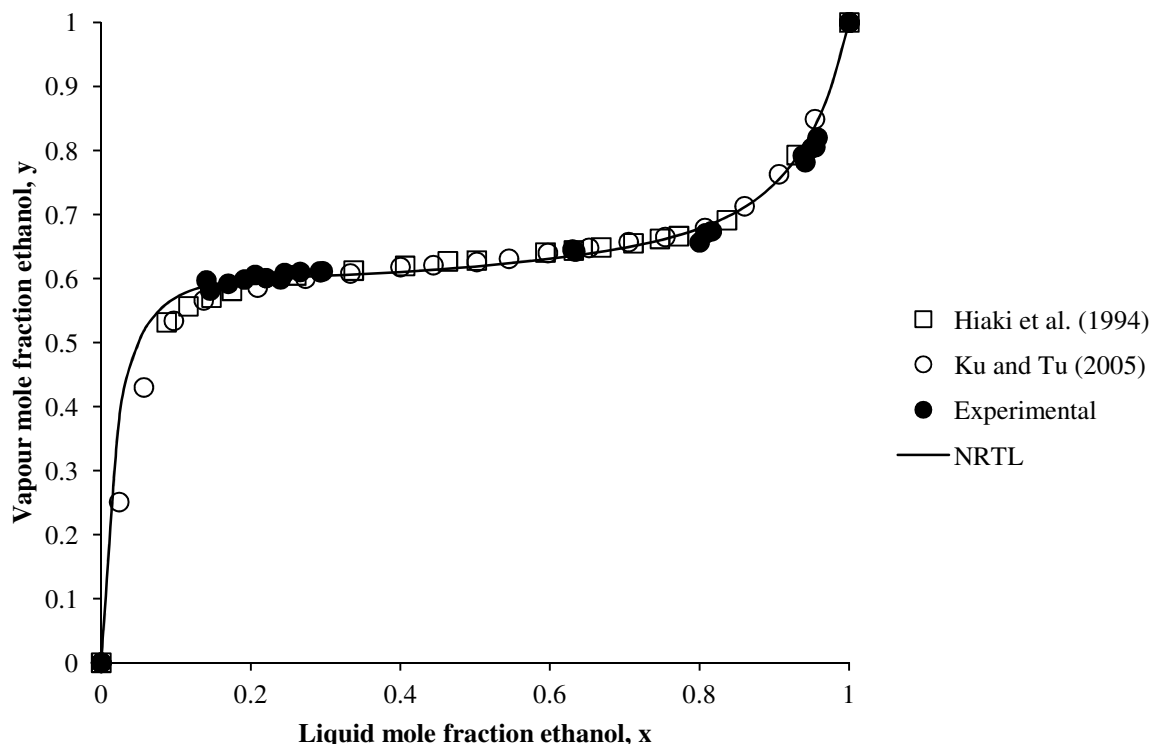


Figure 8-2: Binary x-y phase diagram of measured Ethanol/Isooctane VLE data at 101.325 kPa, compared to data published by Haiki et al. (1994) and Ku and Tu (2005) and to the thermodynamic model NRTL

Table 8-1 quantitatively indicates that the binary VLE data measured in this work, for equipment verification, compares well with the published data and the NRTL prediction. All AAD and AARD % values are similar, if not equal, to that of the published data. Both sets of literature data, as well as the data measured in this work, also adhere to the Herington area test for thermodynamic consistency. The Herington area test is passed by producing a plot of $\ln \frac{y_1}{y_2}$ against x for the measured data, where the area above the zero line and area below the zero line are more or less equal in size (see Tables D-1 and D-2, and Figures D-1 and D-2 in Appendix D).

Table 8-1: AAD and AARD % values for VLE of Ethanol/Isooctane, measured in this work and found in literature, compared to activity coefficient model NRTL with built-in Aspen parameters at 101.325 kPa.

	Temp (°C)	x_{ethanol}	$x_{\text{isooctane}}$	y_{ethanol}	$y_{\text{isooctane}}$
This work					
AAD	0.2951	0.0000	0.0000	0.0098	0.0107
AARD %	0.09	0.00	0.02	1.35	3.64
Hiaki et al. (1994)					
AAD	0.2986	0.0000	0.0000	0.0094	0.0094
AARD %	0.09	0.01	0.00	1.49	2.27
Ku and Tu (2005)					
AAD	0.6031	0.0000	0.0000	0.0187	0.0187
AARD %	0.17	0.04	0.01	4.65	3.73

8.1.2 Ternary VLLE: IPA/Isooctane/Water

The IPA/Isooctane/Water system was selected for the verification of ternary VLLE measurements. IPA/Isooctane/Water was chosen for its similarity to the systems selected for new data measurements. The published VLLE data (Font et al. 2004) available for this system have been measured with an all-glass dynamic recirculating still fitted with an ultrasonic homogenizer. Font et al. (2004) analysed their vapour samples on an online GC with a thermal conductivity detector (TCD) on a column packed with Porapak 80/100. Their organic liquid samples were also analysed with TCD and the water content was determined through Karl Fischer analysis. This was probably done due to the inaccuracy with which TCD determines water content and in the organic liquid samples the water content would be very small. Water analysed with TCD tends to form a peak with an undefined base on a chromatogram (Shimadzu 2011). This makes integration of the peak, to quantify the water content, difficult. It can also prevent sufficient separation of the various components in the sample, on the GC column. The aqueous liquid samples were only analysed on a GC with FID and the water content was calculated with a mass balance. As explained in Section 6.4, online vapour sampling was not used in this work. Since FID tends to give more accurate results and FID cannot detect water, the samples had to undergo two types' of analyses and would be unsuitable for online sampling. Therefore all the samples in this work were analysed on a GC with FID to quantify the non-aqueous components, and with Karl Fischer Titration to determine the water content of each sample.

The organic liquid phase of the measured data is in agreement with the published data (Figure 8-4). The vapour phase of the measured data lies in the same area of the ternary phase diagram as the published data, but is more scattered. The aqueous liquid phase of the measured data does not compare well with the published data, but seems to agree with the UNIFAC (parameters based on LLE) prediction. Other thermodynamic models, such as NRTL and UNIQUAC, all predict larger phase envelopes than UNIFAC and were therefore not included in Figure 8-4. The discrepancy might be explained by the fact that Font et al. (2004) determined the water content of the aqueous liquid samples through mass balance and not Karl Fischer Titration. To test this theory, the aqueous liquid phase compositions measured in this work was altered by keeping the ratio of isooctane to IPA in each sample constant and calculating a different water composition. The results are given in Figure 8-6. This confirms that the discrepancy can definitely be attributed to the fact that Font et al. (2004) did not perform Karl Fischer analyses on their aqueous liquid phase samples. The measured tie lines agree with the published tie lines to some extent, but vary increasingly as the plait point is approached (Figure 8-5). Both the measured and published tie lines disagree with those predicted by UNIFAC. The tie lines predicted by NRTL and UNIQUAC disagreed with the measured and published data even more than those predicted by UNIFAC. Therefore these predictions were not included in Figure 8-5. Due to these uncertainties further verification of ternary VLLE had to be performed.

8.1.3 Ternary VLLE: IPA/DIPE/Water

IPA/DIPE/water was the second system selected for ternary VLLE measurement verification. The published data (Lladosa et al. 2008) for this system have also been measured with an all glass dynamic re-circulating still fitted with an ultrasonic homogenizer, but was not done by the same research group that published the IPA/Isooctane/Water VLLE data. As IPA/DIPE/water is also similar to components set out for measured in this work, it was thought suitable for verification. Lladosa et al. (2008) also analysed their vapour samples on an

online GC with a thermal conductivity detector (TCD) on a column packed with Porapak 80/100. All their samples were analysed on a GC with TCD and no Karl Fischer titrations were performed.

Both the measured organic and aqueous liquid phases compare well with the published data (Figure 8-7) and are accurately predicted by UNIFAC (parameters based on LLE). The measured tie lines agree well with the published data and are adequately predicted by UNIFAC (Figure 8-8). The measured vapour phase however, does not agree with the published data (Figure 8-9) and neither the measured nor the published vapour phase data are in complete agreement with the prediction from thermodynamic models. The discrepancies between the data measured in this work and that of Lladosa et al. (2008) might also be explained by the fact Karl Fischer Titration was additionally used to determine water content in this work. This might especially affect the vapour phase, since such samples tend to be much smaller than liquid phase samples, even more so when taken in the gaseous state. Due to the inconsistency of the vapour phase data, yet another ternary system had to be tested for VLLE verification.

8.1.4 Ternary VLLE: Ethanol/1-Butanol/Water

The last system selected for ternary VLLE verification was Ethanol/1-Butanol/Water. Two sets of published data are available for this system. The first has been measured by Newsham and Vahdat (1977) using the flow method. Newsham and Vahdat (1977) also analysed their samples on a GC with a column packed with Porapak 80/100. No additional analyses were performed to determine the water content of the samples. The second (Gomis, Ruiz & Asensi 2000) has been measured by the same research group that published the IPA/Isooctane/Water VLLE data, using an all glass dynamic recirculating still fitted with an ultrasonic homogenizer and the same analysis techniques. The two sets of published data are in agreement, (although different phase equilibrium equipment were used) and were therefore considered a suitable system to test for verification.

Figure 8-3 illustrates the repeatability and accuracy to which the phase equilibria experiments were performed.

The two organic liquid and aqueous liquid data points cannot be distinguished on the diagram. As stated in the introduction of this section, the marker size of the data points is specifically selected through a sensitivity analysis to account for the uncertainties of the equipment used. These two points were measured in two independent experimental runs. The temperature of the two data points differ by 0.02 °C, within the 0.03 °C uncertainty of the Pt-100's. These two data points are therefore considered repeatable. The accuracy of the data point were tested by taking an overall liquid sample (a mixture of the two liquid phases). According to mass balance rules, this overall sample should therefore lie on the tie line between the organic and aqueous liquid phase if the latter are accurate. This is the case with the two samples in Figure 8-3 and the data is therefore considered accurate.

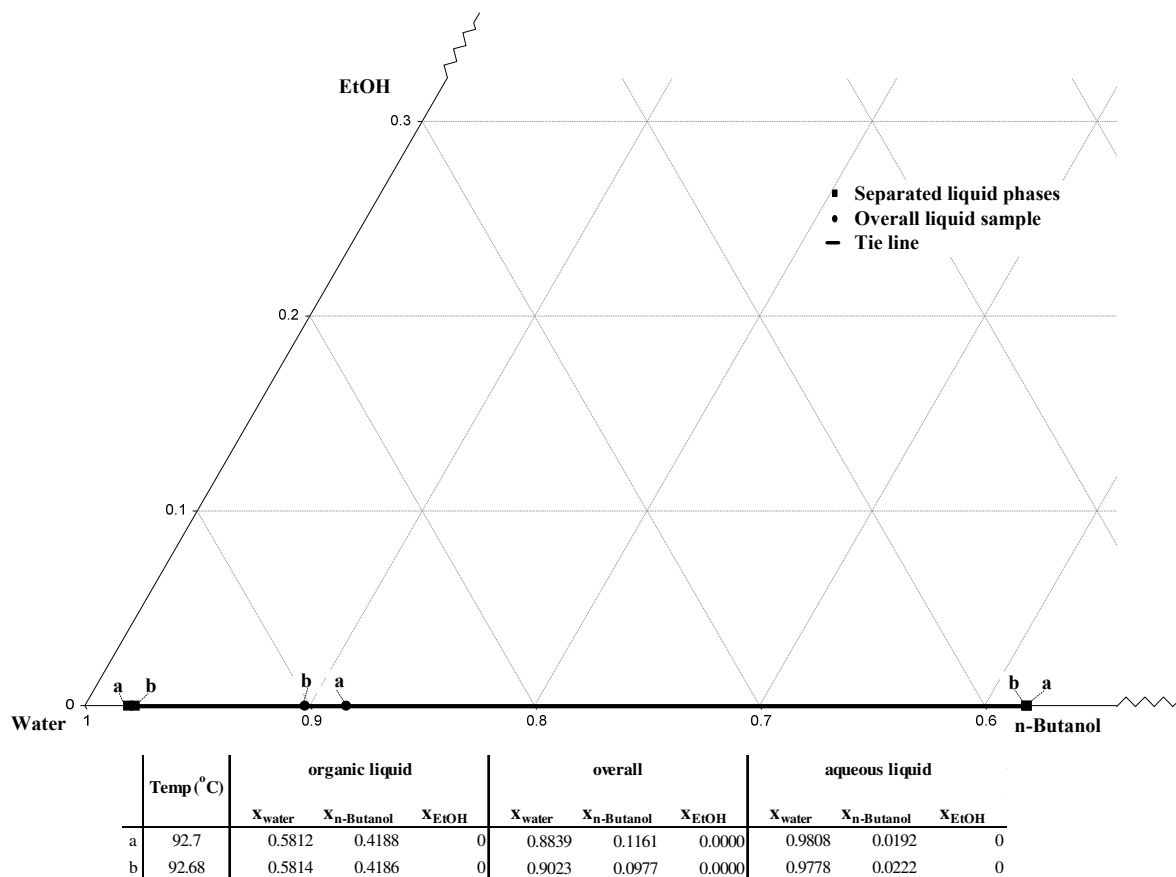


Figure 8-3: Illustration of repeatability and accuracy

The measured vapour, organic liquid and aqueous liquid phases of the ternary system all agree well with both sets of published data (Figure 8-10). The phase envelope description in the legend of Figure 8-10 refers to both liquid phases. The liquid phases are described together in this manner to simplify the diagram, but one can easily distinguish between the organic liquid phase and aqueous counterpart by considering the grouping of the data points. None of the thermodynamic models (NRTL, UNIFAC and UNIQUAC) accurately predicted the published or measured data and were therefore not included in Figure 8-10. The satisfactory measured results concluded the verification of the experimental set-up and method.

To recap, the apparatus used in this work was verified for both binary VLE and ternary VLLE. For binary VLE verification ethanol/isooctane was measured and the results are in agreement with two sets of published data (Hiaki et al. 1994, Ku, Tu 2005). The apparatus was verified for ternary VLLE by data measurements of the ethanol/n-butanol/water system. The data also compared well with two sets of published data (Gomis, Ruiz & Asensi 2000, Newsham, Vahdat 1977).

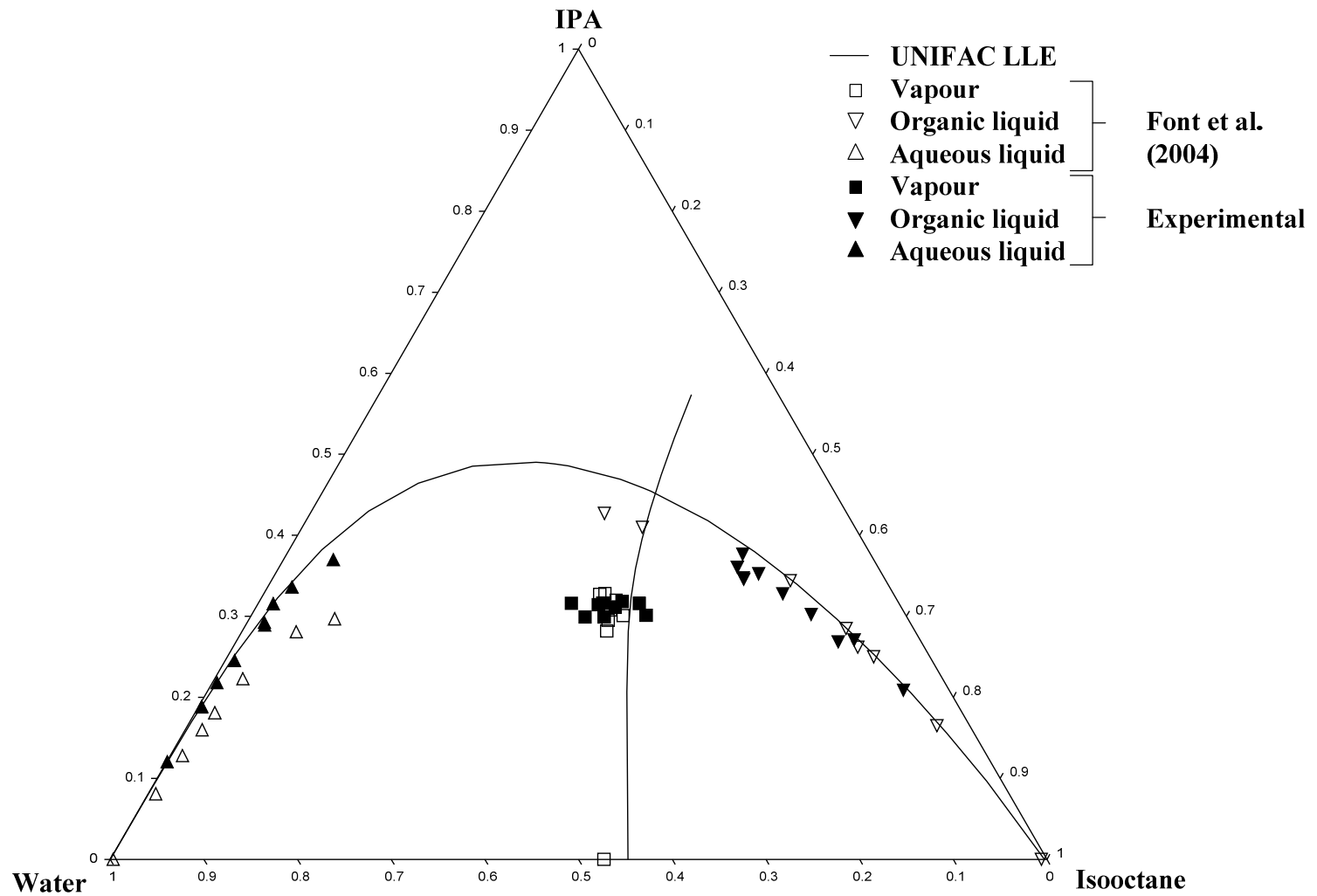


Figure 8-4: Ternary phase diagram of measured IPA/Isooctane/Water VLE data at 101.325 kPa, compared with data published by Font et al. (2004) and the thermodynamic model UNIFAC (parameters based on LLE).

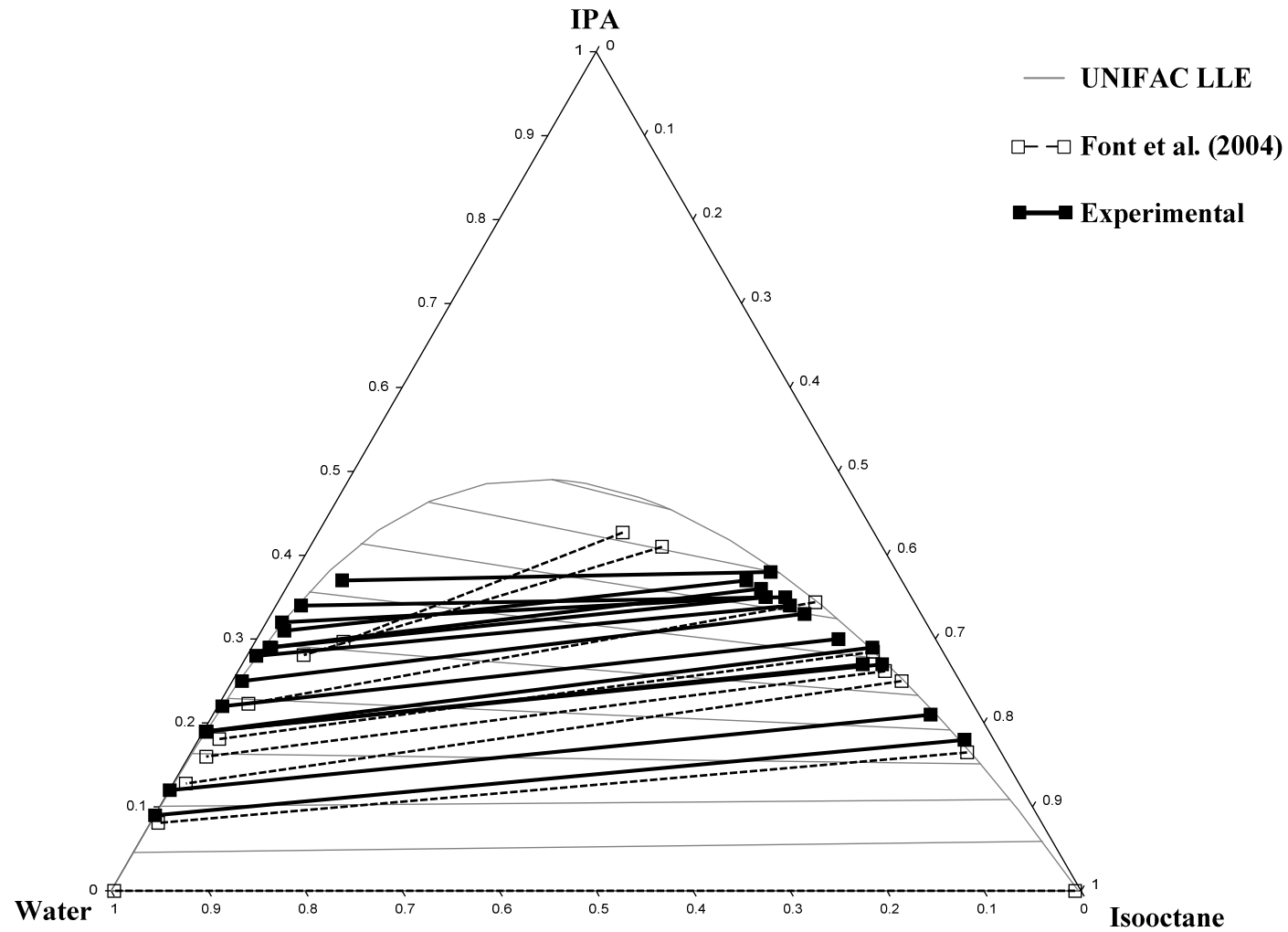


Figure 8-5: Ternary phase diagram of measured IPA/Isooctane/Water tie lines at 101.325 kPa, compared with data published by Font et al. (2004) and the thermodynamic model UNIFAC (parameters based on LLE).

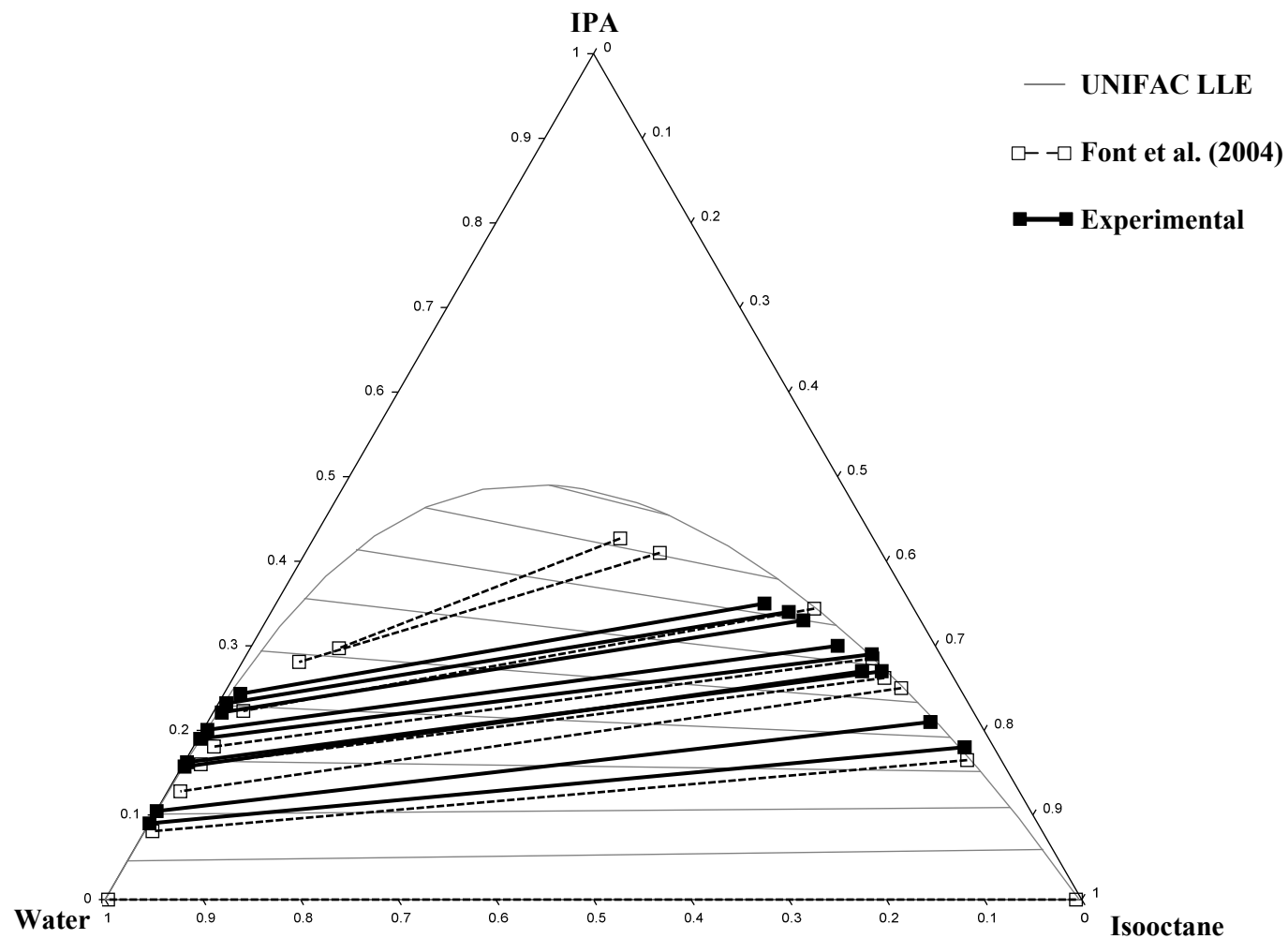


Figure 8-6: Ternary phase diagram of measured IPA/Isooctane/Water tie lines (with corrected aqueous liquid phase compositions) at 101.325 kPa, compared with data published by Font et al. (2004) and the thermodynamic model UNIFAC (parameters based on LLE).

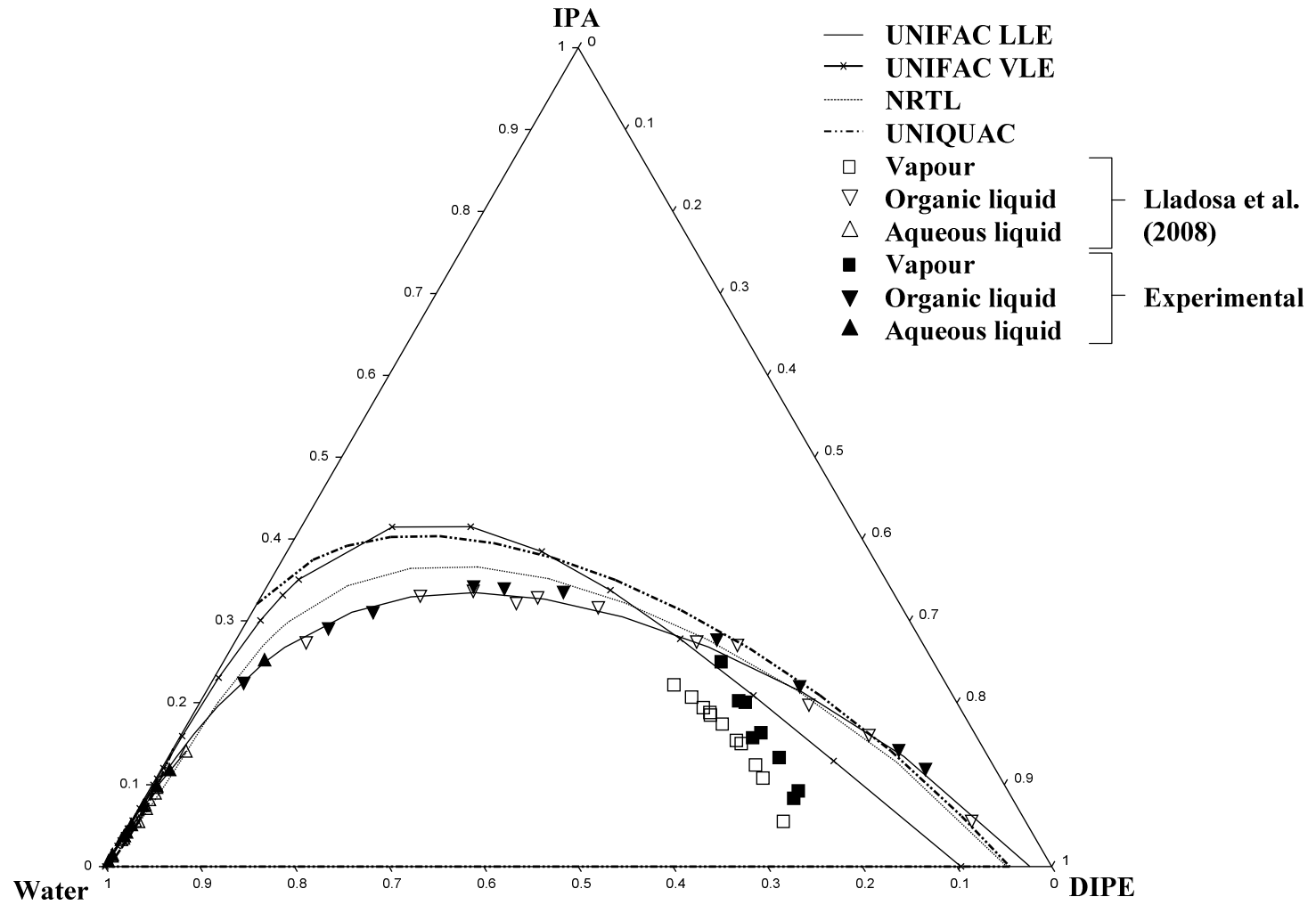


Figure 8-7: Ternary phase diagram of measured IPA/DIPE/Water VLLE data at 101.325 kPa, compared with data published by Lladosa et al. (2008) and the liquid phases of thermodynamic models NRTL and UNIQUAC.

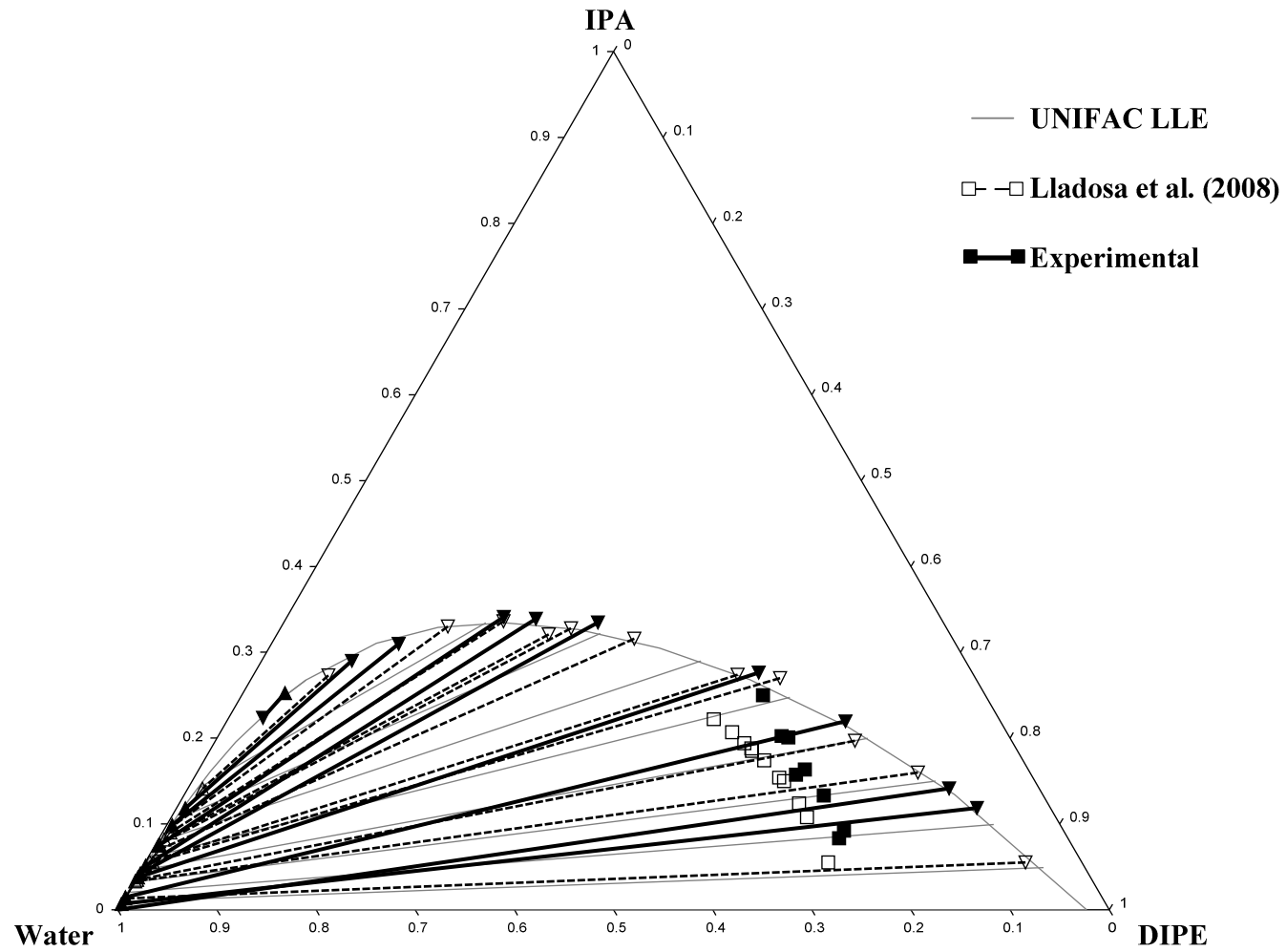


Figure 8-8: Ternary phase diagram of measured IPA/DIPE/Water tie lines at 101.325 kPa, compared with data published by Lladosa et al. (2008) and the thermodynamic model UNIFAC (parameters based on LLE).

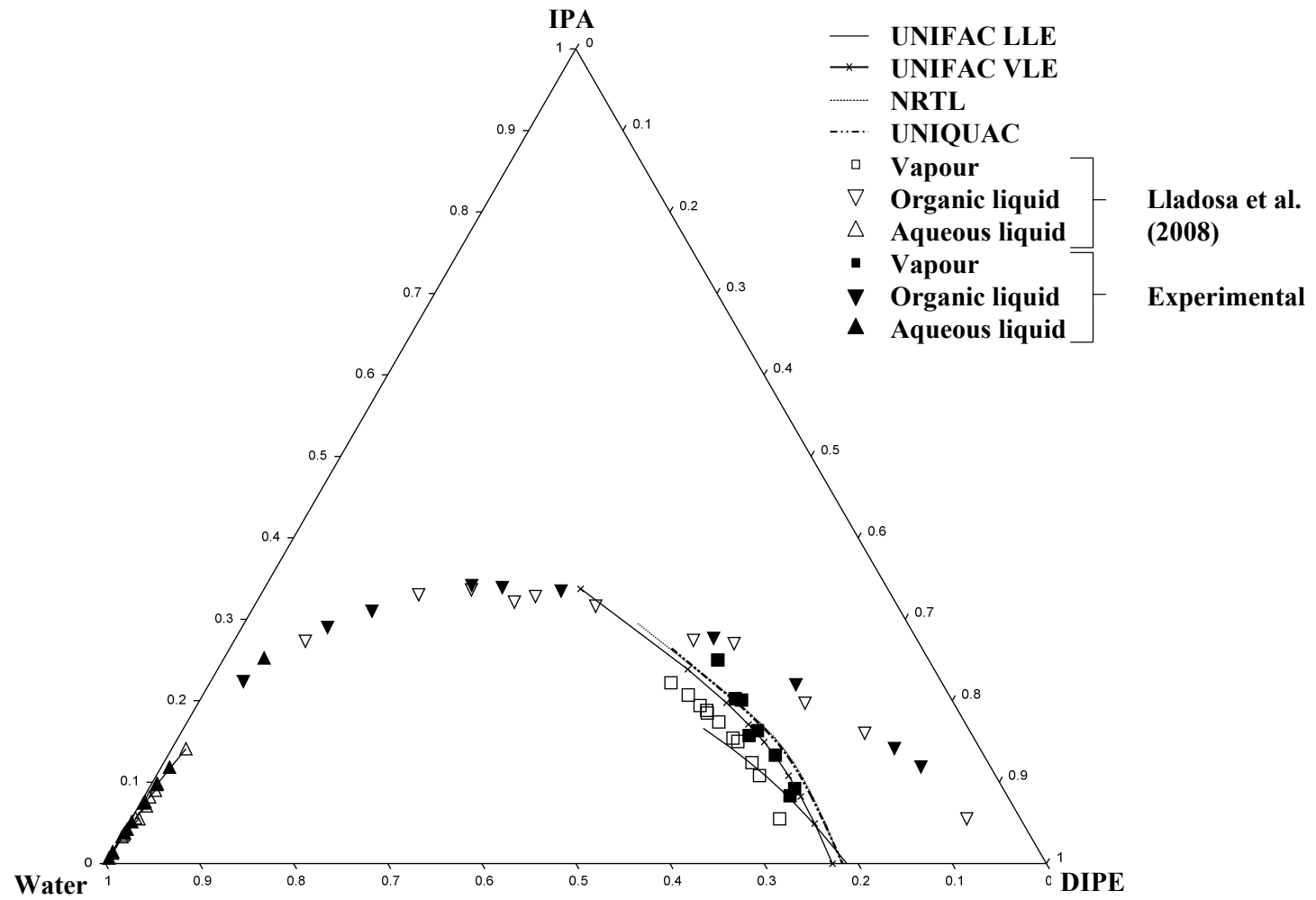


Figure 8-9: Ternary phase diagram of measured IPA/DIPE/Water VLLE data at 101.325 kPa, compared with data published by Lladosa et al. (2008) and the vapour phase of thermodynamic models NRTL and UNIQUAC.

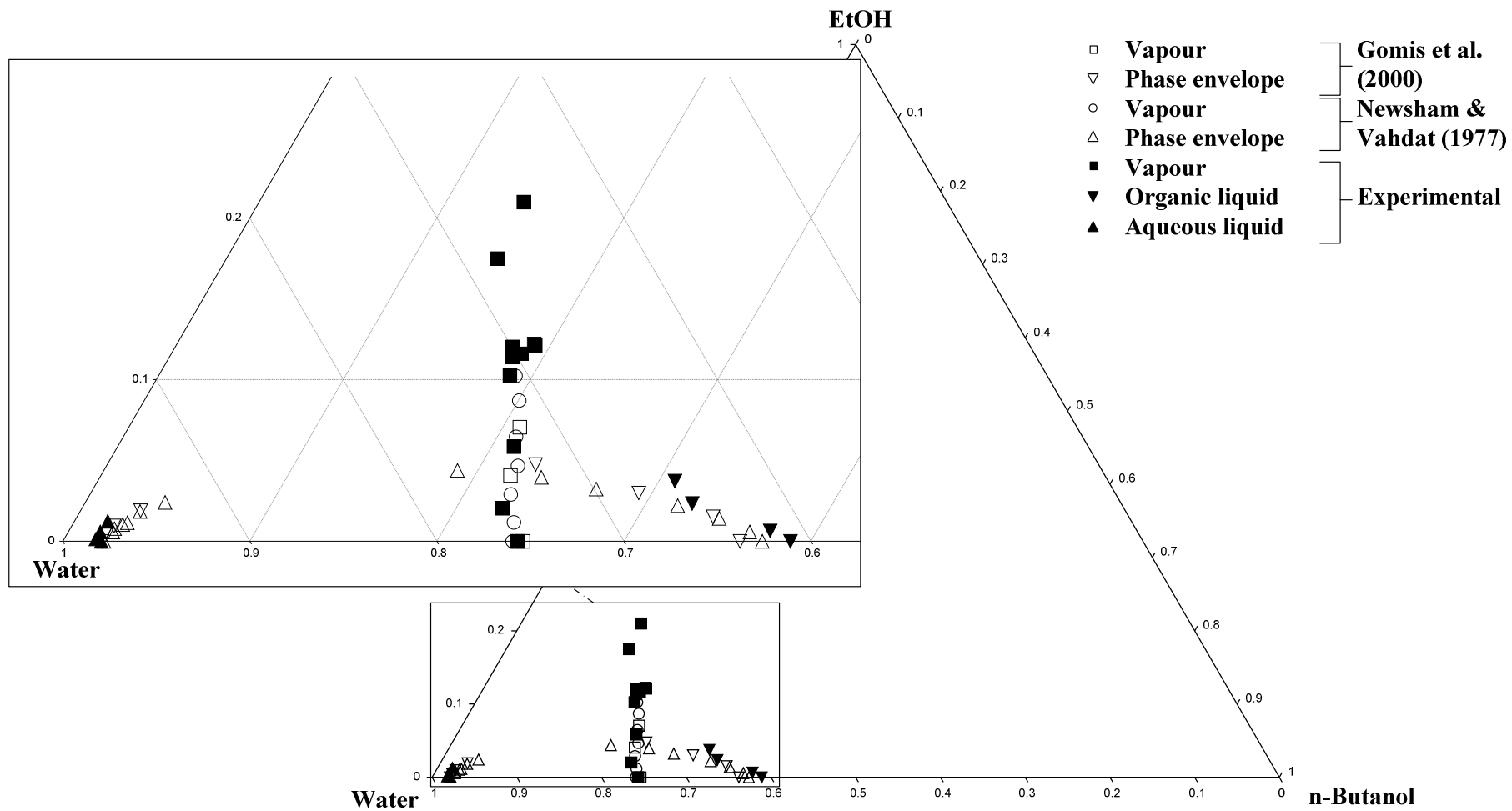


Figure 8-10: Ternary phase diagram of measured Ethanol/n-Butanol/Water VLE data at 101.325 kPa, compared with data published by Newsham and Vahdat (1977) and Gomis et al. (2000).

8.2 NEW PHASE EQUILIBRIUM DATA

In this section the results of the new phase equilibrium measurements and the discussion thereof are provided. As discussed in Section 5.3, the systems studied are ethanol/DIPE/water, n-propanol/DIPE/water and n-propanol/isooctane/water. The ternary heterogeneous azeotropes, calculated from the measured results, are also reported in this section.

Tables with the experimental measurements are included in Appendix C.

8.2.1 Ethanol/DIPE/Water VLLE and VLE

The measured VLLE and VLE data of the system Ethanol/DIPE/Water are plotted in Figures 8-11 and 8-12, respectively. The phase equilibrium data is tabulated in Appendix C in Tables C-5 and C-6. The VLE data were tested for thermodynamic consistency with L-W consistency test as well as the McDermott-Ellis consistency test. The data were found to be thermodynamically consistent. All D values for the L-W test were smaller or equal to 0.647, thus lower than 3 to 5. All D values for the McDermott-Ellis test were smaller than D_{\max} and therefore proved thermodynamic consistency. The liquid phases of the VLLE data were checked for regularity with the Othmer-Tobias correlation and were found to have a regular course, with an r value of 0.991. Detailed tabulated parameter input and results from the L-W test and McDermott-Ellis test calculations are given in Appendix D. The graphical results from the Othmer-Tobias correlation are shown in Appendix E.

Figure 8-13 graphically indicates the existence of a ternary heterogeneous azeotrope. In the upper part of the phase envelope, from temperature 62.07°C to 61.10°C, the organic liquid phase composition lies above that of the corresponding vapour phase. In the lower part of the phase envelope, temperature 61.01°C to 62.16°C, the organic liquid phase composition lies below that of the corresponding vapour phase. This shows that between the points 61.10°C and 61.01°C there is a point upon which the compositions of the aqueous liquid, vapour and organic liquid phases form a straight line. From the lever rule it can be proved that the over-all composition of the aqueous and organic liquid phases on this straight line will be equal to the vapour phase composition, hence the ternary heterogeneous azeotrope exists at this point. The composition and temperature of the ternary azeotrope is determined via numerical interpolation. The result is given in Table 8-2 along with the binary azeotrope for DIPE/Water, measured in this work, and other relevant azeotropic data from literature. The composition of the ternary heterogeneous azeotrope is similar to that compiled by Horsley and Tamplin (1962). Horsley and Tamplin do not supply any information with regard to how the ternary azeotrope they report is measured and the source they give is not available in open literature. It is therefore difficult to explain any differences that might exist. The composition of the binary DIPE/Water azeotrope compares well with the data reported by Lladosa et al. (2008) and Verhoeve (1970) and those compiled by Gmehling et al. (1994).

Table 8-2: Temperature and composition of ternary and binary azeotropes measured for Ethanol/DIPE/Water at 101.325 kPa

Temp (°C)	Composition			Reference
	y_{water}	y_{DIPE}	y_{EtOH}	
61.00	0.1791	0.7070	0.1139	Horsley and Tamplin (1962)
61.04	0.1964	0.6659	0.1377	This work
61.90	0.2480	0.7520	-	Lladosa et al. (2008)
62.16	0.2186	0.7814	-	This work
62.50	0.2200	0.7800	-	Verhoeve (1970)
62.20	0.2147	0.7853	-	Gmehling et al. (1994)
63.00	0.2100	0.7900	-	
78.17	0.0963	-	0.9037	Horsley and Tamplin (1952)
78.00	0.1000	-	0.9000	Gmehling et al. (1994)
78.10	0.1100	-	0.8900	
78.10	0.1090	-	0.8910	
78.10	0.1053	-	0.8947	
78.10	0.1000	-	0.9000	
78.10	0.1030	-	0.8970	
78.12	0.1050	-	0.8950	
78.13	0.1055	-	0.8945	
78.15	0.1060	-	0.8940	
78.15	0.1057	-	0.8943	
78.15	0.1020	-	0.8980	
78.15	0.1000	-	0.9000	
78.16	0.1047	-	0.8953	
78.16	0.0970	-	0.9030	
78.17	0.1067	-	0.8933	
78.17	0.0990	-	0.9010	
78.17	0.0963	-	0.9037	
78.18	0.1100	-	0.8900	
78.18	0.1070	-	0.8930	
78.19	0.1060	-	0.8940	
78.20	0.1100	-	0.8900	
78.20	0.1060	-	0.8940	
78.20	0.0950	-	0.9050	
78.30	0.1060	-	0.8940	
64.00	-	0.6820	0.3180	Benito and Lopez (1992)

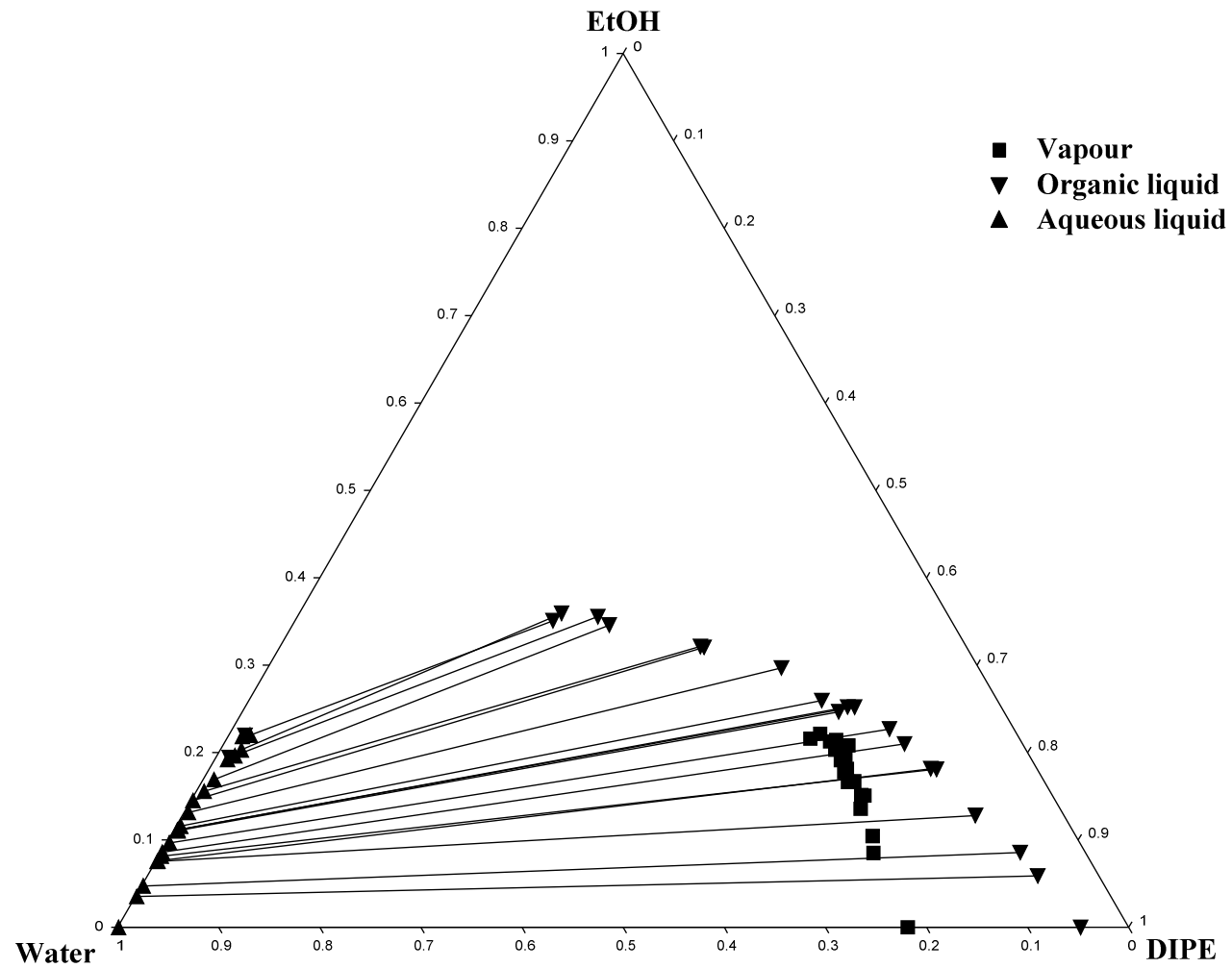


Figure 8-11: Ternary phase diagram of measured Ethanol/DIPE/Water VLE data at 101.325 kPa

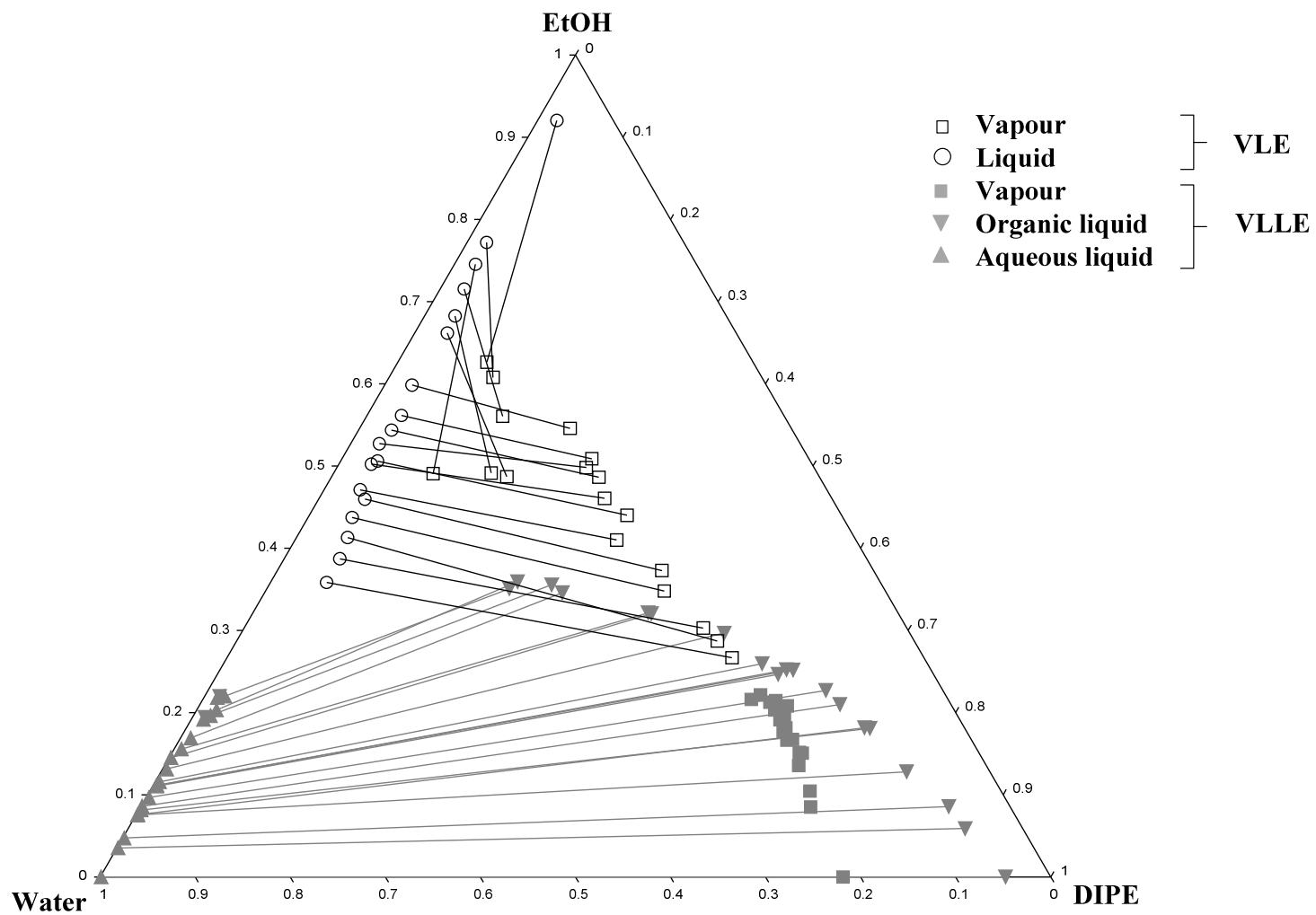


Figure 8-12: Ternary phase diagram of measured Ethanol/DIPE/Water VLE data at 101.325 kPa

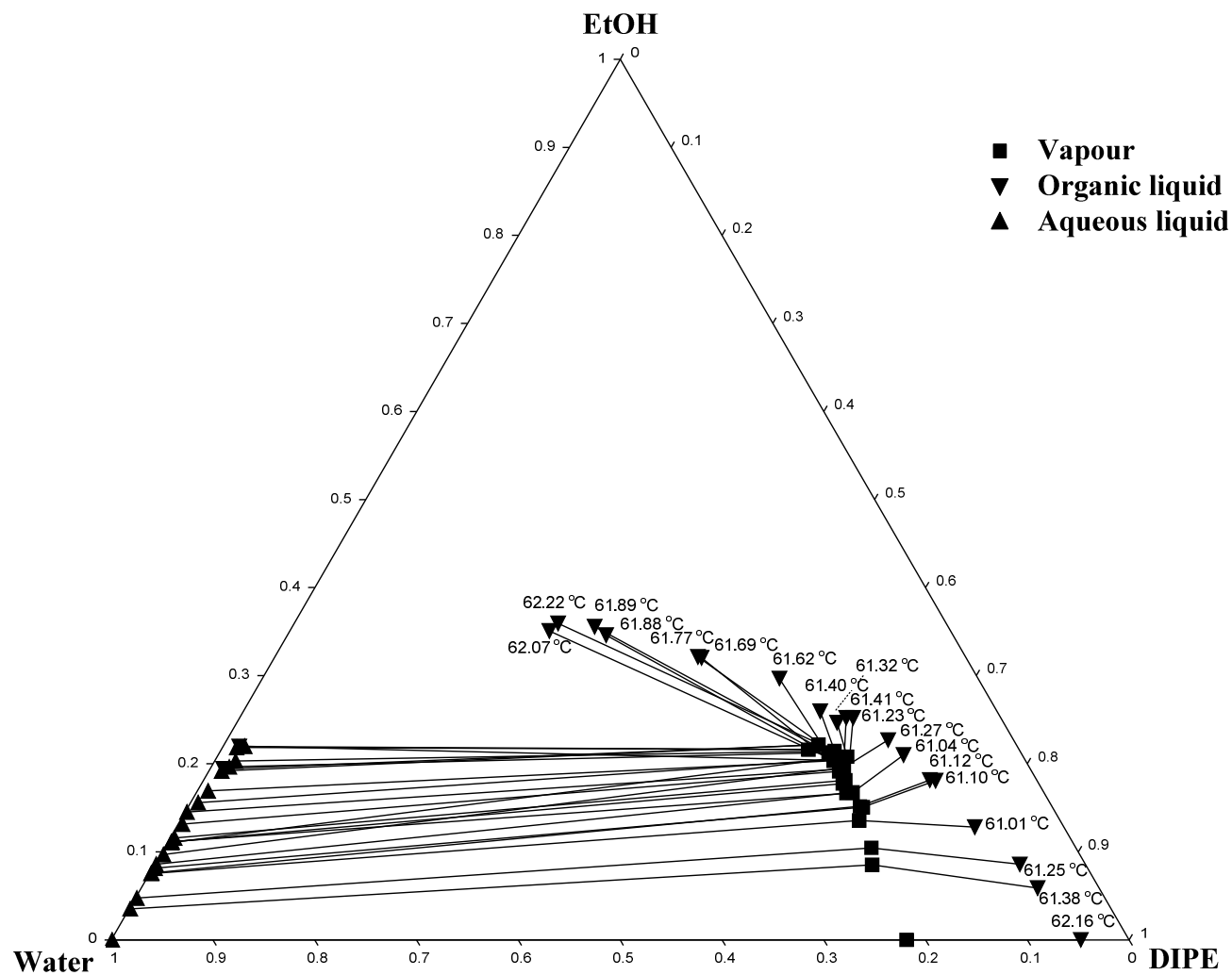


Figure 8-13: Ternary phase diagram for the calculation of the heterogeneous ternary azeotrope from measured Ethanol/DIPE/Water VLE data at 101.325 kPa

8.2.2 n-Propanol/DIPE/Water VLLE and VLE

VLLE and VLE measurements of the system n-Propanol/DIPE/Water are plotted in Figures 8-14 and 8-15, respectively. The VLLE and VLE data are tabulated in Appendix C in Tables C-7 and C-8 respectively. The VLE data passed the L-W consistency test as well as the McDermott-Ellis consistency test and were proven to be thermodynamically consistent. All D values for the L-W test were smaller or equal to 0.350, thus lower than 3 to 5. All D values for the McDermott-Ellis test were smaller than D_{\max} and the data are therefore proved thermodynamic consistent. The liquid phases of the VLLE data were checked for regularity with the Othmer-Tobias correlation and were found to have a regular course, with an r-value of 0.992. Detailed tabulated parameter input and results from the L-W test and McDermott-Ellis test calculations are given in Appendix D. The graphical results from the Othmer-Tobias correlation are given in Appendix E.

Figure 8-16 reveals that no ternary heterogeneous azeotrope exists for the n-Propanol/DIPE/Water system. All the vapour phase compositions lie below the tie-line of the two corresponding liquid phases. Consequently no straight line exists in the phase envelope, upon which corresponding aqueous liquid, organic liquid and vapour phase compositions are found. This indicates that no ternary heterogeneous azeotrope exists. The dehydration of aqueous n-propanol via heterogeneous azeotropic distillation, using DIPE as an entrainer, is therefore seemingly not possible. Table 8-2 presents the binary azeotrope for DIPE/Water measured in this work, along with other relevant azeotropic data from literature. As stated previously, the composition of the binary DIPE/Water azeotrope compares well with the data reported by Lladosa et al. (2008) and Verhoeve (1970) as well as those compiled by Gmehling et al. (1994). From the compilations of Gmehling et al. (1994) it also clear that no binary azeotrope exists between n-Propanol and DIPE.

Table 8-3: Temperature and composition of ternary and binary azeotropes measured for *n*-propanol/DIPE/water at 101.325 kPa

Temp (°C)	Composition			Reference
	Y _{water}	Y _{DIPE}	Y _{n-Propanol}	
61.90	0.2480	0.7520	-	Lladosa et al. (2008)
62.16	0.2186	0.7814	-	This work
62.50	0.2200	0.7800	-	Verhoeve (1970)
87.00	0.5683	-	0.4317	Horsley and Tamplin (1952)
87.55	0.5650	-	0.4350	Gmehling et al. (1994)
87.59	0.5686	-	0.4314	
87.65	0.5680	-	0.4320	
87.66	0.5680	-	0.4320	
87.70	0.5680	-	0.4320	
87.71	0.5670	-	0.4330	
87.71	0.5683	-	0.4317	
87.72	0.5683	-	0.4317	
87.75	0.5684	-	0.4316	
87.75	0.5683	-	0.4317	
87.76	0.5779	-	0.4221	
87.79	0.5820	-	0.4180	
87.80	0.5800	-	0.4200	
87.80	0.5700	-	0.4300	
87.70	0.5680	-	0.4320	
87.80	0.5680	-	0.4320	
88.00	0.5684	-	0.4316	
88.10	0.5671	-	0.4329	

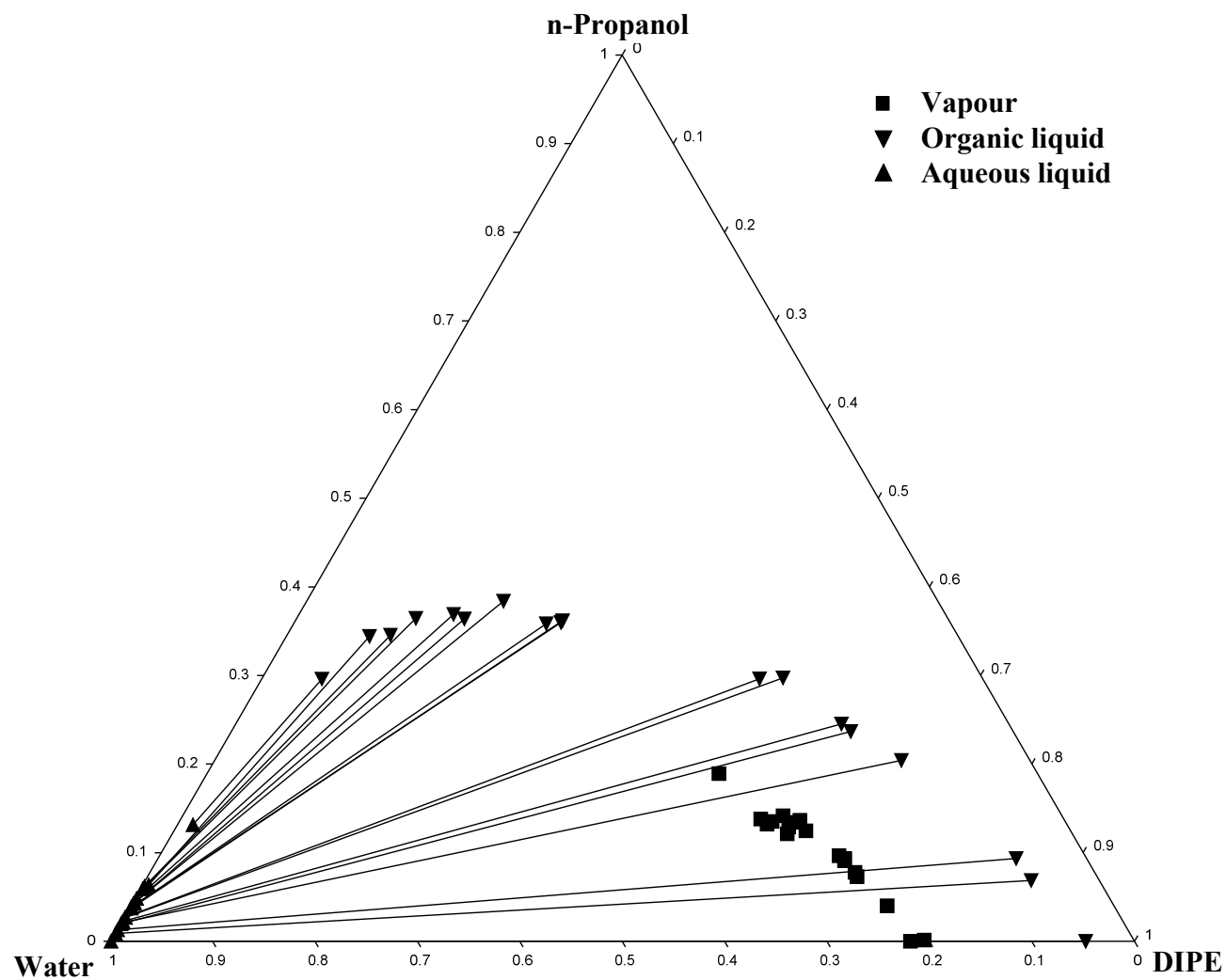


Figure 8-14: Ternary phase diagram of measured n-Propanol/DIPE/Water VLE data at 101.325 kPa

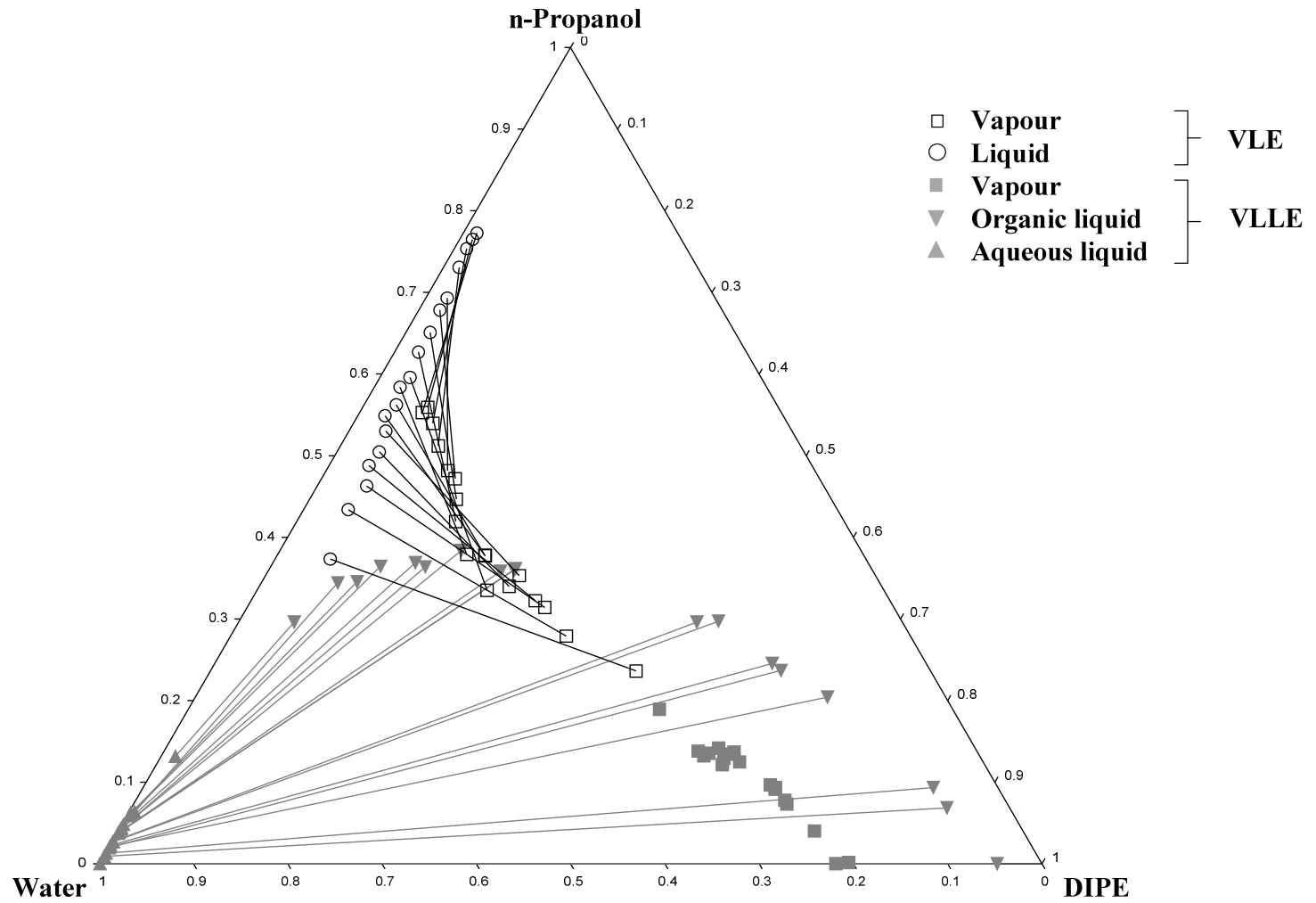


Figure 8-15: Ternary phase diagram of measured n-Propanol/DIPE/Water VLE data at 101.325 kPa

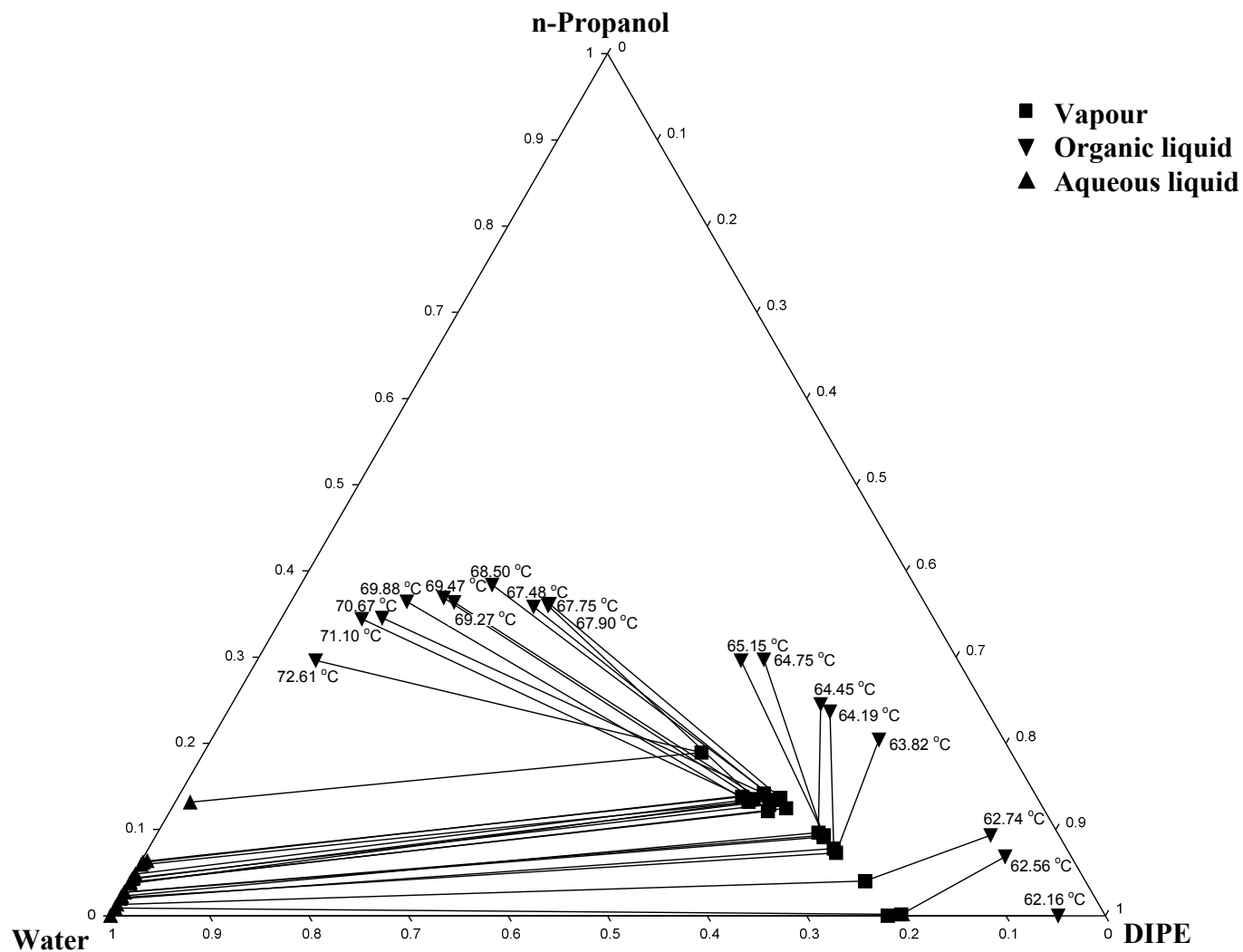


Figure 8-16: Ternary phase diagram for the calculation of the heterogeneous ternary azeotrope from measured n-Propanol/DIPE/Water VLE data at 101.325 kPa

8.2.3 n-Propanol/Isooctane/Water VLLE and VLE

The experimental VLLE and VLE data measured for n-Propanol/Isooctane/Water are presented graphically in Figures 8-17 and 8-18, respectively. The phase equilibrium data is tabulated in Appendix C in Tables C-9 and C-10. The VLE data adhered to the L-W and the McDermott-Ellis consistency tests. Consequently it was established that the data are thermodynamically consistent. All D values for the L-W test were smaller or equal to 3.328, thus lower than 5. All D values for the McDermott-Ellis test were smaller than D_{\max} and the data are therefore proved thermodynamic consistent. The liquid phases of the VLLE data were checked for regularity with the Othmer-Tobias correlation and were found to have a regular course, with an r-value of 0.991. Detailed tabulated parameter input and results from the L-W test and McDermott-Ellis test calculations are given in Appendix D. The graphical results from the Othmer-Tobias correlation are given in Appendix E. The vapour phase compositions in Figure 8-17 seem slightly scattered, but this is also noted in the vapour phase data of Font et al. (2004) in Figure 8-4 for the system IPA/isooctane/water. This might be explained by the nature of the alcohol/isooctane/water systems.

Figure 8-18 illustrates that a ternary heterogeneous azeotrope exists for the n-Propanol/Isooctane/Water system. In the upper part of the phase envelope, from temperature 74.79°C to 74.60°C, the vapour phase compositions lie below the tie-line of the two corresponding liquid phases. Conversely, in the lower part of the phase envelope, temperatures 74.59°C to 79.16°C, the vapour phase compositions lie above the tie-line of the two corresponding liquid phases. This shows that between the points 74.60°C and 74.59°C there is a point upon which the compositions of the aqueous liquid, vapour and organic liquid phases form a straight line. From the lever rule it can be proved that the over-all composition of the aqueous and organic liquid phases on this straight line will be equal to the vapour phase composition, hence the ternary heterogeneous azeotrope exists at this point. The composition and temperature of the ternary azeotrope is determined via numerical interpolation. The result is provided in Table 8-3, along with the binary azeotrope for Isooctane/Water, measured in this work, and other relevant azeotropic data from literature. The composition of the ternary heterogeneous azeotrope is similar to the experimentally determined data compiled by Gmehling et al. (1994). The composition of the binary Isooctane/Water azeotrope compares well with the data reported by Font et al. (2003) and those compiled by Gmehling et al. (1994).

To summarize, VLE and VLLE data were measured for ethanol/DIPE/water, n-propanol/DIPE/water and n-propanol/isooctane/water. All the VLE data were proved to be thermodynamically consistent and LLE section of the VLLE data follows a regular course. The binary DIPE/water and isooctane/water azeotropes were also measured and agreed well with published azeotropic data. The ternary heterogeneous ethanol/DIPE/water and n-propanol/isooctane/water azeotropes were calculated from the measured VLLE data and also agreed fairly well with published azeotropic data.

Table 8-4: Temperature and composition of ternary and binary azeotropes measured for *n*-propanol/isooctane/water at 101.325 kPa

Temp (°C)	Composition			Reference
	Y_{water}	$Y_{\text{isooctane}}$	$Y_{\text{n-Propanol}}$	
73.89	0.3520	0.4400	0.2080	Gmehling et al. (1994)
74.59	0.3899	0.4246	0.1855	This work
79.03	0.4730	0.5270	-	Font et al. (2003)
79.13	0.4710	0.5290	-	This work
78.80	0.4420	0.5580	-	Gmehling et al. (1994)
87.00	0.5683	-	0.4317	Horsley and Tamplin (1952)
87.55	0.5650	-	0.4350	Gmehling et al. (1994)
87.59	0.5686	-	0.4314	
87.65	0.5680	-	0.4320	
87.66	0.5680	-	0.4320	
87.70	0.5680	-	0.4320	
87.71	0.5670	-	0.4330	
87.71	0.5683	-	0.4317	
87.72	0.5683	-	0.4317	
87.75	0.5684	-	0.4316	
87.75	0.5683	-	0.4317	
87.76	0.5779	-	0.4221	
87.79	0.5820	-	0.4180	
87.80	0.5800	-	0.4200	
87.80	0.5700	-	0.4300	
87.70	0.5680	-	0.4320	
87.80	0.5680	-	0.4320	
88.00	0.5684	-	0.4316	
88.10	0.5671	-	0.4329	
76.80	-	0.3095	0.6905	Horsley and Tamplin (1952)
84.78	-	0.5412	0.4533	Hiaki et al. (1994)

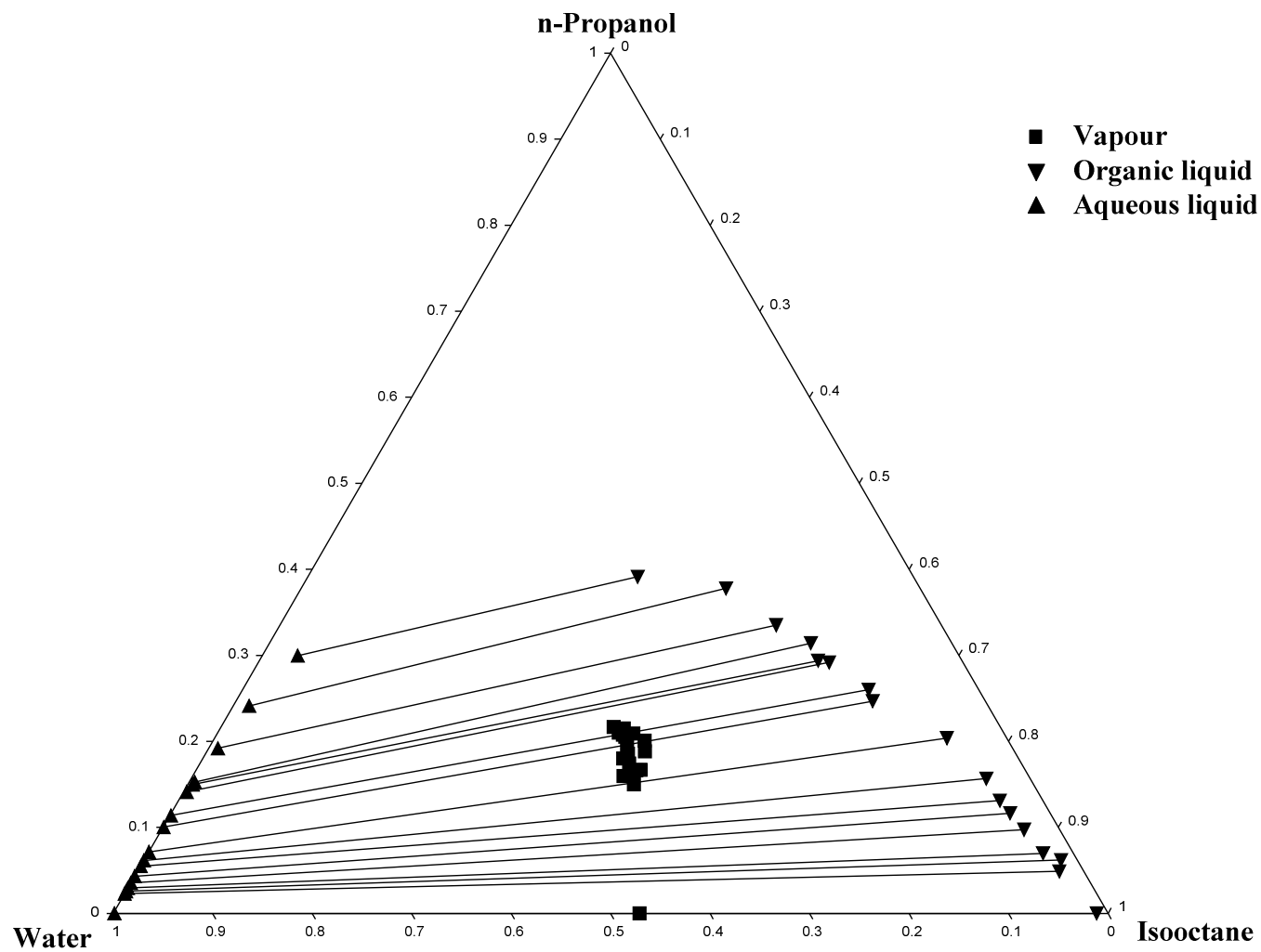


Figure 8-17: Ternary phase diagram of measured n-Propanol/Isooctane/Water VLLE data at 101.325 kPa

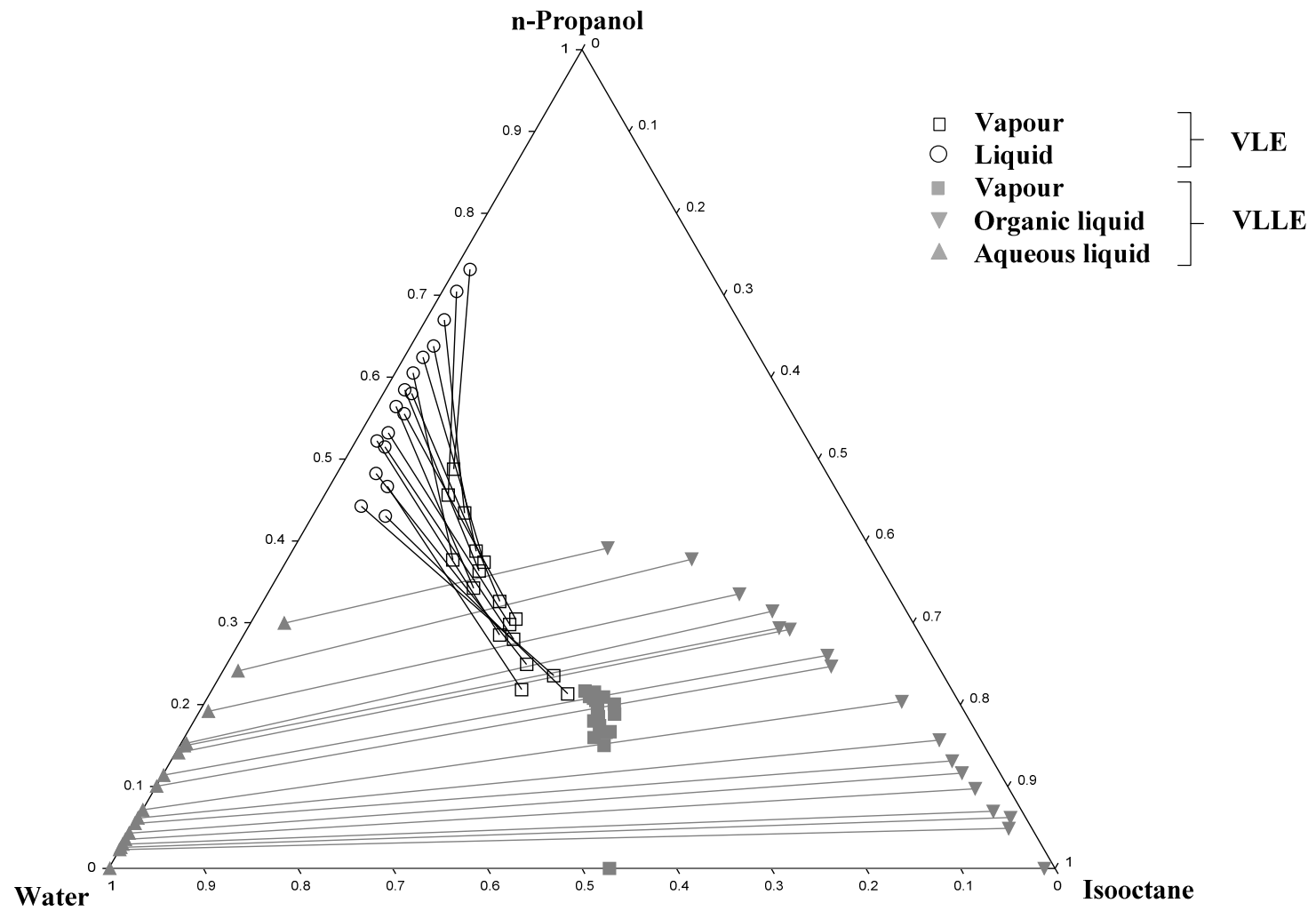


Figure 8-18: Ternary phase diagram of measured n-Propanol/Isooctane/Water VLE data at 101.325 kPa

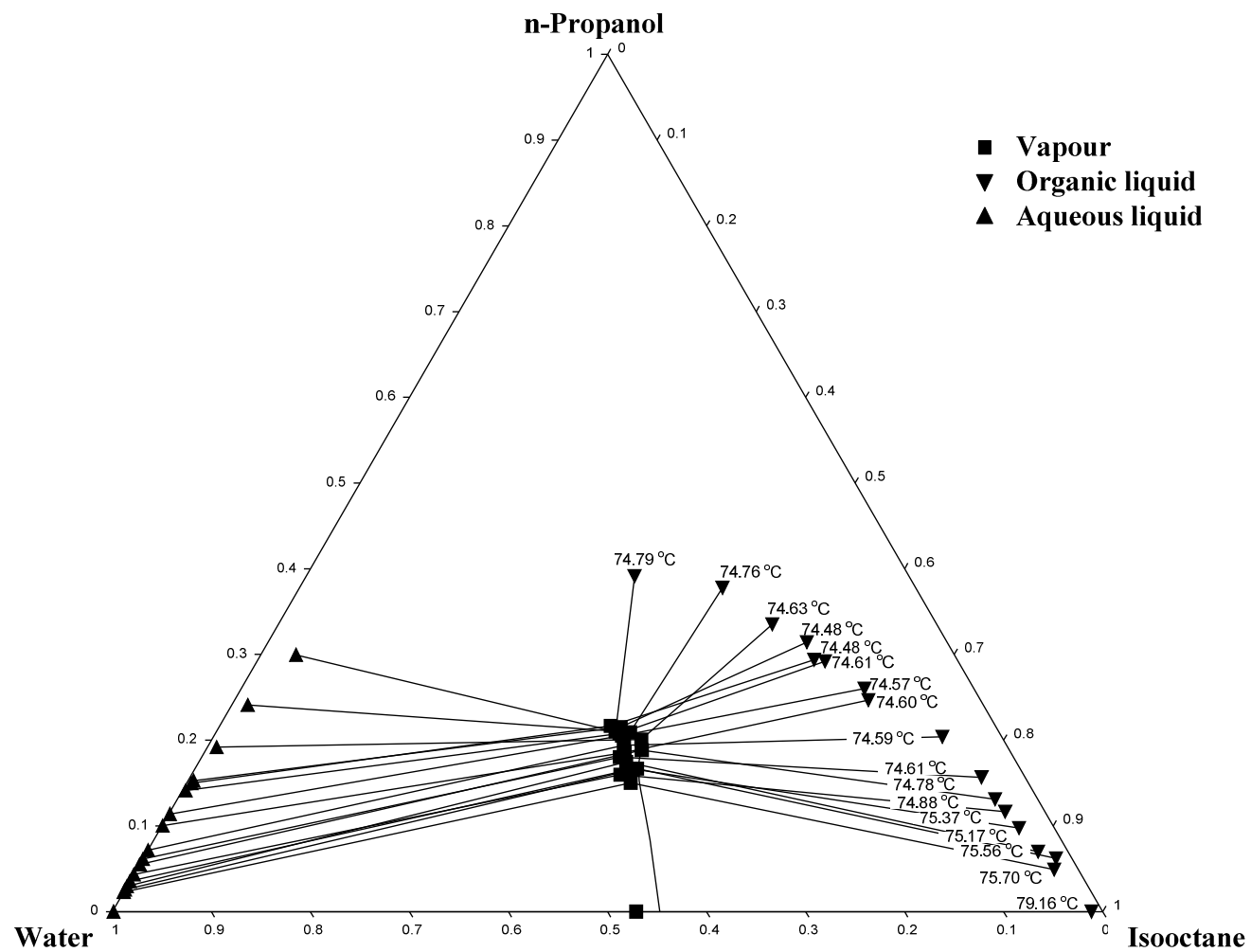


Figure 8-19: Ternary phase diagram for the calculation of the heterogeneous ternary azeotrope from measured n-Propanol/Isooctane/Water VLE data at 101.325 kPa

8.3 ENTRAINER COMPARISON

Considering the data available in literature and the data measured in this work, six entrainers are studied for the dehydration of ethanol via heterogeneous azeotropic distillation, three for isopropanol and three for n-propanol. For comparative purposes and the process of initial elimination, the data for these systems are plotted in Figures 8-20 to 8-22. According to Gomis et al. (2007), the azeotropic distillation process is improved when the amount of water removed from the condenser-decanter (see Section 4.1) of the azeotropic column is increased. Since the distillate from this column has a composition close to that of the ternary heterogeneous azeotrope, the composition of the aqueous phase of the tie line containing the azeotropic point is related to the amount of water removed after condensation and decantation. When the water content of the aqueous phase is lower, a larger quantity of all the components need to be recirculated to separate the same amount of water. Consequently, the production cost will increase. Therefore, a superior entrainer will have the greatest “water carrying capacity”, i.e. the distillate from the azeotropic column will have the largest water composition and the difference in water composition between the two liquid phases formed in the decanter would have to be the largest. The boiling temperature of the ternary heterogeneous azeotrope is also an important factor to consider, since this will influence the amount of energy required.

Figure 8-20 shows that using DIPE as entrainer results in an aqueous liquid phase with the largest water composition. This is also evident from Table 8-5. Benzene results in an aqueous liquid phase with the second largest water composition. Cyclohexane, hexane, heptane and isooctane all yield aqueous liquid phases significantly lower in water content. Therefore, DIPE is used in the separation sequence simulation of ethanol dehydration in Section 9.5. Benzene has commonly been used in the chemical process industry (Norman 1945) and another simulation of ethanol dehydration is therefore performed using Benzene to compare its performance with DIPE.

Table 8-5: Ternary heterogeneous azeotropic compositions of the ethanol/entrainer/water systems at 101.3 kPa

Entrainer	Temp (°C)	Composition								
		organic liquid			aqueous liquid			vapour		
		alcohol	entrainer	water	alcohol	entrainer	water	alcohol	entrainer	water
Cyclohexane ^a	62.39	0.133	0.849	0.018	0.521	0.046	0.433	0.292	0.52	0.188
Hexane ^b	56.06	0.138	0.847	0.016	0.561	0.038	0.401	0.236	0.658	0.105
Heptane ^c	68.68	0.195	0.775	0.03	0.614	0.045	0.341	0.432	0.363	0.205
Isooctane ^d	68.72	0.215	0.758	0.027	0.596	0.082	0.321	0.436	0.366	0.198
Benzene ^e	64.90	0.232	0.664	0.104	0.225	0.021	0.754	0.23	0.55	0.22
DIPE ^f	61.04	0.1475	0.7746	0.0779	0.0777	0.0032	0.9192	0.1377	0.6659	0.1964

^a Gomis et al. (2005)

^b Gomis et al. (2007)

^c Gomis et al. (2006)

^d Font et al. (2003)

^e Norman (1945)

^f This work

Figure 8-21 indicates that using DIPE as entrainer also results in the aqueous liquid phase with the highest water content for the dehydration of IPA, followed by cyclohexane and then isooctane. The exact azeotropic compositions are given in Table 8-6. DIPE is used for the simulation of IPA dehydration separation sequence in Section 8.5 and compared to the cyclohexane commonly used in industry.

Table 8-6: Ternary heterogeneous azeotropic compositions of the IPA/entrainer/water systems at 101.3 kPa

Entrainer	Temp (°C)	Composition								
		organic liquid			aqueous liquid			vapour		
		alcohol	entrainer	water	alcohol	entrainer	water	alcohol	entrainer	water
Cyclohexane ^a	64.3	0.246	0.684	0.07	0.103	0.02	0.877	0.222	0.566	0.212
Isooctane ^b	70.9	0.36	0.51	0.13	0.23	0.03	0.74	0.31	0.38	0.31
DIPE ^c	61.6	0.055	0.888	0.057	0.013	0.001	0.986	0.062	0.683	0.255

^a Verhoeve (1968)

^b Font et al. (2004)

^c Lladosa et al. (2008)

In Figure 8-22 DNPE as entrainer results in the aqueous liquid phase with the highest water content for n-propanol dehydration, again followed by cyclohexane and then isooctane. Table 8-7 also confirms this. In this case the azeotropic tie lines for DNPE and cyclohexane are very similar. As stated in Section 8.2.2, the n-propanol-DIPE-water system does not exhibit a ternary azeotrope and therefore DIPE is not a suitable entrainer for the dehydration of n-propanol via azeotropic distillation. Carlson (1949) however suggested a method for dehydrating aqueous n-propanol which also contains small quantities of ethanol and IPA. In order to investigate DIPE as an entrainer for dehydrating all three alcohols in question, a simulation of the method suggested by Carlson is also performed in Section 8.5. A brief explanation of this method is also provided in Section 8.5.

Table 8-7: Ternary heterogeneous azeotropic compositions of the n-propanol/entrainer/water systems at 101.3 kPa

Entrainer	Temp (°C)	Composition								
		organic liquid			aqueous liquid			vapour		
		alcohol	entrainer	water	alcohol	entrainer	water	alcohol	entrainer	water
Cyclohexane ^a	66.47	0.1558	0.8149	0.0293	0.0441	0	0.9559	0.1324	0.6114	0.2562
Isooctane ^b	74.59	0.2367	0.679	0.0843	0.1003	0.0003	0.8994	0.1855	0.4246	0.3899
DNPE ^c	73.7	0.159	0.783	0.058	0.022	0	0.978	0.203	0.514	0.393

^a Lee and Shen (2003)

^b This work

^c Lladosa et al. (2008)

To reiterate, benzene and DIPE were selected as entrainers for the simulation of ethanol dehydration in Aspen. Cyclohexane and DIPE were selected for the simulation IPA dehydration. DIPE was also selected for the

simulation of n-propanol dehydration, but only when n-propanol forms part of a Fischer Tropsch waste stream consisting of ethanol and IPA as well. The latter refers to a method proposed by Carlson (1949) to specifically use the fact that n-propanol does not form a ternary heterogeneous azeotrope with DIPE and water.

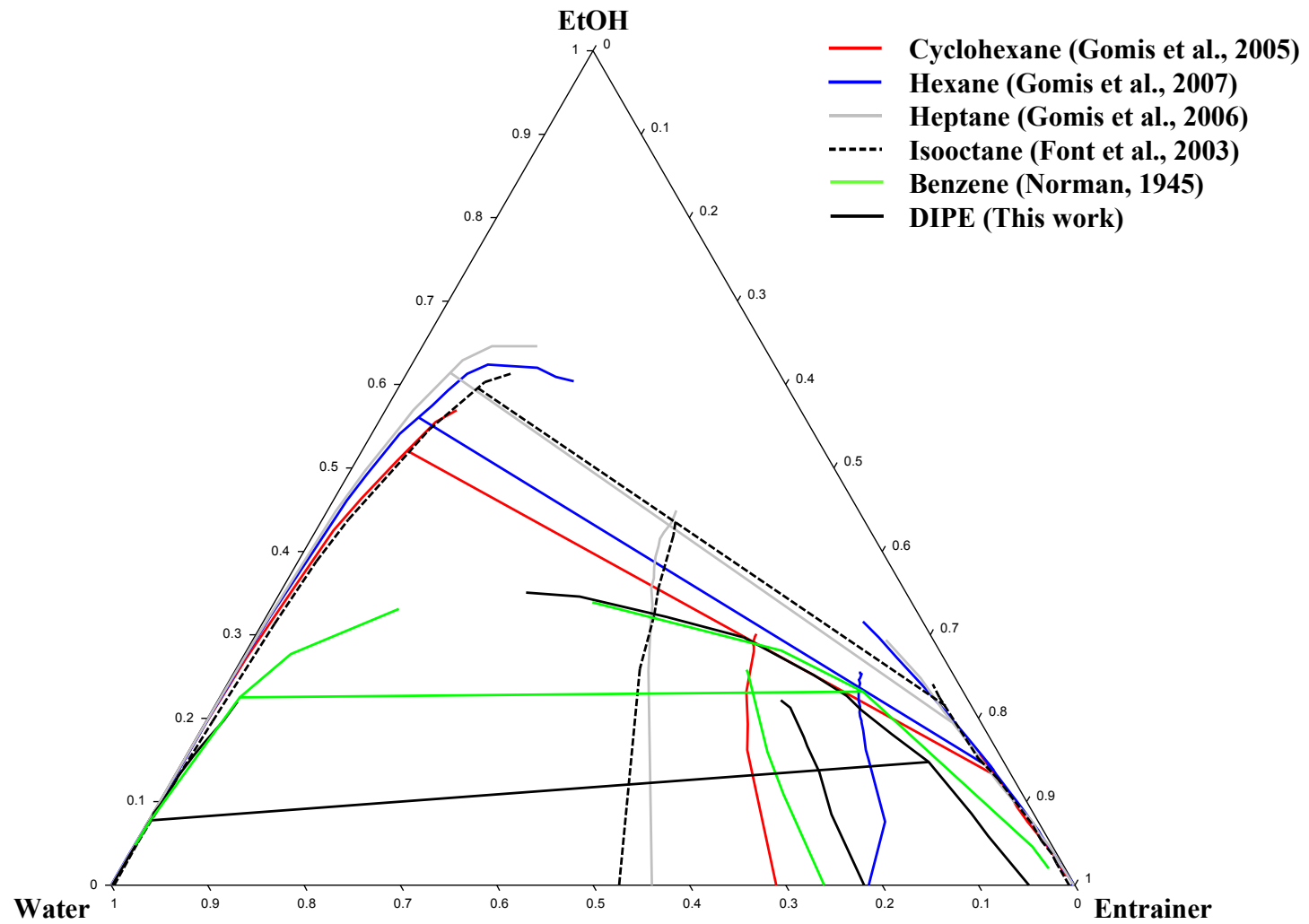


Figure 8-20: Entrainer comparison for ethanol dehydration via heterogeneous azeotropic distillation at 101.325 kPa. Each phase envelope is plotted with its azeotropic tie-line.

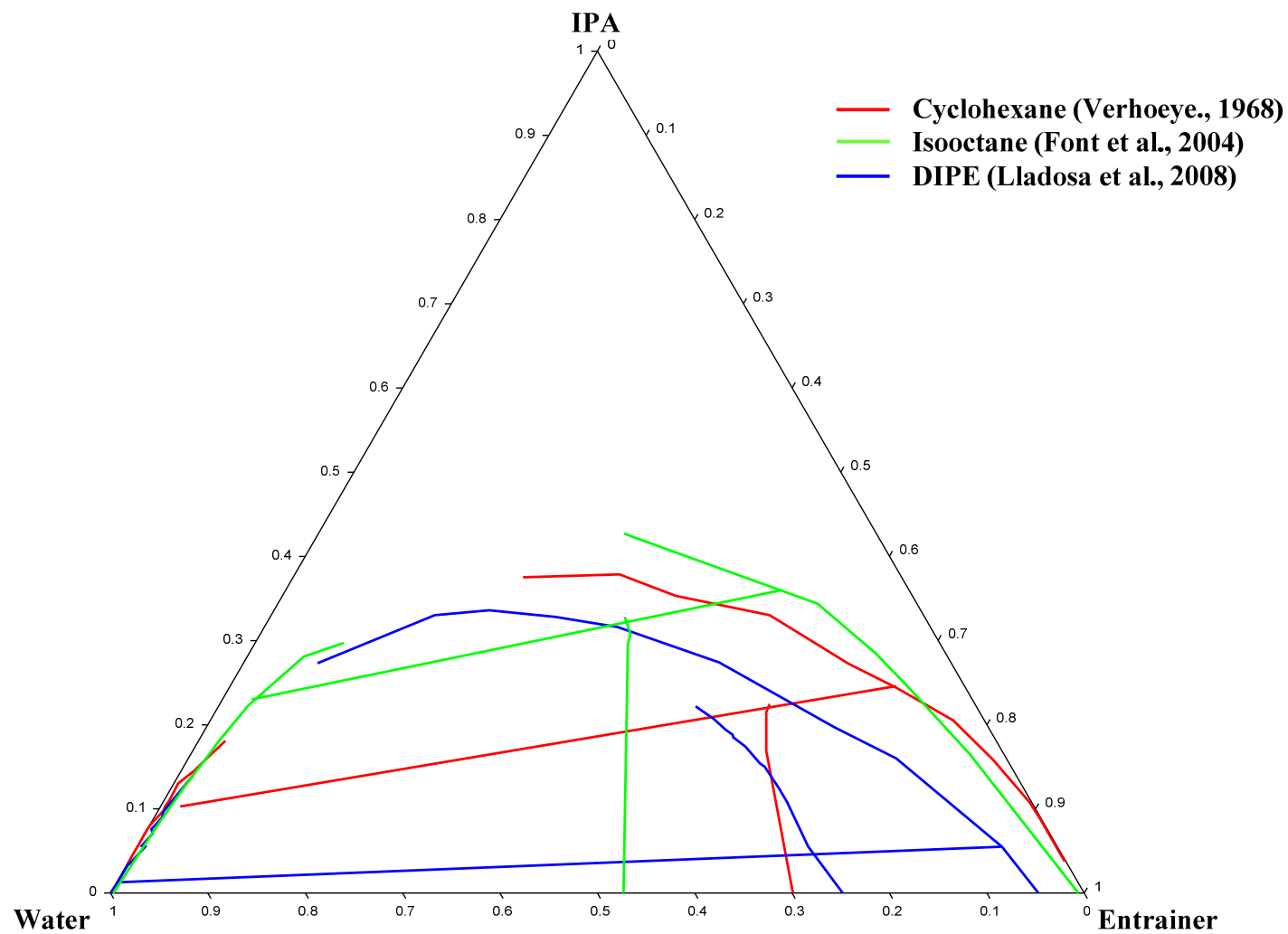


Figure 8-21: Entrainer comparison for IPA dehydration via heterogeneous azeotropic distillation at 101.325 kPa. Each phase envelope is plotted with its azeotropic tie-line.

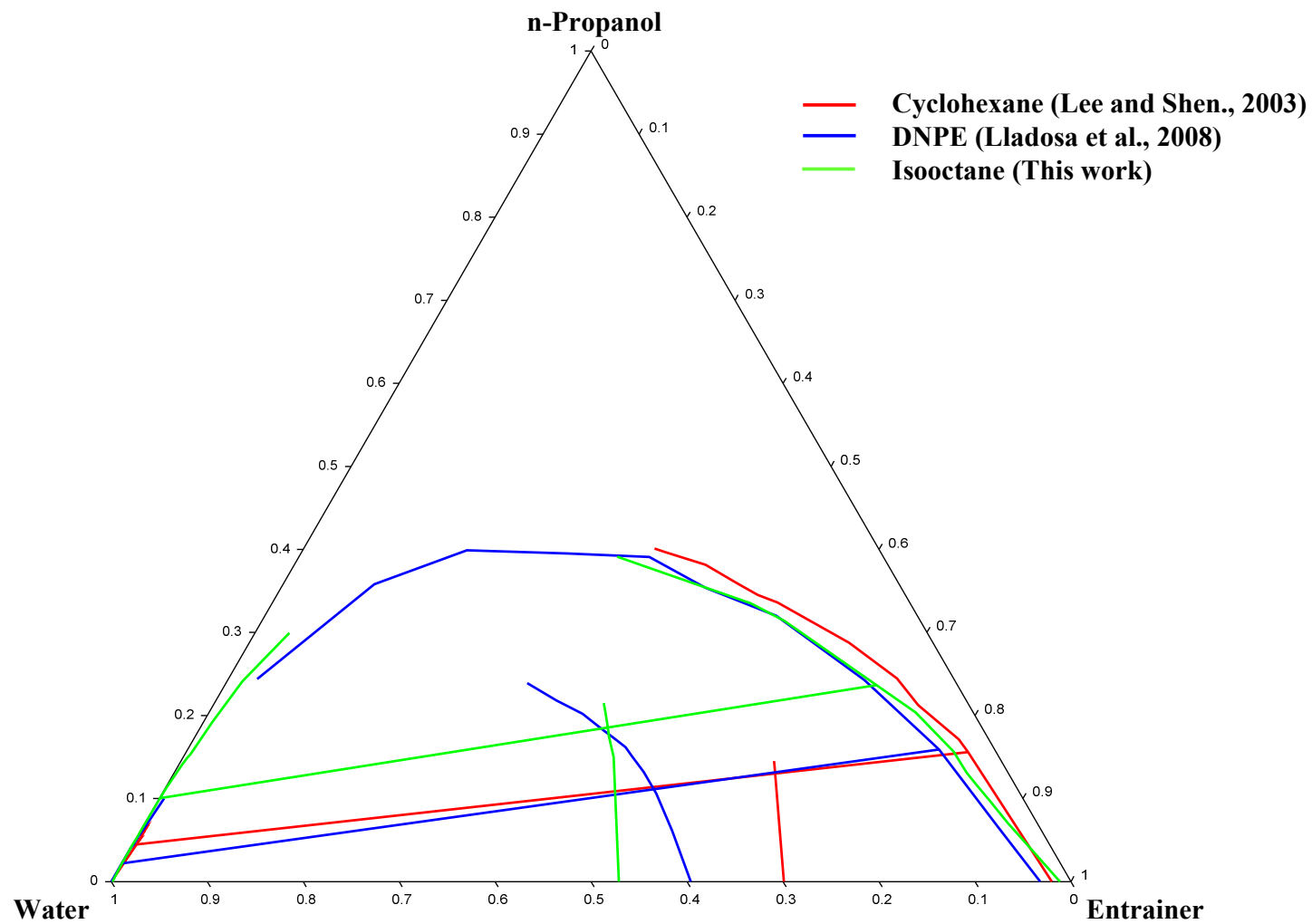


Figure 8-22: Entrainer comparison for n-Propanol dehydration via heterogeneous azeotropic distillation at 101.325 kPa. Each phase envelope is plotted with its azeotropic tie-line.

8.4 THERMODYNAMIC MODELLING

8.4.1 Comparison of data with selected thermodynamic models

As stated in Chapter 1, one of the objectives of this work is to compare the experimental data to thermodynamic models (NRTL, UNIQUAC and UNIFAC). The VLE data predictions are obtained from the simulation program Aspen. All thermodynamic model parameters used in this section are built-in parameters from Aspen. The built-in Aspen parameters used in this work are provided in Appendix F. The estimated data are plotted against the experimental data in Figures 8-23 to 8-25. The azeotropes determined in this work and those obtained from literature (listed in Section 8.2) are indicated on these diagrams by a solid black dot. The model predictions of these azeotropes are also indicated on the diagrams by open dots in a different colour for each model, as indicated in the legend. The model predictions of the phase envelope are plotted against the experimental organic and aqueous liquid phase data. The same is done for the predicted and measured vapour phase values. The three tie-lines of each model and the experimental data are indicated on the diagrams – one in the lower alcohol region, one near the ternary heterogeneous azeotropic region and one in the higher alcohol region, approaching the plait point. The AADs and AARDs between experimental and predicted values for the three systems evaluated in this work are shown in Tables 8-4 to 8-6.

First consider the azeotropes of the **ethanol/DIPE/water** system in Figure 8-23 and Table 8-8. NRTL and UNIFAC (VLE) accurately predict the ethanol/water azeotrope. UNIQUAC predicts a slightly higher ethanol composition, while UNIFAC (LLE) does not predict any ethanol/water azeotrope. For the ethanol/DIPE azeotrope the UNIFAC (LLE) prediction is the closest to the composition found in literature. The predictions from all the other models are also close, but with a somewhat higher ethanol composition. The DIPE/water azeotrope is most accurately predicted by NRTL and UNIQUAC. UNIFAC (VLE) and UNIFAC (LLE) are also close, but with a slightly lower and higher DIPE composition, respectively. With respect to composition the ternary heterogeneous azeotrope is most accurately predicted by UNIFAC (VLE) and UNIFAC (LLE). The ternary azeotropic temperature is most accurately predicted by UNIQUAC and NRTL.

Regarding the phase envelope, NRTL and UNIFAC (LLE) yield the least accurate predictions. Both these models predict a much larger phase envelope and therefore incorrectly include homogeneous phase equilibrium points in the heterogeneous region. The UNIQUAC prediction is a minor improvement, but still overestimates the size of the heterogeneous region around the top of the phase envelope. UNIFAC (VLE) more accurately predicts the phase envelope around the plait point area and the top of the heterogeneous region, but fails to predict the organic liquid phase correctly. The lower two tie-lines are sufficiently predicted by all the models, but only UNIFAC (VLE) accurately predicts the tie-line near the plait point. All the model predictions of the vapour phase are relatively accurate. The UNIFAC (VLE) and UNIFAC (LLE) predictions follow the exact same trend as the experimental data. The NRTL and UNIQUAC predictions however deviate from this trend to some extent in the area of the vapour phase with high ethanol compositions.

Table 8-8: Azeotropes of the ethanol/DIPE/water system measured at 101.3 kPa, with those predicted by Aspen with built-in parameters.

Source	Temp (°C)	Composition		
		ethanol	DIPE	water
UNIFAC (LLE)	60.61	0.1395	0.6727	0.1878
NRTL	60.96	0.1816	0.6336	0.1848
This work	61.04	0.1377	0.6659	0.1964
UNIQUAC	61.14	0.1673	0.6432	0.1895
UNIFAC (VLE)	61.68	0.1430	0.6551	0.2018
UNIFAC (LLE)	61.61	-	0.7879	0.2121
This work	62.16	-	0.7814	0.2186
UNIQUAC	62.45	-	0.7801	0.2199
NRTL	62.46	-	0.7799	0.2201
UNIFAC (VLE)	63.13	-	0.7727	0.2273
UNIFAC (VLE)	78.04	0.8933	-	0.1067
Gmehling et al. (1994)	78.12	0.895	-	0.105
NRTL	78.15	0.8952	-	0.1048
UNIQUAC	78.16	0.8999	-	0.1001
UNIFAC (VLE)	61.53	0.3357	0.6643	-
NRTL	63.86	0.3373	0.6627	-
UNIQUAC	63.87	0.3382	0.6618	-
Benito and Lopez (1992)	64.00	0.318	0.682	-
UNIFAC (LLE)	64.36	0.3290	0.6710	-

According to the AAD and AARD % values for ethanol/DIPE/water in Table 8-4, UNIQUAC and UNIFAC (VLE) most accurately predict the experimental data. The AARD % of temperature predictions for UNIQUAC and UNIFAC (VLE) is 0.01 % and 0.02 % respectively, but the difference is not considered significant since both values are very small. Overall, the AAD and AARD % values from UNIFAC (VLE) are better than those from UNIQUAC, with the only significant exception being the water composition of the organic liquid phase. The accurate prediction of the ternary heterogeneous azeotrope is very important when simulating a heterogeneous azeotropic distillation column. As UNIFAC (VLE) also predicts this azeotrope more accurately than UNIQUAC, it is considered the best model of those studied in this work, to predict ethanol/DIPE/water when using built-in parameters in Aspen. UNIFAC (VLE) predicts an organic liquid phase with a higher water composition than the experimental data indicates. This will lead to a conservative design of the azeotropic column, because in actual fact less water will be refluxed to the column in the organic liquid phase. Therefore the actual energy requirements will be less than that predicted with the built-in Aspen parameters.

The predictions plotted in Figure 8-23 and the high AAD and AARD % values listed in Table 8-4 however indicates that improvements can still be made to these model predictions via parameter regression.

All the models, except for UNIFAC (LLE), predict the composition of the n-propanol/water azeotrope relatively accurately (with a somewhat lower n-propanol composition) in the **n-propanol/DIPE/water** system (Figure

8-24). The azeotropes of this system are also listed in Table 8-9. UNIFAC (LLE) predicts a much higher temperature for the n-propanol/water azeotrope. UNIFAC (VLE) predicts a binary azeotrope between n-propanol and DIPE (89.82 mole % DIPE and 10.18 mole % n-propanol) which does not exist. The DIPE/water azeotrope is most accurately predicted by NRTL and UNIQUAC. UNIFAC (VLE) and UNIFAC (LLE) are also close, but with a slightly lower and higher DIPE composition, respectively. The n-propanol/DIPE/water system exhibits no ternary heterogeneous azeotrope and none of the models predicts one either.

Table 8-9: Azeotropes of the n-propanol/DIPE/water system measured at 101.3 kPa, with those predicted by Aspen with built-in parameters.

Source	Temp (°C)	Composition		
		n-propanol	DIPE	water
UNIFAC (LLE)	61.61	-	0.7879	0.2121
This work	62.16	-	0.7814	0.2186
NRTL	62.46	-	0.7799	0.2201
UNIQUAC	62.75	-	0.7774	0.2226
UNIFAC (VLE)	63.13	-	0.7727	0.2273
UNIQUAC	87.55	0.4229	-	0.5771
NRTL	87.65	0.4249	-	0.5751
Gmehling et al. (1994)	87.66	0.4320	-	0.5680
UNIFAC (VLE)	88.16	0.4226	-	0.5774
UNIFAC (LLE)	92.16	0.3751	-	0.6249
UNIFAC (VLE)	67.69	0.1018	0.8982	-

Regarding the phase envelope, NRTL predicts a much larger heterogeneous region and therefore incorrectly include homogeneous phase equilibrium points in this region. The UNIQUAC prediction is a minor improvement by more accurately predicting the organic liquid phase, but still overestimates the size of the heterogeneous region around the top of the phase envelope. UNIFAC (VLE) predicts the phase envelope around the plait point area and the top of the heterogeneous region slightly more accurate, but fails to predict the organic liquid phase correctly. UNIFAC (LLE) predicts a smaller phase envelope and therefore incorrectly excludes heterogeneous phase equilibrium points from the heterogeneous region. Directionally, all the models predict the tie-lines relatively accurately. NRTL and UNIQUAC most accurately predict the vapour phase, followed by UNIFAC (VLE). The UNIFAC (LLE) vapour phase prediction on the other hand does not compare well with the experimental data at all.

When considering the AAD and AARD % values in Table 8-5, it seems as if UNIFAC (VLE) and UNIFAC (LLE) should, overall, most accurately predict the experimental data. However since UNIFAC (LLE) predicts an n-propanol/DIPE azeotrope that does not exist and UNIFAC (VLE) poorly predicts the n-propanol/water azeotrope, these two can be eliminated as options in this evaluation. The AARD % of temperature predictions by NRTL and UNIQUAC is 0.01 % and 0.02 % respectively, but the difference is not considered significant since both values are very small. Overall the AAD and AARD % values from UNIQUAC are better than those from NRTL, with the only significant exception being the DIPE composition of the aqueous liquid phase. This

AARD % value is very high since the UNIQUAC prediction of the aqueous liquid phase is so close to the n-propanol axis on the diagram, that it almost looks like the model predicts liquid-liquid separation between n-propanol and water. There is however no liquid-liquid separation between these two components. Although this AARD % value is very high, when taking all the phases into account UNIQUAC is considered the best model, of those studied in this work, to predict n-propanol/DIPE/water when using built-in parameters in Aspen. As heterogeneous azeotropic distillation cannot be performed on this system, the only aspects to take into consideration are the prediction of the binary azeotropes, tie lines and phase envelope. UNIQUAC performs best for all of these features.

However, the predictions plotted in Figure 8-24 and the high AAD and AARD % values listed in Table 8-5 indicate that improvements can still be made to these model predictions via parameter regression.

All the models, except UNIFAC (LLE), predict the n-propanol/water azeotrope relatively accurately (with a somewhat lower n-propanol composition) in the **n-propanol/isooctane/water** system (Figure 8-25). The azeotropes of this system are also given in Table 8-10. UNIFAC (LLE) predicts a much higher temperature for the n-propanol/water azeotrope. For the n-propanol/isooctane azeotrope the NRTL prediction is the closest to the composition found in literature. The predictions from UNIFAC (VLE) are also close, but with a somewhat lower n-propanol composition. UNIFAC (LLE) predicts a much higher temperature for this azeotrope. The UNIQUAC prediction has a higher n-propanol composition than found in literature. The isooctane/water azeotrope is most accurately predicted by NRTL and UNIQUAC. UNIFAC (VLE) and UNIFAC (LLE) are also close, but with a slightly higher DIPE composition. The ternary heterogeneous azeotrope is most accurately predicted by UNIFAC (VLE), followed by NRTL and then UNIQUAC. Each predicts a somewhat higher n-propanol composition. UNIFAC (LLE) predicts a ternary azeotrope with a much lower n-propanol composition.

NRTL, UNIQUAC and UNIFAC (VLE) predict a much larger phase envelope and therefore incorrectly include homogeneous phase equilibrium point in the heterogeneous region. UNIFAC (LLE) provides the most accurate prediction of the phase envelope by only slightly over-estimating the size of the heterogeneous region around the plait point. As with the phase envelope, the tie-lines predicted by NRTL, UNIQUAC and UNIFAC (VLE) do not agree well with the experimental data. Even the tie-lines predicted by UNIFAC (LLE) are not in agreement with the experimental data. The lower tie-lines predicted by all the models are still comparable, but the ones close to the ternary azeotrope and plait point exhibit opposite directionalities. The vapour phase is most accurately predicted by UNIFAC (LLE). The vapour phase prediction by UNIQUAC seems to follow the same trend as the experimental data, but extends much farther into the heterogeneous region. The NRTL and UNIFAC (VLE) predictions however deviate from this trend in the area of the vapour phase with high n-propanol compositions.

Table 8-10: Azeotropes of the n-propanol/isooctane/water system measured at 101.3 kPa, with those predicted by Aspen with built-in parameters.

Source	Temp (°C)	Composition		
		n-propanol	isooctane	water
UNIFAC (VLE)	74.16	0.2058	0.4449	0.3493
NRTL	74.25	0.2170	0.4280	0.3550
UNIQUAC	74.55	0.2327	0.4135	0.3538
This work	74.59	0.1855	0.4246	0.3899
UNIFAC (LLE)	77.26	0.1394	0.4647	0.3959
UNIFAC (LLE)	78.92	-	0.5528	0.4472
UNIFAC (VLE)	78.92	-	0.5528	0.4472
This work	79.13	-	0.5290	0.4710
UNIQUAC	79.22	-	0.5471	0.4529
NRTL	79.25	-	0.5464	0.4536
UNIQUAC	87.55	0.4229	-	0.5771
NRTL	87.65	0.4249	-	0.5751
Gmehling et al. (1994)	87.75	0.4316	-	0.5684
UNIFAC (VLE)	88.16	0.4226	-	0.5774
UNIFAC (LLE)	92.16	0.3751	-	0.6249
UNIFAC (VLE)	83.64	0.4484	0.5516	-
NRTL	84.65	0.4506	0.5494	-
UNIQUAC	84.67	0.4729	0.5271	-
Hiaki et al. (1994)	84.78	0.4533	0.5412	-
UNIFAC (LLE)	88.88	0.4563	0.5437	-

As seen in the Figure 8-25, the AARD % values (Table 8-6) also indicate that the experimental data are not accurately predicted by any of the thermodynamic models under investigation, with built-in Aspen parameters. It seems as if overall UNIFAC (LLE) can predict the experimental data better than the rest, with exception of the isooctane composition in the aqueous liquid phase. UNIFAC (LLE), however, poorly predicts the binary n-propanol/water and ternary azeotropes. The isooctane and n-propanol compositions in the aqueous liquid phase are overall poorly predicted by the models with its built-in parameters. The best temperature prediction is by UNIQUAC with an AARD % of 0.03 %, followed by NRTL and UNIFAC (VLE) with 0.05 % each. The difference is again not considered significant since both values are still very small. Although the AAD and AARD % values indicate that UNIFAC (VLE) should be considered after UNIFAC (LLE), its estimation of the phase envelope and tie-lines are so poor that it cannot be used to accurately predict the data.

The predictions plotted in Figure 8-25 and the high AAD and AARD % values listed in Table 8-6 indicates that improvements definitely need to be made to these model predictions via parameter regression. Clearly none of the models considered, with its built-in parameters, accurately predict the VLLE data. As it is, none of the models are deemed suitable for simulating a separation sequence of the n-propanol/isooctane/water system.

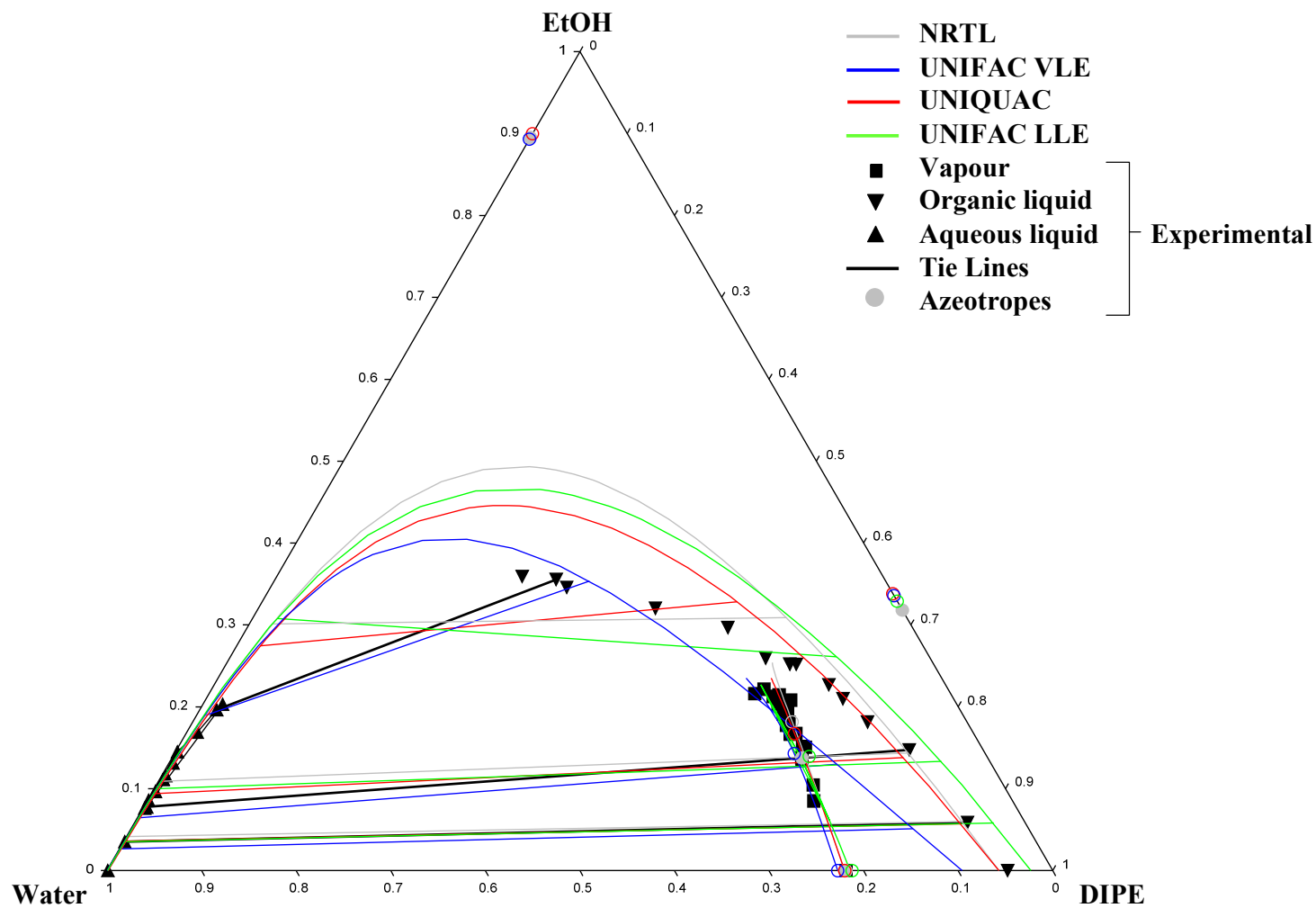


Figure 8-23: Ternary phase diagram of measured Ethanol/DIPE/Water VLLE data at 101.325 kPa and thermodynamic models (with tie lines and azeotropes) with built-in Aspen parameters.

Table 8-11: AAD and AARD % values for VLLE of Ethanol/DIPE/Water by the NRTL, UNIQUAC, UNIFAC (VLE) and UNIFAC (LLE) models with built-in Aspen parameters at 101.325 kPa.

	Temp (°C)	organic liquid			aqueous liquid			vapour			Σ
		X _{DIPE}	X _{ethanol}	X _{water}	X _{DIPE}	X _{ethanol}	X _{water}	Y _{DIPE}	Y _{ethanol}	Y _{water}	
NRTL											
AAD	0.0826	0.0779	0.0652	0.0510	0.0081	0.0716	0.0792	0.0142	0.0192	0.0087	0.4778
AARD %	0.02	24.66	25.34	26.25	120.78	49.60	9.67	2.27	13.58	4.51	276.68
UNIQUAC											
AAD	0.0483	0.0734	0.0529	0.0304	0.0051	0.0413	0.0461	0.0108	0.0142	0.0057	0.3282
AARD %	0.01	18.29	20.93	18.84	99.52	29.54	5.60	1.71	11.19	2.97	208.62
UNIFAC (VLE)											
AAD	0.0585	0.0397	0.0286	0.0439	0.0018	0.0188	0.0197	0.0130	0.0142	0.0100	0.2483
AARD %	0.02	11.43	11.83	36.34	24.57	14.75	2.43	2.12	11.19	5.32	120.01
UNIFAC (LLE)											
AAD	0.1578	0.0819	0.0439	0.0573	0.0063	0.0802	0.0863	0.0236	0.0183	0.0099	0.5655
AARD %	0.05	30.97	16.61	36.06	119.18	67.30	10.16	3.87	12.48	5.06	301.75

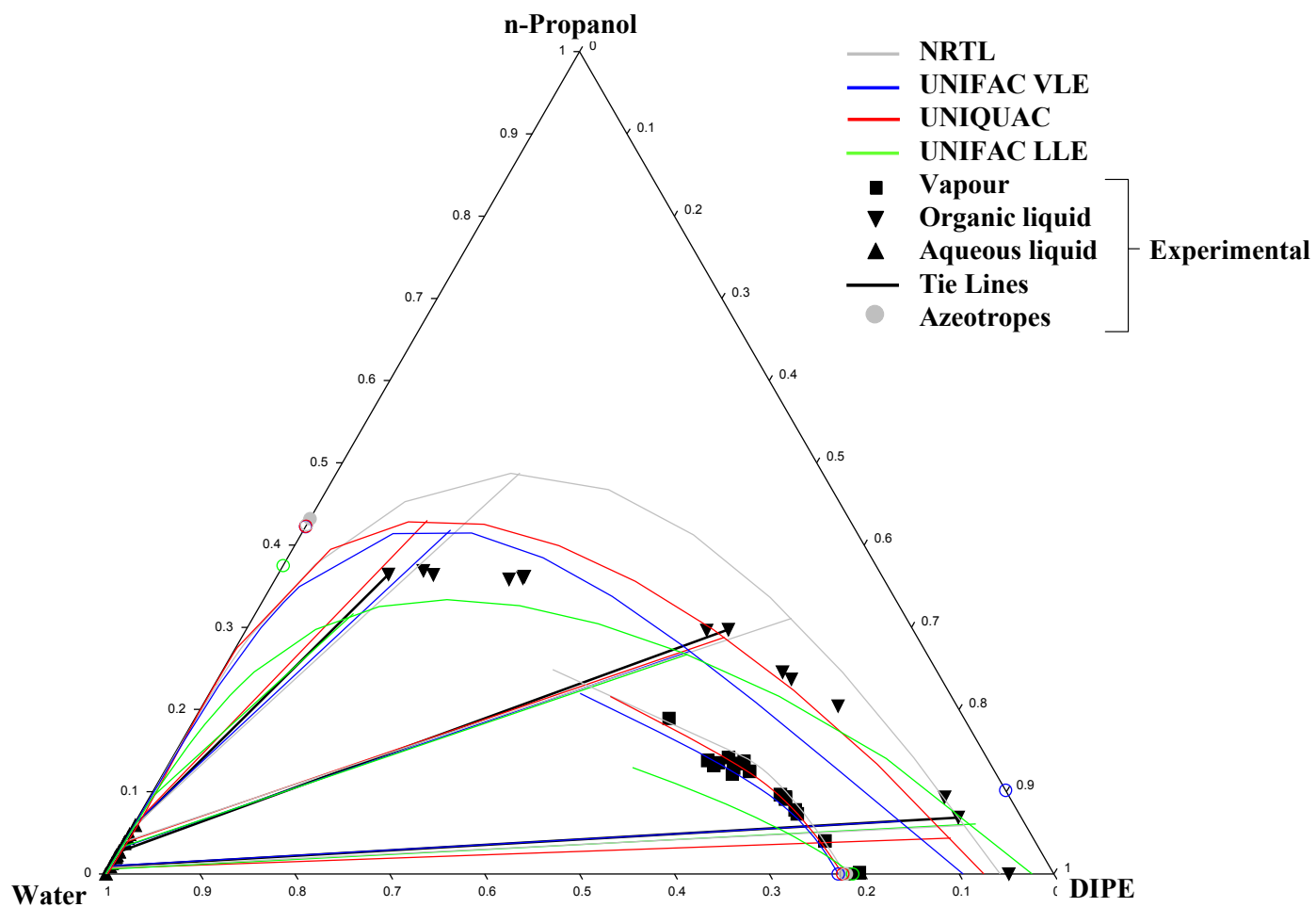


Figure 8-24: Ternary phase diagram of measured n-Propanol/DIPE/Water VLLE data at 101.325 kPa and thermodynamic models (with tie lines and azeotropes) with built-in Aspen parameters.

Table 8-12: AAD and AARD % values for VLLE of *n*-Propanol/DIPE/Water by the NRTL, UNIQUAC, UNIFAC (VLE) and UNIFAC (LLE) models with built-in Aspen parameters at 101.325 kPa.

	Temp (°C)	organic liquid			aqueous liquid			vapour			Σ
		X _{DIPE}	X _{ethanol}	X _{water}	X _{DIPE}	X _{ethanol}	X _{water}	Y _{DIPE}	Y _{ethanol}	Y _{water}	
NRTL											
AAD	0.0265	0.0366	0.1116	0.1370	0.0012	0.0257	0.0254	0.0355	0.0324	0.0075	0.4393
AARD %	0.01	9.79	42.19	41.04	46.92	64.39	2.70	5.84	83.63	2.88	299.38
UNIQUAC											
AAD	0.0842	0.0495	0.0523	0.0688	0.0039	0.0215	0.0249	0.0290	0.0174	0.0132	0.36
AARD %	0.02	25.82	26.74	20.84	179.81	40.01	2.77	4.92	55.96	4.91	361.81
UNIFAC (VLE)											
AAD	0.0652	0.0451	0.0424	0.0721	0.0011	0.0132	0.0133	0.0205	0.0124	0.0138	0.2991
AARD %	0.02	26.16	22.17	29.15	46.35	25.91	1.49	3.38	65.67	5.17	225.45
UNIFAC (LLE)											
AAD	0.0596	0.0866	0.0424	0.0469	0.0010	0.0079	0.0087	0.0418	0.0476	0.0097	0.35
AARD %	0.02	42.01	28.82	18.33	30.85	20.32	0.96	6.88	72.19	3.90	224.28

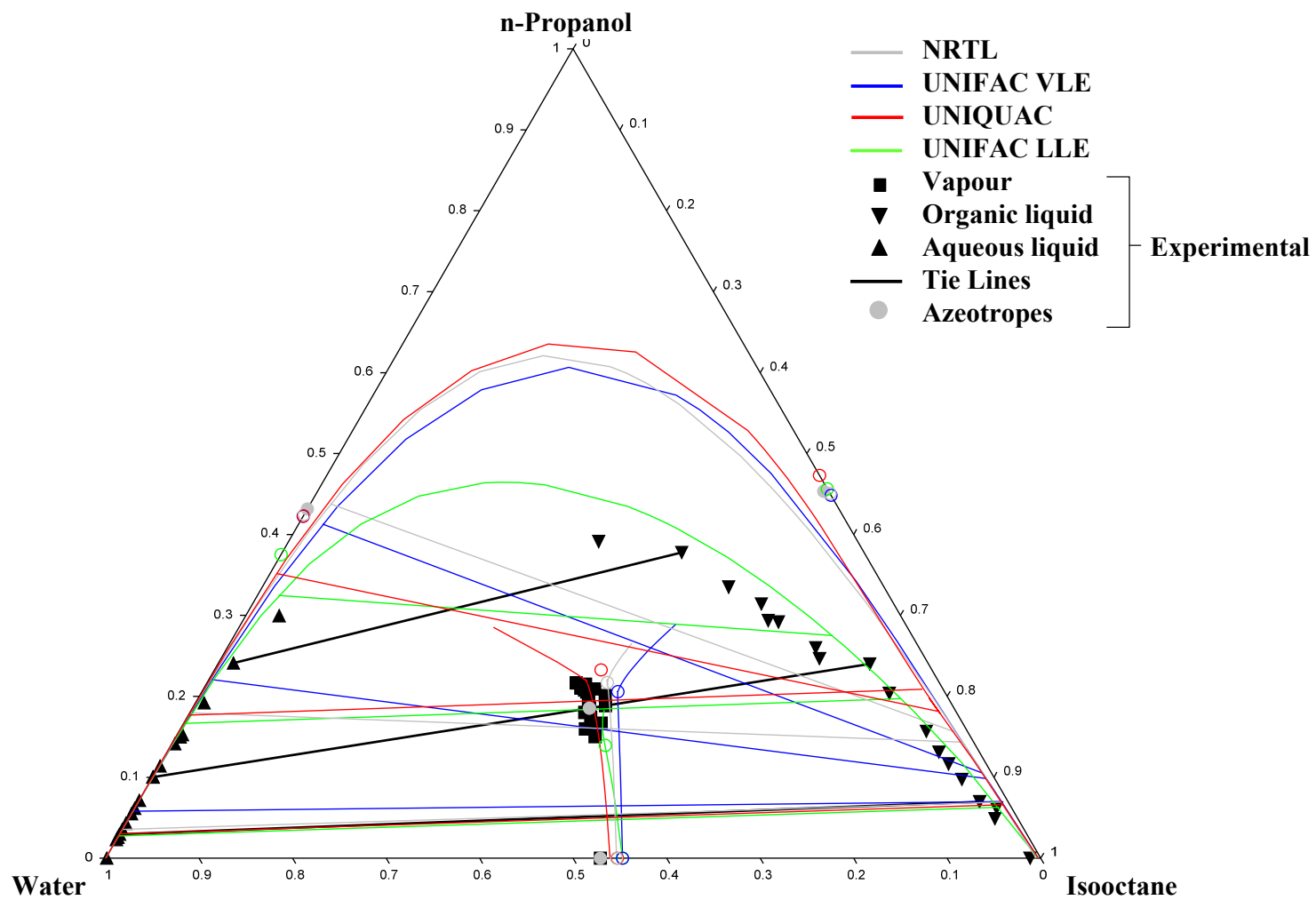


Figure 8-25: Ternary phase diagram of measured n-Propanol/Isooctane/Water VLE data at 101.325 kPa and thermodynamic models (with tie lines and azeotropes) with built-in Aspen parameters.

Table 8-13: AAD and AARD % values for VLLE of *n*-Propanol/Isooctane/Water by the NRTL, UNIQUAC, UNIFAC (VLE) and UNIFAC (LLE) models with built-in Aspen parameters at 101.325 kPa.

	Temp (°C)	organic liquid			aqueous liquid			vapour			Σ
		X _{Isooctane}	X _{n-Propanol}	X _{water}	X _{Isooctane}	X _{n-Propanol}	X _{water}	Y _{Isooctane}	Y _{n-Propanol}	Y _{water}	
NRTL											
AAD	0.1625	0.1611	0.1624	0.0331	0.0022	0.0889	0.0870	0.0274	0.0485	0.0525	0.8258
AARD %	0.05	26.88	86.13	49.60	73.41	127.08	10.11	6.48	58.07	13.45	451.23
UNIQUAC											
AAD	0.1200	0.1311	0.1496	0.0317	0.0025	0.0946	0.0922	0.0274	0.0485	0.0525	0.7500
AARD %	0.03	22.06	74.00	44.06	46.72	117.93	10.81	6.48	58.07	13.45	393.61
UNIFAC (VLE)											
AAD	0.1838	0.1406	0.1237	0.0352	0.0024	0.0696	0.0677	0.0340	0.0365	0.0551	0.7485
AARD %	0.05	23.20	57.57	52.74	131.04	113.43	7.59	8.11	37.75	14.12	445.61
UNIFAC (LLE)											
AAD	0.2898	0.1688	0.1424	0.0396	0.0045	0.0595	0.0634	0.0414	0.0399	0.0081	0.8576
AARD %	0.08	30.86	64.80	38.64	172.39	79.43	7.41	9.81	29.22	2.05	434.68

8.4.2 Regression of data

As set out in Chapter 1, the regression of thermodynamic model parameters on the data measured was performed in this work. The ability of NRTL, UNIQUAC, UNIFAC (VLE) and UNIFAC (LLE) to accurately predict the experimental data with built-in Aspen parameters has been investigated in the previous section and room for improvement has been identified. Areas where these models fall short to correctly predict the VLE data have been high-lighted and some reasons for these shortcomings were given. This section reports on the effort made to improve these model predictions by regressing new parameters for each. The Aspen Plus Data Regression System (DRS) was used to fit parameters of each model to the phase equilibrium data measured in this work and data obtained from literature. The literature data used for regressions are listed in Appendix G. The regressed parameters for each system measured in this work are tabulated in Appendix H. It is important to note that these parameters are not necessarily the optimum parameters that can be obtained for the measured data. The goal was only to improve upon the built-in parameters in Aspen. The NIST Wagner 25 Liquid Vapour Pressure Equation (Appendix F, Table F-1) was used to predict vapour pressure for the regression. In Appendix C, Figures C-1 to C-5, it is shown that the Wagner predictions fit the vapour pressures, as measured in this work, accurately. The regression method followed in this section is explained in Chapter 7. The experimental data together with estimated data with regressed parameters are plotted in Figures 8-26 to 8-29. The ternary phase diagrams are constructed in the same manner as in the previous section. The measured azeotropes as well as those obtained from literature (listed in Section 8-2) are indicated on these diagrams by a solid black dot. The model predictions of the azeotropes are indicated on the diagrams by open dots in a different colour for each model, indicated in the legend. The model predictions of the phase envelope are plotted against the experimental organic and aqueous liquid phase data. The same is done for the estimated and measured vapour phase values. Three tie-lines of each model and the experimental data are indicated on the diagrams – one in the lower alcohol region, one near the ternary heterogeneous azeotropic region and one in the higher alcohol region, approaching the plait point. The AADs and AARDs between experimental and predicted values for the three systems measured in this work are shown in Tables 8-7 to 8-9.

First consider the azeotropes of the **ethanol/DIPE/water** system in Figure 8-26 and Table 8-14. UNIFAC (LLE) most accurately predicts the composition of the ethanol/water azeotrope, followed by UNIFAC (VLE), NRTL and then UNIQUAC all with lower ethanol compositions. The UNIFAC (LLE) prediction of the boiling temperature of this azeotrope is however much lower than that found in literature. With the built-in Aspen parameters UNIFAC (LLE) did not predict any ethanol/water azeotrope and this is of a great improvement. For the NRTL, UNIQUAC and UNIFAC (VLE) of the models the ethanol/water azeotrope is predicted with less accuracy by the regressed parameters. For the ethanol/DIPE azeotrope the UNIFAC (VLE) prediction is the closest to the composition found in literature. NRTL and UNIQUAC predict an ethanol/DIPE azeotrope with a higher ethanol composition. UNIFAC (LLE) predicts an ethanol/DIPE azeotrope with a lower ethanol composition than that found in literature. Only the UNIFAC (VLE) prediction of this azeotrope was improved upon while NRTL, UNIQUAC and UNIFAC (LLE) all predict the azeotrope less accurately with the regressed parameters. The DIPE/water azeotrope is most accurately predicted by NRTL and UNIQUAC. UNIFAC (VLE) and UNIFAC (LLE) are also close, but with a slightly lower and higher DIPE composition, respectively. This indicates there are no significant changes in the prediction of this azeotrope by the regressed parameters. The DIPE/water azeotrope is still accurately predicted. The composition of the ternary heterogeneous azeotrope

is most accurately predicted by NRTL, followed by UNIFAC (VLE), UNIQUAC and UNIFAC (LLE). There is a significant improvement of the ternary azeotrope prediction by NRTL. The boiling temperature of this azeotrope is least accurately predicted by NRTL, but only differs from the measured temperature with 0.63 °C. The prediction by UNIQUAC remained more or less the same, while the predictions by UNIFAC (VLE) and UNIFAC (LLE) are now less accurate.

Table 8-14: Azeotropes of the ethanol/DIPE/water system measured at 101.3 kPa, with those predicted by Aspen with regressed parameters.

Source	Temp (°C)	Composition		
		ethanol	DIPE	water
UNIFAC (VLE)	60.88	0.1180	0.6850	0.1969
This work	61.04	0.1377	0.6659	0.1964
UNIFAC (LLE)	61.27	0.1007	0.6985	0.2008
UNIQUAC	61.30	0.1669	0.6399	0.1932
NRTL	61.67	0.1351	0.6612	0.2036
UNIFAC (VLE)	61.66	-	0.7875	0.2125
UNIFAC (LLE)	61.85	-	0.7856	0.2144
This work	62.16	-	0.7814	0.2186
UNIQUAC	62.42	-	0.7803	0.2197
NRTL	62.64	-	0.7792	0.2208
UNIFAC (LLE)	76.36	0.8903	-	0.1097
UNIQUAC	77.30	0.8100	-	0.1900
NRTL	77.68	0.8573	-	0.1427
UNIFAC (VLE)	77.97	0.8725	-	0.1275
Gmehling et al. (1994)	78.12	0.8950	-	0.1050
Benito and Lopez (1992)	64.00	0.3180	0.6820	-
NRTL	64.21	0.3556	0.6444	-
UNIFAC (VLE)	64.24	0.3310	0.6690	-
UNIQUAC	64.79	0.3544	0.6456	-
UNIFAC (LLE)	64.90	0.2902	0.7098	-

Regarding the phase envelope, UNIQUAC yields the least accurate prediction. It predicts a much larger phase envelope and therefore incorrectly includes homogeneous phase equilibrium points in the heterogeneous region. The regressed parameters for UNIQUAC estimate an even larger heterogeneous region than the built-in Aspen parameters. The NRTL prediction is marginally better than UNIQUAC, but still overestimates the size of the heterogeneous region around the top on the phase envelope. The NRTL phase envelope prediction is however improved by the regressed parameters. The UNIFAC (LLE) phase envelope prediction is also greatly improved by the regressed parameters and it predicts the phase envelope more accurately around the plait point area and the top of the heterogeneous region, but fails to predict the organic liquid phase completely. With the built-in Aspen parameters UNIFAC (VLE) also did not predict the organic liquid phase correctly, but with the regressed parameters it now predicts it more accurately. UNIFAC (VLE) also still predicts the phase envelope most accurately. The lower two tie-lines are sufficiently predicted by all the models, but only UNIFAC (VLE) and

NRTL accurately predict the tie-line near the plait point. The plait point tie-line predictions by UNIQUAC and UNIFAC (LLE) are however greatly improved by the regressed parameters. All the model predictions of the vapour phase are sufficiently accurate.

According to the AAD and AARD values for ethanol/DIPE/water in Table 8-7, UNIFAC (VLE) most accurately predicts the experimental data. The regressed parameters also improved the overall AAD of UNIFAC (VLE) from ca 0.25 to 0.16 and the overall AARD % from ca 120. % to 82 % (compare Tables 8-4 and 8-7). The overall AAD values of NRTL and UNIFAC (LLE) are also improved by the regressed parameters from ca 0.48 to 0.27 and ca 0.57 to 0.24, respectively. The overall AAD value of UNIQUAC was increased by the regressed parameters from ca 0.33 to 0.41 and therefore indicates a decrease in the accuracy of the prediction. This can also be observed when comparing the shapes of the phase envelope in Figures 8-23 and 8-26. Overall the AAD and AARD % values for UNIFAC (VLE) are better than those for NRTL, but NRTL predicts the ternary azeotrope more accurately.

Since the accurate prediction of the ternary heterogeneous azeotrope is very important when simulating a heterogeneous azeotropic distillation column, NRTL with regressed parameters is chosen as thermodynamic model for simulating this separation sequence in Aspen.

The **n-propanol/DIPE/water** system (Figure 8-27) only exhibits two azeotropes namely n-propanol/water and DIPE/water. Also see Table 8-15. NRTL most accurately predicts the n-propanol/water azeotrope, followed by UNIFAC (VLE), UNIFAC (LLE) and then UNIQUAC all with lower ethanol compositions. The UNIFAC (LLE) prediction of the n-propanol/water azeotrope is improved by the regressed parameters and the UNIQUAC prediction with regressed parameters is slightly less accurate than with built-in Aspen parameters. UNIFAC (VLE) still predicts a binary azeotrope between n-propanol and DIPE, which does not exist in reality. As with the built-in Aspen parameters, the DIPE/water azeotrope is most accurately predicted by NRTL and UNIQUAC with the regressed parameters. The UNIFAC (VLE) and UNIFAC (LLE) are improved and also very close to the azeotropic point found in literature. The n-propanol/DIPE/water system exhibits no ternary heterogeneous azeotrope and none of the models predicts one either.

Table 8-15: Azeotropes of the n-propanol/DIPE/water system measured at 101.3 kPa, with those predicted by Aspen with regressed parameters.

Source	Temp (°C)	Composition		
		n-propanol	DIPE	water
UNIFAC (LLE)	61.86	-	0.7856	0.2144
UNIFAC (VLE)	61.95	-	0.7846	0.2154
This work	62.16	-	0.7814	0.2186
UNIQUAC	62.45	-	0.7801	0.2199
NRTL	62.54	-	0.7792	0.2208
NRTL	87.30	0.4294	-	0.5706
UNIQUAC	87.49	0.4032	-	0.5968
Gmehling et al. (1994)	87.66	0.4320	-	0.5680
UNIFAC (LLE)	87.86	0.4162	-	0.5838
UNIFAC (VLE)	88.33	0.4192	-	0.5808
UNIFAC (VLE)	68.45	0.0113	0.9887	-

The regressed parameters for UNIQUAC yield the least accurate prediction of the phase envelope by incorrectly estimating LLE behaviour between n-propanol and water. The NRTL prediction is improved by the regressed parameters since it now estimates a smaller heterogeneous region, but it still includes some of the homogeneous area around the plait point. The regressed parameters for UNIFAC (LLE) also improved its prediction of the phase envelope by enlarging the heterogeneous region it predicts. It does however now overestimate the heterogeneous region around the plait point. With the built-in Aspen parameters UNIFAC (VLE) did not predict the organic liquid phase correctly, but with the regressed parameters it now does. UNIFAC (VLE) most accurately predicts the phase envelope of all the models in question. All the models accurately predict all the tie-lines. All the models also accurately predict of the vapour phase, an improvement made by the regressed parameters. The built-in Aspen parameters predict a vapour phase with a much lower n-propanol composition when using UNIFAC (LLE) than the regressed parameters for UNIFAC (LLE). This is especially an improvement made by the regressed parameters.

The AAD and AARD % values for n-propanol/DIPE/water in Table 8-8 indicate that UNIFAC (VLE) most accurately predicts the experimental data. UNIFAC (VLE) however incorrectly predicts the existence of an n-propanol/DIPE azeotrope. The regressed parameters improved the overall AAD of UNIFAC (VLE) from ca 0.3 to 0.2 and the overall AARD % from ca 225 % to 162 % (compare Tables 8-5 and 8-8). The overall AAD values of NRTL are improved by the regressed parameters from ca 0.44 to 0.39. The overall AAD values of UNIFAC (LLE) increased from 0.35 to 0.48 with the regressed parameters, but the overall AARD % were improved from ca 224 % to 223 %. The overall AAD value of UNIQUAC was increased by the regressed parameters from ca 0.36 to 0.4, but the overall AARD % was improved from ca 362 % to 223 % and therefore suggests an increase in the accuracy of its prediction. This can also be confirmed by the LLE behaviour predicted by the regressed parameters between n-propanol and water in Figure 8-27. Overall the AAD and AARD % values for UNIFAC (VLE) are better than those for NRTL and UNIFAC (LLE), but since UNIFAC

(VLE) incorrectly predicts an n-propanol/DIPE azeotrope it is suggested that NRTL or UNIFAC (LLE) be used for simulations in Aspen.

Only NRTL and UNIQUAC parameters could be determined for the **n-propanol/isooctane/water** system (Figure 8-28). No improvement could be obtained in the UNIFAC (VLE) and (LLE) parameters with the measured data and literature available. Both NRTL and UNIQUAC predict the n-propanol/water azeotrope less accurately with the regressed parameters (Table 8-16 and Figure 8-28). NRTL predicts an n-propanol/water azeotrope with a significantly higher n-propanol composition than that found in literature for the azeotrope and UNIQUAC predicts a significantly lower n-propanol composition. For the n-propanol/isooctane azeotrope the NRTL prediction is the closest to the composition found in literature, but UNIQUAC closest to the boiling temperature. Both the NRTL and UNIQUAC predictions of the n-propanol/isooctane azeotrope remained the same as with the built-in parameters. UNIQUAC predicts an n-propanol/isooctane azeotrope with a higher n-propanol composition than that found in literature. The isooctane/water azeotrope is most accurately predicted by UNIQUAC. Both the NRTL and UNIQUAC predictions of the isooctane/water azeotrope also remained more or less the same as with the built-in parameters. The ternary heterogeneous azeotrope is most accurately predicted by UNIQUAC, as opposed to NRTL with the built-in parameters. There is a small improvement in the ternary azeotrope prediction by UNIQUAC. There is a significant change in the prediction of the ternary azeotrope by NRTL and its accuracy has decreased considerably.

Table 8-16: Azeotropes of the n-propanol/isooctane/water system measured at 101.3 kPa, with those predicted by Aspen with regressed parameters.

Source	Temp (°C)	Composition		
		n-propanol	isooctane	water
This work	74.59	0.1855	0.4246	0.3899
UNIQUAC	75.79	0.2177	0.4058	0.3765
NRTL	76.74	0.1229	0.4985	0.3785
This work	79.13	-	0.5290	0.4710
NRTL	79.23	-	0.5468	0.4532
UNIQUAC	79.64	-	0.5394	0.4606
NRTL	86.68	0.4751	-	0.5249
UNIQUAC	87.60	0.4247	-	0.5753
Gmehling et al. (1994)	87.75	0.4316	-	0.5684
Hiaki et al. (1994)	84.78	0.4533	0.5412	-
UNIQUAC	85.40	0.4743	0.5257	-
NRTL	87.13	0.4496	0.5504	-

Regarding the phase envelope, both the NRTL and UNIQUAC predictions have been improved by the regressed parameters. Both however still predict a much larger phase envelope and therefore incorrectly include homogeneous phase equilibrium points in the heterogeneous region. UNIQUAC predicts a smaller heterogeneous region and is therefore more accurate than NRTL. The directionality of the upper two tie-lines is changed by the regressed parameters from those predicted by the built-in parameters. However, the tie-line still does not agree well with the experimental data. The vapour phase prediction by UNIQUAC with regressed

parameters did not differ from that predicted by the built-in parameters. It still seems to follow the same trend as the experimental data, but extends much farther into the heterogeneous region. The NRTL prediction also now seems to follow the same trend, but deviates from the experimental data around its predicted ternary azeotropic point.

According to the AAD and AARD values for n-propanol/isooctane/water in Table 8-9, UNIQUAC most accurately predicts the experimental data. Overall the AAD and AARD % values from UNIQUAC with regressed parameters are better than with built-in parameters, with the only significant exception being the isooctane composition of the aqueous liquid phase. The overall AAD value of NRTL was increased by the regressed parameters from ca 0.83 to 0.9, but the overall AARD % was improved from ca 451 % to 423 % and therefore suggests an increase in the accuracy of its prediction. Although the regressed parameters slightly improved the VLLE data prediction of these models, the AAD and AARD % values are still unacceptably high. Other, more advanced thermodynamic models might predict the experimental data more accurately. It does not fall into the scope of this project to investigate these more advanced models. When such inaccurate predictions are to be used in a simulation of a heterogeneous azeotropic distillation, the results obtained may differ greatly from what will happen in practice. Therefore it was decided not to simulate a separation sequence for the dehydration of n-propanol with isooctane as entrainer.

To summarize, ethanol/DIPE/water phase equilibrium is best predicted by UNIFAC (VLE) when using built-in Aspen parameters. When new parameters were regressed for the experimental data, the UNIFAC (VLE) parameters were improved even further, but NRTL predicts the composition of the ternary azeotrope more accurately and was therefore selected for simulation. UNIQUAC is considered to predict the n-propanol/DIPE/water phase equilibrium most accurately when using built-in Aspen parameters. With regressed parameters the NRTL and UNIFAC (LLE) predictions are improved and are considered to be most accurate. None of the models predict n-propanol/isooctane/water phase equilibrium accurately with built-in Aspen parameters. The NRTL and UNIQUAC predictions were improved by the regressed parameters, but were still not sufficient of simulation use.

It was found that there is a trade-off between the accurate prediction of the phase envelope with tie lines and ternary heterogeneous and the accurate prediction of the binary azeotropes. If the phase envelope, tie lines and ternary heterogeneous azeotrope predictions are improved, the binary azeotrope predictions are compromised. One has to decide which is more important for the application of the model. In the case of heterogeneous azeotropic distillation, it is more important to predict the phase envelope, tie lines and ternary azeotrope correctly.

The UNIFAC models generally have the lowest AARD % values, which indicate more accurate prediction of the compositions of the vapour and liquid phases. The temperature AAD and AARD % values are similar for all the models, for built-in and regressed parameters. NRTL and UNIQUAC generally predict the azeotropes more accurately. This might be due to the fact that NRTL and UNIQUAC are based on molecular contributions as opposed to UNIFAC that is based on group contributions (Section 3.7 to 3.9).

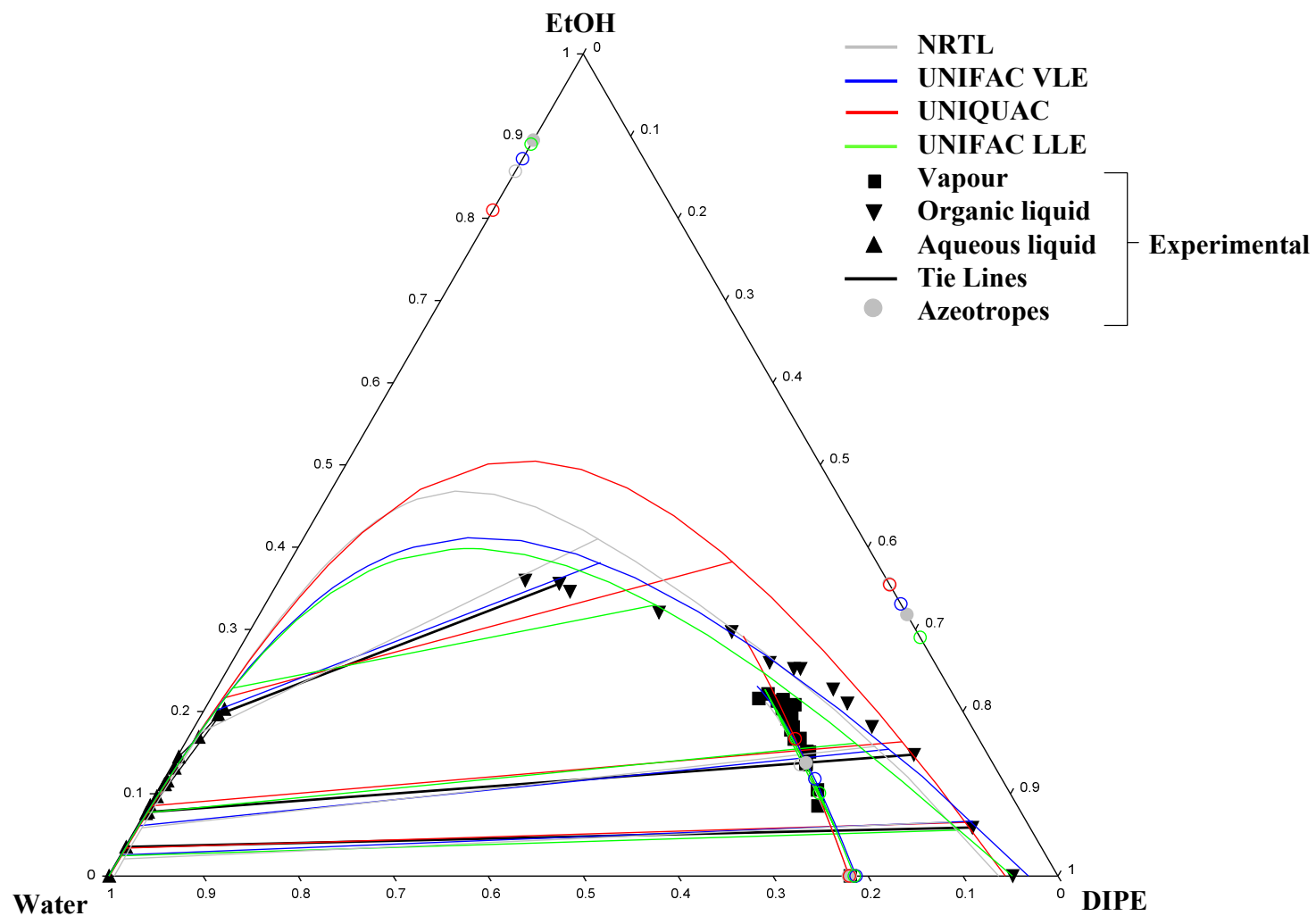


Figure 8-26: Ternary phase diagram of measured Ethanol/DIPE/Water VLLE data at 101.325 kPa and thermodynamic models (with tie lines and azeotropes) with regressed parameters.

Table 8-17: AAD and AARD % values for VLLE of Ethanol/DIPE/Water by the NRTL, UNIQUAC, UNIFAC (VLE) and UNIFAC (LLE) models with regressed parameters at 101.325 kPa.

	Temp (°C)	organic liquid			aqueous liquid			vapour			Σ
		x_{DIPE}	$x_{ethanol}$	x_{water}	x_{DIPE}	$x_{ethanol}$	x_{water}	y_{DIPE}	$y_{ethanol}$	y_{water}	
NRTL											
AAD	0.0598	0.0502	0.0345	0.0376	0.0033	0.0248	0.0226	0.0136	0.0144	0.0124	0.2731
AARD %	0.02	14.14	15.97	18.35	145.93	23.10	2.71	2.20	12.23	6.64	241.28
UNIQUAC											
AAD	0.0724	0.0914	0.0601	0.0460	0.0039	0.0357	0.0388	0.0238	0.0282	0.0070	0.4073
AARD %	0.02	27.11	21.64	25.96	75.25	24.54	4.79	3.85	17.61	3.63	204.40
UNIFAC (VLE)											
AAD	0.0275	0.0296	0.0202	0.0214	0.0011	0.0151	0.0155	0.0095	0.0091	0.0080	0.1572
AARD %	0.01	8.13	10.04	11.63	21.46	13.94	1.89	1.52	8.62	4.27	81.51
UNIFAC (LLE)											
AAD	0.0313	0.0572	0.0294	0.0375	0.0026	0.0194	0.0214	0.0148	0.0181	0.0078	0.2394
AARD %	0.01	15.75	13.36	18.62	32.70	14.77	2.66	2.35	13.49	4.19	117.90

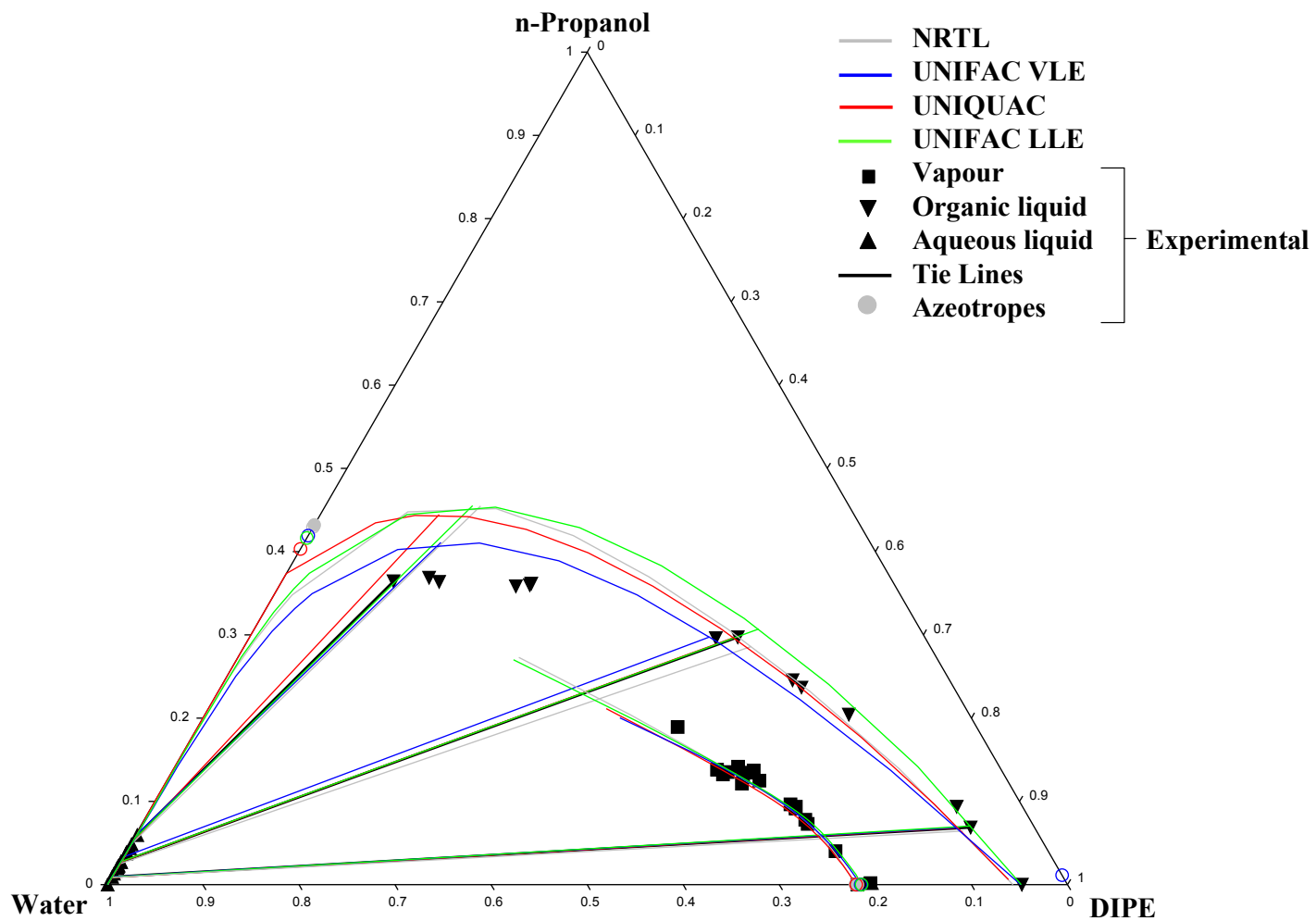


Figure 8-27: Ternary phase diagram of measured n-Propanol/DIPE/Water VLLE data at 101.325 kPa and thermodynamic models (with tie lines and azeotropes) with regressed parameters.

Table 8-18: AAD and AARD % values for VLLE of *n*-Propanol/DIPE/Water by the NRTL, UNIQUAC, UNIFAC (VLE) and UNIFAC (LLE) models with regressed parameters at 101.325 kPa.

	Temp (°C)	organic liquid			aqueous liquid			vapour			Σ
		X _{DIPE}	X _{n-Propanol}	X _{water}	X _{DIPE}	X _{n-Propanol}	X _{water}	Y _{DIPE}	Y _{n-Propanol}	Y _{water}	
NRTL											
AAD	0.0853	0.0690	0.0463	0.1000	0.0009	0.0104	0.0109	0.0310	0.0169	0.0155	0.3861
AARD %	0.02	38.87	22.87	25.97	38.39	21.66	1.22	5.19	67.79	5.75	227.72
UNIQUAC											
AAD	0.0866	0.0625	0.0659	0.1119	0.0009	0.0089	0.0095	0.0262	0.0153	0.0157	0.4033
AARD %	0.03	38.74	29.35	27.38	37.20	18.38	1.07	4.39	60.56	5.77	222.87
UNIFAC (VLE)											
AAD	0.0370	0.0195	0.0346	0.0415	0.0007	0.0129	0.0134	0.0179	0.0105	0.0116	0.1998
AARD %	0.01	10.88	19.81	12.36	20.78	28.19	1.48	2.95	61.16	4.35	161.96
UNIFAC (LLE)											
AAD	0.1206	0.0553	0.0858	0.1223	0.0010	0.0134	0.0142	0.0309	0.0165	0.0163	0.4764
AARD %	0.04	33.18	28.00	28.53	24.11	27.21	1.58	5.20	68.96	6.01	222.82

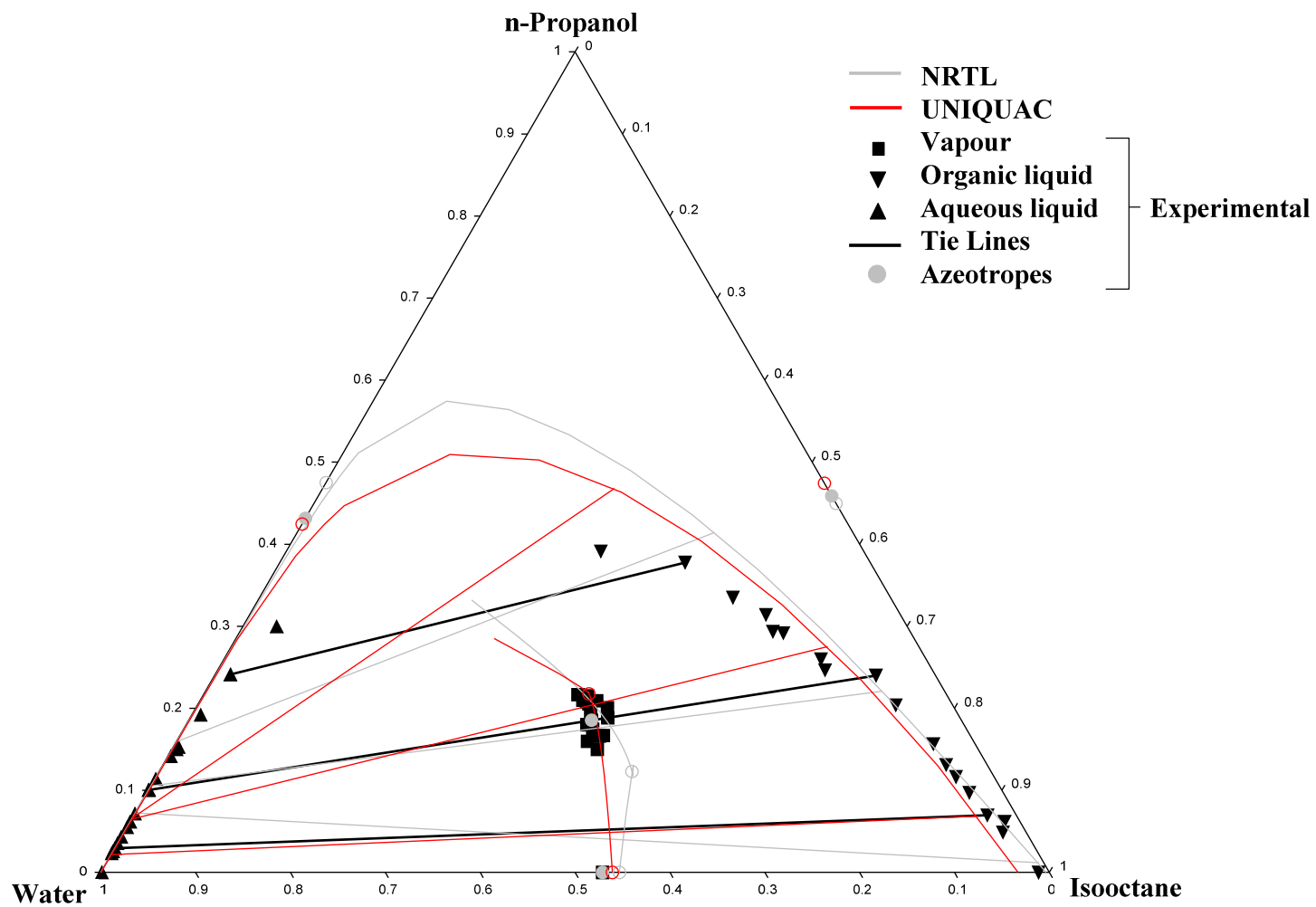


Figure 8-28: Ternary phase diagram of measured *n*-Propanol/Isooctane/Water VLE data at 101.325 kPa and thermodynamic models (with tie lines and azeotropes) with regressed parameters.

Table 8-19: AAD and AARD % values for VLE of *n*-Propanol/Isooctane/Water by the NRTL and UNIQUAC models with regressed parameters at 101.325 kPa.

	Temp (°C)	organic liquid			aqueous liquid			vapour			Σ
		$x_{\text{Isooctane}}$	$x_{\text{n-Propanol}}$	x_{water}	$x_{\text{Isooctane}}$	$x_{\text{n-Propanol}}$	x_{water}	$y_{\text{Isooctane}}$	$y_{\text{n-Propanol}}$	y_{water}	
NRTL											
AAD	0.2802	0.1655	0.1507	0.0195	0.0066	0.0855	0.0908	0.0437	0.0359	0.0218	0.9002
AARD %	0.08	30.53	61.63	25.40	133.93	105.47	11.01	10.16	38.93	5.56	422.69
UNIQUAC											
AAD	0.1474	0.1358	0.1012	0.0526	0.0054	0.0920	0.1459	0.0126	0.0131	0.0097	0.7157
AARD %	0.04	23.51	43.20	62.20	169.71	71.00	17.29	2.92	17.63	2.47	409.96

8.5 SEPARATION SEQUENCE SIMULATIONS

As stipulated in Chapter 1, one of the goals of this work was to construct and simulate separation sequences for the dehydration of ethanol, isopropanol and n-propanol. The layout and functioning of the separation sequences used in this section is explained in chapter 8. The purpose of simulating these separation sequences in Aspen is firstly to illustrate the influence improved regressed parameters have on the simulation results. Secondly, these simulations are performed to provide practical examples of how the chosen entrainer can be used to dehydrate each alcohol in question. And lastly it enables a comparison of this entrainer with those generally used in industry for each specific alcohol dehydration. In this section the comparison of entrainers will be focussed on the purity to which the products can be produced and the flow rates of the streams, i.e. the size of distillation columns required. Sinnott and Towler (2009) provide the following correlation for the diameter of a distillation column:

$$D_c = \sqrt{\frac{4\hat{V}_w}{\pi\rho_v\hat{u}_v}} \quad 8-1$$

where

\hat{V}_w	=	maximum vapour rate, kg/s
ρ_v	=	vapour density, kg/m ³
\hat{u}_v	=	maximum allowable vapour velocity, based on the total column cross sectional area, m/s

Equation 8-1 shows that a larger maximum vapour rate will require a larger column diameter and subsequently a larger distillation column. The average vapour flow rate in a column is can therefore serve as indication of the column size.

The simulation results are shown in the form of detailed flow sheets in Figures 8-27 to 8-35. Some important flow sheet information is also provided in Tables 8-20 to 8-29. The alcohol and water purities provided in these sheets are separation specifications, as used in the simulation of the sequences for the respective columns. The reboiler duties, as provided in these sheets, were also used as simulation specifications. Detailed simulation results are provided in Appendix I. It is important to note the flow sheets provided are not necessarily the most optimum flow sheet possible since determining the optimum flow sheet for each simulation falls outside the scope of this work. These simulations serve as illustration of the importance of accurate model predictions and the comparison that can be drawn between different entrainers for alcohol dehydration. The pupose was not optimization of these flow sheets.

The simulation of **ethanol dehydration** via heterogeneous azeotropic distillation with DIPE as entrainer is used to illustrate the influence improved **regressed parameters** have on simulation results (Figures 8-29 and 8-30, and Tables 8-20 and 8-21). As discovered in the previous two sections, the **built-in Aspen parameters** predict an aqueous liquid phase with a higher ethanol composition around the ternary azeotropic point than the experimental data shows. Therefore the built-in parameters predict that more than 4 times the amount of distillate (D2) from column 2 is recycled than with the regressed parameters (0.178 and 0.039 for built-in and regressed parameters respectively, in Table 8-20). This is also reflected in the larger vapour flow rate in column 1 with built-in parameters (15.04 kg/sec), than with regressed parameters (12.14 kg/sec). The respective

condenser duties of the second column for the two flow sheets does not differ that much (ca -1920 kW and -1930 kW) although the flows of D2 differ significantly, since the compositions of the two D2 streams differ greatly. The significant difference in average vapour flow rates in the recovery column, between built-in and regressed parameters, indicates that this column might be under-designed when using built-in parameters and will in all likelihood flood. The significantly higher reflux ratio in the second column, with regressed parameters, indicate that more stages might be required than the built-in parameters predicted. The large difference in flow between the D2 streams will however result in over-design of column 1 when using built-in Aspen parameters, to accommodate the large flow to the column and the larger vapour flow rate in the column (refer to Equation 8-1). The organic liquid phase around the ternary azeotropic point is also predicted with a higher ethanol composition and with a lower DIPE composition by the built-in parameters and a greater amount of organic liquid phase is refluxed to column 1 (5.551 and 4.059 for built-in and regressed parameters respectively, in Table 8-20). With the larger recycle of D2 and organic reflux in Figure 8-29, a larger distillate (D1) is produced from column 1 and therefore the condenser duty is larger (ca -6400 kW) as opposed to that in Figure 8-30 (ca -5270 kW). The reboiler duty (ca 6540 kW) predicted by the built-in parameters for column 1 is also significantly higher than that predicted by the regressed parameters (ca 5410 kW).

Table 8-20: Flow sheet information for the azeotropic column (C1) of ethanol dehydration with DIPE as entrainer, comparing built-in Aspen parameters with regressed parameters.

Flows and ratios			
	Built-in	Regressed	
D ₂ /F ratio	0.178	0.039	
Organic reflux/F ratio	5.551	4.059	
Average vapour flow rate	15.04	12.14	kg/sec
Condenser			
Temperature	334.41	335.31	K
Duty	-6407.26	-5273.49	kW
Distillate rate*	0.1727	0.1409	kmol/sec
Reflux rate**	0.1745	0.1423	kmol/sec
Reflux ratio	1.01	1.01	
*Vapour flow at top of column			
**Liquid flow at top of column			
Reboiler			
Temperature	349.51	349.84	K
Duty	6544.24	5412.52	kW
Bottoms rate*	0.0142	0.0136	kmol/sec
Boilup rate**	0.1694	0.1364	kmol/sec
Boilup ratio	11.94	10.03	
*Liquid flow at top of column			
**Vapour flow at top of column			

The overall energy balance of the flow sheet simulated with built-in Aspen parameters is ca -1220 kW as opposed to ca 204 kW from the regressed parameters provided full energy integration can be achieved. This all

indicates that when built-in Aspen parameters do not accurately predict experimental phase equilibrium data, it is of great importance to first regress more reliable parameters before simulations can be performed.

Table 8-21: Flow sheet information for the recovery column (C2) of ethanol dehydration with DIPE as entrainer, comparing built-in Aspen parameters with regressed parameters.

Flow			
	Built-in	Regressed	
Average vapour flow rate	0.93	1.46	kg/sec
Condenser			
Temperature	342.83	348.72	K
Duty	-1917.47	-1933.83	kW
Distillate rate*	0.0049	0.0011	kmol/sec
Reflux rate**	0.0421	0.0478	kmol/sec
Reflux ratio	8.53	44.55	
*Vapour flow at top of column			
**Liquid flow at top of column			
Reboiler			
Temperature	373.17	373.15	K
Duty	2000.00	2000.00	kW
Bottoms rate*	0.0139	0.0135	kmol/sec
Boilup rate**	0.0490	0.0490	kmol/sec
Boilup ratio	3.53	3.63	
*Liquid flow at top of column			
**Vapour flow at top of column			

The simulation performed for **ethanol dehydration with DIPE** as entrainer, using the regressed parameters (Figure 8-30) can be compared to a simulation of **ethanol dehydration with benzene** as entrainer (Figure 8-31), as a way of quantitatively assessing the separation capabilities of the two entrainers. Important flow sheet information of these two sequences is also provided in Tables 8-22 and 8-23. The benzene simulation was performed with parameters supplied by Christo Crause (2011). These parameters can be found in Appendix H, Table H-11. As stated in chapter 6, benzene has originally been used for ethanol dehydration to first establish the method of heterogeneous azeotropic distillation. Since then it has commonly been used as entrainer for ethanol dehydration. From Figure 8-20 in Section 8.3 it is clear that the aqueous liquid phase around the azeotropic point of the ethanol/benzene/water system has a larger ethanol and lower water composition than that of the ethanol/DIPE/water system. Therefore in the ethanol/DIPE/water system more water is removed from the azeotropic column (C1) through the aqueous liquid phase and less ethanol is carried to the recovery column (C2). Subsequently less distillate from column 2 need to be recycled since less ethanol is lost to the aqueous liquid phase when using DIPE as entrainer. This can be seen in Figures 8-30 and 8-31. It is also evident from the D2/F ratios of 1.055 and 0.039 for benzene and DIPE respectively. The recycled D2 stream for ethanol/benzene/water is two orders of magnitude larger than for ethanol/DIPE/water. The vapour flow rate in the benzene column is also larger than the DIPE column (13.76 compared to 12.14 in Table 8-22). A larger azeotropic column will therefore be required when benzene is used as entrainer, due to a larger flow to the

column and a larger vapour flow in the column (Equation 8-1). The condenser and reboiler duties of the azeotropic column are also significantly higher when using benzene (ca -8720 kW and 8770 kW respectively) as opposed to using DIPE (ca -5270 kW and 5410 kW respectively) as entrainer. This indicates that the azeotropic column and energy requirements for ethanol dehydration with benzene as entrainer could be much larger than for DIPE. The difference in average vapour flow and significant difference in reflux ratio in the second column, indicates that a larger (more stages) recovery column might be required when using DIPE as entrainer.

Table 8-22: Flow sheet information for the azeotropic columns, C1, of ethanol dehydration with benzene and DIPE as entrainers respectively.

Flows and ratios			
	Benzene	DIPE	
D ₂ /F ratio	1.055	0.039	
Organic reflux/F ratio	4.281	4.059	
Average vapour flow rate	13.76	12.14	kg/sec
Condenser			
Temperature	337.59	335.31	K
Duty	-8702.19	-5273.49	kW
Distillate rate*	0.2229	0.1409	kmol/sec
Reflux rate**	0.1935	0.1423	kmol/sec
Reflux ratio	0.87	1.01	
*Vapour flow at top of column			
**Liquid flow at top of column			
Reboiler			
Temperature	351.08	349.84	K
Duty	8768.90	5412.52	kW
Bottoms rate*	0.0098	0.0136	kmol/sec
Boilup rate**	0.2248	0.1364	kmol/sec
Boilup ratio	22.97	10.03	
*Liquid flow at top of column			
**Vapour flow at top of column			

Table 8-23: Flow sheet information for the recovery columns, C2, of ethanol dehydration with benzene and DIPE as entrainers respectively.

Flow			
	Benzene	DIPE	
Average vapour flow rate	1.05	1.46	kg/sec
Condenser			
Temperature	342.27	348.72	K
Duty	-1831.28	-1933.83	kW
Distillate rate*	0.0293	0.0011	kmol/sec
Reflux rate**	0.0148	0.0478	kmol/sec
Reflux ratio	0.50	44.55	
*Vapour flow at top of column			
**Liquid flow at top of column			
Reboiler			
Temperature	373.16	373.15	K
Duty	2000.00	2000.00	kW
Bottoms rate*	0.0135	0.0135	kmol/sec
Boilup rate**	0.0490	0.0490	kmol/sec
Boilup ratio	3.63	3.63	
*Liquid flow at top of column			
**Vapour flow at top of column			

As previously said (Chapter 5), aqueous IPA originating from the semiconductor manufacturing industry is traditionally dehydrated using cyclohexane as an entrainer. From Figure 8-21 it is evident that DIPE is also a potential entrainer for **IPA dehydration**. Figures 8-32 and 8-33 contain detailed flow sheets for IPA dehydration using cyclohexane and DIPE as entrainers, respectively. Tables 8-24 and 8-25 contain important flow sheet information of these sequences. The IPA/cyclohexane simulation has been performed by Arifin and Chien (2007). Only the information provided by Arifin and Chien (2007) could be listed in Tables 8-24 and 8-25. In this work, the IPA/DIPE/water simulation was performed in Aspen with its built-in parameters. These parameters adequately predict the IPA/DIPE/water phase equilibrium data measured by Lladosa et al. (2008). The flow sheets can be used to compare the separation capacity of cyclohexane and DIPE as entrainers. Figure 8-21 in Section 8.3 shows that the aqueous liquid phase around the azeotropic point of the IPA/cyclohexane/water system has a larger IPA and lower water composition than that of the IPA/DIPE/water system. Consequently, in the IPA/DIPE/water system more water is removed from the azeotropic column (C1) through the aqueous liquid phase and less distillate from column 2 need to be recycled since less IPA is lost to the aqueous liquid phase. This can be seen in Figures 8-32 to 8-33 and Table 8-24. The recycled D2 stream for IPA/cyclohexane/water is an order of magnitude larger than for IPA/DIPE/water. Compare the D_2/F ratios of 1.092 and 0.183 (Table 8-24) for cyclohexane and DIPE respectively. The recycle flow to the azeotropic column is therefore much larger and a larger column will be required when cyclohexane is used as entrainer. The condenser and reboiler duties of the azeotropic column are lower when using cyclohexane (ca -3990 kW and 4450 kW respectively) as opposed to using DIPE (ca -4810 kW and 5010 kW respectively) as entrainer.

However, the condenser and reboiler duties of the recovery column (C2) are higher when using cyclohexane (ca -1940 kW and 2140 kW respectively) as opposed to using DIPE (ca -920 kW and 1000 kW respectively) as entrainer. The overall energy balance of the flow sheet simulated with cyclohexane as entrainer is ca 650 kW as opposed to 280 kW when using DIPE as entrainer providing full energy integration can be implemented. This indicates that the simulation results, using DIPE as an entrainer, is definitely comparable with that of cyclohexane, if not better.

Table 8-24: Flow sheet information for the azeotropic columns, C₁, of IPA dehydration with cyclohexane and DIPE as entrainers respectively.

Feed ratios			
	Cyclohexane	DIPE	
D ₂ /F ratio	1.092	0.183	
Organic reflux/F ratio	2.461	3.958	
Average vapour flow rate	-	11.30	kg/sec
Condenser			
Temperature	-	334.87	K
Duty	-3988.63	-4806.72	kW
Distillate rate*	0.1126	0.1258	kmol/sec
Reflux rate**	-	0.9758	kmol/sec
Reflux ratio	-	0.99	
*Vapour flow at top of column			
**Liquid flow at top of column			
Reboiler			
Temperature	-	354.93	K
Duty	4448.38	5007.56	kW
Bottoms rate*	0.0139	0.0139	kmol/sec
Boilup rate**	-	0.1236	kmol/sec
Boilup ratio	-	8.91	
*Liquid flow at top of column			
**Vapour flow at top of column			

Table 8-25: Flow sheet information for the recovery columns, C₂, of IPA dehydration with cyclohexane and DIPE as entrainers respectively.

Flow			
	Cyclohexane	DIPE	
Average vapour flow rate	-	0.02	kg/sec
Condenser			
Temperature	-	338.69	K
Duty	-1943.71	-923.22	kW
Distillate rate*	0.0303	0.0051	kmol/sec
Reflux rate**	-	0.0160	kmol/sec
Reflux ratio	-	3.15	
*Vapour flow at top of column			
**Liquid flow at top of column			
Reboiler			
Temperature	-	373.17	K
Duty	2137.83	1000.00	kW
Bottoms rate*	0.0139	0.0139	kmol/sec
Boilup rate**	-	0.0245	kmol/sec
Boilup ratio	-	1.76	
*Liquid flow at top of column			
**Vapour flow at top of column			

The experimental results given in Section 8.2 shows that n-propanol/DIPE/water does not exhibit any ternary heterogeneous azeotrope. Therefore, one would think that heterogeneous azeotropic distillation cannot be used to **dehydrate aqueous n-propanol**. However, as stated in chapter 5, Carlson (1949) proposed a method for recovering the alcohols from a crude aqueous n-propanol cut also containing ethanol and IPA. The proposed method is based on azeotropic distillation and employs DIPE as entrainer. The crude aqueous n-propanol cut, which Carlson (1949) refers to in his patent, is produced in the Fischer Tropsch process. The separation sequence is similar to those previously discussed. The only difference is that the bottoms produced from the azeotropic column are n-propanol although no ternary azeotrope exists between n-propanol, DIPE and water. The ethanol, IPA and water in the feed are entrained overhead in the azeotropic column due to the low-boiling ternary azeotropes it forms with DIPE. A simulation of the abovementioned method was performed in this work with Aspen. A flow sheet with the simulation results obtained is shown in Figure 8-34 and important flow sheet information is listed in Tables 8-26 and 8-27. The results Carlson (1949) obtained along with the comparative results from the simulation performed in this work are given in Table 8-28. A similar bottoms product stream was obtained. The composition of the feed stream is taken from Carlson's patent. An n-propanol stream with a purity of 99 mole % is produced as bottoms of the azeotropic column (C1). In this stream 94.78 % of the n-propanol fed to the column, is recovered. The second column (C2) produces nearly pure water as bottoms. The distillate of the C2 can be used for processing and recovery of valuable by-products. This simulation serves as illustration that DIPE can even be utilized for n-propanol dehydration in certain cases, depending on the quality of the feed stream.

Table 8-26: Flow sheet information for the azeotropic column, C_1 , of *n*-propanol dehydration from a Fischer Tropsch waste stream with DIPE as entrainer.

Flow		
Average vapour flow rate	3.23	kg/sec
Condenser		
Temperature	344.14	K
Duty	-3068.30	kW
Distillate rate*	0.0761	kmol/sec
Reflux rate**	0.0598	kmol/sec
Reflux ratio	0.78	
*Vapour flow at top of column		
**Liquid flow at top of column		
Reboiler		
Temperature	369.95	K
Duty	3409.62	kW
Bottoms rate*	0.0100	kmol/sec
Boilup rate**	0.0100	kmol/sec
Boilup ratio	8.18	
*Liquid flow at top of column		
**Vapour flow at top of column		

Table 8-27: Flow sheet information for the second column (producing nearly pure water) of *n*-propanol dehydration from a Fischer Tropsch waste stream with DIPE as entrainer.

Flow		
Average vapour flow rate	0.95	kg/sec
Condenser		
Temperature	349.80	K
Duty	-1922.14	kW
Distillate rate*	0.0020	kmol/sec
Reflux rate**	0.0442	kmol/sec
Reflux ratio	22.30	
*Vapour flow at top of column		
**Liquid flow at top of column		
Reboiler		
Temperature	373.17	K
Duty	2000.00	kW
Bottoms rate*	0.0150	kmol/sec
Boilup rate**	0.0490	kmol/sec
Boilup ratio	3.27	
*Liquid flow at top of column		
**Vapour flow at top of column		

Table 8-28: Bottoms from the azeotropic column of Carlson's (1945) example compared to the simulation in this work.

Component	Carlson (1949) wt %	This work wt %
n-propanol	97.5*	99.7
acid	0.1	0.0
ester	0.4	0.0
aldehyde	0.7	0.0
ketone	0.0	0.0
water	1.7	0.3

*(97.5-99.5 wt %)

DIPE can also be used for the **recovery of ethanol** when a waste stream from the Fischer Tropsch process has a high ethanol composition. Typical compositions of such ethanol-rich streams can be found in literature (Nel, de Klerk 2007). An example of such a simulation is given in Figure 8-35 and flow sheet information is provided on this figure and in Tables 8-29 and 8-30.

Table 8-29: Flow sheet information for the azeotropic column, C1, of ethanol dehydration from a Fischer Tropsch waste stream with DIPE as entrainer.

Flow		
Average vapour flow rate	10.12	kg/sec
Condenser		
Temperature	334.30	K
Duty	-4436.19	kW
Distillate rate*	0.1199	kmol/sec
Reflux rate**	0.1254	kmol/sec
Reflux ratio	1.05	
*Vapour flow at top of column		
**Liquid flow at top of column		
Reboiler		
Temperature	353.45	K
Duty	4907.81	kW
Bottoms rate*	0.0099	kmol/sec
Boilup rate**	0.1265	kmol/sec
Boilup ratio	12.78	
*Liquid flow at top of column		
**Vapour flow at top of column		

An ethanol-rich stream is fed to an azeotropic column (C1). Water, IPA and some the ethanol is entrained to the distillate of the azeotropic column. The bottoms (B1) of C1 mainly consist of ethanol and n-propanol. This stream is then fed to a standard distillation column where ethanol is recovered as distillate (D2). The ethanol purity in D2 is only 94.25 mole %, but it is well beyond the ethanol/water and ethanol/MEK azeotropes. In this stream 68.53 % of the ethanol fed to the column, is recovered. This may not be the optimum flow sheet for ethanol recovery from a Fischer Tropsch waste stream, but is used as illustration that DIPE can even be employed for ethanol dehydration and recovery in certain cases, depending on the quality of the feed stream.

Table 8-30: Flow sheet information for the second column (producing nearly pure water) of ethanol dehydration from a Fischer Tropsch waste stream with DIPE as entrainer.

Flow		
Average vapour flow rate	8.06	kg/sec
Condenser		
Temperature	350.64	K
Duty	-6918.57	kW
Distillate rate*	0.0070	kmol/sec
Reflux rate**	0.1713	kmol/sec
Reflux ratio	24.47	
*Vapour flow at top of column		
**Liquid flow at top of column		
Reboiler		
Temperature	363.29	K
Duty	7000.00	kW
Bottoms rate*	0.0029	kmol/sec
Boilup rate**	0.1808	kmol/sec
Boilup ratio	62.36	
*Liquid flow at top of column		
**Vapour flow at top of column		

To reiterate, DIPE is considered a feasible replacement for benzene as entrainer for ethanol dehydration. It may even deliver better, more cost and energy effective result than benzene. DIPE is found to be comparable with cyclohexane for IPA dehydration and DIPE can also be used for the recovery of ethanol and/or n-propanol from aqueous Fischer Tropsch waste streams, depending on the composition of the stream. Throughout the simulations the number of stages in the columns was kept constant to simplify the comparison between flow sheets. Significantly high reflux ratios however indicate that more stages might be necessary in that specific column. There is a trade-off between the reflux ratio and number of stages in a column. Fewer stages will need a higher reflux ratio, but will result in high utility costs. On the otherhand more stages will require a lower reflux ratio, but will increase the capital cost.

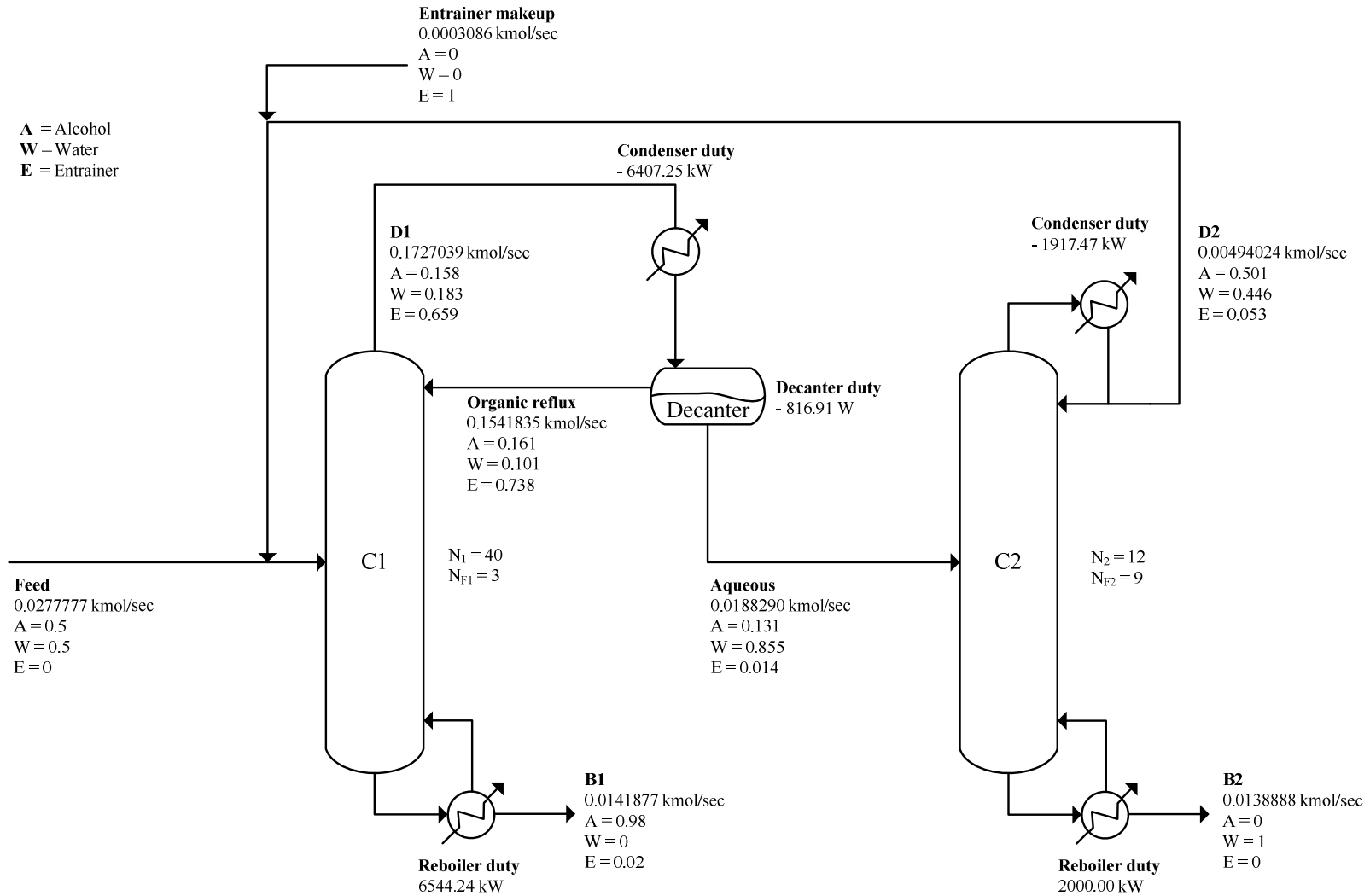


Figure 8-29: Flow sheet of the dehydration of ethanol via heterogeneous azeotropic distillation with DIPE as entrainer. All compositions are in mole fractions. The simulation was performed with Aspen using NRTL and its built-in parameters.

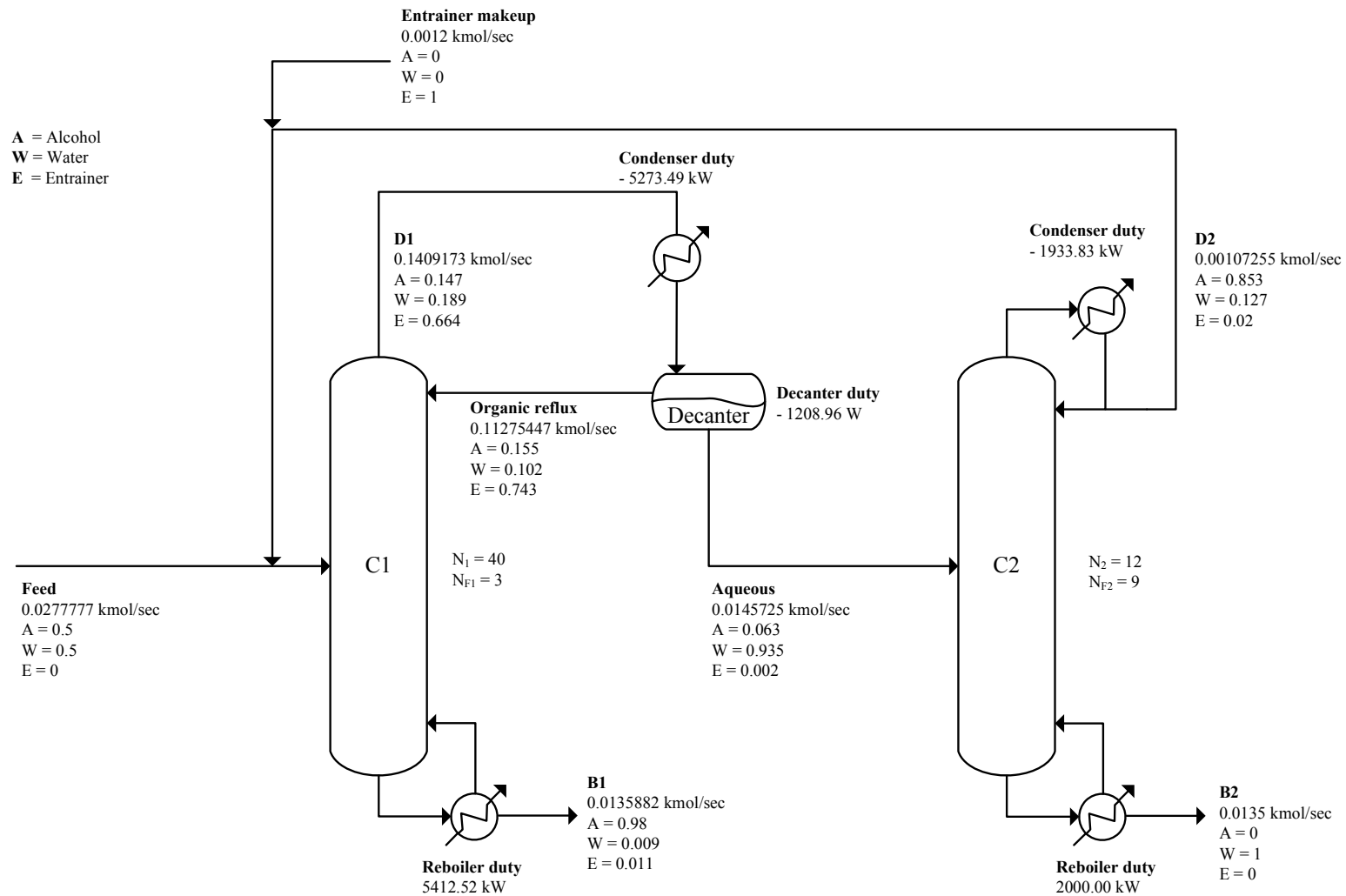


Figure 8-30: Flow sheet of the dehydration of ethanol via heterogeneous azeotropic distillation with DIPE as entrainer. All compositions are in mole fractions. The simulation was performed with Aspen using NRTL with parameters regressed in this work.

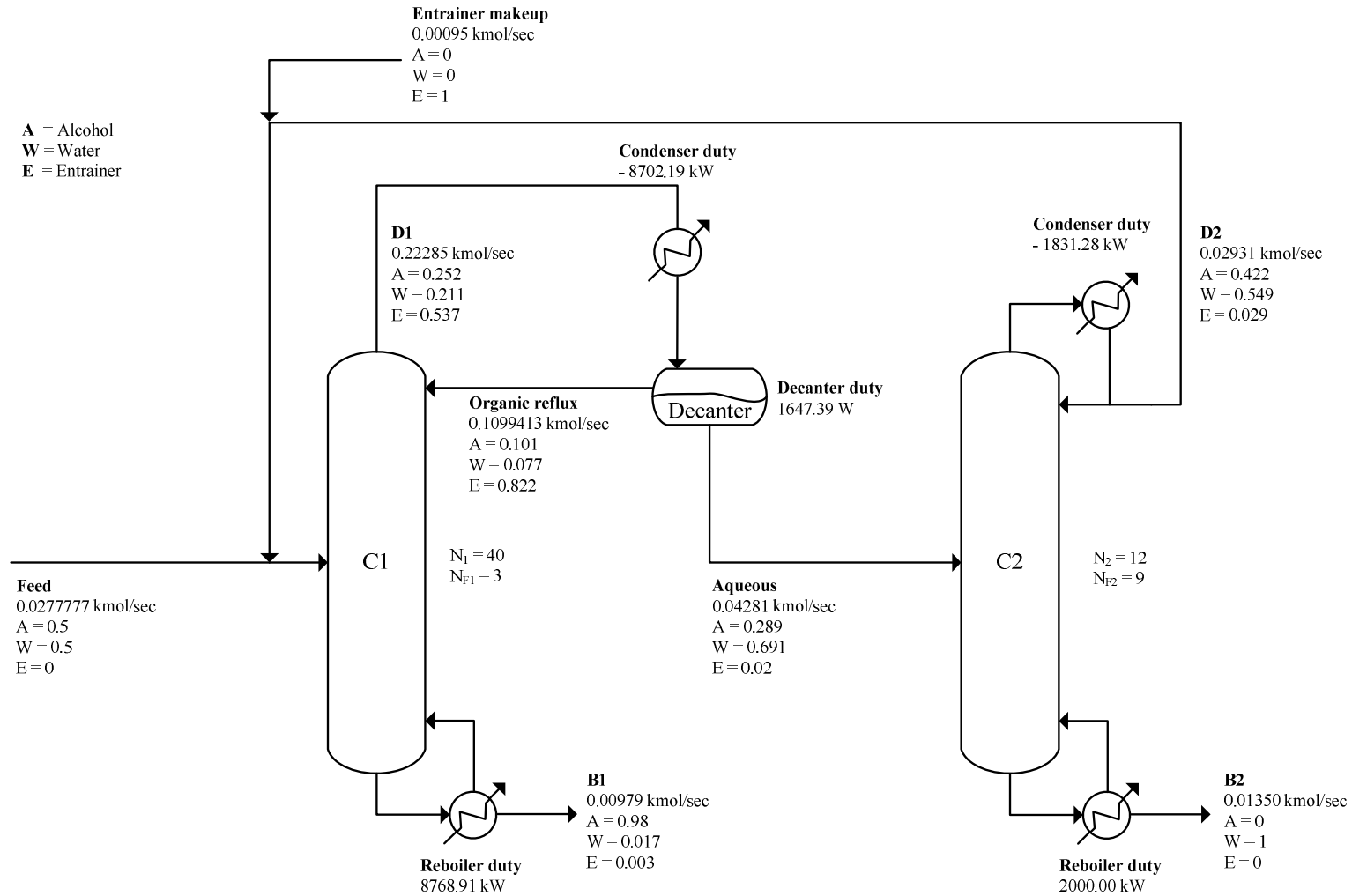


Figure 8-31: Flow sheet of the dehydration of ethanol via heterogeneous azeotropic distillation with benzene as entrainer. All compositions are in mole fractions. The simulation was performed with Aspen using NRTL with parameters supplied by Christo Crause (2011).

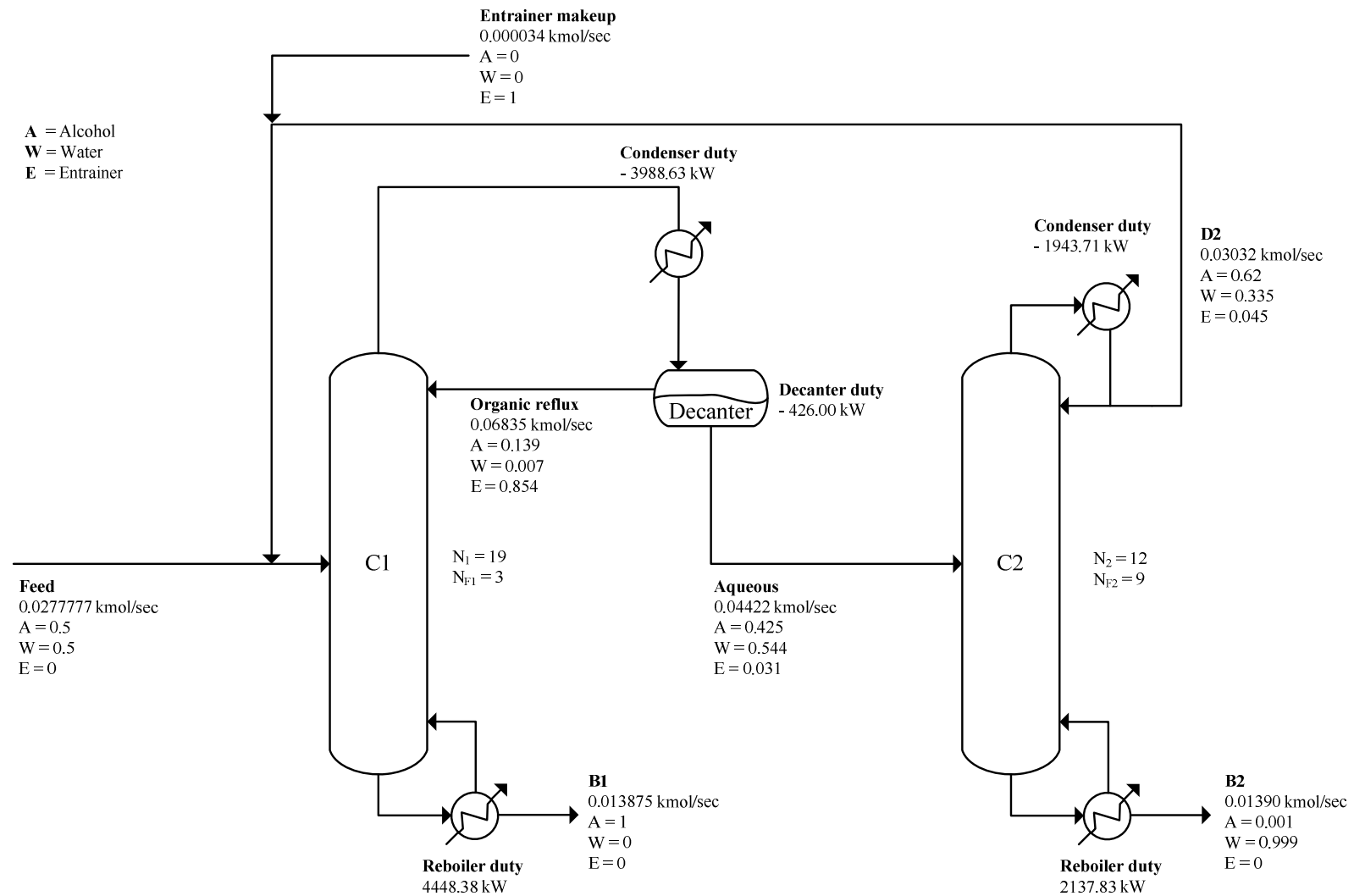


Figure 8-32: Flow sheet of the dehydration of IPA via heterogeneous azeotropic distillation with cyclohexane as entrainer. All compositions are in mole fractions. The simulation was performed by Arifin and Chien (2007).

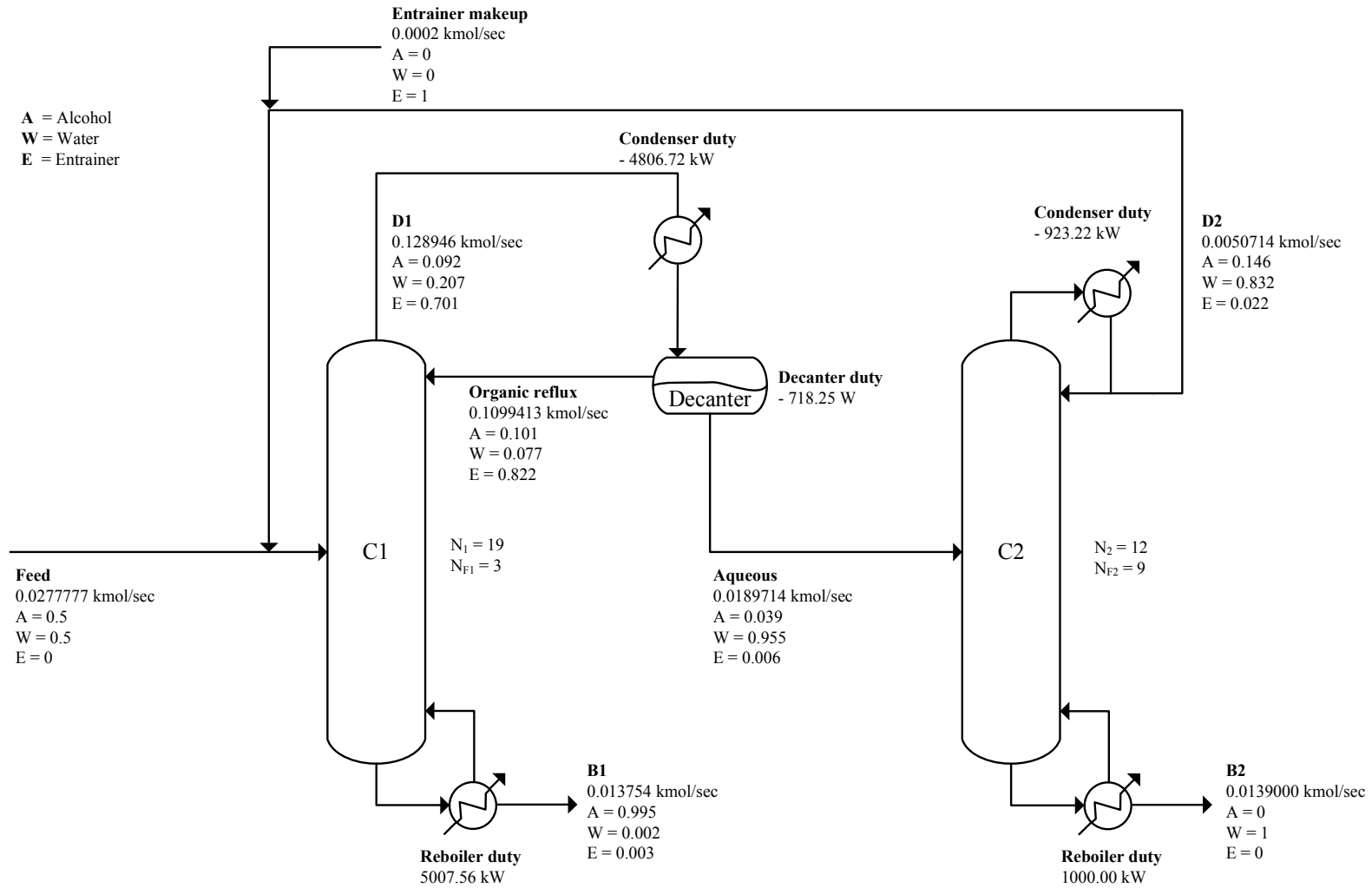


Figure 8-33: Flow sheet of the dehydration of IPA via heterogeneous azeotropic distillation with DIPE as entrainer. All compositions are in mole fractions. The simulation was performed with Aspen using NRTL and its built-in parameters.

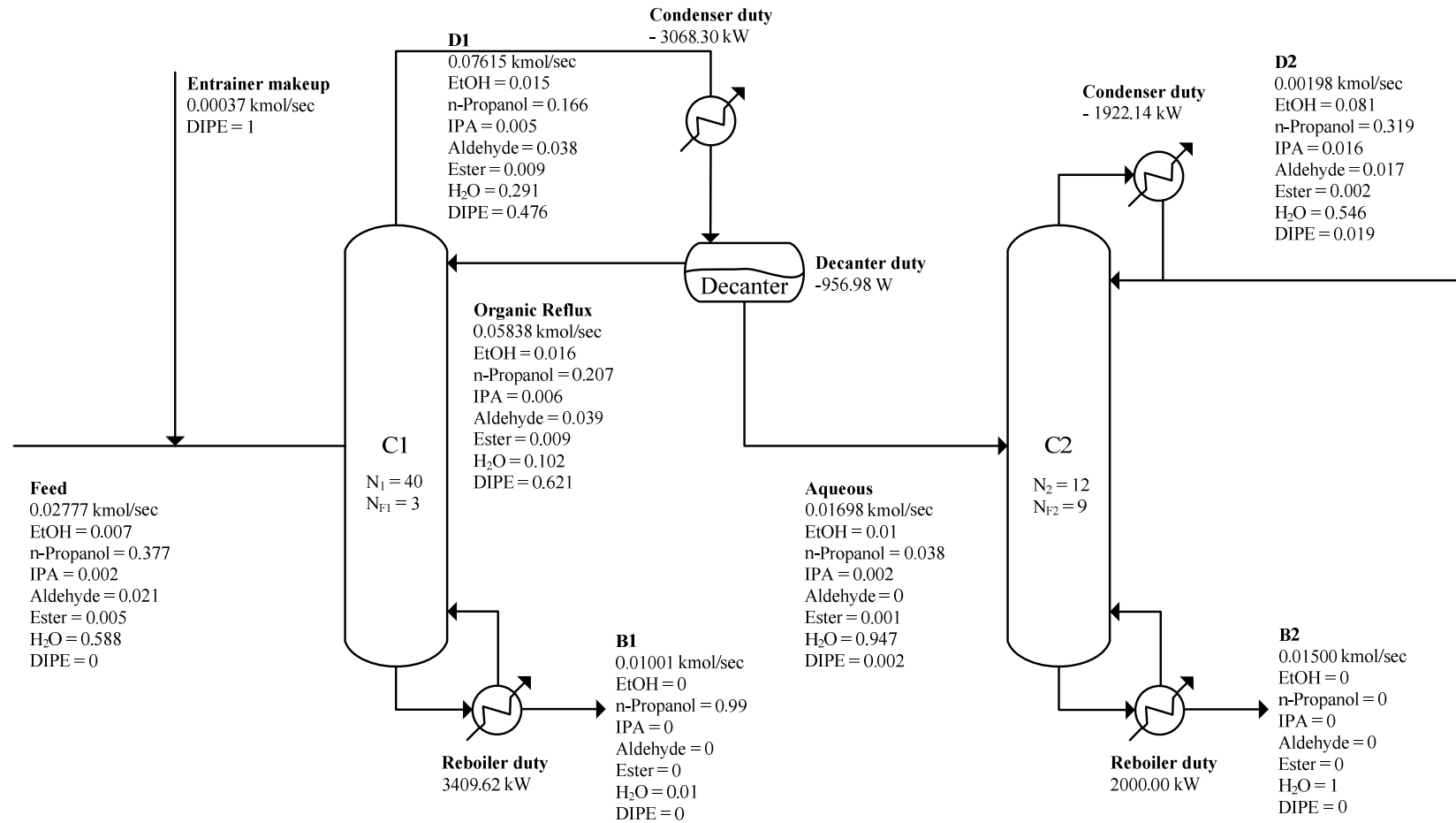


Figure 8-34: Flow sheet of the recovery of n-propanol from a typical aqueous Fischer Tropsch stream, contaminated with other close-boiling oxygenated components (Carlson 1949). DIPE is used as entrainer. All compositions are in mole fractions. The simulation was performed with Aspen using NRTL.

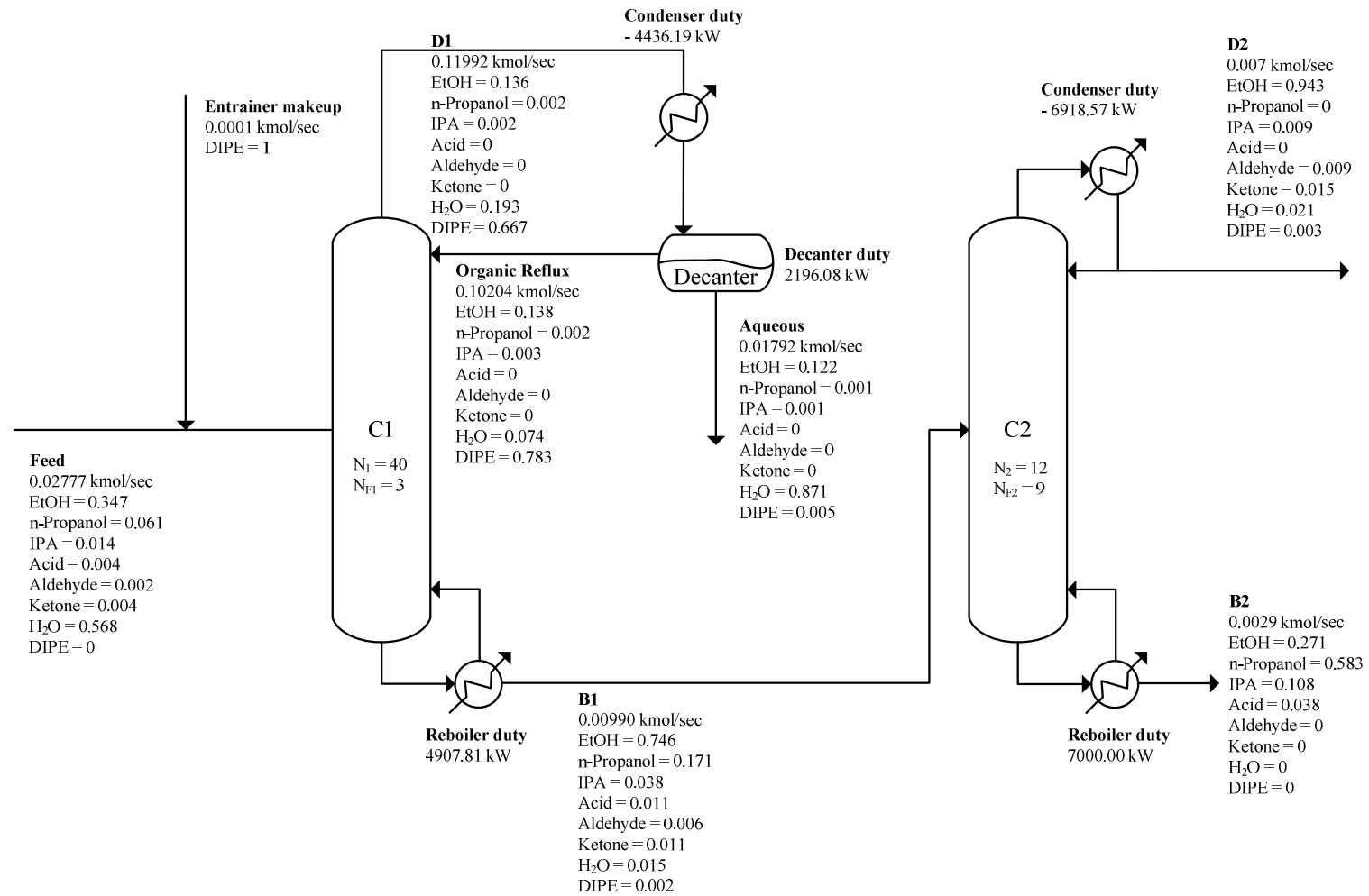


Figure 8-35: Flow sheet of the recovery of ethanol from a typical aqueous Fischer Tropsch stream, contaminated with other close-boiling oxygenated components (Nel, de Klerk 2007). DIPE is used as entrainer. All compositions are in mole fractions. The simulation was performed with Aspen using NRTL.

9 CONCLUSIONS AND RECOMMENDATIONS

In this work the formation of alcohol/water azeotropes in the process industry was studied, as well as some entrainers that can be used to separate these azeotropes via heterogeneous azeotropic distillation. Through the study of literature pertaining to the abovementioned topics, the equipment acquired and the experimental work, regressions and simulations performed, the following conclusions were reached:

- Isobaric VLLE at standard atmospheric conditions can be accurately measured with a dynamic Gillespie unit (as acquired for this work) equipped with an ultrasonic homogenizer to prevent liquid-liquid separation. The equipment can be operated in a pressure range of 2.5 mbar to 3 bar and up to a temperature of 250 °C. The equilibrium temperatures are measured with an accuracy of 0.03°C and the pressure can be regulated at 101.3 kPa with an accuracy of 0.35% FSO (Full Scale Output). The relative accuracy of the compositional measurements is 2%.
- The equipment was firstly verified by measuring data as also available in literature. It was verified for isobaric binary VLE by measuring ethanol/isooctane at 101.3 kPa (Hiaki et al. 1994, Ku, Tu 2005). The measured data compared well with the published data and the NRTL prediction in Aspen, of ethanol/isooctane. All AAD and AARD % values for the measured data from the NRTL prediction are similar, if not equal, to that of the published data. The equipment was verified for ternary VLLE by measuring ethanol/n-butanol/water at 101.3 kPa (Gomis, Ruiz & Asensi 2000, Newsham, Vahdat 1977). The measured data agreed well with all the phases of both sets of published data. None of the thermodynamic models (NRTL, UNIFAC and UNIQUAC) accurately predicted the published or measured data and therefore no AAD or AARD % comparisons could be performed.
- VLE and VLLE data were measured for ethanol/water/DIPE, n-propanol/water/DIPE and n-propanol/water/isooctane. The VLE data were found thermodynamically consistent by the L-W and McDermott-Ellis consistency tests. Although no thermodynamic consistency test could be found explicitly for VLLE data, the LLE component of the data followed a regular trend according to the Othmer-Tobias correlation. The reliability of the measured VLLE data was also confirmed through thorough verification of the phase equilibrium equipment and the mass balances performed on the samples. The binary DIPE/water and isooctane/water azeotropes, as well as the ternary ethanol/DIPE/water and n-propanol/isooctane/water azeotropes measured in this work, agree well with those found in literature.
- With built-in Aspen parameters the ethanol/DIPE/water VLLE behaviour was best predicted by UNIFAC (VLE), n-propanol/DIPE/water by UNIQUAC and n-propanol/isooctane/water by UNIFAC (LLE). There is however room for improvement. The regressed parameters generally improved the model predictions and indicated that experimental VLLE data were necessary to evaluate and improve the estimations made by thermodynamic models. With the regressed parameters, NRTL most accurately predicted the ethanol/DIPE/water and n-propanol/DIPE/water VLLE. Although the regressed parameters improved the NRTL and UNIQUAC predictions made for

n-propanol/isooctane/water, these models are considered unsuitable for accurate prediction of the VLLE behaviour of this system. None of the models studied predict the measured data perfectly, even with regressed parameters.

- Indications are that DIPE might be the superior entrainer, of those considered in this work, for ethanol and IPA dehydration via heterogeneous azeotropic distillation, potentially outperforming benzene and cyclohexane generally used in industry for such dehydration. This is based on the comparison of VLLE data of the various entrainers.
- Separation sequences were simulated for the dehydration of ethanol, isopropanol and n-propanol. Firstly, the built-in Aspen parameters for NRTL were compared to the regressed parameters for the ethanol/DIPE/water system by simulating a separation sequence using each set of parameters respectively. Significantly larger stream flows and condenser and reboiler duties were predicted by the built-in parameters in the azeotropic column. Therefore, when using these parameters to simulate such a separation sequences, the azeotropic column might be grossly over-designed. The average vapour flow rate and reflux ratio in the recovery column were however underestimated by the built-in parameters and might therefore be underdesigned when using built-in parameters to simulate the sequence. This indicates the importance of regressing more reliable parameters based on accurate experimental data.
- The separation sequence simulated with the regressed parameters for ethanol/DIPE/water was also compared to a simulation performed for ethanol/benzene/water with the same separation sequence. The comparison of these simulations revealed that, when using benzene as entrainer, the flow to the azeotropic column from the recycle and reflux streams can be much larger than with DIPE, thus requiring a larger column. Subsequently, the condenser and reboiler requirements would also be higher, although the amount of relatively pure ethanol recovered as bottoms would stay the same or may even be less. Since benzene is carcinogenic and DIPE costs more or less the same as benzene, DIPE may be a better entrainer for ethanol dehydration. However, DIPE still poses the risk of forming explosive peroxides. Therefore, the carcinogenic effects of benzene would have to be weighed against the possible explosive peroxides of DIPE.
- A separation sequence for the dehydration of IPA with DIPE as entrainer was also simulated and compared to simulation in literature for IPA dehydration with cyclohexane as entrainer. The organic reflux stream to the azeotropic column is larger when using DIPE, but the recycle stream from the recovery column is smaller than with cyclohexane. The condenser and reboiler duty requirements of the azeotropic column is larger when using DIPE, but condenser and reboiler duties for the recovery column is smaller than with cyclohexane. Therefore, the two separation sequences are definitely comparable. The overall energy requirements on the cyclohexane sequence are, however, more than twice as large as with DIPE. Consequently DIPE is considered a reasonable alternative to cyclohexane as entrainer for IPA dehydration.

- Two separation sequences were simulated for the recovery of n-propanol and ethanol, respectively, from typical Fischer Tropsch waste streams. It was found that, although n-propanol/DIPE/water does not form a ternary azeotrope, n-propanol can still be recovered with DIPE as entrainer via heterogeneous azeotropic distillation if the aqueous waste stream also contains ethanol and/or IPA. The last two separation sequence simulated in this work, serves as a practical application of DIPE as entrainer for the recovery of ethanol from an aqueous Fischer Tropsch waste stream with a high ethanol composition.

As anticipated in Section 1.2, DIPE is found to be a valid alternative entrainer for benzene and cyclohexane based on cost, separation ability and safety. There undoubtedly may exist an even better entrainer than DIPE, but from the data available in literature and the measurements made in this work DIPE is superior. NRTL with built-in Aspen parameters did not predict the VLLE data most accurately, unlike what was anticipated in Section 1.2. With regressed parameters, NRTL is overall the best model of those considered in this work, for the simulation of heterogeneous azeotropic distillation. The UNIFAC models also predict the phase envelope and vapour phase well, but not the azeotropes. It is suggested that more sophisticated thermodynamic models be investigated to predict VLLE data, especially for n-propanol/isooctane/water, since the models studied in this work still fall short of completely predicting the phase equilibrium.

Online GC analysis of the vapour phase samples from the VLE/VLLE measuring unit might be considered. It is however recommended that an FID detector be used. In that case, provision should be made to analyse the water content of the samples, as it would be more accurate than merely calculating it by mass balance.

It is recommended that VLLE data be measured for ethanol/DNPE/water and IPA/DNPE/water in order to fully compare DIPE and DNPE as entrainers, since the Aspen azeotrope predictions are not in agreement for the different property models. It is also recommended that higher alcohols should be considered, such as sec-butanol and isobutanol.

When simulating a heterogeneous azeotropic distillation sequence one might even consider using different sets of parameters for different units in the sequence. For the azeotropic column it is important that the azeotropes, especially the ternary heterogeneous azeotrope are accurately predicted. For a pre-concentrator or recovery column one might rather use a set of parameters that will predict the phase equilibrium behaviour away from the azeotrope, accurately.

10 REFERENCES

- Abrams, D.S. & Prausnitz, J.M. 1975, "Statistical thermodynamics of liquid mixtures: a new expression for the excess Gibbs energy of partly or completely miscible systems", *AIChE Journal*, vol. 21, no. 1, pp. 116-128.
- Arce, A., Marchiaro, A., Rodríguez, O. & Soto, A. 2002, "Liquid-liquid equilibrium of diisopropyl ether ethanol water system at different temperatures", *Journal of Chemical & Engineering Data*, vol. 47, no. 3, pp. 529-532.
- Arce, A., Martínez-Ageitos, J. & Soto, A. 1996, "VLE for water ethanol 1-octanol mixtures. Experimental measurements and correlations", *Fluid Phase Equilibria*, vol. 122, no. 1-2, pp. 117-129.
- Arifin, S. & Chien, I.L. 2007, "Combined preconcentrator/recovery column design for isopropyl alcohol dehydration process", *Industrial & Engineering Chemistry Research*, vol. 46, no. 8, pp. 2535-2543.
- Asensi, J.C., Moltó, J., del Mar Olaya, M., Ruiz, F. & Gomis, V. 2002, "Isobaric vapour-liquid equilibria data for the binary system 1-propanol+1-pentanol and isobaric vapour-liquid-liquid equilibria data for the ternary system water+1-propanol+1-pentanol at 101.3 kPa", *Fluid Phase Equilibria*, vol. 200, no. 2, pp. 287-293.
- Aslam, N. & Sunol, A.K. 2006, "Sensitivity of azeotropic states to activity coefficient model parameters and system variables", *Fluid Phase Equilibria*, vol. 240, no. 1, pp. 1-14.
- Aspen Technology, I. 2009, *Aspen Plus 7.1*.
- Barbaudy, J. 1926, "Système alcool éthylique-benzène-eau. I étude de la surface de trouble", *Recueil des Travaux Chimiques des Pays-Bas*, vol. 45, no. 3, pp. 207-213.
- BASF 2011, *n-Propanol (CP)*. Available: http://www.basf.com/group/corporate/en/brand/N_PROPANOL_CP [2011, 10/04].
- Benito, G.G. & Lopez, A.C. 1992, "Vapor-liquid equilibrium data for the binary systems formed by diisopropyl ether with ethanol, n-propanol and ethyl, isopropyl and propyl acetates", *Revue roumaine de chimie*, vol. 37, pp. 973-973.
- Berg, L. 1969, "Azeotropic and extractive distillation: Selecting the agent for distillation", *Chemical Engineering Progress*, vol. 65, no. 9, pp. 52-57.
- Blackford, D. & York, R. 1965, "Vapor-Liquid Equilibria of the System Acrylonitrile-Acetonitrile-Water.", *Journal of Chemical and Engineering Data*, vol. 10, no. 4, pp. 313-318.
- Bossen, B.S., Joergensen, S.B. & Gani, R. 1993, "Simulation, design, and analysis of azeotropic distillation operations", *Industrial & Engineering Chemistry Research*, vol. 32, no. 4, pp. 620-633.
- Brignole, E.A., Bottini, S. & Gani, R. 1986, "A strategy for the design and selection of solvents for separation processes.", *Fluid Phase Equilibria*, vol. 29, pp. 125-132.
- Cairns, B.P. & Furzer, I.A. 1990, "Multicomponent three-phase azeotropic distillation. 1. Extensive experimental data and simulation results", *Industrial & Engineering Chemistry Research*, vol. 29, no. 7, pp. 1349-1363.
- Cairns, B.P. & Furzer, I.A. 1990, "Multicomponent three-phase azeotropic distillation. 3. modern thermodynamic models and multiple solutions", *Industrial & Engineering Chemistry Research*, vol. 29, no. 7, pp. 1383-1395.

- California Office of Environmental Health Hazard Assessment 2011, *Chronic Toxicity Summary - n-Hexane*. Available: http://oehha.ca.gov/air/chronic_rels/pdf/110543.pdf [2011, 10/06].
- Carlson, C.S. 1949, *Recovery of Normal Propyl Alcohol from Oxygenated Compounds*, 202-42, US Patent 2,489,619.
- Carniti, P., Cori, L. & Ragaini, V. 1978, "A critical analysis of the hand and Othmer-Tobias correlations", *Fluid Phase Equilibria*, vol. 2, no. 1, pp. 39-47.
- Challis, A.A.L. 1954, *Azeotropic distillation of propyl amines*, US Patent 2,691,624.
- Crause, C. 2011, *Ethanol/Water/Benzene*, email, 14 October.
- Dawe, R.A., Newsham, D.M.T. & Ng, S.B. 1973, "Vapor-liquid equilibria in mixtures of water, 1-propanol, and 1-butanol", *Journal of Chemical and Engineering Data*, vol. 18, no. 1, pp. 44-49.
- de Villiers, W.E., French, R.N. & Koplos, G.J. 2002, "Navigate phase equilibria via residue curve maps", *Chemical Engineering Progress*, vol. 98, pp. 66.
- Doherty, M.F. & Malone, M.F. 2001, *Conceptual design of distillation systems*, McGraw-Hill New York.
- Doherty, M.F. & Perkins, J.D. 1978, "On the dynamics of distillation processes I: The simple distillation of multicomponent non-reacting, homogeneous liquid mixtures", *Chemical Engineering Science*, vol. 33, no. 3, pp. 281-301.
- Dohrn, R., Peper, S., Fonseca, J.M.S. 2010, "High-pressure fluid-phase equilibria: Experimental methods and systems investigated (2000-2004)", *Fluid Phase Equilibria*, vol. 288, pp.1-54.
- Dunn, C.L., Millar, R.W., Pierotti, G.J., Shiras, R.N. & Souders Jr, M. 1945, "Toluene Recovery by Extractive Distillation", *Transactions of the American Institute of Chemical Engineers*, vol. 41, pp. 631.
- Elly, M., Landa, M. & Wisniak, J. 2003, *PRO-VLE 2.0. Vapor-liquid equilibria computer program*, Ben-Gurion University of the Negev, Beer-Sheva.
- Ewell, R.H., Harrison, J.M. & Berg, L. 1944, "Azeotropic distillation", *Industrial & Engineering Chemistry*, vol. 36, no. 10, pp. 871-875.
- Felder, R.M. & Rousseau, R.W. 2000, *Elementary principles of chemical processes*, John Wiley and Sons, United States of America.
- Fien, G.J.A.F. & Liu, Y.A. 1994, "Heuristic synthesis and shortcut design of separation processes using residue curve maps: a review", *Industrial & Engineering Chemistry Research*, vol. 33, no. 11, pp. 2505-2522.
- Fleming, H.L. & Slater, C.S. 1992, *Membrane Handbook*, WSW Ho and KK Sirkar, Van Nostrand Reinhold, New York.
- Font, A., Asensi, J.C., Ruiz, F. & Gomis, V. 2004, "Isobaric vapor-liquid and vapor-liquid-liquid equilibria data for the system water isopropanol isooctane", *Journal of Chemical & Engineering Data*, vol. 49, no. 4, pp. 765-767.
- Font, A., Asensi, J.C., Ruiz, F. & Gomis, V. 2003, "Application of isooctane to the dehydration of ethanol. Design of a column sequence to obtain absolute ethanol by heterogeneous azeotropic distillation", *Industrial & Engineering Chemistry Research*, vol. 42, no. 1, pp. 140-144.
- Foucher, E.R., Doherty, M.F. & Malone, M.F. 1991, "Automatic screening of entrainers for homogeneous azeotropic distillation", *Industrial & Engineering Chemistry Research*, vol. 30, no. 4, pp. 760-772.

- Frolich, P.K. & Lewis, W.K. 1928, "Synthesis of Alcohols Higher than Methanol from Carbon Monoxide and Hydrogen", *Industrial & Engineering Chemistry*, vol. 20, no. 4, pp. 354-359.
- Furzer, I.A. 1994, "Synthesis of entrainers in heteroazeotropic distillation systems", *The Canadian Journal of Chemical Engineering*, vol. 72, no. 2, pp. 358-364.
- Furzer, I.A. 1985, "Ethanol Dehydration Column Efficiencies Using UNIFAC", *American Institute of Chemical Engineers*, vol. 31, no. 8, pp. 1389-1392.
- Ghanadzadeh, H., Ghanadzadeh, A. & Bahrpaima, K. 2009, "Measurement and prediction of tie-line data for mixtures of (water, 1-propanol, diisopropyl ether): LLE diagrams as a function of temperature", *Fluid Phase Equilibria*, vol. 277, no. 2, pp. 126-130.
- Gmehling, J., Menke, J., Krafczyk, J. & Fischer, K. 1994, *Azeotropic Data Part I*, VCH Publishers, New York, USA.
- Gmehling, J., Menke, J., Krafczyk, J. & Fischer, K. 1994, *Azeotropic Data Part II*, VCH Publishers, New York, USA.
- Gomis, V., Font, A., Pedraza, R. & Saquete, M.D. 2007, "Isobaric vapor-liquid and vapor-liquid-liquid equilibrium data for the water-ethanol-hexane system", *Fluid Phase Equilibria*, vol. 259, no. 1, pp. 66-70.
- Gomis, V., Font, A., Pedraza, R. & Saquete, M.D. 2005, "Isobaric vapor-liquid and vapor-liquid-liquid equilibrium data for the system water + ethanol +cyclohexane", *Fluid Phase Equilibria*, vol. 235, no. 1, pp. 7-10.
- Gomis, V., Font, A. & Saquete, M.D. 2006, "Vapour-liquid-liquid and vapour-liquid equilibrium of the system water + ethanol + heptane at 101.3 kPa", *Fluid Phase Equilibria*, vol. 248, no. 2, pp. 206-210.
- Gomis, V., Pedraza, R., Francés, O., Font, A. & Asensi, J.C. 2007, "Dehydration of ethanol using azeotropic distillation with isooctane", *Industrial & Engineering Chemistry Research*, vol. 46, no. 13, pp. 4572-4576.
- Gomis, V., Pequenín, A. & Asensi, J.C. 2010, "A review of the isobaric (vapor-liquid-liquid) equilibria of multicomponent systems and the experimental methods used in their investigation", *The Journal of Chemical Thermodynamics*, vol 42, pp. 823-828.
- Gomis, V., Pequenín, A. & Asensi, J.C. 2009, "Isobaric vapor-liquid-liquid equilibrium and vapor-liquid equilibrium for the system water-ethanol-1, 4-dimethylbenzene at 101.3 kPa", *Fluid Phase Equilibria*, vol. 281, no. 1, pp. 1-4.
- Gomis, V., Ruiz, F. & Asensi, J.C. 2000, "The application of ultrasound in the determination of isobaric vapour-liquid-liquid equilibrium data", *Fluid Phase Equilibria*, vol. 172, no. 2, pp. 245-259.
- Guinot, H. & Clark, F.W. 1938, "Azeotropic distillation in industry", *Chemical Engineering Research and Design*, vol. 16, no. a, pp. 189-199.
- Hala, E., Pick, J., Frjed, V. & Vilim, O. 1967, *Vapour-liquid equilibrium*, Pergamon, Oxford.
- Ham-let Advanced Control Technology 2011, *Corrosion Data*. Available: www.ham-let.com/resources/dr.aspx?rid=24&lng=3 [2011, 06/10].
- Hand, D.B. 1930, "Dimeric distribution", *The Journal of Physical Chemistry*, vol. 34, no. 9, pp. 1961-2000.
- Hanson, G.R., Venturelli, P.J. & Fleckenstein, A.E. 2011, *Drugs and society*, Jones & Bartlett Learning.

- Harrison, K. 2000, October 2002-last update, *Cyclohexane @ 3DChem.com*. Available: <http://www.3dchem.com/molecules.asp?ID=176> [2011, 10/06].
- Helmenstine, A. 2011, *Gasoline & Octane Ratings*. Available: <http://chemistry.about.com/cs/howthingswork/a/aa070401a.htm> [2011, 10/07].
- Herington, E. F. G., 1951. "Test for the Consistency of Experimental Isobaric Vapour-liquid Equilibrium Data", *Journal Institute of Petroleum*, vol 37, pp. 457-470.
- Hiaki, T., Takahashi, K., Tsuji, T., Hongo, M. & Kojima, K. 1994, "Vapor-Liquid Equilibria of Ethanol with 2, 2, 4-trimethylpentane or Octane at 101.3 kPa", *Journal of Chemical and Engineering Data*, vol. 39, no. 4, pp. 720-722.
- Hilmen, E.K. 2000, *Separation of azeotropic mixtures: tools for analysis and studies on batch distillation operation*, PhD dissertation, Norwegian University of Science and Technology.
- Hlavaty, K. & Linek, J. 1973, "Liquid-Liquid Equilibria in Four Ternary Acetic Acid Organic Solvent-Water Systems at 24.6 C", *Collection of Czechoslovak Chemical Communications*, vol. 38, pp. 374.
- Hömmerich, U. & Rautenbach, R. 1998, "Design and optimization of combined pervaporation/distillation processes for the production of MTBE", *Journal of Membrane Science*, vol. 146, no. 1, pp. 53-64.
- Horsley, L.H. & Tamplin, W.S. 1962, *Azeotropic data II*, American Chemical Society, Washington.
- Horsley, L.H. & Tamplin, W.S. 1952, *Azeotropic data*, American Chemical Society, Washington.
- Hu, H.S. 2009, "Determination of vapour-liquid and vapour-liquid-liquid equilibrium of the chloroform-water and trichloroethylene-water binary mixtures", *Fluid Phase Equilibria*, vol. 289, no. 1, pp. 80-89 .
- Hunsmann, W. & Simmrock, K.H. 1966, "Separation of water, formic acid and acetic acid by azeotrope distillation", *Chemie Ingenieur Technik*, vol. 38, pp. 1053-1059.
- Hwang, I.C., Park, S.J. & Choi, J.S. 2008, "Liquid-liquid equilibria for the binary system of di-isopropyl ether (DIPE) and water in between 288.15 and 323.15 K and the ternary systems of DIPE, water and C1-C4 alcohols at 298.15 K", *Fluid Phase Equilibria*, vol. 269, no. 1-2, pp. 1-5.
- In, R.E.T. 1963, *Liquid Extraction*, McGraw-Hill, New York.
- International Programme on Chemical Safety 1990, *Environmental Health Criteria 103: 2-Propanol* [Homepage of World Health Organization], [Online]. Available: <http://www.inchem.org/documents/ehc/ehc/ehc103.htm#SubSectionNumber:3.2.2> [2010, 06/22].
- Ivonne, R.D., Vincent, G. & Xavier, J. 2001, "Heterogeneous entrainer selection for the separation of azeotropic and close boiling temperature mixtures by heterogeneous batch distillation", *Industrial & Engineering Chemistry Research*, vol. 40, no. 22, pp. 4935-4950.
- Iwakabe, K. & Kosuge, H. 2001, "Isobaric vapor-liquid-liquid equilibria with a newly developed still", *Fluid Phase Equilibria*, vol. 192, no. 1-2, pp. 171-186.
- Julka, V., Chiplunkar, M. & O'Young, L. 2009, "Selecting Entrainers for Azeotropic Distillation", *Chemical Engineering Progress*, vol. 105, no. 3, pp. 47-53.
- Knauf, R., Meyer-Blumenroth, U. & Semel, J. 1998, "Membrane Processes in the Chemical Industry", *Chemie Ingenieur Technik*, vol. 70, no. 10, pp. 1265-1270.

- Kojima, K., Ochi, K. & Nakazawa, Y. 1969, "Relationship between liquid activity coefficient and composition for ternary systems", *International Chemical Engineering*, vol. 9, pp. 342–347.
- Kojima, K., Tochigi, K., Seki, H. & Watase, K. 1968, "Determination of vapor–liquid equilibrium from boiling point curve", *Kagaku Kogaku Ronbunshu*, vol. 32, pp. 149–153.
- Koretsky, M.D. 2004, *Engineering and chemical thermodynamics*, Wiley.
- Krupatkin, I.L. & Bodin, M.A. 1947, "Homogenization of binary layering by a third component", *Zhurnal Obshchei Khimii*, vol. 17, pp. 1993–1998.
- Ku, H.C. & Tu, C.H. 2005, "Isobaric vapor-liquid equilibria for mixtures of acetone, ethanol, and 2, 2, 4-trimethylpentane at 101.3 kPa", *Fluid Phase Equilibria*, vol. 231, no. 1, pp. 99–108.
- Kunesh, J.G., Kister, H.Z., Lockett, M.J. & Fair, J.R. 1995, "Distillation: Still towering over other options", *Chemical Engineering Progress*, vol. 91, no. 10, pp. 43–54.
- Kurihara, K., Nakamichi, M. & Kojima, K. 1993, "Isobaric vapor-liquid equilibria for methanol-ethanol-water and the three constituent binary systems", *Journal of Chemical and Engineering Data*, vol. 38, no. 3, pp. 446–449.
- Lee, L. & Shen, H. 2003, "Azeotropic Behavior of a Water + n-Propanol + Cyclohexane Mixture Using Cyclohexane as an Entrainer for Separating the Water + n-Propanol Mixture at 760 mm Hg", *Industrial & Engineering Chemistry Research*, vol. 42, pp. 5905–5914.
- Lin, S.H. & Wang, C.S. 2004, "Recovery of isopropyl alcohol from waste solvent of a semiconductor plant", *Journal of Hazardous Materials*, vol. 106, no. 2–3, pp. 161–168.
- Lladosa, E., Cháfer, A., Montón, J.B. & Martínez, N.F. 2011, "Liquid–Liquid and Vapor–Liquid–Liquid Equilibrium of the 4-Methyl-2-pentanone 2-Butanol Water System", *Journal of Chemical & Engineering Data*, .
- Lladosa, E., Montón, J.B., Burguet, M.C. & de la Torre, J. 2008, "Isobaric (vapour liquid liquid) equilibrium data for (di-n-propyl ether n-propyl alcohol water) and (diisopropyl ether isopropyl alcohol water) systems at 100 kPa", *The Journal of Chemical Thermodynamics*, vol. 40, no. 5, pp. 867–873.
- Lladosa, E., Montón, J.B., de la Torre, J. & Martínez, N.F. 2011, "Liquid–Liquid and Vapor–Liquid–Liquid Equilibrium of the 2-Butanone 2-Butanol Water System", *Journal of Chemical & Engineering Data*, vol. 56, no. 5, pp. 1755–1761 .
- Luyben, W.L. & Chien, I.L. 2010, *Design and Control of Distillation Systems for Separating Azeotropes*, Wiley, New Jersey.
- Malanowski, S. 1982, "Experimental methods for vapour-liquid equilibria. II. Dew-and bubble-point method", *Fluid Phase Equilibria*, vol. 9, no. 3, pp. 311–317.
- Malanowski, S., Anderko, A. & Malanowski, S. 1992, *Modelling phase equilibria: thermodynamic background and practical tools*, Wiley New York.
- Malesinski, W. 1965, *Azeotropy and other theoretical problems of vapour-liquid equilibrium*, Interscience, London.
- Marples, M. 1939, *Dehydration of Ethanol*, 202–42, US Patent 2,173,692.

- Marrufo, B., Loras, S. & Sanchotello, M. 2009, "Isobaric Vapor–Liquid Equilibria for Binary and Ternary Mixtures with Cyclohexane, Cyclohexene, and 2-Methoxyethanol at 100 kPa", *Journal of Chemical & Engineering Data*, vol. 55, no. 1, pp. 62-68.
- Marshall, R.J. 2006-2011, *Chemical Engineering - Economic Indicators*, McGraw-Hill Pub. Co., Albany, N.Y.
- McDermott, C. & Ellis, S.R.M. 1965, "A multicomponent consistency test", *Chemical Engineering Science*, vol. 20, no. 4, pp. 293-296.
- Nel, R.J.J. & de Klerk, A. 2007, "Fischer Tropsch Aqueous Phase Refining by Catalytic Alcohol Dehydration", *Industrial & Engineering Chemistry Research*, vol. 46, no. 11, pp. 3558-3565.
- Newsham, D.M.T. & Vahdat, N. 1977, "Prediction of vapour-liquid-liquid equilibria from liquid-liquid equilibria Part I: Experimental results for the systems methanol-water-n-but", *The Chemical Engineering Journal*, vol. 13, no. 1, pp. 27-31.
- Nexant Chem Systems 2006, *PERP Program - Ethanol. New Report Alert*. Available: <http://www.chemsystems.com/reports/search/docs/abstracts/0405-8-abs.pdf> [2011, 10/04].
- Norman, W.S. 1945, "The Dehydration of Ethanol by Azeotropic Distillation", *Transactions of the Institution of Chemical Engineers*, vol. 23, pp. 66.
- Norman, W. 1945, "The dehydration of allyl alcohol by azeotropic distillation", *Transactions of the Institution of Chemical Engineers*, vol. 23, pp. 76–88.
- Occupational Safety and Health Administration (OSHA) 2010, 12 January 2010-last update, *Benzene*. Available: <http://www.osha.gov/SLTC/benzene/index.html> [2010, 06/28].
- Occupational Safety and Health Administration (OSHA) 2009, 15 May 2009-last update, *Occupational Safety and Health Guideline for n-Hexane*. Available: <http://www.osha.gov/SLTC/healthguidelines/n-hexane/recognition.html> [2010, 06/28].
- Occupational Safety and Health Administration (OSHA) 1999, 22 April 1999-last update, *Cyclohexane*. Available: <http://www.osha.gov/SLTC/healthguidelines/cyclohexane/index.html> [2010, 06/28].
- Orchillés, A.V., Miguel, P.J., Vercher, E. & Martínez-Andreu, A. 2009, "Isobaric Vapor–Liquid and Liquid–Liquid Equilibria for Chloroform Methanol 1-Ethyl-3-methylimidazolium Trifluoromethanesulfonate at 100 kPa", *Journal of Chemical & Engineering Data*, vol. 55, no. 3, pp. 1209-1214.
- Othmer, D.F. & Tobias, P.E. 1942, "Tie line correlation", *Industrial & Engineering Chemistry*, vol. 34, no. 6, pp. 690.
- Pequenín, A., Asensi, J.C. & Gomis, V. 2011, "Experimental Determination of Quaternary and Ternary Isobaric Vapor-Liquid-Liquid Equilibrium and Vapor-Liquid Equilibrium for the Systems Water-Ethanol-Hexane-Toluene and Water-Hexane-Toluene at 101.3 kPa", *Journal of Chemical & Engineering Data*, vol. 56, no. 11, pp. 3994-3998 .
- Pequenín, A., Asensi, J.C. & Gomis, V. 2009, "Isobaric Vapor–Liquid–Liquid Equilibrium and Vapor–Liquid Equilibrium for the Quaternary System Water–Ethanol–Cyclohexane–Isooctane at 101.3 kPa", *Journal of Chemical & Engineering Data*, vol. 55, no. 3, pp. 1227-1231.
- Pham, H.N. & Doherty, M.F. 1990, "Design and synthesis of heterogeneous azeotropic distillations - I. Heterogeneous phase diagrams", *Chemical Engineering Science*, vol. 45, no. 7, pp. 1823-1836.
- Pham, H.N. & Doherty, M.F. 1990, "Design and synthesis of heterogeneous azeotropic distillations II. Residue curve maps", *Chemical Engineering Science*, vol. 45, no. 7, pp. 1837-1843.

- Pham, H.N. & Doherty, M.F. 1990, "Design and synthesis of heterogeneous azeotropic distillations III. Column sequences", *Chemical Engineering Science*, vol. 45, no. 7, pp. 1845-1854.
- Prausnitz, J.M., Lichtenthaler, R.N. & de Azevedo, E.G. 1999, *Molecular thermodynamics of fluid-phase equilibria*, Prentice Hall, Upper Saddle River, N.J.
- Raal, J.D. & Mühlbauer, A.L. 1998, *Phase equilibria: measurement and computation*, Taylor and Francis, Washington D.C.
- Refining online 2011, *FCC Octane MON Versus RON* [Homepage of Refining online], [Online]. Available: http://www.refiningonline.com/engelhardkb/crep/tcr4_29.htm [2011, 11/06].
- Reinders, W. & De Minjer, C.H. 1947, "Vapour-liquid equilibria in ternary systems. VI. The system water-acetone-chloroform", *Recueil des Travaux Chimiques des Pays-Bas*, vol. 66, no. 9, pp. 573-604.
- Renon, H. & Prausnitz, J.M. 1968, "Local compositions in thermodynamic excess functions for liquid mixtures", *American Institute of Chemical Engineers*, vol. 14, no. 1, pp. 135-144.
- Rovaglio, M., Faravelli, T., Biardi, G., Gaffuri, P. & Soccol, S. 1992, "Precise composition control of heterogeneous azeotropic distillation towers", *Computers & Chemical Engineering*, vol. 16, pp. S181-S188.
- Sandler, S.I. 1999, *Chemical and Engineering Thermodynamics*, 3rd edn, John Wiley & Sons, New York.
- Schweitzer, P.A. 1997, *Handbook of separation techniques for chemical engineers*, McGraw-Hill, New York.
- ScienceLab.com 2011, *Material Safety Data Sheet Listing*. Available: <http://www.sciencelab.com/msdsList.php> [2011, 10/06].
- Seader, J.D. & Henley, E.J. 2006, *Separation Process Principles*, John Wiley & Sons, USA.
- Segura, H. 20 January 2011, *Assessment of thermodynamic consistency test*, Department of Chemical Engineering, University of Concepcion, Concepcion, Chile.
- Shimadzu 2011, *GC Data Sheet*. Available: http://www.shimadzu.com.br/analitica/aplicacoes/cromatografos/gc_ms/ca180-917a.pdf [2011, 11/05].
- Sinnott, R. & Towler, G. 2009, *Chemical Engineering Design*, 5th edn, Butterworth-Heinemann, United Kingdom.
- Smith, J.M., Van Ness, H.C. & Abbott, M.M. 2005, *Introduction to chemical engineering thermodynamics*, McGraw-Hill, Boston.
- Smith, R. 1995, *Chemical process design*, McGraw-Hill, New York.
- Swietoslowski, W. 1963, *Azeotropy and polyazeotropy*, Polish Scientific Publishers, Warszawa.
- Szitkai, Z., Lelkes, Z., Rev, E. & Fonyo, Z. 2002, "Optimization of hybrid ethanol dehydration systems", *Chemical Engineering and Processing*, vol. 41, no. 7, pp. 631-646.
- Tassios, D.P., Ditsler, D.E., Kumar, R., Prausnitz, J.M., King, C.J., Furter, W.F., Black, C. & Golding, R.A. 1972, "Extractive and Azeotropic Distillation", *Advances in Chemistry Series*, vol. 115.
- The Physical Sciences Initiative 2011, *Petrol and Octane Numbers*. Available: http://chemistry.slss.ie/resources/downloads/ch_cw_petrol.pdf [2011, 11/06].

- Torcal, M., García-Abarrio, S., Pardo, J.I., Mainar, A.M. & Urieta, J.S. 2010, "P, ρ , T Measurements and Isobaric Vapor– Liquid– Equilibria of the 1, 3, 3-Trimethyl-2-oxabicyclo [2, 2, 2] octane Propan-1-ol Mixture: Cubic and Statistical Associating Fluid Theory-Based Equation of State Analysis", *Journal of Chemical & Engineering Data*, vol. 55, no. 12, pp. 5932-5940 .
- Treybal, R.E. 1963, *Liquid-Liquid Extraction*, McGraw-Hill, New York.
- U.S. Department of Health and Human Services, Public Health Service, National Toxicology Program 2010, *Report on Carcinogens*.
- United States Department of Labour - Occupational Safety & Health Administration 2011, *Benzene*. Available: <http://www.osha.gov/SLTC/benzene/> [2011, 10/06].
- Unruh, J.D., Ryan, D.A. & Dugan, S.L. 1999, *Process for the production of n-propanol*, C07C 29/14, US Patent 5,866,725.
- Van Hoof, V., Van den Abeele, L., Buekenhoudt, A., Dotremont, C. & Leysen, R. 2004, "Economic comparison between azeotropic distillation and different hybrid systems combining distillation with pervaporation for the dehydration of isopropanol", *Separation and Purification Technology*, vol. 37, no. 1, pp. 33-49.
- Van Winkle, M. 1967, *Distillation*, McGraw-Hill, New York.
- Van Zandijcke, F. & Verhoeve, L. 1974, "The vapour-liquid equilibrium of ternary systems with limited miscibility at atmospheric pressure", *Journal of Applied Chemistry and Biotechnology*, vol. 24, no. 12, pp. 709-729.
- Verhoeve, L.A.J. 1970, "System 2-isopropoxypropane-2-propanol-water", *Journal of Chemical and Engineering Data*, vol. 15, no. 2, pp. 222-226.
- Verhoeve, L.A.J. 1968, "System cyclohexane-2-propanol-water", *Journal of Chemical & Engineering Data*, vol. 13, no. 4, pp. 462-467.
- Walas, S.M. 1985, *Phase equilibria in Chemical Engineering*, Butterworth Boston, Stoneham, USA.
- Wang, C., Chen, Y. & Ying, A. 2011, "Measurement and Calculation of Liquid–Liquid Equilibria of Ternary and Quaternary Systems Containing Water, Propan-1-ol, and 2, 2, 4-Trimethylpentane (TMP) with 2, 2'-Oxybis (propane) (DIPE) or Dimethyl Carbonate (DMC)", *Journal of Chemical & Engineering Data*, vol. 56, no. 11, pp. 4466-4472 .
- Wang, C.J., Wong, D.S.H., Chien, I.L., Shih, R.F., Liu, W.T. & Tsai, C.S. 1998, "Critical reflux, parametric sensitivity, and hysteresis in azeotropic distillation of isopropyl alcohol water cyclohexane", *Industrial & Engineering Chemistry Research*, vol. 37, no. 7, pp. 2835-2843.
- Wang, S.J., Lee, C.J., Jang, S.S. & Shieh, S.S. 2008, "Plant-wide design and control of acetic acid dehydration system via heterogeneous azeotropic distillation and divided wall distillation", *Journal of Process Control*, vol. 18, no. 1, pp. 45-60.
- Webb, W.H.A. 1937, "Industrial Alcohol", *Chemical Engineering Research and Design*, vol. 15, pp. 243-252.
- Weir, R.D. & de Loos, T.W. 2005, *Measurement of the thermodynamic properties of multiple phases*, Elsevier Science Ltd.
- Widagdo, S. & Seider, W.D. 1996, "Journal review. Azeotropic distillation", *American Institute of Chemical Engineers*, vol. 42, no. 1, pp. 96-130.

- Widagdo, S., Seider, W.D. & Sebastian, D.H. 1992, "Dynamic analysis of heterogeneous azeotropic distillation", *American Institute of Chemical Engineers*, vol. 38, no. 8, pp. 1229-1242.
- Wilson, G.M. & Deal, C.H. 1962, "Activity coefficients and molecular structure. Activity coefficients in changing environments-solutions of groups", *Industrial & Engineering Chemistry Fundamentals*, vol. 1, no. 1, pp. 20-23.
- Wisniak, J. 1993, "A new test for the thermodynamic consistency of vapor-liquid equilibrium", *Industrial & Engineering Chemistry Research*, vol. 32, no. 7, pp. 1531-1533.
- Wisniak, J. 1994, "Herington Test for Thermodynamic Consistency", *Industrial & Engineering Chemistry Research*, vol. 33, no. 7, pp. 177-180.
- Wisniak, J. 14 September 2011, *PRO-VLE 2.0 Vapor-Liquid Equilibria Computer Program*, Department of Chemical Engineering Ben-Gurion University, Beer-Sheva, Negev.
- Wisniak, J., Apelblat, A. & Segura, H. 1997, "An assessment of thermodynamic consistency tests for vapor-liquid equilibrium data", *Physics and Chemistry of Liquids*, vol. 35, no. 1, pp. 1-58.
- Wisniak, J. & Segura, H. 1997, "Heteroazeotropy and analytical models for phase equilibria", *Industrial & Engineering Chemistry Research*, vol. 36, no. 1, pp. 253-263.
- Wisniak, J. & Tamir, A. 1977, "Vapor-liquid equilibria in the ternary systems water-formic acid-acetic acid and water-acetic acid-propionic acid", *Journal of Chemical and Engineering Data*, vol. 22, no. 3, pp. 253-260.
- Yorizane, M., Yoshimura, S. & Yamamoto, T. 1967, "Measurement of the ternary vapor-liquid equilibrium (Isopropyl alcohol-water-isopropyl ether system)", *Kagaku Kogaku Ronbunshu*, vol. 31, pp. 451-457.
- Young, S. 1902, "The preparation of absolute alcohol from strong spirit", *Journal of the Chemical Society*, vol. 81, pp. 707-717.
- Younis, O.A.D., Pritchard, D.W. & Anwar, M.M. 2007, "Experimental isobaric vapour-liquid-liquid equilibrium data for the quaternary systems water (1)-ethanol (2)-acetone (3)-n-butyl acetate (4) and water (1)-ethanol (2)-acetone (3)-methyl ethyl ketone (4) and their partially miscible-constituent ternaries", *Fluid Phase Equilibria*, vol. 251, no. 2, pp. 149-160.
- Zemp, R.J. & Francesconi, A.Z. 1992, "Salt effect on phase equilibria by a recirculating still", *Journal of Chemical and Engineering Data*, vol. 37, no. 3, pp. 313-316.
- Zhang, J.W., Bai, P. & Zhang, W. 2011, "Isobaric Vapor Liquid Equilibrium (VLE) Data of the Systems Ethylene Glycol-Glycerol and 1, 2-Propylene Glycol-Ethylene Glycol at 20Pa", *Advanced Materials Research*, vol. 301, pp. 235-240.

A. MSDS FORMS

All MSDS information was obtained from ScienceLab.com (ScienceLab.com 2011). Additional corrosion data was obtained from Ham-let (Ham-let Advanced Control Technology 2011).

Table A-1: Benzene MSDS

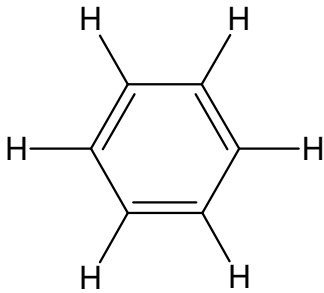
Benzene	
	
Physical Data	
Appearance:	Colourless to light yellow liquid
Molecular Weight:	78.11
Chemical Formula:	C ₆ H ₆
Odour:	Aromatic. Gasoline-like.
SG(water = 1):	0.7257
Boiling point (°C):	80.1
Melting point (°C):	5.5
Vapour pressure (kPa):	10
Vapour density (air = 1):	2.8
Corrosion resistance:	<p>Excellent for alloy20, monel, flexible graphite and teflon-reinforced or NGR</p> <p>Good for aluminium, brass, carbon steel, ductile iron/cast iron, 316 stainless steel, 17-4PH, hastelloy C and viton</p> <p>Poor for delrin</p> <p>Do not use for buna N (nitrile) and EPDM/EPR</p> <p>Non-corrosive in presence of glass</p>
Hazards	
Very hazardous in case of eye contact or inhalation. Hazardous in case of skin contact or ingestion.	
Fire and Explosion Data	
Flammability:	Flammable
Flash point (closed cup, °C):	-11.1
Auto-ignition Temperature (°C):	497.78
Upper Flame Limit (volume % in air):	7.8
Lower Flame Limit (volume % in air):	1.2

Table A-2: Cyclohexane MSDS

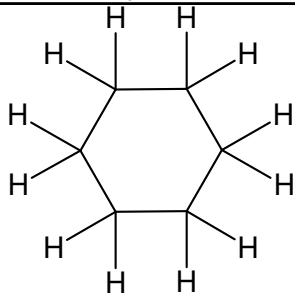
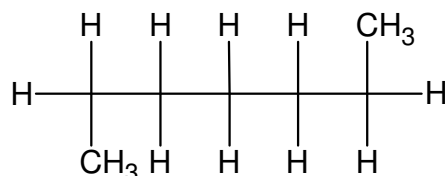
Cyclohexane	
	
Physical Data	
Appearance:	Clear, colourless liquid
Molecular Weight:	84.16
Chemical Formula:	C ₆ H ₁₂
Odour:	Chloroform-like, solvent mild sweet odour
SG(water = 1):	0.7781
Boiling point (°C):	80.7
Melting point (°C):	6.47
Vapour pressure (kPa):	12.9
Vapour density (air = 1):	2.98
Corrosion resistance:	<p>Excellent for aluminium, braas, carbon steel, ductile iron/cast iron, 316 stainless steel, alloy20, delrin, viton and teflon-reinforced or NGR</p> <p>Good for monel and hastelloy C</p> <p>Poor for buna N (nitrile)</p> <p>Do not use for EPDM/EPR</p> <p>Not considered corrosive for glass</p>
Hazards	
Slightly hazardous in the case of skin contact, eye contact, ingestion or inhalation.	
Fire and Explosion Data	
Flammability:	Flammable
Flash point (closed cup, °C):	-18
Auto-ignition Temperature (°C):	245
Upper Flame Limit (volume % in air):	8.4
Lower Flame Limit (volume % in air):	1.3

Table A-3: Hexane MSDS

Hexane



Physical Data

Appearance:	Colourless liquid
Molecular Weight:	86.18
Chemical Formula:	CH ₃ (CH ₂) ₄ CH ₃
Odour:	Gasoline-like smell
SG(water = 1):	0.66
Boiling point (°C):	68
Melting point (°C):	-95
Vapour pressure (kPa):	17.3
Vapour density (air = 1):	2.97
Corrosion resistance:	Excellent for aluminum, 316 stainless steel, alloy20, hastelloy C, buna N (nitrile), delrin, viton, teflon reinforced or NGR Good for brass, carbon steel, ductile iron/cast iron and monel

Do not use for EPDM/EPR

Hazards

Hazardous in case of skin contact, ingestion or inhalation. Slightly hazardous in the case of eye contact.

Fire and Explosion Data

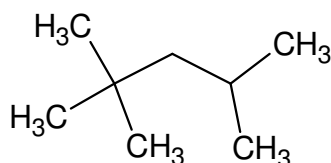
Flammability:	Flammable
Flash point (closed cup, °C):	-22.5
Auto-ignition Temperature (°C):	225
Upper Flame Limit (volume % in air):	7.5
Lower Flame Limit (volume % in air):	1.15

Table A-4: Heptane MSDS

Heptane	
Physical Data	
Appearance:	Clear, colourless liquid
Molecular Weight:	100.21
Chemical Formula:	CH ₃ (CH ₂) ₅ CH ₃
Odour:	Hydrocarbon, gasoline-like
SG(water = 1):	0.6838
Boiling point (°C):	98.4
Melting point (°C):	-90.7
Vapour pressure (kPa):	5.3
Vapour density (air = 1):	3.5
Corrosion resistance:	<p>Excellent for aluminum, brass, 316 stainless steel, alloy 20, hastelloy C, buna N (nitrile), delrin, viton, teflon reinforced or NGR</p> <p>Good for carbon steel, ductile iron/cast iron and monel</p> <p>Do not use for EPDM/EPR</p> <p>Not considered to be corrosive for metals and glass</p>
Hazards	
Slightly hazardous in case of skin contact, eye contact, ingestion or inhalation.	
Fire and Explosion Data	
Flammability:	Flammable
Flash point (closed cup, °C):	-4
Auto-ignition Temperature (°C):	203.89
Upper Flame Limit (volume % in air):	6.7
Lower Flame Limit (volume % in air):	1.05

Table A-5: Isooctane MSDS

Isooctane



Physical Data

Appearance:	Clear, colourless liquid
Molecular Weight:	114.23
Chemical Formula:	C ₈ H ₁₈
Odour:	Mild hydrocarbon odour
SG(water = 1):	0.692
Boiling point (°C):	99.24
Melting point (°C):	-107.36
Vapour pressure (kPa):	5.47
Vapour density (air = 1):	3.9

Excellent for brass, carbon steel, 316 stainless steel, monel, delrin, flexible graphite, teflon-reinforced

Corrosion resistance: Good for aluminum, ductile iron/cast iron, alloy 20

Poor for hastelloy C, buna N

Non-corrosive in the presence of glass

Do not use for EPDM/EPR, viton

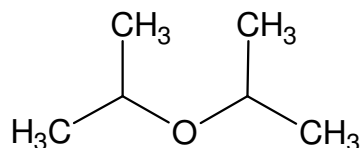
Hazards

Hazardous in case of eye contact, ingestion and inhalation. Slightly hazardous in case of skin contact.

Fire and Explosion Data

Flammability:	Flammable
Flash point (closed cup, °C):	-12
Auto-ignition Temperature (°C):	415
Upper Flame Limit (volume % in air):	6
Lower Flame Limit (volume % in air):	1.1

Table A-6: DIPE MSDS

DIPE**Physical Data**

Appearance:	Colourless liquid
Molecular Weight:	102.18
Chemical Formula:	$(\text{CH}_3)_2\text{CHOCH}(\text{CH}_3)_2$
Odour:	Ethereal
SG(water = 1):	0.7257
Boiling point ($^{\circ}\text{C}$):	68.5
Melting point ($^{\circ}\text{C}$):	-86
Vapour pressure (kPa):	15.87
Vapour density (air = 1):	3.52
Corrosion resistance:	Excellent for aluminum, brass, carbon steel, 316 stainless steel, hastelloy C, buna N, delrin, viton, teflon reinforced
	Good for ductile iron/cast iron, alloy 20
	Do not use for EPDM/EPR
	Non-corrosive in the presence of glass

Hazards

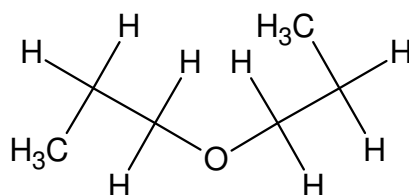
Forms explosive peroxides on prolonged storage. Very hazardous in case of eye contact, ingestion and inhalation. Hazardous in case of skin contact.

Fire and Explosion Data

Flammability:	Flammable
Flash point (closed cup, $^{\circ}\text{C}$):	-28
Auto-ignition Temperature ($^{\circ}\text{C}$):	443
Upper Flame Limit (volume % in air):	7.9
Lower Flame Limit (volume % in air):	1.4

Table A-7: DNPE MSDS

DNPE



Physical Data

Appearance:	Colourless liquid
Molecular Weight:	102.18
Chemical Formula:	(C ₃ H ₇) ₂ O
Odour:	Ethereal
SG(water = 1):	0.7257
Boiling point (°C):	89-91
Melting point (°C):	-122
Vapour pressure (kPa):	7.33
Vapour density (air = 1):	3.53
Corrosion resistance:	Excellent for aluminum, brass, carbon steel, 316 stainless steel, hastelloy C, buna N, delrin, viton, teflon reinforced
	Good for ductile iron/cast iron, alloy 20
	Do not use for EPDM/EPR
	Non-corrosive in the presence of glass

Hazards

May form peroxides during prolonged storage. Slightly hazardous in case of skin contact, eye contact, ingestion or inhalation. May cause burns in the case of skin or eye contact.

Fire and Explosion Data

Flammability:	Extremely flammable
Flash point (closed cup, °C):	-28
Auto-ignition Temperature (°C):	443
Upper Flame Limit (volume % in air):	7.9
Lower Flame Limit (volume % in air):	1.4

B. CALIBRATION CERTIFICATES



TC Ltd, Units 1-8, Brimington Rd North, Chesterfield, S41 9BE, United Kingdom
 Email: callab@tc.co.uk - Web: www.tc.co.uk
 Tel: 01895 252222 - Fax: 01895 273540

KALIBRIERSCHEIN

Datum der Messung: 23 Dezember 2010
 Auftraggeber: Pilodist GmbH
 Anschrift Auftraggeber: Auf Der KaiserFuhr 43 53127 Bonn
 Bostell-Nr. Auftraggeber: Fax Vom 14.12.2010
 Auftrag-Nr. TC GmbH: AU23339
 Auftragsdatum: 14 Dezember 2010
 Kalibriergegenstand: Pt100 6.0mm x 70mm
 Serien Nr. AU23339/1A
 Typenbezeichnung: 15-1-6.0-4-70-CE1A-R100-1/10-2MTRS RT47/NO BRAID/SMALL
 Platin-Widerstandsthermometer
 Umgebungstemperatur: 20°C +/- 2°C

Seite 1 von 1
 Zugelassener
 Unterzeichner:
 L R Walker
 K M Donaldson

Donaldson

Kalibrierschein-Nr:
 10034-1A

Kalibrierverfahren: Das Thermometer wurde durch Vergleich mit zwei Referenz-Widerstandsthermometern kalibriert. Die Kalibrierung erfolgte in einem gerührtem Wasserbad der Firma Grant und einem Hart Trockenblock-Kalibrator. Alle Messungen können auf nationale Normale zurückgeführt werden. Die Widerstände wurden mit Präzisions-Digitalmultimetern gemessen. Alle Messungen wurden unter kontrollierten Umgebungsbedingungen unter Verwendung von Geräten mit bekannten und zurückverfolgbaren Werten durchgeführt. Die Temperaturmessungen lassen sich auf die internationale Temperaturskala ITS-90 zurückführen. Die Umrechnung der Widerstandswerte des Thermometers erfolgte gemäß IEC60751:2008.

Referenz-Temperatur (°C)	Widerstand Prüfling (Ω)	Temperatur kalkuliert gem. IEC (°C)	Fehler (°C)
49.88	119.367	49.92	0.04
199.83	175.836	199.95	0.12

Die Eintauchtiefe des geprüften Thermometers betrug 150mm

Kalibriert von: T Heath

Datum der Kalibrierung: 23 Dezember 2010

Die angegebenen signifikanten Stellen erleichtern dem Anwender des Kalibrierscheins die Interpolation, sie entsprechen nicht der tatsächlichen Messunsicherheit. Die Angaben zur Messgröße erfolgen ohne Berücksichtigung der Messunsicherheit.

Bemerkung: Es liegt in der Verantwortung des Anwenders die Langzeitdrift sowie die Messunsicherheit unter den Bedingungen der Nutzung zu bestimmen.

Dieser Kalibrierschein wurde gemäß der internen Kalibriervorschrift der TC Gruppe ausgestellt. Er dokumentiert, in Übereinstimmung mit dem internationalen Einheitsystem (SI), die Rückführung auf nationale Normale des National Physical Laboratory (NPL) oder andere anerkannte nationale Einrichtungen. Dieser Kalibrierschein darf nur vollständig und unverändert weiterverarbeitet werden. Auszüge oder Änderungen bedürfen der schriftlichen Genehmigung des ausstellenden Kalibrierlaboratoriums.



TC Ltd, Units 1-6, Birmingham Rd North, Chesterfield, S41 9BE, United Kingdom
 Email: callab@tc.co.uk - Web: www.tc.co.uk
 Tel: 01895 252222 - Fax: 01895 273540

KALIBRIERSCHEIN

Datum der Messung: 23 Dezember 2010
 Auftraggeber: Pilodist GmbH
 Anschrift Auftraggeber: Auf Der KaiserFühr 43 53127 Bonn
 Bestell-Nr. Auftraggeber: Fax Vom 14.12.2010
 Auftrag-Nr. TC GmbH: AU23339
 Auftragsdatum: 14 Dezember 2010
 Kalibriergegenstand: Pt100 6.0mm x 200mm
 Serien Nr.: AU23339/1B
 Typenbezeichnung: 16-1-6 0-4-200-CE1A-R100-1/10-2Mtrs RT47/NO BRAID/SMALL
 Platin-Widerstandsthermometer
 Umgebungstemperatur: 20°C +/- 2°C

Seite 1 von 1
 Zugelassener
 Unterzeichner:
 L R Walker
 K M Donaldson

K Donaldson

Kalibrierschein-Nr:
 10034-1B

Kalibrierverfahren: Das Thermometer wurde durch Vergleich mit zwei Referenz-Widerstandsthermometern kalibriert. Die Kalibrierung erfolgte in einem gerühmtem Wasserbad der Firma Grant und einem Hart Trockenblock-Kalibrator. Alle Messungen können auf nationale Normale zurückgeführt werden. Die Widerstände wurden mit Präzisions-Digitalmultimetern gemessen. Alle Messungen wurden unter kontrollierten Umgebungsbedingungen unter Verwendung von Geräten mit bekannten und zurückverfügbaren Werten durchgeführt. Die Temperaturmessungen lassen sich auf die Internationale Temperaturskala ITS-90 zurückführen. Die Umrechnung der Widerstandswerte des Thermometers erfolgte gemäß IEC60751:2008.

Referenz-Temperatur (°C)	Widerstand Prüfling (Ω)	Temperatur kalkuliert gem. IEC (°C)	Fehler (°C)
49.88	119.369	49.93	0.05
199.83	175.832	199.93	0.10

Die Eintauchtiefe des geprüften Thermometers betrug 150mm

Kalibriert von: T Heath

Datum der Kalibrierung: 23 Dezember 2010

Die angegebenen signifikanten Stellen entsprechen dem Anwender des Kalibrierscheins die Interpolation, sie entsprechen nicht der tatsächlichen Messunsicherheit. Die Angaben zur Messgröße erfolgen ohne Berücksichtigung der Messunsicherheit.

Bemerkung: Es liegt in der Verantwortung des Anwenders die Langzeitstabilität sowie die Messunsicherheit unter den Bedingungen der Nutzung zu bestimmen.

Dieser Kalibrierschein wurde gemäß den internen Kalibrierverfahren der TC Gruppe ausgestellt. Er dokumentiert, in Übereinstimmung mit dem internationalen Einheitensystem (SI), die Rückführung auf nationale Normale des National Physical Laboratory (NPL) oder andere anerkannte nationale Einrichtungen. Dieser Kalibrierschein darf nur vollständig und unverändert weiterverarbeitet werden. Auszüge oder Änderungen bedürfen der schriftlichen Genehmigung des ausstellenden Kalibrierlaboratoriums.

Abnahmeprüfzeugnis Inspection certificate		DIN EN 10204/3.1	Formblatt FB 27 – WB 04	
Besteller:	VTU Umwelt- und Verfahrenstechnik GmbH			
Customer:	Auf der Kaiserfuhr 43, 53127 Bonn			
Auftragsnummer (Besteller):	telefonisch (Herr Joub)	Bestelldatum:	13.12.2011	
Order-No. (Customer):		Date:		
Auftrag Nr.:	2230054			
Job-No.:				
Stück: 1	Typ: 31151S	Nenngröße: DMU 03	Anzeigebereich: 0 / 4 bar	
Quantity:	Type:	Diameter:	Range:	
Artikelbezeichnung:	Druckmessumformer DMU 03			
Seriennummer:	1000076701			
Messbereich:	0 – 4 bar			
Anfang Signalausgang (V):	0			
Ende Signalausgang (V):	10			
Kalibrierzertifikat Nr. :	21031238			
Kalibrierdatum:	19.01.2011			
Angaben zum Kalibrieraufbau				
Raumtemperatur:	24,0°C	Medium: Stickstoff		
Druckreferenz:	Hersteller GE Druck	Type DPI 515		
	Genauigkeit: 0..10bar: 0,03% rdg+0,01%fs	SN-Nr.: 51501519		
Multimeter:	Hersteller Hewlett Packard	Type 34401 A		
	Genauigkeit: 10V--> 0,0035%rdg +0,0005%fs	SN-Nr.: 3148 A 06495		
Kalibrierwiderstand:	Hersteller n/a	Type n/a		
	Genauigkeit: n/a	SN-Nr.: n/a		
Version: 2 / Index: 0	AFRISO-EURO-INDEX GmbH	D-74363 Güglingen	Seite: 1 von 2	



Abnahmeprüfzeugnis
Inspection certificate

DIN EN 10204/3.1

Formblatt
FB 27 – WB 04

Messwerte:

Eingang in %	Eingang bar	Ausgang Seil V	Ausgang Ist									
			gemessen in bar						gemittelt			
			1. Zyklus		2. Zyklus		3. Zyklus		steigend	fallend	steigend	
			steigend	fallend	steigend	fallend	steigend	fallend				
0,0	0,000	0,000	0,018	0,018	0,018	0,018	0,018	0,018	0,018	0,018	0,018	0,018
10,0	0,400	1,000	1,014	1,014	1,015	1,014	1,014	1,013	1,014	1,014	1,014	1,014
20,0	0,800	2,000	2,010	2,010	2,010	2,010	2,010	2,010	2,010	2,010	2,010	2,010
30,0	1,200	3,000	3,010	3,010	3,010	3,010	3,010	3,009	3,010	3,010	3,010	3,010
40,0	1,600	4,000	3,999	3,998	4,000	3,999	3,999	3,998	3,999	3,999	3,999	3,999
50,0	2,000	5,000	5,000	5,000	5,000	4,999	4,999	4,999	5,000	4,999	5,000	5,000
60,0	2,400	6,000	5,997	5,997	5,997	5,997	5,997	5,997	5,997	5,997	5,997	5,997
70,0	2,800	7,000	6,991	6,991	6,991	6,991	6,990	6,989	6,991	6,990	6,991	6,991
80,0	3,200	8,000	7,993	7,993	7,993	7,993	7,992	7,993	7,993	7,993	7,993	7,993
90,0	3,600	9,000	8,992	8,992	8,993	8,992	8,992	8,992	8,992	8,992	8,992	8,992
100,0	4,000	10,000	9,999	9,999	9,999	9,999	9,999	9,999	9,999	9,999	9,999	9,999

Auswertung nach IEC60770-1 Abweichung $\leq \pm$ % FSO: Soll: 0,35 Ist: 0,18

Hiemit bescheinigen wir, dass das Produkt unter Verwendung einwandfreier Werkstoffe und nach dem Stand der Technik gefertigt wurden.
Die Bestellvorschriften wurden eingehalten.
Die Endkontrolle ergab keine Beanstandungen.
Die Messergebnisse wurden dem Vorlieferantenzeugnis entnommen.

We herewith certify that this product has been manufactured with the utmost care according to the approved technical standards.
Goods have been manufactured in accordance with order sheet.
The order of working and testing operations corresponds to the test and inspection program of Afriso on the subject.
The measurements were taken from our supplier certificate.



21.01.2011
Datum

[Signature]
i.A. Hans-Joachim
Unterschrift

Telefon ☎ (07135) 102 0 • Telefax (07135) 102 147

SA Metrology

23 Platinum Business Park
Taurus Street
Brackenfell
Tel 0834502615 / Fax (086) 540 2284



SA Metrology

Certificate of Calibration

This certificate is issued in accordance with the ISO 17025:2005 International Standard and is traceable through the National Metrology Laboratory (NML) in Pretoria, SANAS recognised National or International Laboratories

Manufacturer : Afriso
Description : Pressure Transducer
Model No : 311148S
Serial No : 1307171
Asset No : Unknown
Calibrated for : CME Metrology
Cape Town
Temperature : 20 °C ± 3 °C
Relative humidity : 48 %RH ± 5 %RH
Date of calibration : 23 December 2010
Issue Date : 29 December 2010
Calibrated by : P Coetsee

This Report is issued without alteration. Copyright of this Report is owned by SAME and may not be reproduced other than in full, except with the prior written approval of SAMET. The values given in this Report were correct at the time of Test. Subsequently the accuracy will depend on factors such as care exercised in handling the instrument and frequency of use. Retest should be performed after a period, which has been chosen to ensure that, under normal circumstances, the instruments accuracy remains within the desired limits. The uncertainties of measurement were estimated for a coverage factor of $k=2$ which approximates a 95% confidence level.

Technical Signatory
ZW de Witt
Report no SM31504

Calibration Certificate

1. Standards and equipment

Ref	Make	Model	Description	Serial no
50	Fluke	5500A	Calibrator	7270009
201	Fluke	716	Pressure calibrator	7047016
219	Fluke	8506A	DMM True RMS 7.5 Digit	6275404
19	Fluke	525A	Calibrator	9005276
220	Aquatech Inc	DBX1	Precision Digital Barograph	220
230	Fluke	700P01	Pressure Module:	79900103
236	Fluke	700P09	Pressure Module	1500 PSIG
238	Druck	DPI-701	Pressure Calibrator	701051 5805
221	Fluke	700P07	Pressure Module:	73950703
237	Druck	DPI-601	Digital Pressure Calibrator	601478906

2. Procedure

- 2.1 The UUT (Unit under test) was partially calibrated in terms of the manufacturers' accuracy specification, with reference to the typical manufacturers recommended procedure
- 2.2 The UUT was subjected to pressure using filtered air pressure in a direct comparison method against a Certified Digital Pressure transducer in a split system configuration supported by a Process Calibrator.
- 2.3 Calibration procedure no SM P2 001 was used

3. Results

3.1 Decreasing Pressure

Range	Applied Value	UUT Down Pressure	Correction	Tolerance	Measurement uncertainty
1 Bar To 0 Bar	1.0000 Bar	10.000 V	0.0000 Bar	± 0.35 %	± 0.1 %
	0.9980 Bar	9.980 V	0.0000 Bar	± 0.35 %	± 0.1 %
	0.9960 Bar	9.960 V	0.0000 Bar	± 0.35 %	± 0.1 %
	0.9940 Bar	9.940 V	0.0000 Bar	± 0.35 %	± 0.1 %
	0.9800 Bar	9.801 V	-0.0001 Bar	± 0.35 %	± 0.1 %
	0.8000 Bar	8.002 V	-0.0002 Bar	± 0.35 %	± 0.1 %


 Technical Signatory
 ZW de Witt
 Report no SM31504

Calibration Certificate

3.1 Increasing Pressure

Range	Applied Value	UUT Up Pressure	Correction	Tolerance	Measurement uncertainty
1 Bar To 0 Bar	0.8000 Bar	8.003 V	-0.0003 Bar	± 0.35 %	± 0.1 %
	0.9800 Bar	9.802 V	-0.0002 Bar	± 0.35 %	± 0.1 %
	0.9940 Bar	9.941 V	-0.0001 Bar	± 0.35 %	± 0.1 %
	0.9960 Bar	9.960 V	0.0000 Bar	± 0.35 %	± 0.1 %
	0.9980 Bar	9.980 V	0.0000 Bar	± 0.35 %	± 0.1 %
	1.0000 Bar	10.000 V	0.0000 Bar	± 0.35 %	± 0.1 %

4. Comments

Bold - highlights indicate out of tolerance values



Technical Signatory
ZW de Witt
Report no SM31504

C. EXPERIMENTAL DATA

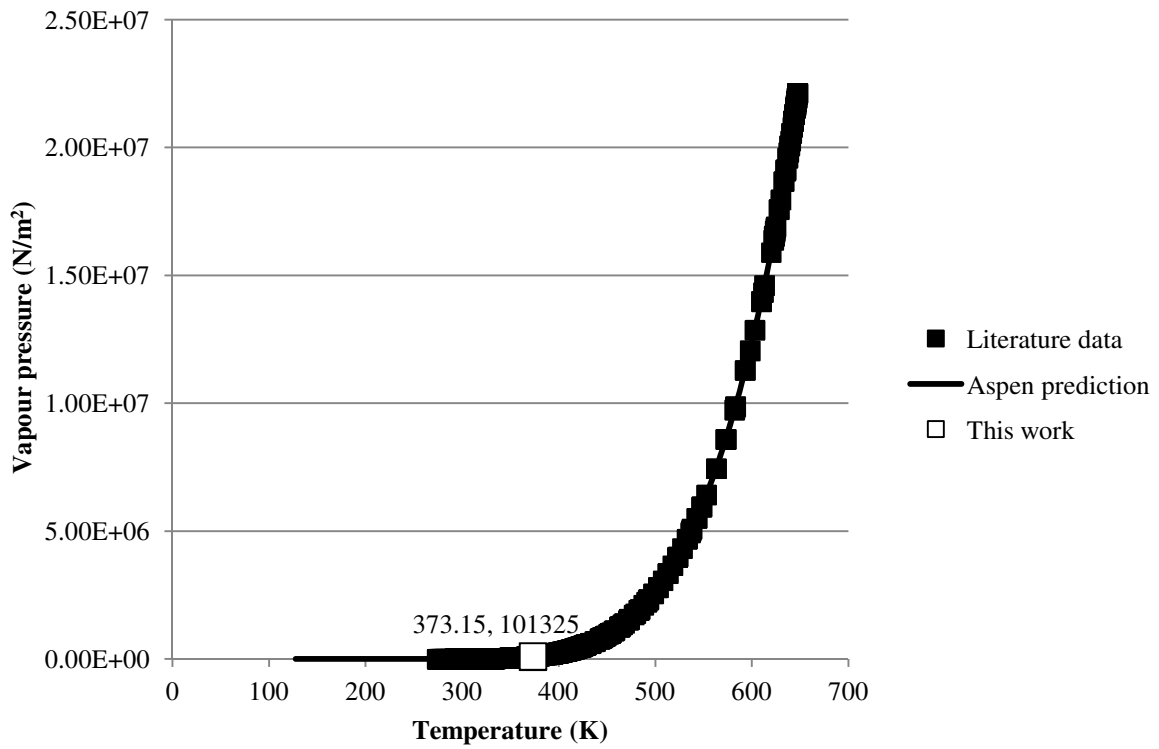


Figure C-1: Water vapour pressure curve.

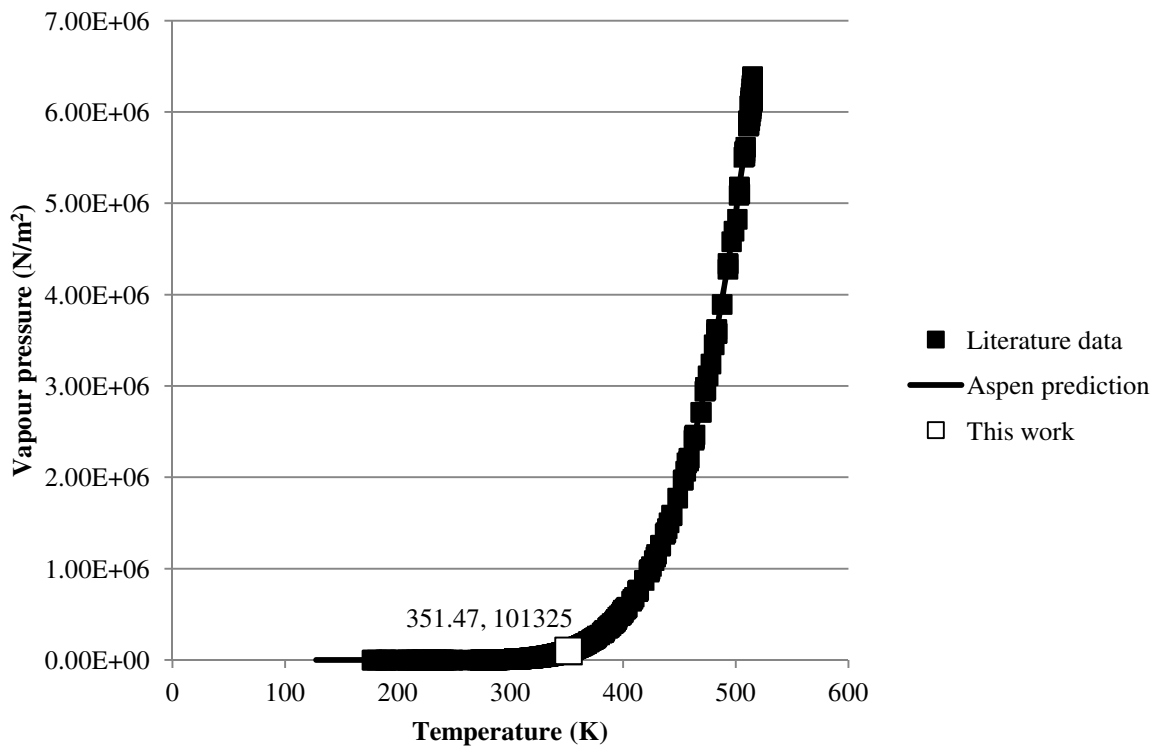


Figure C-2: Ethanol vapour pressure curve.

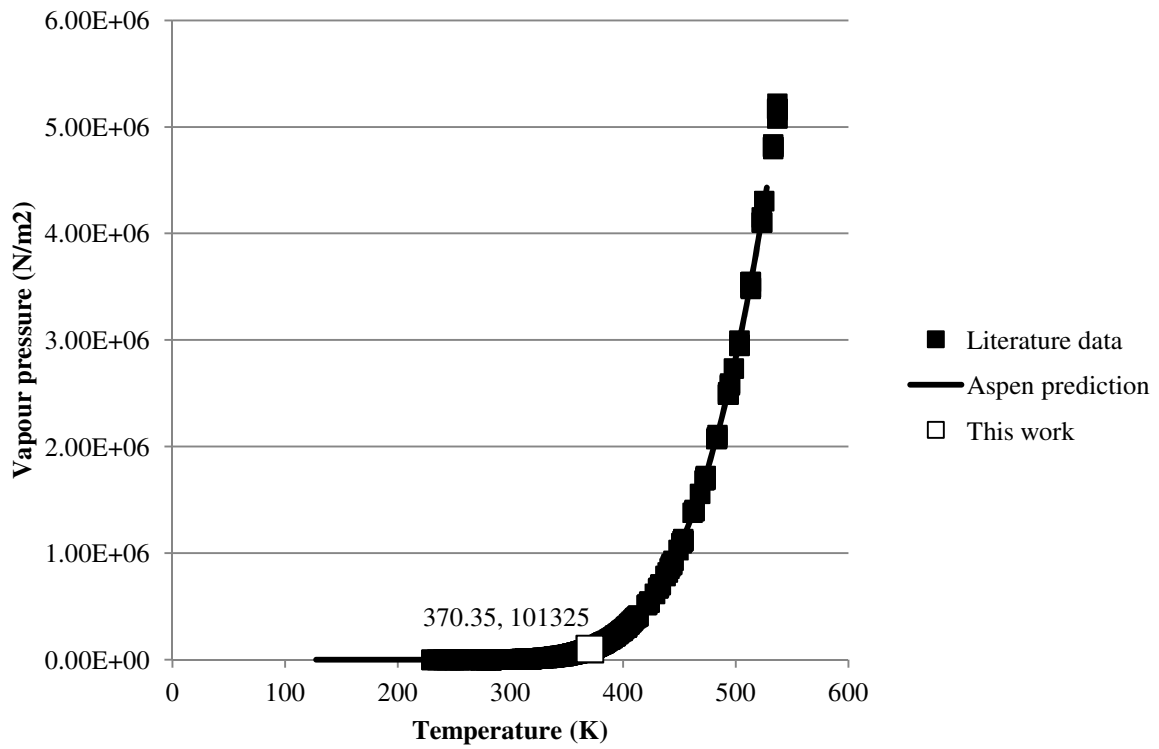


Figure C-3: n-Propanol vapour pressure curve.

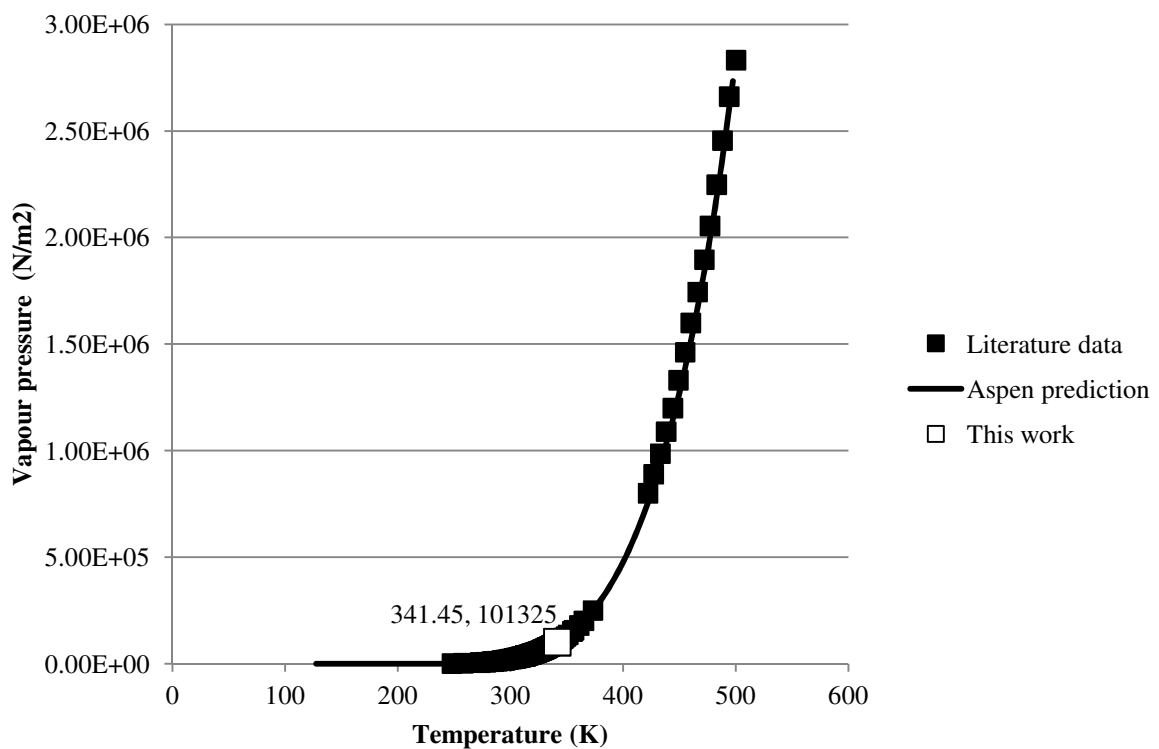


Figure C-4: DIPE vapour pressure curve.

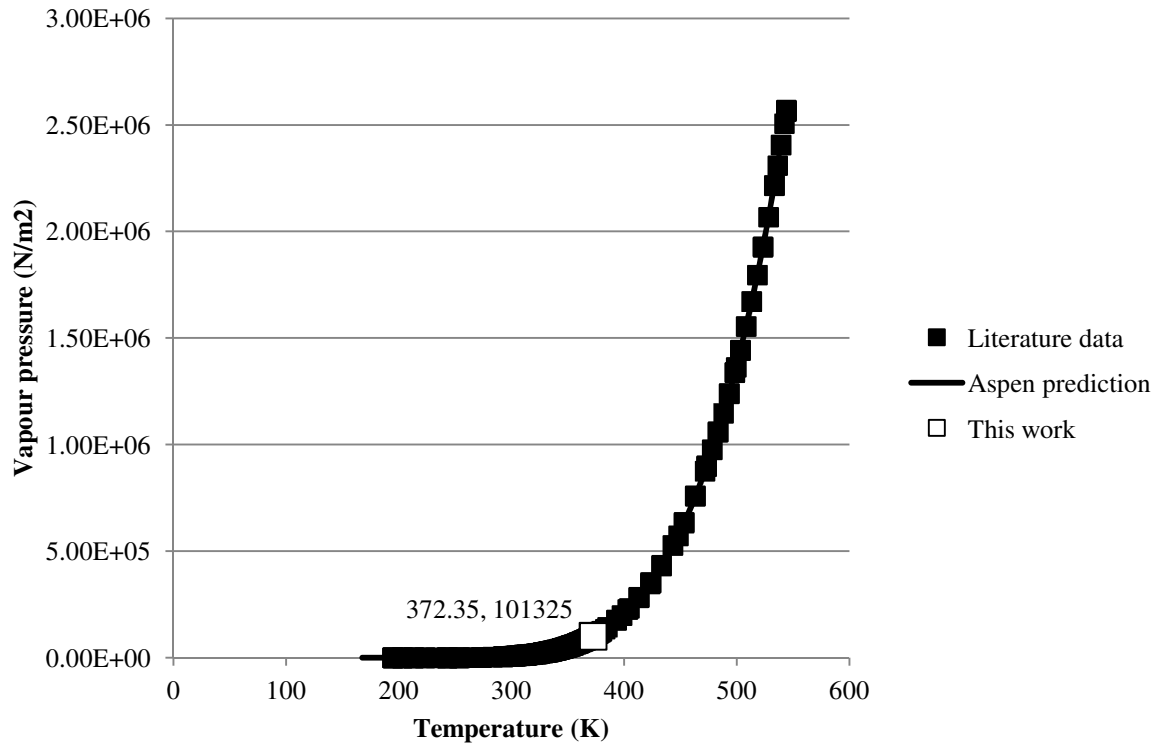


Figure C-5: Isooctane vapour pressure curve.

Table C-1: Binary VLE data (mole fraction) of Ethanol/Isooctane at 101.325 kPa

Temp (°C)	x_{ethanol}	$x_{\text{isooctane}}$	y_{ethanol}	$y_{\text{isooctane}}$
99.20	0.0000	1.0000	0.0000	1.0000
71.64	0.2962	0.7038	0.6113	0.3887
71.79	0.2930	0.7070	0.6100	0.3900
71.80	0.2922	0.7078	0.6112	0.3888
72.50	0.2058	0.7942	0.6056	0.3944
72.50	0.2203	0.7797	0.6007	0.3993
72.50	0.1914	0.8086	0.5986	0.4014
73.20	0.1698	0.8302	0.5920	0.4080
73.33	0.1406	0.8594	0.5971	0.4029
73.33	0.1456	0.8544	0.5813	0.4187
78.32	1.0000	0.0000	1.0000	0.0000
78.32	1.0000	0.0000	1.0000	0.0000
78.30	1.0000	0.0000	1.0000	0.0000
73.60	0.9377	0.0623	0.7921	0.2079
73.65	0.9412	0.0588	0.7817	0.2183
71.45	0.8161	0.1839	0.6740	0.3260
71.47	0.8078	0.1922	0.6706	0.3294
71.47	0.7999	0.2001	0.6566	0.3434
71.42	0.6299	0.3701	0.6454	0.3546
71.42	0.6337	0.3663	0.6422	0.3578
71.90	0.2398	0.7602	0.5988	0.4012
71.85	0.2451	0.7549	0.6087	0.3913
71.85	0.2659	0.7341	0.6103	0.3897
74.27	0.9494	0.0506	0.8034	0.1966
74.40	0.9544	0.0456	0.8053	0.1947
74.50	0.9575	0.0425	0.8201	0.1799

Table C-2: Ternary VLLE data (mole fraction) of IPA/Isooctane/Water at 101.325 kPa

Temp (°C)	organic liquid			aqueous liquid			vapour		
	x_{water}	$x_{\text{isooctane}}$	x_{IPA}	x_{water}	$x_{\text{isooctane}}$	x_{IPA}	y_{water}	$y_{\text{isooctane}}$	y_{IPA}
70.96	0.0488	0.7424	0.2088	0.8790	0.0005	0.1205	0.3436	0.3572	0.2992
71.08	0.0704	0.6586	0.2710	0.8081	0.0032	0.1887	0.0802	0.5263	0.3935
71.05	0.0886	0.6429	0.2685	0.8085	0.0033	0.1882	0.3218	0.3638	0.3144
71.01	0.1181	0.5540	0.3279	0.7447	0.0099	0.2454	0.2773	0.4214	0.3013
70.98	0.1328	0.5277	0.3395	0.7098	0.0096	0.2806	0.2632	0.4124	0.3244
70.98	0.1505	0.5022	0.3473	0.6682	0.0161	0.3156	0.3053	0.3833	0.3114
70.91	0.0748	0.6399	0.2852	0.8082	0.0024	0.1894	0.3214	0.3528	0.3258
70.98	0.1005	0.5971	0.3024	0.7771	0.0047	0.2182	0.3230	0.3776	0.2994
71.01	0.1508	0.5033	0.3459	0.6905	0.0201	0.2894	0.2773	0.4068	0.3160
71.09	0.1496	0.4937	0.3567	0.7164	0.1171	0.1665	0.3313	0.3404	0.3282
71.15	0.1365	0.4869	0.3766	0.5769	0.0532	0.3699	0.3159	0.3676	0.3165
71.06	0.1316	0.5159	0.3525	0.6380	0.0258	0.3362	0.3496	0.3342	0.3162
71.08	0.1594	0.4709	0.3696	0.6637	0.0236	0.3127	0.3245	0.3405	0.3350
71.02	0.1502	0.4891	0.3607	0.6891	0.0181	0.2928	0.2944	0.3872	0.3183

Table C-3: Ternary VLLE data (mole fraction) of IPA/DIPE/Water at 101.325 kPa

Temp (°C)	organic liquid			aqueous liquid			vapour		
	X _{water}	X _{DIPE}	X _{IPA}	X _{water}	X _{DIPE}	X _{IPA}	Y _{water}	Y _{DIPE}	Y _{DIPE}
62.55	0.2154	0.5082	0.2764	0.9610	0.0015	0.0376	0.20432	0.69459	0.10109
63.36	0.3484	0.3169	0.3347	0.9559	0.0018	0.0423	0.19018	0.59232	0.21751
63.98	0.4088	0.2522	0.3390	0.9463	0.0024	0.0513	0.2373	0.6054	0.1573
64.47	0.4400	0.2187	0.3413	0.9220	0.0034	0.0746	0.2293	0.5682	0.2024
65.85	0.6189	0.0910	0.2900	0.8727	0.0090	0.1183	0.2242	0.5258	0.2500
66.66	0.7417	0.0347	0.2236	0.7052	0.0424	0.2524	0.22346	0.57587	0.20067
65.17	0.5619	0.1282	0.3099	0.8958	0.0055	0.0986	0.2254	0.6112	0.1634
61.78	0.0741	0.8073	0.1186	0.9930	0.0004	0.0067	0.2308	0.6858	0.0834
62.28	0.1564	0.6241	0.2195	0.9849	0.0005	0.0146	0.2214	0.6454	0.1332

Table C-4: Ternary VLLE data (mole fraction) of Ethanol/n-Butanol/Water at 101.325 kPa

Temp (°C)	organic liquid			aqueous liquid			vapour		
	X _{water}	X _{n-Butanol}	X _{EtOH}	X _{water}	X _{n-Butanol}	X _{EtOH}	Y _{water}	Y _{n-Butanol}	Y _{EtOH}
92.70	0.5812	0.4188	0.0000	0.9808	0.0192	0.0000	0.7571	0.2429	0.0000
91.00	0.5953	0.3332	0.0715	0.9590	0.0223	0.0187	0.6868	0.1920	0.1212
91.11	0.6586	0.2887	0.0527	0.9476	0.0238	0.0286	0.6803	0.1449	0.1748
92.68	0.5814	0.4186	0.0000	0.9778	0.0222	0.0000	0.7570	0.2430	0.0000
91.41	0.6397	0.3114	0.0489	0.9688	0.0178	0.0134	0.7027	0.1835	0.1139
90.16	0.8469	0.0806	0.0725	0.8634	0.0910	0.0456	0.6488	0.1415	0.2098
91.17	0.6311	0.3096	0.0593	0.9621	0.0176	0.0203	0.6967	0.1872	0.1160
91.33	0.6474	0.2943	0.0583	0.9678	0.0152	0.0170	0.7098	0.1877	0.1025
92.74	0.6110	0.3890	0.0000	0.9795	0.0205	0.0000	0.6670	0.3330	0.0000
92.68	0.6186	0.3749	0.0065	0.9816	0.0170	0.0014	0.7548	0.2248	0.0204
92.16	0.6518	0.3248	0.0234	0.9771	0.0171	0.0058	0.7296	0.2119	0.0585
91.63	0.6542	0.3086	0.0372	0.9697	0.0179	0.0124	0.6993	0.1805	0.1202

Table C-5: Ternary VLE data (mole fraction) of Ethanol/DIPE/Water at 101.325 kPa

Temp (°C)	organic liquid			aqueous liquid			vapour		
	X _{water}	X _{DIPE}	X _{EtOH}	X _{water}	X _{DIPE}	X _{EtOH}	Y _{water}	Y _{DIPE}	Y _{EtOH}
61.01	0.0877	0.7844	0.1280	0.9231	0.0015	0.0754	0.1974	0.6670	0.1356
61.04	0.1168	0.6733	0.2099	0.9128	0.0011	0.0860	0.1826	0.6219	0.1956
61.10	0.0997	0.7194	0.1809	0.9161	0.0024	0.0815	0.1861	0.6631	0.1507
61.12	0.1051	0.7134	0.1815	0.9221	0.0019	0.0760	0.1888	0.6597	0.1515
61.23	0.1451	0.6029	0.2520	0.8845	0.0038	0.1116	0.1944	0.6391	0.1665
61.25	0.0644	0.8498	0.0857	0.9510	0.0016	0.0474	0.2010	0.6945	0.1045
61.27	0.1232	0.6499	0.2269	0.9004	0.0029	0.0967	0.1879	0.6447	0.1674
61.32	0.1635	0.5899	0.2466	0.8852	0.0042	0.1105	0.1731	0.6188	0.2081
61.38	0.0605	0.8805	0.0589	0.9636	0.0012	0.0353	0.2100	0.7049	0.0851
61.40	0.1738	0.5667	0.2595	0.8798	0.0044	0.1158	0.1881	0.6306	0.1813
61.41	0.1520	0.5959	0.2521	0.8852	0.0036	0.1112	0.1927	0.6299	0.1775
61.62	0.1951	0.5081	0.2968	0.8644	0.0043	0.1314	0.1891	0.6196	0.1913
61.69	0.2599	0.4197	0.3204	0.8530	0.0019	0.1451	0.1866	0.6195	0.1938
61.77	0.2629	0.4157	0.3214	0.8365	0.0077	0.1557	0.1798	0.6147	0.2055
61.88	0.3408	0.3132	0.3459	0.8201	0.0108	0.1691	0.1886	0.6081	0.2034
61.89	0.3473	0.2972	0.3555	0.7858	0.0178	0.1964	0.1889	0.5982	0.2128
62.07	0.3941	0.2551	0.3508	0.7590	0.0211	0.2199	0.1880	0.6081	0.2039
62.16	0.0476	0.9524	0.0000	0.9991	0.0009	0.0000	0.2186	0.7814	0.0000
62.22	0.3813	0.2594	0.3593	0.7761	0.0208	0.2031	0.1821	0.6034	0.2145
62.24	0.7927	0.0131	0.1942	0.7954	0.0127	0.1919	0.1945	0.5840	0.2215
63.14	0.7644	0.0160	0.2196	0.7674	0.0141	0.2184	0.2070	0.5770	0.2160

Table C-6: Ternary VLE data (mole fraction) of Ethanol/DIPE/Water at 101.325 kPa

Temp (°C)	X _{water}	X _{DIPE}	X _{EtOH}	Y _{water}	Y _{DIPE}	Y _{EtOH}
65.06	0.5826	0.0590	0.3584	0.2020	0.5313	0.2667
66.84	0.5542	0.0586	0.3872	0.2141	0.4830	0.3029
67.49	0.5332	0.0538	0.4130	0.2072	0.5056	0.2872
68.98	0.5162	0.0464	0.4374	0.2326	0.4195	0.3479
69.25	0.4917	0.0486	0.4597	0.2226	0.4046	0.3728
70.65	0.4909	0.0380	0.4711	0.2515	0.3384	0.4100
71.11	0.4552	0.0388	0.5060	0.2257	0.3342	0.4401
72.08	0.4636	0.0341	0.5023	0.2390	0.3003	0.4607
72.28	0.4216	0.0347	0.5437	0.2322	0.2815	0.4863
73.01	0.4024	0.0362	0.5615	0.2284	0.2628	0.5088
73.09	0.4427	0.0301	0.5272	0.2396	0.2623	0.4981
73.68	0.3039	0.0343	0.6618	0.3287	0.1842	0.4871
73.93	0.3727	0.0288	0.5985	0.2327	0.2215	0.5458
74.2	0.2853	0.0321	0.6826	0.3429	0.1656	0.4915
74.92	0.2595	0.0252	0.7154	0.2963	0.1432	0.5605
75.69	0.2324	0.0221	0.7455	0.4044	0.1049	0.4907
76.09	0.2075	0.0205	0.7720	0.2828	0.1094	0.6078
76.35	0.0594	0.0202	0.9204	0.2799	0.0936	0.6265

Table C-7: Ternary VLE data (mole fraction) of *n*-Propanol/DIPE/Water at 101.325 kPa

Temp (°C)	organic liquid			aqueous liquid			vapour		
	X _{water}	X _{DIPE}	X _{n-Propanol}	X _{water}	X _{DIPE}	X _{n-Propanol}	Y _{water}	Y _{DIPE}	Y _{n-Propanol}
62.16	0.0476	0.9524	0.0000	0.9991	0.0009	0.0000	0.2186	0.7814	0.0000
62.56	0.0665	0.8649	0.0686	0.9900	0.0009	0.0091	0.2042	0.7942	0.0016
62.74	0.0686	0.8380	0.0934	0.9861	0.0010	0.0129	0.2214	0.7386	0.0401
63.82	0.1254	0.6704	0.2042	0.9778	0.0011	0.0211	0.2341	0.6929	0.0730
64.19	0.1584	0.6048	0.2368	0.9794	0.0008	0.0198	0.2339	0.6882	0.0779
64.45	0.1634	0.5912	0.2454	0.9764	0.0009	0.0227	0.2399	0.6635	0.0965
64.75	0.1945	0.5083	0.2972	0.9716	0.0014	0.0270	0.2375	0.6713	0.0912
65.15	0.2179	0.4859	0.2962	0.9716	0.0011	0.0273	0.2362	0.6705	0.0934
67.48	0.3951	0.2465	0.3584	0.9606	0.0013	0.0381	0.2584	0.6169	0.1247
67.75	0.3798	0.2603	0.3599	0.9596	0.0015	0.0389	0.2783	0.6004	0.1213
67.90	0.3774	0.2609	0.3617	0.9611	0.0016	0.0373	0.2583	0.6050	0.1368
68.50	0.4242	0.1920	0.3839	0.9560	0.0015	0.0425	0.2629	0.6027	0.1344
69.27	0.4721	0.1640	0.3638	0.9542	0.0021	0.0437	0.2731	0.5980	0.1289
69.47	0.4802	0.1510	0.3688	0.9500	0.0017	0.0482	0.2860	0.5787	0.1353
69.88	0.5192	0.1163	0.3644	0.9386	0.0022	0.0592	0.2925	0.5753	0.1322
70.67	0.5537	0.1009	0.3455	0.9355	0.0026	0.0619	0.2722	0.5861	0.1417
71.10	0.5746	0.0810	0.3443	0.9306	0.0059	0.0636	0.2958	0.5662	0.1380
72.61	0.6451	0.0588	0.2961	0.8534	0.0151	0.1316	0.3111	0.4997	0.1892

Table C-8: Ternary VLE data (mole fraction) of *n*-Propanol/DIPE/Water at 101.325 kPa

Temp (°C)	X _{water}	X _{DIPE}	X _{n-Propanol}	Y _{water}	Y _{DIPE}	Y _{n-Propanol}
73.27	0.5683	0.0585	0.3733	0.3125	0.4514	0.2361
76.21	0.5189	0.0472	0.4339	0.3651	0.3560	0.2789
77.91	0.4848	0.0523	0.4629	0.3703	0.3157	0.3140
78.36	0.4699	0.0422	0.4879	0.3763	0.3015	0.3222
79.97	0.4505	0.0448	0.5046	0.3952	0.2650	0.3398
80.15	0.4311	0.0389	0.5301	0.3780	0.2690	0.3530
81.07	0.4224	0.0287	0.5489	0.4018	0.2209	0.3772
81.21	0.4037	0.0340	0.5623	0.4020	0.2199	0.3781
82.02	0.3889	0.0272	0.5839	0.4206	0.2003	0.3791
82.43	0.3724	0.0317	0.5959	0.4211	0.2440	0.3349
83.01	0.3480	0.0252	0.6269	0.4122	0.1685	0.4193
84.28	0.3235	0.0256	0.6509	0.3980	0.1555	0.4466
84.45	0.2995	0.0222	0.6783	0.3865	0.1417	0.4718
85.18	0.2843	0.0226	0.6931	0.3898	0.1287	0.4816
86.32	0.2530	0.0165	0.7306	0.3844	0.1036	0.5120
87.63	0.2335	0.0130	0.7536	0.3762	0.0841	0.5396
87.98	0.2216	0.0135	0.7649	0.3719	0.0688	0.5592
88.36	0.2131	0.0143	0.7727	0.3807	0.0664	0.5528

Table C-9: Ternary VLLE data (mole fraction) of *n*-Propanol/Isooctane/Water at 101.325 kPa

Temp (°C)	organic liquid			aqueous liquid			vapour		
	X _{water}	X _{Isooctane}	X _{n-Propanol}	X _{water}	X _{Isooctane}	X _{n-Propanol}	Y _{water}	Y _{Isooctane}	Y _{n-Propanol}
74.48	0.1446	0.5617	0.2937	0.8452	0.0049	0.1499	0.3899	0.4246	0.1855
74.48	0.1417	0.5441	0.3142	0.8415	0.0057	0.1528	0.3793	0.4056	0.2151
74.57	0.1106	0.6293	0.2601	0.8848	0.0012	0.1139	0.3826	0.4120	0.2053
74.59	0.0601	0.7361	0.2038	0.9282	0.0003	0.0715	0.3865	0.4195	0.1940
74.60	0.1133	0.6401	0.2467	0.8990	0.0006	0.1004	0.3885	0.3948	0.2167
74.61	0.0440	0.7993	0.1567	0.9383	0.0002	0.0615	0.3975	0.4225	0.1801
74.61	0.1345	0.5736	0.2919	0.8554	0.0033	0.1413	0.3838	0.4083	0.2079
74.63	0.1661	0.4988	0.3351	0.7988	0.0093	0.1919	0.3654	0.4338	0.2008
74.76	0.1951	0.4271	0.3778	0.7426	0.0161	0.2412	0.3725	0.4183	0.2092
74.78	0.0431	0.8256	0.1312	0.9448	0.0002	0.0550	0.3713	0.4403	0.1885
74.79	0.2771	0.3316	0.3913	0.6647	0.0357	0.2996	0.3868	0.4031	0.2101
74.88	0.0402	0.8433	0.1165	0.9568	0.0000	0.0432	0.4070	0.4331	0.1598
75.17	0.0304	0.8998	0.0698	0.9704	0.0000	0.0296	0.3941	0.4315	0.1744
75.37	0.0357	0.8669	0.0974	0.9645	0.0000	0.0355	0.3912	0.4425	0.1663
75.56	0.0162	0.9217	0.0621	0.9742	0.0001	0.0257	0.3867	0.4464	0.1669
75.70	0.0245	0.9266	0.0489	0.9770	0.0000	0.0230	0.4015	0.4484	0.1501
79.16	0.0114	0.9886	0.0000	0.9988	0.0012	0.0000	0.4710	0.5290	0.0000

Table C-10: Ternary VLE data (mole fraction) of n-Propanol/Isooctane/Water at 101.325 kPa

Temp (°C)	1 st GC injection					
	X _{water}	X _{isooctane}	X _{n-Propanol}	Y _{water}	Y _{isooctane}	Y _{n-Propanol}
75.63	0.4865	0.0629	0.4506	0.4060	0.3702	0.2238
76.55	0.5127	0.0471	0.4403	0.4075	0.3366	0.2559
76.61	0.4778	0.0750	0.4473	0.4572	0.3359	0.2069
77.56	0.4765	0.0416	0.4820	0.4345	0.3191	0.2463
78.95	0.4504	0.0333	0.5163	0.4318	0.2869	0.2813
79.78	0.4381	0.0285	0.5334	0.4268	0.2728	0.3004
80.44	0.4096	0.0330	0.5573	0.4138	0.2653	0.3209
81.08	0.5891	0.3546	0.0564	0.4354	0.2429	0.3217
81.16	0.3898	0.0298	0.5804	0.4253	0.2551	0.3196
81.84	0.4142	0.0215	0.5643	0.4434	0.2145	0.3422
82.51	0.3971	0.0270	0.5758	0.4263	0.2075	0.3662
82.51	0.3559	0.0205	0.6236	0.4165	0.2095	0.3740
83.23	0.3384	0.0267	0.6348	0.4176	0.1928	0.3896
83.24	0.3764	0.0208	0.6028	0.4475	0.1740	0.3785
84.42	0.3101	0.0185	0.6714	0.4081	0.1624	0.4295
86.16	0.2803	0.0168	0.7029	0.4120	0.1277	0.4603
87.12	0.2529	0.0186	0.7285	0.3943	0.1291	0.4766
Temp (°C)	2 nd GC injection					
	X _{water}	X _{isooctane}	X _{n-Propanol}	Y _{water}	Y _{DIPE}	Y _{n-Propanol}
75.63	0.4924	0.0773	0.4303	0.4083	0.3785	0.2132
76.55	0.5121	0.0457	0.4423	0.4120	0.3525	0.2355
76.61	0.4722	0.0613	0.4665	0.4544	0.3271	0.2185
77.56	0.4764	0.0413	0.4823	0.4339	0.3170	0.2491
78.95	0.4508	0.0344	0.5148	0.4322	0.2881	0.2797
79.78	0.4385	0.0295	0.5319	0.4274	0.2747	0.2980
80.44	0.4102	0.0346	0.5552	0.4176	0.2779	0.3045
81.08	0.4555	0.0224	0.5221	0.4443	0.2705	0.2852
81.16	0.3899	0.0300	0.5801	0.4238	0.2501	0.3261
81.84	0.4143	0.0216	0.5641	0.4433	0.2144	0.3423
82.51	0.3949	0.0206	0.5845	0.4270	0.2097	0.3633
82.51	0.3558	0.0200	0.6242	0.4165	0.2095	0.3740
83.23	0.3377	0.0243	0.6380	0.4181	0.1945	0.3874
83.24	0.3759	0.0191	0.6051	0.4479	0.1752	0.3768
84.42	0.3104	0.0197	0.6699	0.4070	0.1591	0.4340
86.16	0.2800	0.0153	0.7047	0.4130	0.1308	0.4561
87.12	0.2523	0.0160	0.7316	0.3917	0.1207	0.4876

D. THERMODYNAMIC CONSISTENCY TESTS*Table D-1: Herington consistency test results for ethanol/isooctane VLE measured by Hiaki et al. (1994).*

Area above the zero line:	A	= 0.51513
Area below the zero line:	B	= 0.54258
D	= $100 \cdot \text{ABS}(A-B)/(A+B)$	= 2.5946
J	= $150 \cdot (T_{\text{max}} - T_{\text{min}})/T_{\text{min}}$	= 1.793
ABS(D-J)	= 0.8016	
Net area multiplied by 100	= A*	= -2.7444
Criteria to Pass:	ABS(D-J)<10 (for isobaric data set)	or ABS(A*)<3

Table D-2: Herington consistency test results for ethanol/isooctane VLE measured by Ku and Tu (2005).

Area above the zero line:	A	= 0.47473
Area below the zero line:	B	= 0.53946
D	= $100 \cdot \text{ABS}(A-B)/(A+B)$	= 6.3819
J	= $150 \cdot (T_{\text{max}} - T_{\text{min}})/T_{\text{min}}$	= 12.146
ABS(D-J)	= 5.7641	
Net area multiplied by 100	= A*	= -6.4725
Criteria to Pass:	ABS(D-J)<10 (for isobaric data set)	or ABS(A*)<3

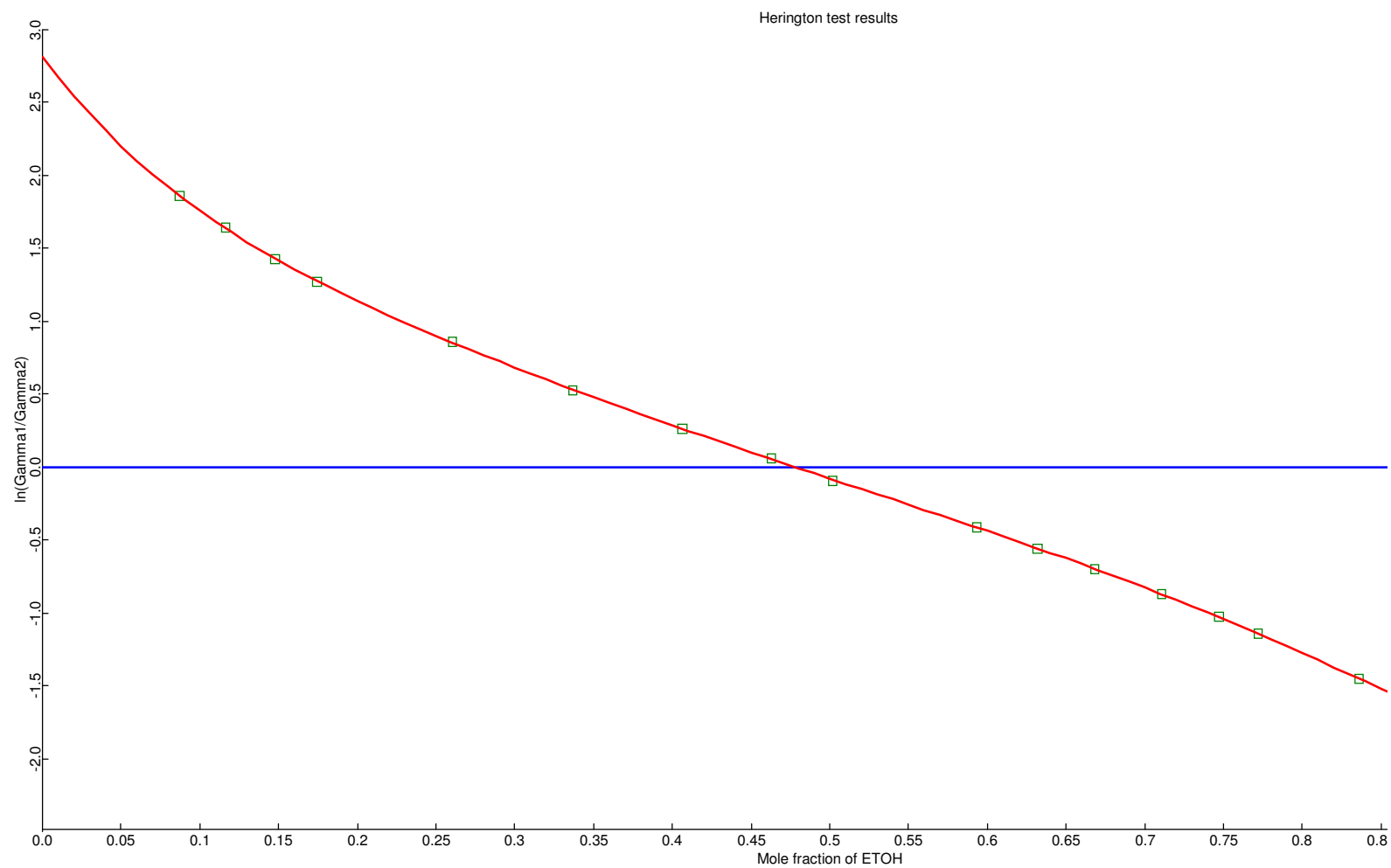


Figure D-1: Graphical Herington consistency test results for ethanol/isooctane VLE measured by Hiaki et al. (1994).

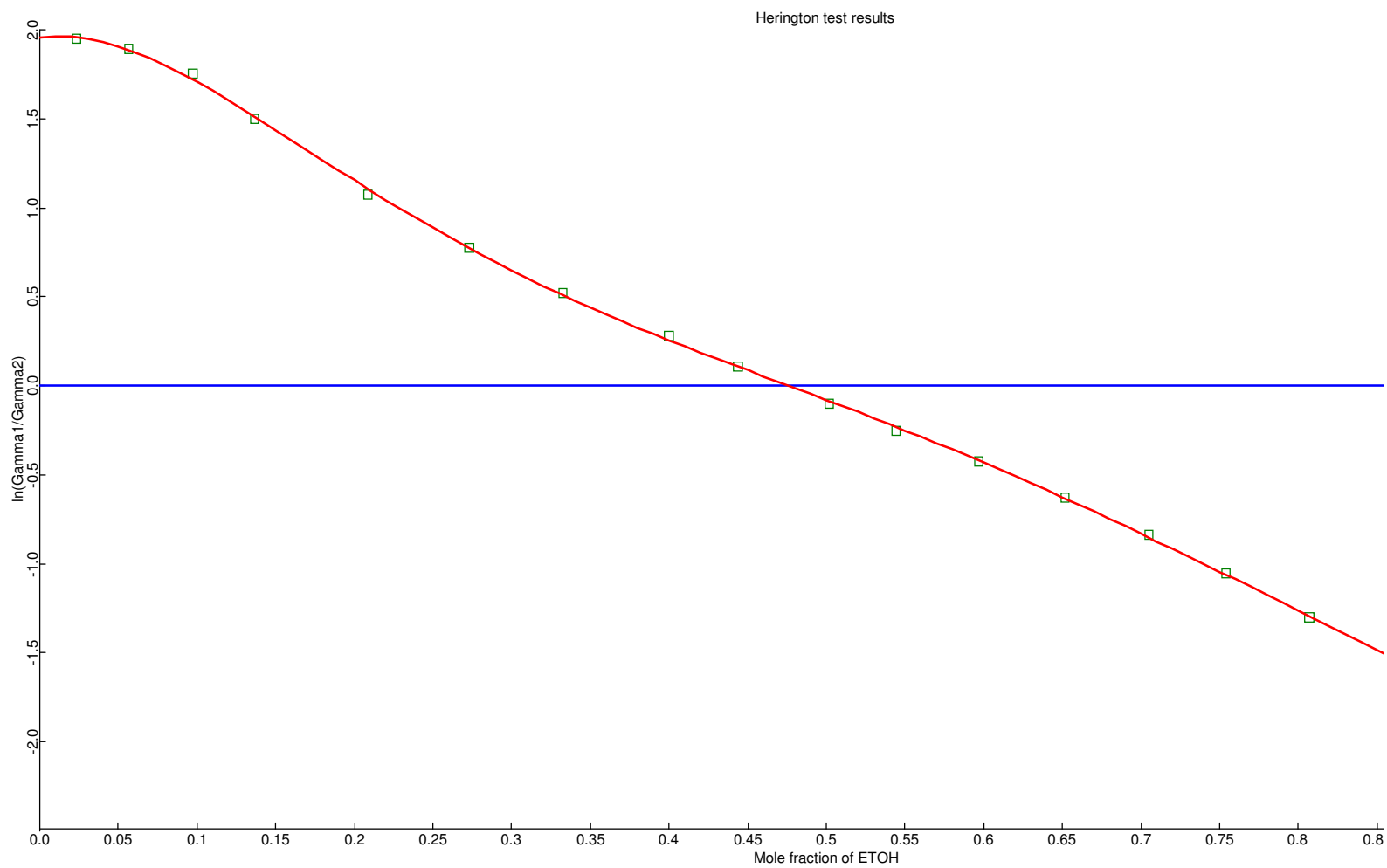


Figure D-2: Graphical Herington consistency test results for ethanol/isooctane VLE measured by Ku and Tu (2005).

Table D-3: Parameter input for PRO-VLE 2.0 software

Parameter	Symbol	Water	Ethanol	n-Propanol	Isooctane	DIPE
	A	8.108 ^a	8.112 ^a	7.744 ^a	6.888 ^a	6.852 ^b
Antoine constants: $\log P = A - B/(t+C)$; (mmHg; deg C)	B	1750.286 ^a	1592.864 ^a	1437.686 ^a	1319.529 ^a	1143.07 ^b
	C	235 ^a	226.184 ^a	198.463 ^a	211.625 ^a	219.34 ^b
Critical temperature	T _c (K)	647.13 ^c	513.92 ^c	536.78 ^c	543.96 ^c	500.05 ^c
Critical pressure	P _c (atm)	217.683 ^c	60.681 ^c	51.077 ^c	25.342 ^c	28.426 ^c
Critical volume	V _c (cm ³ /mol)	55.948 ^c	167 ^c	219 ^c	468 ^c	386 ^c
Boiling temperature	T _b (K)	373.15 ^c	351.44 ^c	370.35 ^c	372.388 ^c	341.45 ^c
Acentric factor	ω	0.345 ^c	0.645 ^c	0.622 ^c	0.303 ^c	0.339 ^c
Liquid molar volume	V ^L (cm ³ /mol)	18.506 ^c	62.694 ^c	82.075 ^c	182.949 ^c	151.659 ^c
Heat of vaporization	ΔH_v (cal/mol)	9751.243 ^c	9237.165 ^c	9954.063 ^c	7414.054 ^c	6962.811 ^c
Moment dipole	μ (debye)	1.845 ^c	1.687 ^c	1.675 ^c	0 ^c	1.128 ^c

^a Felder and Rousseau (2000)^b Reddick et al. (1986)^c Aspen Plus v7.1

Table D-4: L-W consistency test results for Ethanol/DIPE/Water VLE

Wisniak L-W test						
T (K)	x_{water}	x_{DIPE}	L_i	W_i	L_i/W_i	D
338.21	0.583	0.059	25.552	25.743	0.99	0.372
339.99	0.554	0.059	23.149	23.308	0.99	0.342
340.64	0.533	0.054	22.062	22.209	0.99	0.332
342.13	0.516	0.046	20.239	20.363	0.99	0.305
342.4	0.492	0.049	19.419	19.542	0.99	0.316
343.8	0.491	0.038	18.06	18.158	0.99	0.271
344.26	0.455	0.039	16.814	16.907	0.99	0.276
345.23	0.464	0.034	16.054	16.129	1	0.233
345.43	0.422	0.035	14.932	15.009	0.99	0.257
346.16	0.402	0.036	13.774	13.84	1	0.239
346.24	0.443	0.03	14.61	14.669	1	0.202
346.83	0.304	0.034	10.964	11.032	0.99	0.309
347.08	0.373	0.029	12.249	12.302	1	0.216
347.35	0.285	0.032	10.052	10.113	0.99	0.303
348.07	0.259	0.025	8.815	8.864	0.99	0.277
348.84	0.232	0.022	7.476	7.514	0.99	0.254
349.24	0.207	0.021	6.545	6.578	1	0.251
349.5	0.059	0.02	3.071	3.111	0.99	0.647

Table D-5: McDermott-Ellis consistency test results for Ethanol/DIPE/Water VLE

McDermott-Ellis test				
T (K)	x_{water}	x_{DIPE}	D_i	D_{maxi}
338.21	0.583	0.059	0	0.291
339.99	0.554	0.059	-0.127	0.289
340.64	0.533	0.054	0.143	0.28
342.13	0.516	0.046	-0.008	0.266
342.4	0.492	0.049	0.079	0.259
343.8	0.491	0.038	-0.072	0.253
344.26	0.455	0.039	0.012	0.25
345.23	0.464	0.034	0.01	0.249
345.43	0.422	0.035	-0.027	0.245
346.16	0.402	0.036	0.011	0.247
346.24	0.443	0.03	0.142	0.26
346.83	0.304	0.034	-0.099	0.249
347.08	0.373	0.029	0.083	0.251
347.35	0.285	0.032	0.039	0.221
348.07	0.259	0.025	-0.116	0.229
348.84	0.232	0.022	0.138	0.222
349.24	0.207	0.021	0.059	0.251
349.5	0.059	0.02	0	0.197

Table D-6: L-W consistency test results for n-Propanol/DIPE/Water VLE

Wisniak L-W test						
T (K)	x_{water}	x_{DIPE}	L_i	W_i	L_i/W_i	D
346.42	0.568	0.058	24.203	24.373	0.99	0.350
349.36	0.519	0.047	21.378	21.507	0.99	0.301
351.06	0.485	0.052	19.468	19.572	0.99	0.266
351.51	0.47	0.042	19.202	19.303	0.99	0.262
353.12	0.451	0.045	17.48	17.553	1	0.208
353.3	0.431	0.039	17.378	17.453	1	0.215
354.22	0.422	0.029	16.661	16.72	1	0.177
354.36	0.404	0.034	16.351	16.413	1	0.189
355.17	0.389	0.027	15.65	15.7	1	0.159
355.58	0.372	0.032	15.095	15.141	1	0.152
356.16	0.348	0.025	14.591	14.632	1	0.140
357.43	0.324	0.026	13.244	13.269	1	0.094
357.6	0.299	0.022	13.083	13.109	1	0.099
358.33	0.284	0.023	12.302	12.319	1	0.069
359.47	0.253	0.016	11.211	11.214	1	0.013
360.78	0.234	0.013	9.924	9.911	1	0.066
361.13	0.222	0.014	9.53	9.514	1	0.084
361.51	0.213	0.014	9.109	9.09	1	0.104

Table D-7: McDermott-Ellis consistency test results for n-Propanol/DIPE/Water VLE

McDermott-Ellis test				
T (K)	x_{water}	x_{DIPE}	D_i	D_{maxi}
346.42	0.568	0.058	0.036	0.261
349.36	0.519	0.047	-0.03	0.248
351.06	0.485	0.052	-0.001	0.243
351.51	0.47	0.042	-0.043	0.241
353.12	0.451	0.045	-0.013	0.236
353.3	0.431	0.039	0.037	0.233
354.22	0.422	0.029	-0.009	0.232
354.36	0.404	0.034	-0.031	0.231
355.17	0.389	0.027	-0.166	0.233
355.58	0.372	0.032	0.192	0.234
356.16	0.348	0.025	-0.048	0.223
357.43	0.324	0.026	0.037	0.219
357.6	0.299	0.022	-0.029	0.219
358.33	0.284	0.023	-0.017	0.217
359.47	0.253	0.016	-0.04	0.211
360.78	0.234	0.013	0.017	0.213
361.13	0.222	0.014	-0.038	0.211
361.51	0.213	0.014	0	0.208

Table D-8: L-W consistency test results for n-Propanol/Isooctane/Water VLE

Wisniak L-W test						
T (K)	x_{water}	$x_{\text{Isooctane}}$	L_i	W_i	L_i/W_i	D
348.78	0.492	0.077	23.078	24.667	0.94	3.328
349.7	0.512	0.046	22.152	23.188	0.96	2.285
349.76	0.472	0.061	22.009	23.306	0.94	2.862
350.71	0.476	0.041	21.033	21.974	0.96	2.188
352.1	0.451	0.034	19.557	20.353	0.96	1.994
352.93	0.438	0.03	18.683	19.381	0.96	1.834
353.59	0.41	0.035	17.953	18.72	0.96	2.091
354.23	0.456	0.022	17.418	17.965	0.97	1.546
354.31	0.39	0.03	17.168	17.845	0.96	1.934
354.99	0.414	0.022	16.541	17.064	0.97	1.556
355.66	0.395	0.021	15.814	16.309	0.97	1.541
355.66	0.356	0.02	15.704	16.195	0.97	1.539
356.38	0.338	0.024	14.941	15.485	0.96	1.788
356.39	0.376	0.019	15.029	15.486	0.97	1.498
357.57	0.31	0.02	13.667	14.113	0.97	1.605
359.31	0.28	0.015	11.835	12.181	0.97	1.441
360.27	0.252	0.016	10.799	11.138	0.97	1.545

Table D-9: McDermott-Ellis consistency test results for n-Propanol/Isooctane/Water VLE

McDermott-Ellis test				
T (K)	x_{water}	$x_{\text{Isooctane}}$	D_i	D_{maxi}
348.78	0.492	0.077	0.012	0.268
349.7	0.512	0.046	0.015	0.267
349.76	0.472	0.061	0	0.263
350.71	0.476	0.041	-0.009	0.246
352.1	0.451	0.034	-0.015	0.241
352.93	0.438	0.03	-0.049	0.243
353.59	0.41	0.035	-0.07	0.25
354.23	0.456	0.022	0.097	0.247
354.31	0.39	0.03	0.029	0.237
354.99	0.414	0.022	-0.017	0.228
355.66	0.395	0.021	0.016	0.229
355.66	0.356	0.02	-0.014	0.232
356.38	0.338	0.024	0.01	0.228
356.39	0.376	0.019	0.016	0.226
357.57	0.31	0.02	-0.066	0.219
359.31	0.28	0.015	-0.01	0.217
360.27	0.252	0.016	0	0.212

E. OTHMER-TOBIAS CORRELATIONS

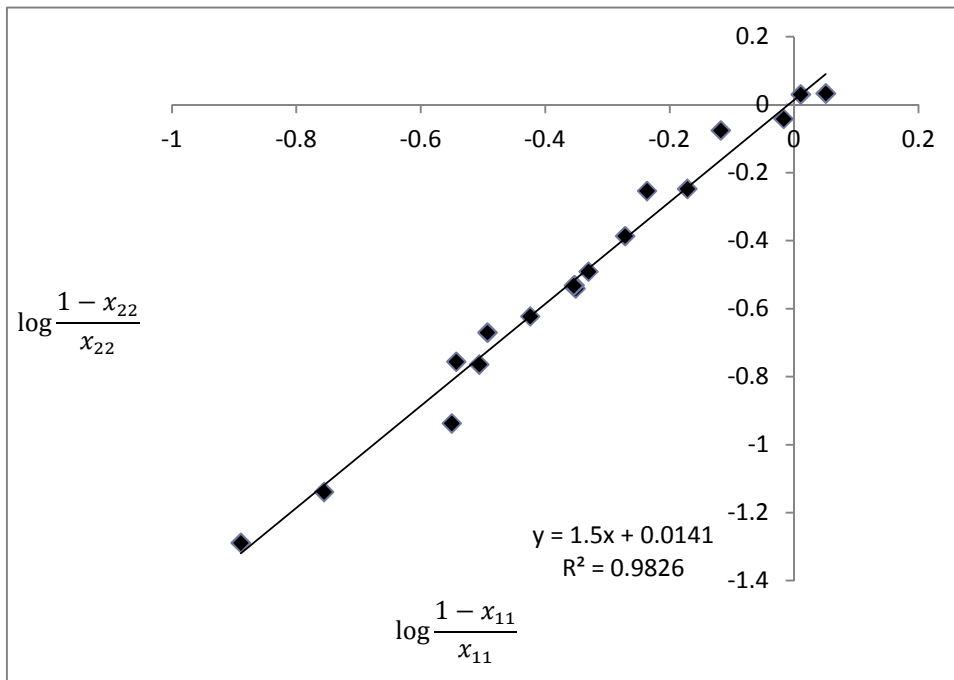


Figure E-1: Othmer-Tobias Correlation for Ethanol/DIPE/Water liquid phases

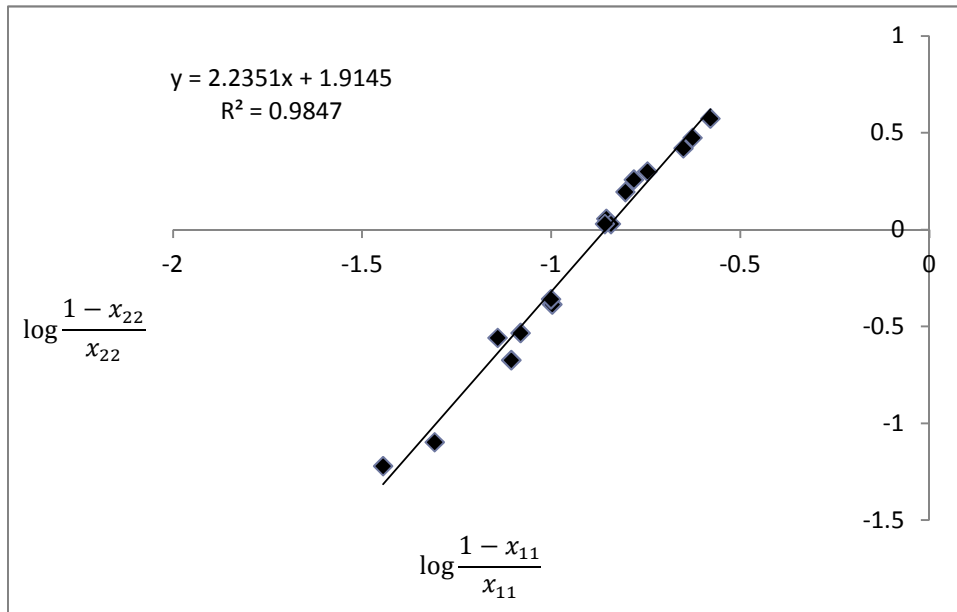


Figure E-2: Othmer-Tobias Correlation for n-Propanol/DIPE/Water liquid phases

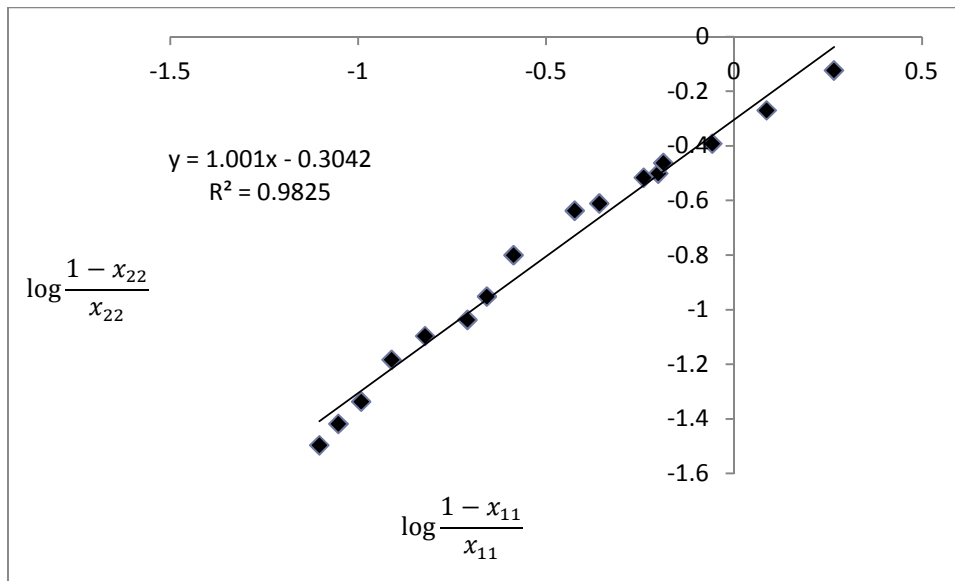


Figure E-3: Othmer-Tobias Correlation for n-Propanol/Isooctane/Water liquid phases

F. BUILT-IN ASPEN PARAMETERS*Table F-1: Aspen Plus NIST Wagner 25 Liquid Vapour Pressure Equation Parameters.*

Parameters	Components				
	Ethanol	Isooctane	n-Propanol	DIPE	Water
C ₁	-8.362345	-7.595284	-8.095994	-7.802337	-7.91302
C ₂	0.2131663	1.933648	0.9204644	2.085983	2.103149
C ₃	-3.486578	-2.709663	-6.592563	-2.925522	-2.676236
C ₄	-0.4440908	-2.746997	1.457953	-3.66026	-1.544579
lnP _{ci}	15.64879	14.7586	15.44415	14.86236	16.91285
T _{ci}	514.7877	543.9092	536.7353	500.1721	647.3084
T _{lower}	127.5	165.786	148.753	187.782	273.16
T _{upper}	514.7877	543.9092	536.7353	500.1721	647.3084

$$\ln p_i^{*,l} \left[\frac{N}{m^2} \right] = \ln p_{ci} + (C_{1i}(1 - T_{ri}) + C_{2i}(1 - T_{ri})^{1.5} + C_{3i}(1 - T_{ri})^{2.5} + C_{4i}(1 - T_{ri})^5) / T_{ri}$$

For $T_{lower} \leq T \leq T_{upper}$ [K]

Where $T_{ri} = T/T_{ci}$

Table F-2: Aspen UNIFAC groups used in this work.

Group number	Description
1300	Water
1605	Ether
1200	Primary alcohol
1015	CH3
3000	P1

Table F-3: Built-in Aspen parameters for NRTL.

Component i Component j	Ethanol n-Propanol	Ethanol Water	Ethanol DIPE	Ethanol Isooctane	n-Propanol Water	n-Propanol DIPE	n-Propanol Isooctane	Water DIPE	Water Isooctane
Temperature units	K	K	K	K	K	K	K	K	K
Source	APV73 VLE-IG	APV73 VLE-IG	APV73 VLE-IG	APV73 VLE-IG	APV73 VLE-IG	APV73 VLE-IG	APV73 VLE-IG	APV73 LLE-ASPEN	APV73 LLE-ASPEN
Property units:									
aij	8.2606	-0.8009	0	0	-1.7411	0	0	8.0209	13.6508329
aji	-9.721	3.4578	0	0	5.4486	0	0	0.035	-7.35503268
bij	-2846.6829	246.18	285.113	525.4371	576.4458	244.2234	294.2462	-766.4165	-142.098998
bji	3409.6863	-586.0809	231.8151	745.3775	-861.1792	202.4844	511.3716	422.9778	4167.6657
cij	0.3	0.3	0.3	0.47	0.3	0.3	0.3	0.2	0.2
dij	0	0	0	0	0	0	0	0	0
eij	0	0	0	0	0	0	0	0	0
ejj	0	0	0	0	0	0	0	0	0
fij	0	0	0	0	0	0	0	0	0
fji	0	0	0	0	0	0	0	0	0
Tlower	313.15	298.14	333.65	298.15	298.15	337.85	328.37	293.15	273.15
Tupper	370.31	373.15	341.75	323.15	373.15	356.15	348.52	333.15	323.15

G. DATA FROM LITERATURE FOR REGRESSIONS*Table G-1: Isobaric phase equilibrium data at 101.3 kPa, used from literature and this work, for parameter regressions.*

Components	Data type	Set No.	Source
ethanol/water	VLE	1	Kojima et al. (1968)
		2	Kojima et al. (1969)
		3	Zemp and Francesconi (1992)
		4	Kurihara et al. (1993)
		5	Arce et al. (1996)
n-propanol/water	VLE	6	Kojima et al. (1968)
		7	Smirvo (1959)
		8	Dawe and Newsham (1973)
ethanol/DIPE	VLE	9	Benito and Lopez (1992)
n-propanol/DIPE		10	Benito and Lopez (1992)
n-propanol/isooctane		11	Hiaki et al. (1994)
DIPE/water	VLE	12	Yorizane et al. (1967)
		13	Hunsmann and Simmrock (1966)
DIPE/water	LLE	14	Krupatkin and Bodin (1947)
		15	Hlavaty and Linek (1973)
		16	Hwang et al.(2008)
isooctane/water	LLE	17	Maczynski et al. (2004)
	LLE	18	Arce et al. (2002)
ethanol/DIPE/water	LLE	19	Hwang et al. (2008)
	VLE	20	
	Organic VLE (VLLE)	21	
	Aqueous VLE (VLLE)	22	This work
	LLE (VLLE)	23	
	Ternary Azeotrope	24	
n-propanol/DIPE/water	LLE	25	Ghanadzadeha and Ghanadzadeha (2009)
	LLE	26	Hwang et al. (2008)
	LLE	27	Wang et al. (2011)
	VLE	28	
	Organic VLE (VLLE)	29	This work
Aqueous VLE (VLLE)	30		
LLE (VLLE)	31		
n-propanol/isooctane/water	LLE	32	Wang et al. (2011)
	VLE	33	
	Organic VLE (VLLE)	34	
	Aqueous VLE (VLLE)	35	This work
	LLE (VLLE)	36	
Ternary Azeotrope	37		

Table G-2: Weighting of data from Table G-1, used in parameter regressions.

Set No.	Ethanol/DIPE/Water				n-Propanol/DIPE/Water				n-Propanol/Isooctane/Water			
	NRTL	UNIQUAC	UNIFAC	UNIFAC LLE	NRTL	UNIQUAC	UNIFAC	UNIFAC LLE	NRTL	UNIQUAC	UNIFAC	UNIFAC LLE
1												
2	1		1	1								
3												
4												
5		1		1								
6												1
7						1						1
8					1	1		1	5	1	1	1
9	1	1	2	2								
10					5	5	10	11				
11									5		0.5	2
12							0.5					
13												
14		1		1	1	1	1	1				
15												
16	0.9		0.5									
17									1	1	1	1
18												
19												
20												
21	1	2	2	3								
22			1									
23	1.2	5	5	5								
24		3										
25												
26												
27												
28					1		1	1				
29							1					
30							1					
31					1	3	10	5				
32												
33												
34									3	3	1	10
35										3	1	1
36									8	3	10	5
37										1		

H. REGRESSED PARAMETERS*Table H-1: NRTL Model Parameters of the Water (1) + DIPE (2) + Ethanol (3) ternary mixture.*

i, j	A _{ij}	A _{ji}	B _{ij}	B _{ji}	C _{ij}
1, 2	5.43	-8.58	3166.61	68.94	0.018
1, 3	-2.76	-5.14	1549.35	2063.90	0.783
2, 3	-4.19	-1.70	3058.67	-882.89	-0.037

Table H-2: UNIQUAC Model Parameters of the Water (1) + DIPE (2) + Ethanol (3) ternary mixture.

i, j	A _{ij}	A _{ji}	B _{ij}	B _{ji}
1, 2	-1.06	-0.47	205.64	-451.87
1, 3	-0.60	2.87	253.03	-1252.70
2, 3	28.89	-20.81	-10000.00	7046.36

Table H-3: UNIFAC (vapour-liquid equilibrium calculations) Model Parameters of the Water (1) + DIPE (2) + Ethanol (3) ternary mixture.

Functional Group	G1	G2	G3
G1	112.05	-540.44	-191.11
G2	1280.62	8352.31	-87.59
G3	382.49	308.66	-15.13

G1: Group number for water

G2: Group number for >CH-O- (ether)

G3: Group number for -OH (primary alcohol)

Table H-4: UNIFAC (liquid-liquid equilibrium calculations) Model Parameters of the Water (1) + DIPE (2) + Ethanol (3) ternary mixture.

Functional Group	G1	G2	G3
G1	74.99	-569.74	-724.03
G2	14498.00	-252.54	22.16
G3	14498.00	-396.72	-358.18

G1: Group number for water

G2: Group number for >CH-O- (ether)

G3: Group number for -OH (primary alcohol)

Table H-5: NRTL Model Parameters of the Water (1) + DIPE (2) + n-Propanol (3) ternary mixture.

i, j	A _{ij}	A _{ji}	B _{ij}	B _{ji}	C _{ij}
1, 2	12.79	-3.77	-1534.89	817.44	0.078
1, 3	4.68	-1.36	-726.32	727.43	0.490
2, 3	10.77	-12.94	-3578.69	4662.83	-0.299

Table H-6: UNIQUAC Model Parameters of the Water (1) + DIPE (2) + n-Propanol (3) ternary mixture.

i, j	A _{ij}	A _{ji}	B _{ij}	B _{ji}
1, 2	-1.11	-0.29	220.73	-505.39
1, 3	0.09	-1.13	-297.36	403.12
2, 3	6.67	-3.95	-2605.41	1475.09

Table H-7: UNIFAC (vapour-liquid equilibrium calculations) Model Parameters of the Water (1) + DIPE (2) + n-Propanol (3) ternary mixture.

Functional Group	G1	G2	G3
G1	187.84	-562.75	-2165.07
G2	1317.04	9996.80	-2008.30
G3	551.61	0.00	-1972.51

G1: Group number for water

G2: Group number for >CH-O- (ether)

G3: Group number for -OH (primary alcohol)

Table H-8: UNIFAC (liquid-liquid equilibrium calculations) Model Parameters of the Water (1) + DIPE (2) + n-Propanol (3) ternary mixture.

Functional Group	G1	G2	G3
G1	32.05	-570.06	-2047.18
G2	1271.14	-252.54	1615.56
G3	200.53	-827.65	-2157.85

G1: Group number for water

G2: Group number for >CH-O- (ether)

G3: Special group number for n-Propanol

Table H-9: NRTL Model Parameters of the Water (1) + Isooctane (2) + n-Propanol (3) ternary mixture.

i, j	A _{ij}	A _{ji}	B _{ij}	B _{ji}	C _{ij}
1, 2	-6.40	4.95	1077.59	1197.54	-0.072
1, 3	12.15	10.22	-5966.13	-1960.98	-0.071
2, 3	6.74	6.12	-1190.28	-1567.63	0.660

Table H-10: UNIQUAC Model Parameters of the Water (1) + Isooctane (2) + n-Propanol (3) ternary mixture.

i, j	A _{ij}	A _{ji}	B _{ij}	B _{ji}
1, 2	4.76	7.58	-1853.99	-3454.91
1, 3	1.57	-0.76	-710.64	182.83
2, 3	0.49	-0.76	-575.28	370.68

Table H-11: NRTL Model Parameters of the Water + Ethanol + Benzene mixture, regressed by Christo Crause (2011).

Component i Component j Temperature units Parameters:	WATER ETHANOL C	WATER BENZENE C	ETHANOL BENZENE C
aij	0.08905	0.49132	-0.11046
aji	5.68039	-1.00517	0.15438
bij	102.981	1980.909	408.146
bji	-894.595	1770.413	410.987
cij	0.3	0.28546	0.501486
dij	0	0	0
eij	0	0	0
eji	0	0	0
fij	0.0044966	0	0
fji	-0.0094041	0	0
Tlower	0	0	0
Tupper	1000	1000	1000

I. DETAILED SIMULATION RESULTS

Table I-1: Stream results for the dehydration of ethanol via heterogeneous azeotropic distillation with DIPE as entrainer. The simulation was performed with Aspen using NRTL with built-in Aspen parameters.

Streams	AQUEOUS	B1	B2	D1	D2	FF	MAKEUP	ORGANIC
Mole Flow kmol/sec								
ETHANOL	0.0025	0.0139	0.0000	0.0273	0.0025	0.0139	0.0000	0.0248
DIPE	0.0003	0.0003	0.0000	0.1138	0.0003	0.0000	0.0003	0.1138
H2O	0.0161	0.0000	0.0139	0.0317	0.0022	0.0139	0.0000	0.0156
Mole Frac								
ETHANOL	0.1314	0.9800	0.0000	0.1579	0.5007	0.5000	0.0000	0.1608
DIPE	0.0138	0.0195	0.0000	0.6587	0.0527	0.0000	1.0000	0.7381
H2O	0.8548	0.0005	1.0000	0.1834	0.4466	0.5000	0.0000	0.1010
Total Flow kmol/sec	0.0188	0.0142	0.0139	0.1727	0.0049	0.0278	0.0003	0.1542
Total Flow kg/sec	0.4305	0.6689	0.2502	13.4506	0.1803	0.8901	0.0315	13.0516
Total Flow cum/sec	0.0005	0.0009	0.0003	4.7390	0.0002	0.0010	0.0000	0.0179
Temperature K	313.57	349.51	373.17	334.41	342.83	298.15	313.00	313.56
Pressure N/sqm	101325	101325	101325	101325	101325	101325	101325	101325
Vapor Frac	0	0	0	1	0	0	0	0
Liquid Frac	1	1	1	0	1	1	1	1
Solid Frac	0	0	0	0	0	0	0	0
Enthalpy J/kmol	-284400277	-271741670	-280077310	-287161830	-279847307	-281769936	-347945343	-329182077
Enthalpy J/kg	-12438768	-5763777.3	-15546529	-3687124.7	-7668058.2	-8793724.8	-3405334.3	-3888750.5
Enthalpy Watt	-5354982.8	-3855408.7	-3889937.7	-49593970	-1382511.5	-7826942.7	-107375.93	-50754435
Entropy J/kmol-K	-189328.44	-331789.23	-146101.87	-451495.84	-265607.38	-251938.12	-735212.94	-608602.26
Entropy J/kg-K	-8280.63	-7037.42	-8109.82	-5797.15	-7277.87	-7862.71	-7195.51	-7189.65
Density kmol/cum	39.57	15.57	50.97	0.04	21.33	26.46	6.90	8.62
Density kg/cum	904.64	734.14	918.27	2.84	778.36	847.93	705.07	730.10
Average MW	22.86	47.15	18.02	77.88	36.50	32.04	102.18	84.65
Liq Vol 60F cum/sec	0.0005	0.0008	0.0003	0.0183	0.0002	0.0011	0.0000	0.0179

Table I-2: Azeotropic column information for the dehydration of ethanol via heterogeneous azeotropic distillation with DIPE as entrainer. The simulation was performed with Aspen using NRTL with built-in Aspen parameters.

Stage	Temperature K	Pressure N/sqm	Heat duty Watt	Vapour (mole fraction)			1 st Liquid (mole fraction)			2 nd Liquid (mole fraction)		
				ETHANOL	DIPE	H2O	ETHANOL	DIPE	H2O	ETHANOL	DIPE	H2O
1	334.41	101325	-6407250	0.1579	0.6587	0.1834	0.1699	0.7225	0.1077	0.1699	0.7225	0.1077
2	334.45	101325	0	0.1663	0.6531	0.1807	0.1852	0.7017	0.1131	0.1852	0.7017	0.1131
3	334.47	101325	0	0.1801	0.6339	0.1860	0.1743	0.0255	0.8002	0.2343	0.6053	0.1604
4	334.46	101325	0	0.1792	0.6347	0.1861	0.1720	0.0250	0.8030	0.2317	0.6099	0.1583
5	334.44	101325	0	0.1763	0.6373	0.1864	0.1642	0.0233	0.8126	0.2229	0.6255	0.1516
6	334.30	101325	0	0.1650	0.6359	0.1991	0.2199	0.5944	0.1857	0.2199	0.5944	0.1857
7	334.30	101325	0	0.1651	0.6359	0.1990	0.2200	0.5944	0.1856	0.2200	0.5944	0.1856
8	334.31	101325	0	0.1652	0.6359	0.1990	0.2201	0.5944	0.1855	0.2201	0.5944	0.1855
9	334.31	101325	0	0.1653	0.6358	0.1989	0.2203	0.5943	0.1854	0.2203	0.5943	0.1854
10	334.31	101325	0	0.1655	0.6358	0.1987	0.2206	0.5942	0.1852	0.2206	0.5942	0.1852
11	334.31	101325	0	0.1658	0.6357	0.1985	0.2210	0.5941	0.1849	0.2210	0.5941	0.1849
12	334.32	101325	0	0.1662	0.6356	0.1982	0.2215	0.5940	0.1845	0.2215	0.5940	0.1845
13	334.32	101325	0	0.1668	0.6354	0.1978	0.2223	0.5938	0.1840	0.2223	0.5938	0.1840
14	334.33	101325	0	0.1676	0.6352	0.1972	0.2234	0.5935	0.1832	0.2234	0.5935	0.1832
15	334.34	101325	0	0.1688	0.6349	0.1963	0.2249	0.5931	0.1820	0.2249	0.5931	0.1820
16	334.36	101325	0	0.1704	0.6345	0.1951	0.2272	0.5925	0.1804	0.2272	0.5925	0.1804
17	334.39	101325	0	0.1728	0.6338	0.1933	0.2303	0.5917	0.1780	0.2303	0.5917	0.1780
18	334.43	101325	0	0.1762	0.6330	0.1908	0.2348	0.5906	0.1746	0.2348	0.5906	0.1746
19	334.48	101325	0	0.1810	0.6318	0.1872	0.2410	0.5892	0.1698	0.2410	0.5892	0.1698
20	334.55	101325	0	0.1877	0.6304	0.1820	0.2495	0.5876	0.1630	0.2495	0.5876	0.1630
21	334.66	101325	0	0.1968	0.6286	0.1747	0.2608	0.5857	0.1535	0.2608	0.5857	0.1535
22	334.80	101325	0	0.2089	0.6266	0.1645	0.2753	0.5840	0.1406	0.2753	0.5840	0.1406
23	334.99	101325	0	0.2246	0.6247	0.1507	0.2930	0.5830	0.1240	0.2930	0.5830	0.1240
24	335.24	101325	0	0.2435	0.6235	0.1329	0.3128	0.5831	0.1041	0.3128	0.5831	0.1041
25	335.53	101325	0	0.2649	0.6236	0.1115	0.3331	0.5845	0.0824	0.3331	0.5845	0.0824
26	335.85	101325	0	0.2868	0.6249	0.0883	0.3518	0.5868	0.0614	0.3518	0.5868	0.0614
27	336.16	101325	0	0.3069	0.6273	0.0658	0.3673	0.5894	0.0433	0.3673	0.5894	0.0433
28	336.43	101325	0	0.3237	0.6299	0.0464	0.3791	0.5917	0.0292	0.3791	0.5917	0.0292
29	336.64	101325	0	0.3364	0.6323	0.0312	0.3875	0.5935	0.0190	0.3875	0.5935	0.0190

Table I-3: Azeotropic column information (continued) for the dehydration of ethanol via heterogeneous azeotropic distillation with DIPE as entrainer. The simulation was performed with Aspen using NRTL with built-in Aspen parameters.

Stage	Temperature	Pressure	Heat duty	Vapour (mole fraction)			1 st Liquid (mole fraction)			2 nd Liquid (mole fraction)		
	K	N/sqm	Watt	ETHANOL	DIPE	H2O	ETHANOL	DIPE	H2O	ETHANOL	DIPE	H2O
30	336.79	101325	0	0.3455	0.6342	0.0203	0.3931	0.5948	0.0121	0.3931	0.5948	0.0121
31	336.89	101325	0	0.3516	0.6355	0.0129	0.3969	0.5956	0.0076	0.3969	0.5956	0.0076
32	336.96	101325	0	0.3557	0.6363	0.0081	0.3995	0.5959	0.0047	0.3995	0.5959	0.0047
33	337.00	101325	0	0.3585	0.6366	0.0050	0.4018	0.5953	0.0029	0.4018	0.5953	0.0029
34	337.04	101325	0	0.3609	0.6360	0.0030	0.4053	0.5929	0.0018	0.4053	0.5929	0.0018
35	337.07	101325	0	0.3647	0.6335	0.0018	0.4138	0.5851	0.0011	0.4138	0.5851	0.0011
36	337.13	101325	0	0.3737	0.6252	0.0011	0.4391	0.5602	0.0007	0.4391	0.5602	0.0007
37	337.41	101325	0	0.4005	0.5988	0.0007	0.5200	0.4795	0.0005	0.5200	0.4795	0.0005
38	339.11	101325	0	0.4861	0.5134	0.0005	0.7241	0.2754	0.0005	0.7241	0.2754	0.0005
39	344.72	101325	0	0.7038	0.2957	0.0005	0.9132	0.0863	0.0006	0.9132	0.0863	0.0006
40	349.51	101325	6544238.41	0.9076	0.0919	0.0006	0.9800	0.0195	0.0005	0.9800	0.0195	0.0005

Table I-4: Recovery column information for the dehydration of ethanol via heterogeneous azeotropic distillation with DIPE as entrainer. The simulation was performed with Aspen using NRTL with built-in Aspen parameters.

Stage	Temperature	Pressure	Heat duty	Vapour (mole fraction)			Liquid (mole fraction)		
	K	N/sqm	Watt	ETHANOL	DIPE	H2O	ETHANOL	DIPE	H2O
1	342.83	101325	-1917466.3	0.4040	0.3726	0.2235	0.5007	0.0527	0.4466
2	355.12	101325	0	0.5007	0.0527	0.4466	0.1835	0.0009	0.8156
3	366.85	101325	0	0.2176	0.0065	0.7759	0.0253	0.0000	0.9746
4	370.99	101325	0	0.0759	0.0056	0.9185	0.0068	0.0000	0.9932
5	371.45	101325	0	0.0590	0.0056	0.9355	0.0051	0.0000	0.9949
6	371.49	101325	0	0.0574	0.0056	0.9370	0.0050	0.0000	0.9950
7	371.49	101325	0	0.0573	0.0056	0.9371	0.0050	0.0000	0.9950
8	371.49	101325	0	0.0573	0.0056	0.9371	0.0050	0.0000	0.9950
9	371.49	101325	0	0.0573	0.0056	0.9371	0.0050	0.0000	0.9950
10	373.00	101325	0	0.0064	0.0000	0.9936	0.0005	0.0000	0.9995
11	373.15	101325	0	0.0007	0.0000	0.9993	0.0001	0.0000	0.9999
12	373.17	101325	2000000	0.0001	0.0000	0.9999	0.0000	0.0000	1.0000

Table I-5: Stream results for the dehydration of ethanol via heterogeneous azeotropic distillation with DIPE as entrainer. The simulation was performed with Aspen using NRTL with parameters regressed in this work.

STREAMS	AQUEOUS	B1	B2	D1	D2	FEED	MAKEUP	ORGANIC
Mole Flow kmol/sec								
ETHANOL	0.0009	0.0133	0.0000	0.0207	0.0009	0.0139	0.0000	0.0198
DIPE	0.0000	0.0002	0.0000	0.0935	0.0000	0.0000	0.0012	0.0947
H2O	0.0136	0.0001	0.0135	0.0266	0.0001	0.0139	0.0000	0.0130
Mole Frac								
ETHANOL	0.0628	0.9800	0.0001	0.1472	0.8525	0.5000	0.0000	0.1554
DIPE	0.0015	0.0111	0.0000	0.6638	0.0198	0.0000	1.0000	0.7427
H2O	0.9357	0.0089	0.9999	0.1890	0.1277	0.5000	0.0000	0.1019
Total Flow kmol/sec	0.0146	0.0136	0.0135	0.1409	0.0011	0.0278	0.0012	0.1275
Total Flow kg/sec	0.2900	0.6310	0.2432	10.9936	0.0468	0.8901	0.1226	10.8262
Total Flow cum/sec	0.0003	0.0009	0.0003	3.8772	0.0001	0.0010	0.0002	0.0148
Temperature K	314.032378	349.836505	373.14517	335.311422	348.718561	298.15	313	314.01011
Pressure N/sqm	101325	101325	101325	101325	101325	101325	101325	101325
Vapor Frac	0	0	0	1	0	0	0	0
Liquid Frac	1	1	1	0	1	1	1	1
Solid Frac	0	0	0	0	0	0	0	0
Enthalpy J/kmol	-284137132	-271374372	-280079558	-287503626	-273511416	-281643461	-347945343	-329812625
Enthalpy J/kg	-14277877	-5843731.1	-15544724	-3685253	-6273240.6	-8789777.6	-3405334.3	-3885554.3
Enthalpy Watt	-4140602.7	-3687513.6	-3781074	-40514231	-293354.76	-7823429.5	-417534.41	-42065865
Entropy J/kmol-K	-170158.66	-327318.25	-146118.42	-452368.07	-308293.31	-251306.33	-735212.94	-610857.82
Entropy J/kg-K	-8550.46	-7048.42	-8109.73	-5798.50	-7071.00	-7842.99	-7195.51	-7196.57
Density kmol/cum	47.40	15.83	50.96	0.04	17.07	26.46	6.90	8.59
Density kg/cum	943.23	735.09	918.24	2.84	744.37	847.93	705.07	729.28
Average MW	19.90	46.44	18.02	78.01	43.60	32.04	102.18	84.88
Liq Vol 60F cum/sec	0.0003	0.0008	0.0002	0.0149	0.0001	0.0011	0.0002	0.0148

Table I-6: Azeotropic column information for the dehydration of ethanol via heterogeneous azeotropic distillation with DIPE as entrainer. The simulation was performed with Aspen using NRTL with parameters regressed in this work.

Stage	Temperature K	Pressure N/sqm	Heat duty Watt	Vapour (mole fraction)			1 st Liquid (mole fraction)			2 nd Liquid (mole fraction)		
				ETHANOL	DIPE	H2O	ETHANOL	DIPE	H2O	ETHANOL	DIPE	H2O
1	335.31	101325	-5273490	0.1472	0.6638	0.1890	0.1688	0.7239	0.1073	0.1688	0.7239	0.1073
2	335.40	101325	0	0.1611	0.6537	0.1852	0.1929	0.6915	0.1156	0.1929	0.6915	0.1156
3	335.51	101325	0	0.1827	0.6237	0.1935	0.2596	0.5751	0.1653	0.2596	0.5751	0.1653
4	335.73	101325	0	0.1980	0.6233	0.1787	0.2733	0.5746	0.1521	0.2733	0.5746	0.1521
5	335.93	101325	0	0.2128	0.6228	0.1644	0.2864	0.5740	0.1396	0.2864	0.5740	0.1396
6	336.11	101325	0	0.2270	0.6222	0.1508	0.2987	0.5734	0.1278	0.2987	0.5734	0.1278
7	336.26	101325	0	0.2404	0.6216	0.1380	0.3103	0.5728	0.1169	0.3103	0.5728	0.1169
8	336.41	101325	0	0.2530	0.6209	0.1261	0.3211	0.5721	0.1068	0.3211	0.5721	0.1068
9	336.53	101325	0	0.2647	0.6202	0.1152	0.3311	0.5715	0.0975	0.3311	0.5715	0.0975
10	336.64	101325	0	0.2755	0.6195	0.1050	0.3403	0.5708	0.0889	0.3403	0.5708	0.0889
11	336.74	101325	0	0.2854	0.6188	0.0958	0.3487	0.5702	0.0811	0.3487	0.5702	0.0811
12	336.83	101325	0	0.2945	0.6182	0.0873	0.3564	0.5696	0.0739	0.3564	0.5696	0.0739
13	336.91	101325	0	0.3029	0.6176	0.0795	0.3635	0.5691	0.0674	0.3635	0.5691	0.0674
14	336.97	101325	0	0.3106	0.6170	0.0724	0.3700	0.5686	0.0614	0.3700	0.5686	0.0614
15	337.04	101325	0	0.3176	0.6164	0.0659	0.3759	0.5681	0.0560	0.3759	0.5681	0.0560
16	337.09	101325	0	0.3241	0.6159	0.0600	0.3814	0.5677	0.0510	0.3814	0.5677	0.0510
17	337.14	101325	0	0.3300	0.6155	0.0546	0.3864	0.5672	0.0464	0.3864	0.5672	0.0464
18	337.18	101325	0	0.3354	0.6150	0.0496	0.3910	0.5668	0.0422	0.3910	0.5668	0.0422
19	337.22	101325	0	0.3404	0.6146	0.0450	0.3952	0.5665	0.0383	0.3952	0.5665	0.0383
20	337.26	101325	0	0.3449	0.6142	0.0408	0.3991	0.5662	0.0348	0.3991	0.5662	0.0348
21	337.29	101325	0	0.3491	0.6139	0.0370	0.4026	0.5658	0.0315	0.4026	0.5658	0.0315
22	337.32	101325	0	0.3530	0.6136	0.0335	0.4059	0.5656	0.0285	0.4059	0.5656	0.0285
23	337.35	101325	0	0.3565	0.6133	0.0302	0.4089	0.5653	0.0258	0.4089	0.5653	0.0258
24	337.37	101325	0	0.3598	0.6130	0.0272	0.4117	0.5650	0.0232	0.4117	0.5650	0.0232
25	337.40	101325	0	0.3628	0.6127	0.0245	0.4143	0.5648	0.0209	0.4143	0.5648	0.0209
26	337.42	101325	0	0.3656	0.6125	0.0219	0.4167	0.5646	0.0187	0.4167	0.5646	0.0187
27	337.44	101325	0	0.3682	0.6122	0.0196	0.4189	0.5644	0.0167	0.4189	0.5644	0.0167
28	337.45	101325	0	0.3706	0.6120	0.0174	0.4209	0.5642	0.0149	0.4209	0.5642	0.0149
29	337.47	101325	0	0.3728	0.6118	0.0154	0.4228	0.5640	0.0131	0.4228	0.5640	0.0131

Table I-7: Azeotropic column information (continued) for the dehydration of ethanol via heterogeneous azeotropic distillation with DIPE as entrainer. The simulation was performed with Aspen using NRTL with parameters regressed in this work.

Stage	Temperature	Pressure	Heat duty	Vapour (mole fraction)			1 st Liquid (mole fraction)			2 nd Liquid (mole fraction)		
	K	N/sqm	Watt	ETHANOL	DIPE	H2O	ETHANOL	DIPE	H2O	ETHANOL	DIPE	H2O
30	337.48	101325	0	0.3749	0.6116	0.0135	0.4246	0.5638	0.0116	0.4246	0.5638	0.0116
31	337.50	101325	0	0.3768	0.6114	0.0118	0.4264	0.5635	0.0101	0.4264	0.5635	0.0101
32	337.51	101325	0	0.3787	0.6111	0.0102	0.4283	0.5629	0.0087	0.4283	0.5629	0.0087
33	337.52	101325	0	0.3808	0.6105	0.0087	0.4309	0.5616	0.0075	0.4309	0.5616	0.0075
34	337.54	101325	0	0.3835	0.6091	0.0074	0.4353	0.5583	0.0064	0.4353	0.5583	0.0064
35	337.57	101325	0	0.3882	0.6056	0.0062	0.4450	0.5495	0.0054	0.4450	0.5495	0.0054
36	337.64	101325	0	0.3987	0.5962	0.0051	0.4702	0.5250	0.0048	0.4702	0.5250	0.0048
37	337.91	101325	0	0.4256	0.5700	0.0044	0.5425	0.4528	0.0047	0.5425	0.4528	0.0047
38	339.30	101325	0	0.5030	0.4927	0.0043	0.7342	0.2599	0.0059	0.7342	0.2599	0.0059
39	344.67	101325	0	0.7104	0.2840	0.0056	0.9247	0.0675	0.0077	0.9247	0.0675	0.0077
40	349.84	101325	5412518.59	0.9192	0.0732	0.0076	0.9800	0.0111	0.0089	0.9800	0.0111	0.0089

Table I-8: Recovery column information for the dehydration of ethanol via heterogeneous azeotropic distillation with DIPE as entrainer. The simulation was performed with Aspen using NRTL with parameters regressed in this work.

Stage	Temperature	Pressure	Heat duty	Vapour (mole fraction)			Liquid (mole fraction)		
	K	N/sqm	Watt	ETHANOL	DIPE	H2O	ETHANOL	DIPE	H2O
1	348.72	101325	-1933826.3	0.7670	0.1346	0.0984	0.8525	0.0198	0.1277
2	351.51	101325	0	0.8525	0.0198	0.1277	0.8452	0.0023	0.1525
3	352.01	101325	0	0.8453	0.0027	0.1520	0.8184	0.0003	0.1813
4	352.23	101325	0	0.8192	0.0007	0.1801	0.7820	0.0001	0.2179
5	352.49	101325	0	0.7836	0.0005	0.2159	0.7331	0.0000	0.2669
6	352.89	101325	0	0.7357	0.0005	0.2638	0.6631	0.0000	0.3369
7	353.66	101325	0	0.6673	0.0005	0.3322	0.5517	0.0000	0.4482
8	355.66	101325	0	0.5584	0.0005	0.4411	0.3139	0.0000	0.6861
9	363.68	101325	0	0.3261	0.0005	0.6734	0.0462	0.0000	0.9538
10	371.63	101325	0	0.0593	0.0000	0.9407	0.0059	0.0000	0.9941
11	372.98	101325	0	0.0075	0.0000	0.9925	0.0007	0.0000	0.9993
12	373.15	101325	2000000	0.0009	0.0000	0.9991	0.0001	0.0000	0.9999

Table I-9: Stream results for the dehydration of ethanol via heterogeneous azeotropic distillation with benzene as entrainer. The simulation was performed with Aspen using NRTL with parameters supplied by Christo Crause (2011).

STREAMS	AQUEOUS	B1	B2	D1	D2	FEED	MAKE-UP	ORGANIC
Mole Flow kmol/sec								
BENZENE	0.0008	0.0000	0.0000	0.1198	0.0008	0.0000	0.0095	0.1284
ETHANOL	0.0124	0.0096	0.0000	0.0561	0.0124	0.0139	0.0000	0.0438
H2O	0.0296	0.0002	0.0135	0.0470	0.0161	0.0139	0.0000	0.0174
Mole Frac								
BENZENE	0.0196	0.0030	0.0000	0.5374	0.0287	0.0000	1.0000	0.6775
ETHANOL	0.2893	0.9800	0.0000	0.2519	0.4225	0.5000	0.0000	0.2308
H2O	0.6911	0.0170	1.0000	0.2107	0.5488	0.5000	0.0000	0.0917
Total Flow kmol/sec	0.0428	0.0098	0.0135	0.2229	0.0293	0.0278	0.0095	0.1895
Total Flow kg/sec	1.1691	0.4473	0.2432	12.7866	0.9259	0.8901	0.7421	12.3596
Total Flow cum/sec	0.0013	0.0006	0.0003	6.1732	0.0011	0.0010	0.0009	0.0143
Temperature K	311.85531	351.081992	373.15531	337.589396	342.273695	298.15	313	311.72302
Pressure N/sqm	101325	101325	101325	101325	101325	101325	101325	101325
Vapor Frac	0	0	0	1	0	0	0	0
Liquid Frac	1	1	1	0	1	1	1	1
Solid Frac	0	0	0	0	0	0	0	0
Enthalpy J/kmol	-275785623	-269405615	-280077780	-62769386	-268051767	-282016863	51135882.8	-54852409
Enthalpy J/kg	-10098281	-5896335.7	-15545808	-1093970.8	-8485072	-8801431.1	654634.489	-841194.05
Enthalpy Watt	-11806137	-2637224	-3781050	-13988203	-7856358.2	-7833801.8	485790.887	-10396814
Entropy J/kmol-K	-211768.26	-320530.06	-146107.08	-132941.14	-225542.69	-252763.8	-246098.06	-257069.11
Entropy J/kg-K	-7754.19	-7015.27	-8109.72	-2316.95	-7139.46	-7888.48	-3150.51	-3942.31
Density kmol/cum	31.96	16.10	50.97	0.04	25.68	26.46	10.97	13.22
Density kg/cum	872.90	735.66	918.26	2.07	811.10	847.93	857.09	862.18
Average MW	27.31	45.69	18.02	57.38	31.59	32.04	78.11	65.21
Liq Vol 60F cum/sec	0.0013	0.0006	0.0002	0.0147	0.0011	0.0011	0.0008	0.0142

Table I-10: Azeotropic column information for the dehydration of ethanol via heterogeneous azeotropic distillation with benzene as entrainer. The simulation was performed with Aspen using NRTL with parameters supplied by Christo Crause (2011).

Stage	Temperature	Pressure	Heat duty	Vapour (mole fraction)			1 st Liquid (mole fraction)			2 nd Liquid (mole fraction)		
	K	N/sqm	Watt	BENZENE	ETHANOL	H2O	BENZENE	ETHANOL	H2O	BENZENE	ETHANOL	H2O
1	337.59	101325	8702190	0.5374	0.2519	0.2107	0.0142	0.2440	0.7418	0.7382	0.1993	0.0625
2	337.84	101325	0	0.5531	0.2279	0.2191	0.0058	0.1613	0.8329	0.8414	0.1274	0.0312
3	336.83	101325	0	0.5597	0.1723	0.2680	0.5383	0.2034	0.2584	0.5383	0.2034	0.2584
4	336.83	101325	0	0.5597	0.1723	0.2680	0.5383	0.2034	0.2584	0.5383	0.2034	0.2584
5	336.83	101325	0	0.5597	0.1723	0.2680	0.5383	0.2034	0.2584	0.5383	0.2034	0.2584
6	336.83	101325	0	0.5597	0.1723	0.2680	0.5383	0.2034	0.2584	0.5383	0.2034	0.2584
7	336.83	101325	0	0.5597	0.1723	0.2680	0.5383	0.2034	0.2584	0.5383	0.2034	0.2584
8	336.83	101325	0	0.5597	0.1723	0.2680	0.5383	0.2034	0.2584	0.5383	0.2034	0.2584
9	336.83	101325	0	0.5597	0.1723	0.2680	0.5383	0.2034	0.2584	0.5383	0.2034	0.2584
10	336.83	101325	0	0.5597	0.1723	0.2680	0.5383	0.2034	0.2583	0.5383	0.2034	0.2583
11	336.83	101325	0	0.5597	0.1723	0.2680	0.5383	0.2034	0.2583	0.5383	0.2034	0.2583
12	336.83	101325	0	0.5597	0.1723	0.2680	0.5383	0.2034	0.2583	0.5383	0.2034	0.2583
13	336.83	101325	0	0.5597	0.1724	0.2680	0.5382	0.2034	0.2583	0.5382	0.2034	0.2583
14	336.83	101325	0	0.5596	0.1724	0.2680	0.5382	0.2035	0.2583	0.5382	0.2035	0.2583
15	336.83	101325	0	0.5596	0.1724	0.2679	0.5382	0.2036	0.2583	0.5382	0.2036	0.2583
16	336.83	101325	0	0.5596	0.1725	0.2679	0.5381	0.2036	0.2582	0.5381	0.2036	0.2582
17	336.83	101325	0	0.5596	0.1726	0.2679	0.5381	0.2038	0.2581	0.5381	0.2038	0.2581
18	336.83	101325	0	0.5595	0.1728	0.2678	0.5380	0.2040	0.2580	0.5380	0.2040	0.2580
19	336.84	101325	0	0.5594	0.1730	0.2676	0.5378	0.2044	0.2578	0.5378	0.2044	0.2578
20	336.84	101325	0	0.5592	0.1733	0.2674	0.5376	0.2049	0.2575	0.5376	0.2049	0.2575
21	336.84	101325	0	0.5590	0.1739	0.2671	0.5372	0.2057	0.2571	0.5372	0.2057	0.2571
22	336.84	101325	0	0.5586	0.1747	0.2667	0.5367	0.2069	0.2564	0.5367	0.2069	0.2564
23	336.85	101325	0	0.5580	0.1759	0.2660	0.5359	0.2087	0.2554	0.5359	0.2087	0.2554
24	336.86	101325	0	0.5572	0.1778	0.2650	0.5347	0.2114	0.2539	0.5347	0.2114	0.2539
25	336.88	101325	0	0.5560	0.1807	0.2634	0.5329	0.2156	0.2515	0.5329	0.2156	0.2515
26	336.91	101325	0	0.5541	0.1850	0.2609	0.5303	0.2219	0.2479	0.5303	0.2219	0.2479
27	336.95	101325	0	0.5514	0.1915	0.2571	0.5265	0.2314	0.2421	0.5265	0.2314	0.2421
28	337.02	101325	0	0.5474	0.2014	0.2511	0.5212	0.2456	0.2331	0.5212	0.2456	0.2331
29	337.13	101325	0	0.5419	0.2163	0.2418	0.5143	0.2667	0.2189	0.5143	0.2667	0.2189

Table I-11: Azeotropic column information (continued) for the dehydration of ethanol via heterogeneous azeotropic distillation with benzene as entrainer. The simulation was performed with Aspen using NRTL with parameters supplied by Christo Crause (2011).

Stage	Temperature K	Pressure N/sqm	Heat duty Watt	Vapour (mole fraction)			1 st Liquid (mole fraction)			2 nd Liquid (mole fraction)		
				BENZENE	ETHANOL	H2O	BENZENE	ETHANOL	H2O	BENZENE	ETHANOL	H2O
30	337.32	101325	0	0.5348	0.2382	0.2270	0.5066	0.2965	0.1968	0.5066	0.2965	0.1968
31	337.63	101325	0	0.5267	0.2693	0.2040	0.4999	0.3352	0.1648	0.4999	0.3352	0.1648
32	338.09	101325	0	0.5197	0.3096	0.1707	0.4962	0.3788	0.1249	0.4962	0.3788	0.1249
33	338.67	101325	0	0.5158	0.3550	0.1292	0.4954	0.4199	0.0847	0.4954	0.4199	0.0847
34	339.27	101325	0	0.5148	0.3978	0.0873	0.4943	0.4536	0.0522	0.4943	0.4536	0.0522
35	339.76	101325	0	0.5135	0.4329	0.0536	0.4830	0.4862	0.0308	0.4830	0.4862	0.0308
36	340.16	101325	0	0.5018	0.4669	0.0314	0.4249	0.5550	0.0201	0.4249	0.5550	0.0201
37	341.26	101325	0	0.4417	0.5381	0.0202	0.2484	0.7336	0.0180	0.2484	0.7336	0.0180
38	345.60	101325	0	0.2586	0.7233	0.0181	0.0747	0.9067	0.0186	0.0747	0.9067	0.0186
39	349.76	101325	0	0.0778	0.9035	0.0187	0.0158	0.9662	0.0181	0.0158	0.9662	0.0181
40	351.08	101325	8768904.59	0.0163	0.9655	0.0181	0.0030	0.9800	0.0170	0.0030	0.9800	0.0170

Table I-12: Recovery column information for the dehydration of ethanol via heterogeneous azeotropic distillation with benzene as entrainer. The simulation was performed with Aspen using NRTL with parameters supplied by Christo Crause (2011).

Stage	Temperature K	Pressure N/sqm	Heat duty Watt	Vapour			Liquid		
				BENZENE	ETHANOL	H2O	BENZENE	ETHANOL	H2O
1	342.27	101325	-1831275.2	0.3933	0.3666	0.2401	0.0287	0.4225	0.5488
2	358.95	101325	0	0.0287	0.4225	0.5488	0.0001	0.0887	0.9112
3	363.31	101325	0	0.0191	0.3111	0.6697	0.0000	0.0435	0.9565
4	363.83	101325	0	0.0191	0.2957	0.6852	0.0000	0.0397	0.9603
5	363.88	101325	0	0.0191	0.2944	0.6865	0.0000	0.0394	0.9606
6	363.88	101325	0	0.0191	0.2943	0.6867	0.0000	0.0393	0.9607
7	363.88	101325	0	0.0191	0.2943	0.6867	0.0000	0.0393	0.9607
8	363.88	101325	0	0.0191	0.2943	0.6867	0.0000	0.0393	0.9607
9	363.88	101325	0	0.0191	0.2943	0.6867	0.0000	0.0393	0.9607
10	371.84	101325	0	0.0000	0.0504	0.9496	0.0000	0.0040	0.9960
11	373.03	101325	0	0.0000	0.0051	0.9949	0.0000	0.0004	0.9996
12	373.16	101325	2000000	0.0000	0.0005	0.9995	0.0000	0.0000	1.0000

Table I-13: Stream results for the dehydration of IPA via heterogeneous azeotropic distillation with DIPE as entrainer. The simulation was performed with Aspen using NRTL with built-in Aspen parameters.

Streams	AQUEOUS	B1	B2	D1	D2	FF	MAKEUP	ORGANIC
Mole Flow kmol/sec								
DIPE	0.0001	0.0000	0.0000	0.0904	0.0001	0.0000	0.0002	0.0905
IPA	0.0007	0.0138	0.0000	0.0119	0.0007	0.0139	0.0000	0.0111
H2O	0.0181	0.0000	0.0139	0.0267	0.0042	0.0139	0.0000	0.0085
Mole Frac								
DIPE	0.0059	0.0034	0.0000	0.7012	0.0222	0.0000	1.0000	0.8214
IPA	0.0389	0.9950	0.0000	0.0921	0.1455	0.5000	0.0000	0.1011
H2O	0.9552	0.0016	1.0000	0.2068	0.8323	0.5000	0.0000	0.0775
Total Flow kmol/sec	0.0190	0.0139	0.0139	0.1289	0.0051	0.0278	0.0002	0.1102
Total Flow kg/sec	0.3823	0.8349	0.2504	10.4318	0.1319	1.0849	0.0204	10.0699
Total Flow cum/sec	0.0004	0.0012	0.0003	3.5432	0.0002	0.0013	0.0000	0.0140
Temperature K	313.73	354.93	373.17	334.87	338.69	298.15	298.15	313.69
Pressure N/sqm	101325	101325	101325	101325	101325	101325	101325	101325
Vapor Frac	0	0	0	1	0	0	0	0
Liquid Frac	1	1	1	0	1	1	1	1
Solid Frac	0	0	0	0	0	0	0	0
Enthalpy J/kmol	-286396176	-307281811	-280077249	-294051972	-288575480	-302531145	-351285603	-339108902
Enthalpy J/kg	-14212162	-5106812.8	-15546642	-3634732.8	-11096306	-7746165.6	-3438025.3	-3710169
Enthalpy Watt	-5433349.9	-4263667.4	-3893073.8	-37916831	-1463495.3	-8403643	-70257.121	-37361178
Entropy J/kmol-K	-173714.66	-422795.12	-146101.16	-474459.58	-206383.23	-308543.34	-746073.33	-657294.35
Entropy J/kg-K	-8620.44	-7026.56	-8109.84	-5864.72	-7935.85	-7900.11	-7301.81	-7191.42
Density kmol/cum	46.86	12.00	50.97	0.04	32.82	21.47	7.05	7.89
Density kg/cum	944.20	722.22	918.27	2.94	853.66	838.41	720.63	721.14
Average MW	20.15	60.17	18.02	80.90	26.01	39.06	102.18	91.40
Liq Vol 60F cum/sec	0.0004	0.0011	0.0003	0.0142	0.0001	0.0013	0.0000	0.0138

Table I-14: Azeotropic column information for the dehydration of IPA via heterogeneous azeotropic distillation with DIPE as entrainer. The simulation was performed with Aspen using NRTL with built-in Aspen parameters.

Stage	Temperature	Pressure	Heat duty	Vapour (mole fraction)			1 st Liquid (mole fraction)			2 nd Liquid (mole fraction)		
	K	N/sqm	Watt	DIPE	IPA	H2O	DIPE	IPA	H2O	DIPE	IPA	H2O
1	334.87	101325	-4806720	0.7012	0.0921	0.2068	0.7012	0.0921	0.2068	0.8021	0.1082	0.0898
2	334.89	101325	0	0.6944	0.0991	0.2065	0.6944	0.0991	0.2065	0.7800	0.1226	0.0974
3	334.74	101325	0	0.6610	0.1100	0.2290	0.6610	0.1100	0.2290	0.6047	0.1867	0.2086
4	334.77	101325	0	0.6607	0.1114	0.2279	0.6607	0.1114	0.2279	0.6042	0.1891	0.2067
5	334.83	101325	0	0.6602	0.1140	0.2258	0.6602	0.1140	0.2258	0.6035	0.1936	0.2030
6	334.93	101325	0	0.6594	0.1189	0.2218	0.6594	0.1189	0.2218	0.6026	0.2017	0.1956
7	335.12	101325	0	0.6585	0.1278	0.2137	0.6585	0.1278	0.2137	0.6031	0.2158	0.1810
8	335.48	101325	0	0.6590	0.1432	0.1978	0.6590	0.1432	0.1978	0.6083	0.2375	0.1542
9	336.08	101325	0	0.6645	0.1671	0.1684	0.6645	0.1671	0.1684	0.6206	0.2650	0.1144
10	336.93	101325	0	0.6777	0.1975	0.1248	0.6777	0.1975	0.1248	0.6359	0.2923	0.0718
11	337.84	101325	0	0.6939	0.2278	0.0783	0.6939	0.2278	0.0783	0.6454	0.3153	0.0393
12	338.57	101325	0	0.7039	0.2533	0.0428	0.7039	0.2533	0.0428	0.6408	0.3391	0.0201
13	339.13	101325	0	0.6989	0.2793	0.0218	0.6989	0.2793	0.0218	0.6072	0.3821	0.0107
14	339.98	101325	0	0.6630	0.3255	0.0115	0.6630	0.3255	0.0115	0.5059	0.4874	0.0067
15	342.62	101325	0	0.5545	0.4383	0.0072	0.5545	0.4383	0.0072	0.3088	0.6860	0.0053
16	347.98	101325	0	0.3408	0.6535	0.0056	0.3408	0.6535	0.0056	0.1273	0.8684	0.0043
17	352.40	101325	0	0.1411	0.8544	0.0046	0.1411	0.8544	0.0046	0.0413	0.9555	0.0032
18	354.31	101325	0	0.0455	0.9511	0.0034	0.0455	0.9511	0.0034	0.0121	0.9856	0.0023
19	354.93	101325	5007556.31	0.0131	0.9845	0.0024	0.0131	0.9845	0.0024	0.0034	0.9950	0.0016

Table I-15: Recovery column information for the dehydration of IPA via heterogeneous azeotropic distillation with DIPE as entrainer. The simulation was performed with Aspen using NRTL with built-in Aspen parameters.

Stage	Temperature	Pressure	Heat duty	Vapour (mole fraction)			Liquid (mole fraction)		
	K	N/sqm	Watt	DIPE	IPA	H2O	DIPE	IPA	H2O
1	338.69	101325	-923219.74	0.5425	0.2214	0.2361	0.0222	0.1455	0.8323
2	368.28	101325	0	0.0222	0.1455	0.8323	0.0001	0.0069	0.9930
3	371.95	101325	0	0.0051	0.0388	0.9561	0.0000	0.0015	0.9985
4	372.08	101325	0	0.0051	0.0344	0.9605	0.0000	0.0013	0.9987
5	372.08	101325	0	0.0051	0.0342	0.9607	0.0000	0.0013	0.9987
6	372.08	101325	0	0.0051	0.0342	0.9607	0.0000	0.0013	0.9987
7	372.08	101325	0	0.0051	0.0342	0.9607	0.0000	0.0013	0.9987
8	372.08	101325	0	0.0051	0.0342	0.9607	0.0000	0.0013	0.9987
9	372.08	101325	0	0.0051	0.0342	0.9607	0.0000	0.0013	0.9987
10	373.11	101325	0	0.0000	0.0020	0.9980	0.0000	0.0001	0.9999
11	373.16	101325	0	0.0000	0.0001	0.9999	0.0000	0.0000	1.0000
12	373.17	101325	1000000	0.0000	0.0000	1.0000	0.0000	0.0000	1.0000

Table I-17: Stream results (continued) for the recovery of n-propanol from a Fischer-Tropsch waste water stream via heterogeneous azeotropic distillation with DIPE as entrainer. The simulation was performed with Aspen using NRTL.

Streams	AQUEOUS	B1	B2	D1	D2	FF	MAKEUP	ORGANIC
Enthalpy J/kmol	-285244553	-289389658	-280077252	-276187176	-285067821	-291786260	-351285603	-325481066
Enthalpy J/kg	-14098827	-4848856.8	-15546634	-4038685.3	-7704095.3	-8183377.3	-3438025.3	-3958654.9
Enthalpy Watt	-4844170	-2897741.3	-4201158.8	-21030522	-565151.32	-8105174	-12997.567	-19268605
Entropy J/kmol-K	-172633.2	-406737.79	-146101.18	-369700.77	-262974.03	-275070.15	-746073.33	-579646.54
Entropy J/kg-K	-8532.77	-6815.08	-8109.84	-5406.13	-7107.00	-7714.56	-7301.81	-7049.94
Density kmol/cum	46.72	12.15	50.97	0.04	21.54	24.38	7.05	8.98
Density kg/cum	945.33	725.21	918.27	2.42	796.89	869.28	720.63	738.10
Average MW	20.23	59.68	18.02	68.39	37.00	35.66	102.18	82.22
Liq Vol 60F cum/sec	0.0004	0.0007	0.0003	0.0069	0.0001	0.0012	0.0000	0.0066

Table I-18: Azeotropic column information for the vapour phase for the recovery of n-propanol from a Fischer-Tropsch waste water stream via heterogeneous azeotropic distillation with DIPE as entrainer. The simulation was performed with Aspen using NRTL.

Stage	Temperature K	Pressure N/sqm	Heat duty Watt	Vapour (mole fraction)								
				DIPE	IPA	H2O	ETHANOL	N-PROPAN	ACID	ALDEHYDE	MEK	ESTER
1	344.14	101325	-3068300	0.4761	0.0050	0.2909	0.0148	0.1661	0.0000	0.0379	0.0004	0.0087
2	358.08	101325	0	0.0730	0.0077	0.4938	0.0168	0.3624	0.0000	0.0402	0.0003	0.0059
3	360.16	101325	0	0.0039	0.0058	0.5562	0.0117	0.3947	0.0000	0.0247	0.0001	0.0029
4	360.53	101325	0	0.0002	0.0047	0.5655	0.0084	0.4074	0.0000	0.0131	0.0000	0.0007
5	360.68	101325	0	0.0000	0.0037	0.5697	0.0059	0.4136	0.0000	0.0069	0.0000	0.0002
6	360.77	101325	0	0.0000	0.0029	0.5722	0.0041	0.4172	0.0000	0.0036	0.0000	0.0000
7	360.81	101325	0	0.0000	0.0022	0.5737	0.0029	0.4194	0.0000	0.0019	0.0000	0.0000
8	360.84	101325	0	0.0000	0.0017	0.5746	0.0020	0.4207	0.0000	0.0010	0.0000	0.0000
9	360.86	101325	0	0.0000	0.0013	0.5753	0.0014	0.4215	0.0000	0.0005	0.0000	0.0000
10	360.87	101325	0	0.0000	0.0010	0.5757	0.0010	0.4221	0.0000	0.0003	0.0000	0.0000
11	360.88	101325	0	0.0000	0.0008	0.5760	0.0007	0.4225	0.0000	0.0001	0.0000	0.0000
12	360.88	101325	0	0.0000	0.0006	0.5762	0.0005	0.4227	0.0000	0.0001	0.0000	0.0000
13	360.88	101325	0	0.0000	0.0004	0.5763	0.0003	0.4229	0.0000	0.0000	0.0000	0.0000
14	360.89	101325	0	0.0000	0.0003	0.5764	0.0002	0.4230	0.0000	0.0000	0.0000	0.0000
15	360.89	101325	0	0.0000	0.0003	0.5765	0.0002	0.4231	0.0000	0.0000	0.0000	0.0000
16	360.89	101325	0	0.0000	0.0002	0.5765	0.0001	0.4232	0.0000	0.0000	0.0000	0.0000
17	360.89	101325	0	0.0000	0.0001	0.5766	0.0001	0.4232	0.0000	0.0000	0.0000	0.0000
18	360.89	101325	0	0.0000	0.0001	0.5766	0.0001	0.4232	0.0000	0.0000	0.0000	0.0000
19	360.89	101325	0	0.0000	0.0001	0.5766	0.0000	0.4233	0.0000	0.0000	0.0000	0.0000
20	360.89	101325	0	0.0000	0.0001	0.5766	0.0000	0.4233	0.0000	0.0000	0.0000	0.0000
21	360.89	101325	0	0.0000	0.0000	0.5766	0.0000	0.4233	0.0000	0.0000	0.0000	0.0000
22	360.89	101325	0	0.0000	0.0000	0.5766	0.0000	0.4233	0.0000	0.0000	0.0000	0.0000
23	360.89	101325	0	0.0000	0.0000	0.5766	0.0000	0.4233	0.0000	0.0000	0.0000	0.0000
24	360.89	101325	0	0.0000	0.0000	0.5766	0.0000	0.4233	0.0000	0.0000	0.0000	0.0000
25	360.89	101325	0	0.0000	0.0000	0.5767	0.0000	0.4233	0.0000	0.0000	0.0000	0.0000
26	360.89	101325	0	0.0000	0.0000	0.5767	0.0000	0.4233	0.0000	0.0000	0.0000	0.0000
27	360.89	101325	0	0.0000	0.0000	0.5766	0.0000	0.4233	0.0000	0.0000	0.0000	0.0000
28	360.89	101325	0	0.0000	0.0000	0.5766	0.0000	0.4234	0.0000	0.0000	0.0000	0.0000
29	360.89	101325	0	0.0000	0.0000	0.5766	0.0000	0.4234	0.0000	0.0000	0.0000	0.0000

Table I-19: Azeotropic column information (continued) for the vapour phase for the recovery of n-propanol from a Fischer-Tropsch waste water stream via heterogeneous azeotropic distillation with DIPE as entrainer. The simulation was performed with Aspen using NRTL.

Stage	Temperature	Pressure	Heat duty	Vapour (mole fraction)								
	K	N/sqm	Watt	DIPE	IPA	H2O	ETHANOL	N-PROPAN	ACID	ALDEHYDE	MEK	ESTER
30	360.89	101325	0	0.0000	0.0000	0.5763	0.0000	0.4236	0.0000	0.0000	0.0000	0.0000
31	360.90	101325	0	0.0000	0.0000	0.5756	0.0000	0.4244	0.0000	0.0000	0.0000	0.0000
32	360.92	101325	0	0.0000	0.0000	0.5730	0.0000	0.4270	0.0000	0.0000	0.0000	0.0000
33	360.99	101325	0	0.0000	0.0000	0.5644	0.0000	0.4356	0.0000	0.0000	0.0000	0.0000
34	361.26	101325	0	0.0000	0.0000	0.5383	0.0000	0.4617	0.0000	0.0000	0.0000	0.0000
35	362.19	101325	0	0.0000	0.0000	0.4730	0.0000	0.5270	0.0000	0.0000	0.0000	0.0000
36	364.18	101325	0	0.0000	0.0000	0.3576	0.0000	0.6424	0.0000	0.0000	0.0000	0.0000
37	366.56	101325	0	0.0000	0.0000	0.2237	0.0000	0.7763	0.0000	0.0000	0.0000	0.0000
38	368.38	101325	0	0.0000	0.0000	0.1187	0.0000	0.8813	0.0000	0.0000	0.0000	0.0000
39	369.43	101325	0	0.0000	0.0000	0.0563	0.0000	0.9437	0.0000	0.0000	0.0000	0.0000
40	369.95	101325	3409618.1	0.0000	0.0000	0.0246	0.0000	0.9753	0.0000	0.0000	0.0000	0.0000

Table I-20: Azeotropic column information for the 1st liquid phase phase for the recovery of n-propanol from a Fischer-Tropsch waste water stream via heterogeneous azeotropic distillation with DIPE as entrainer. The simulation was performed with Aspen using NRTL.

Stage	Temperature K	Pressure N/sqm	Heat duty Watt	1 st Liquid (mole fraction)								
				DIPE	IPA	H2O	ETHANOL	N-PROPAN	ACID	ALDEHYDE	MEK	ESTER
1	344.14	101325	-3068300	0.0947	0.0088	0.3690	0.0186	0.4609	0.0000	0.0423	0.0002	0.0053
2	358.08	101325	0	0.0051	0.0064	0.4508	0.0119	0.5020	0.0000	0.0222	0.0001	0.0015
3	360.16	101325	0	0.0002	0.0042	0.5058	0.0075	0.4699	0.0000	0.0117	0.0000	0.0006
4	360.53	101325	0	0.0000	0.0033	0.5095	0.0053	0.4756	0.0000	0.0061	0.0000	0.0001
5	360.68	101325	0	0.0000	0.0026	0.5117	0.0037	0.4788	0.0000	0.0032	0.0000	0.0000
6	360.77	101325	0	0.0000	0.0020	0.5130	0.0026	0.4808	0.0000	0.0017	0.0000	0.0000
7	360.81	101325	0	0.0000	0.0015	0.5138	0.0018	0.4820	0.0000	0.0009	0.0000	0.0000
8	360.84	101325	0	0.0000	0.0012	0.5144	0.0012	0.4827	0.0000	0.0004	0.0000	0.0000
9	360.86	101325	0	0.0000	0.0009	0.5148	0.0009	0.4832	0.0000	0.0002	0.0000	0.0000
10	360.87	101325	0	0.0000	0.0007	0.5150	0.0006	0.4836	0.0000	0.0001	0.0000	0.0000
11	360.88	101325	0	0.0000	0.0005	0.5152	0.0004	0.4838	0.0000	0.0001	0.0000	0.0000
12	360.88	101325	0	0.0000	0.0004	0.5153	0.0003	0.4839	0.0000	0.0000	0.0000	0.0000
13	360.88	101325	0	0.0000	0.0003	0.5154	0.0002	0.4841	0.0000	0.0000	0.0000	0.0000
14	360.89	101325	0	0.0000	0.0002	0.5155	0.0001	0.4841	0.0000	0.0000	0.0000	0.0000
15	360.89	101325	0	0.0000	0.0002	0.5155	0.0001	0.4842	0.0000	0.0000	0.0000	0.0000
16	360.89	101325	0	0.0000	0.0001	0.5155	0.0001	0.4842	0.0000	0.0000	0.0000	0.0000
17	360.89	101325	0	0.0000	0.0001	0.5156	0.0000	0.4843	0.0000	0.0000	0.0000	0.0000
18	360.89	101325	0	0.0000	0.0001	0.5156	0.0000	0.4843	0.0000	0.0000	0.0000	0.0000
19	360.89	101325	0	0.0000	0.0001	0.5156	0.0000	0.4843	0.0000	0.0000	0.0000	0.0000
20	360.89	101325	0	0.0000	0.0000	0.5156	0.0000	0.4843	0.0000	0.0000	0.0000	0.0000
21	360.89	101325	0	0.0000	0.0000	0.5156	0.0000	0.4843	0.0000	0.0000	0.0000	0.0000
22	360.89	101325	0	0.0000	0.0000	0.5156	0.0000	0.4843	0.0000	0.0000	0.0000	0.0000
23	360.89	101325	0	0.0000	0.0000	0.5156	0.0000	0.4843	0.0000	0.0000	0.0000	0.0000
24	360.89	101325	0	0.0000	0.0000	0.5156	0.0000	0.4843	0.0000	0.0000	0.0000	0.0000
25	360.89	101325	0	0.0000	0.0000	0.5156	0.0000	0.4843	0.0000	0.0000	0.0000	0.0000
26	360.89	101325	0	0.0000	0.0000	0.5156	0.0000	0.4843	0.0000	0.0000	0.0000	0.0000
27	360.89	101325	0	0.0000	0.0000	0.5156	0.0000	0.4844	0.0000	0.0000	0.0000	0.0000
28	360.89	101325	0	0.0000	0.0000	0.5156	0.0000	0.4844	0.0000	0.0000	0.0000	0.0000
29	360.89	101325	0	0.0000	0.0000	0.5154	0.0000	0.4846	0.0000	0.0000	0.0000	0.0000

Table I-21: Azeotropic column information (continued) for the 1st liquid phase phase for the recovery of n-propanol from a Fischer-Tropsch waste water stream via heterogeneous azeotropic distillation with DIPE as entrainer. The simulation was performed with Aspen using NRTL.

Stage	Temperature K	Pressure N/sqm	Heat duty Watt	1 st Liquid (mole fraction)								
				DIPE	IPA	H2O	ETHANOL	N-PROPAN	ACID	ALDEHYDE	MEK	ESTER
30	360.89	101325	0	0.0000	0.0000	0.5147	0.0000	0.4853	0.0000	0.0000	0.0000	0.0000
31	360.90	101325	0	0.0000	0.0000	0.5124	0.0000	0.4876	0.0000	0.0000	0.0000	0.0000
32	360.92	101325	0	0.0000	0.0000	0.5047	0.0000	0.4953	0.0000	0.0000	0.0000	0.0000
33	360.99	101325	0	0.0000	0.0000	0.4813	0.0000	0.5186	0.0000	0.0000	0.0000	0.0000
34	361.26	101325	0	0.0000	0.0000	0.4231	0.0000	0.5769	0.0000	0.0000	0.0000	0.0000
35	362.19	101325	0	0.0000	0.0000	0.3199	0.0000	0.6801	0.0000	0.0000	0.0000	0.0000
36	364.18	101325	0	0.0000	0.0000	0.2004	0.0000	0.7995	0.0000	0.0000	0.0000	0.0000
37	366.56	101325	0	0.0000	0.0000	0.1068	0.0000	0.8931	0.0000	0.0000	0.0000	0.0000
38	368.38	101325	0	0.0000	0.0000	0.0512	0.0000	0.9487	0.0000	0.0000	0.0000	0.0000
39	369.43	101325	0	0.0000	0.0000	0.0230	0.0000	0.9769	0.0001	0.0000	0.0000	0.0000
40	369.95	101325	3409618.1	0.0000	0.0000	0.0098	0.0000	0.9900	0.0002	0.0000	0.0000	0.0000

Table I-22: Azeotropic column information for the 2nd liquid phase phase for the recovery of n-propanol from a Fischer-Tropsch waste water stream via heterogeneous azeotropic distillation with DIPE as entrainer. The simulation was performed with Aspen using NRTL.

Stage	Temperature K	Pressure N/sqm	Heat duty Watt	2 nd Liquid (mole fraction)								
				DIPE	IPA	H2O	ETHANOL	N-PROPAN	ACID	ALDEHYDE	MEK	ESTER
1	344.14	101325	-3068300	0.0947	0.0088	0.3690	0.0186	0.4609	0.0000	0.0423	0.0002	0.0053
2	358.08	101325	0	0.0051	0.0064	0.4508	0.0119	0.5020	0.0000	0.0222	0.0001	0.0015
3	360.16	101325	0	0.0002	0.0042	0.5058	0.0075	0.4699	0.0000	0.0117	0.0000	0.0006
4	360.53	101325	0	0.0000	0.0033	0.5095	0.0053	0.4756	0.0000	0.0061	0.0000	0.0001
5	360.68	101325	0	0.0000	0.0026	0.5117	0.0037	0.4788	0.0000	0.0032	0.0000	0.0000
6	360.77	101325	0	0.0000	0.0020	0.5130	0.0026	0.4808	0.0000	0.0017	0.0000	0.0000
7	360.81	101325	0	0.0000	0.0015	0.5138	0.0018	0.4820	0.0000	0.0009	0.0000	0.0000
8	360.84	101325	0	0.0000	0.0012	0.5144	0.0012	0.4827	0.0000	0.0004	0.0000	0.0000
9	360.86	101325	0	0.0000	0.0009	0.5148	0.0009	0.4832	0.0000	0.0002	0.0000	0.0000
10	360.87	101325	0	0.0000	0.0007	0.5150	0.0006	0.4836	0.0000	0.0001	0.0000	0.0000
11	360.88	101325	0	0.0000	0.0005	0.5152	0.0004	0.4838	0.0000	0.0001	0.0000	0.0000
12	360.88	101325	0	0.0000	0.0004	0.5153	0.0003	0.4839	0.0000	0.0000	0.0000	0.0000
13	360.88	101325	0	0.0000	0.0003	0.5154	0.0002	0.4841	0.0000	0.0000	0.0000	0.0000
14	360.89	101325	0	0.0000	0.0002	0.5155	0.0001	0.4841	0.0000	0.0000	0.0000	0.0000
15	360.89	101325	0	0.0000	0.0002	0.5155	0.0001	0.4842	0.0000	0.0000	0.0000	0.0000
16	360.89	101325	0	0.0000	0.0001	0.5155	0.0001	0.4842	0.0000	0.0000	0.0000	0.0000
17	360.89	101325	0	0.0000	0.0001	0.5156	0.0000	0.4843	0.0000	0.0000	0.0000	0.0000
18	360.89	101325	0	0.0000	0.0001	0.5156	0.0000	0.4843	0.0000	0.0000	0.0000	0.0000
19	360.89	101325	0	0.0000	0.0001	0.5156	0.0000	0.4843	0.0000	0.0000	0.0000	0.0000
20	360.89	101325	0	0.0000	0.0000	0.5156	0.0000	0.4843	0.0000	0.0000	0.0000	0.0000
21	360.89	101325	0	0.0000	0.0000	0.5156	0.0000	0.4843	0.0000	0.0000	0.0000	0.0000
22	360.89	101325	0	0.0000	0.0000	0.5156	0.0000	0.4843	0.0000	0.0000	0.0000	0.0000
23	360.89	101325	0	0.0000	0.0000	0.5156	0.0000	0.4843	0.0000	0.0000	0.0000	0.0000
24	360.89	101325	0	0.0000	0.0000	0.5156	0.0000	0.4843	0.0000	0.0000	0.0000	0.0000
25	360.89	101325	0	0.0000	0.0000	0.5156	0.0000	0.4843	0.0000	0.0000	0.0000	0.0000
26	360.89	101325	0	0.0000	0.0000	0.5156	0.0000	0.4843	0.0000	0.0000	0.0000	0.0000
27	360.89	101325	0	0.0000	0.0000	0.5156	0.0000	0.4844	0.0000	0.0000	0.0000	0.0000
28	360.89	101325	0	0.0000	0.0000	0.5156	0.0000	0.4844	0.0000	0.0000	0.0000	0.0000
29	360.89	101325	0	0.0000	0.0000	0.5154	0.0000	0.4846	0.0000	0.0000	0.0000	0.0000

Table I-23: Azeotropic column information (continued) for the 2nd liquid phase phase for the recovery of n-propanol from a Fischer-Tropsch waste water stream via heterogeneous azeotropic distillation with DIPE as entrainer. The simulation was performed with Aspen using NRTL.

Stage	Temperature K	Pressure N/sqm	Heat duty Watt	2 nd Liquid (mole fraction)								
				DIPE	IPA	H2O	ETHANOL	N-PROPAN	ACID	ALDEHYDE	MEK	ESTER
30	360.89	101325	0	0.0000	0.0000	0.5147	0.0000	0.4853	0.0000	0.0000	0.0000	0.0000
31	360.90	101325	0	0.0000	0.0000	0.5124	0.0000	0.4876	0.0000	0.0000	0.0000	0.0000
32	360.92	101325	0	0.0000	0.0000	0.5047	0.0000	0.4953	0.0000	0.0000	0.0000	0.0000
33	360.99	101325	0	0.0000	0.0000	0.4813	0.0000	0.5186	0.0000	0.0000	0.0000	0.0000
34	361.26	101325	0	0.0000	0.0000	0.4231	0.0000	0.5769	0.0000	0.0000	0.0000	0.0000
35	362.19	101325	0	0.0000	0.0000	0.3199	0.0000	0.6801	0.0000	0.0000	0.0000	0.0000
36	364.18	101325	0	0.0000	0.0000	0.2004	0.0000	0.7995	0.0000	0.0000	0.0000	0.0000
37	366.56	101325	0	0.0000	0.0000	0.1068	0.0000	0.8931	0.0000	0.0000	0.0000	0.0000
38	368.38	101325	0	0.0000	0.0000	0.0512	0.0000	0.9487	0.0000	0.0000	0.0000	0.0000
39	369.43	101325	0	0.0000	0.0000	0.0230	0.0000	0.9769	0.0001	0.0000	0.0000	0.0000
40	369.95	101325	3409618.1	0.0000	0.0000	0.0098	0.0000	0.9900	0.0002	0.0000	0.0000	0.0000

Table I-27: Stream results (continued) for the recovery of ethanol from a Fischer-Tropsch waste water stream via heterogeneous azeotropic distillation with DIPE as entrainer. The simulation was performed with Aspen using NRTL.

Streams	AQUEOUS	B1	D1	FF	MAKEUP	ORGANIC	B2	D2
Enthalpy J/kmol	-284003873	-276388434	-288007411	-285855658	-351285603	-332200756	-290949804	-270570065
Enthalpy J/kg	-12935531	-5605985.3	-3686277.5	-9095778.7	-3438025.3	-3774506.3	-5170444.3	-5829356.2
Enthalpy Watt	-5088834.3	-2736245.5	-34536811	-7940435	-35128.56	-33917103	-843754.43	-1893990.5
Entropy J/kmol-K	-183314.72	-332479.11	-453510.16	-247669.52	-746073.33	-631330.82	-368313.8	-322045.08
Entropy J/kg-K	-8349.44	-6743.67	-5804.59	-7880.72	-7301.81	-7173.26	-6545.27	-6938.37
Density kmol/cum	41.60	14.98	0.04	27.38	7.05	8.23	13.08	15.86
Density kg/cum	913.31	738.36	2.85	860.53	720.63	723.99	736.21	736.06
Average MW	21.96	49.30	78.13	31.43	102.18	88.01	56.27	46.42
Liq Vol 60F cum/sec	0.0004	0.0006	0.0127	0.0010	0.0000	0.0123	0.0002	0.0004

Table I-28: Azeotropic column information for the vapour phase for the recovery of ethanol from a Fischer-Tropsch waste water stream via heterogeneous azeotropic distillation with DIPE as entrainer. The simulation was performed with Aspen using NRTL.

Stage	Temperature K	Pressure N/sqm	Heat duty Watt	Vapour (mole fraction)							
				DIPE	IPA	H2O	ETHANOL	N-PROPAN	ACID	ALDEHYDE	MEK
1	334.30	101325	-4436190	0.6667	0.0023	0.1929	0.1362	0.0016	0.0000	0.0002	0.0002
2	334.44	101325	0	0.6791	0.0025	0.1963	0.1185	0.0030	0.0000	0.0003	0.0003
3	332.80	101325	0	0.6030	0.0023	0.2916	0.0974	0.0049	0.0000	0.0004	0.0004
4	332.80	101325	0	0.6030	0.0023	0.2916	0.0974	0.0049	0.0000	0.0004	0.0004
5	332.80	101325	0	0.6030	0.0023	0.2916	0.0974	0.0049	0.0000	0.0004	0.0004
6	332.80	101325	0	0.6030	0.0023	0.2916	0.0974	0.0049	0.0000	0.0004	0.0004
7	332.80	101325	0	0.6030	0.0023	0.2916	0.0974	0.0049	0.0000	0.0004	0.0004
8	332.80	101325	0	0.6030	0.0023	0.2916	0.0974	0.0049	0.0000	0.0004	0.0004
9	332.80	101325	0	0.6030	0.0023	0.2916	0.0974	0.0049	0.0000	0.0004	0.0004
10	332.80	101325	0	0.6030	0.0023	0.2916	0.0974	0.0049	0.0000	0.0004	0.0004
11	332.80	101325	0	0.6029	0.0023	0.2916	0.0974	0.0049	0.0000	0.0004	0.0004
12	332.80	101325	0	0.6029	0.0023	0.2916	0.0974	0.0049	0.0000	0.0004	0.0004
13	332.80	101325	0	0.6029	0.0023	0.2916	0.0974	0.0049	0.0000	0.0004	0.0004
14	332.80	101325	0	0.6029	0.0023	0.2916	0.0974	0.0049	0.0000	0.0004	0.0004
15	332.80	101325	0	0.6029	0.0023	0.2916	0.0975	0.0049	0.0000	0.0004	0.0004
16	332.80	101325	0	0.6029	0.0023	0.2916	0.0975	0.0049	0.0000	0.0004	0.0004
17	332.80	101325	0	0.6029	0.0023	0.2915	0.0976	0.0049	0.0000	0.0004	0.0004
18	332.80	101325	0	0.6029	0.0023	0.2914	0.0977	0.0049	0.0000	0.0004	0.0004
19	332.80	101325	0	0.6029	0.0023	0.2913	0.0978	0.0049	0.0000	0.0004	0.0004
20	332.80	101325	0	0.6028	0.0023	0.2911	0.0981	0.0049	0.0000	0.0004	0.0004
21	332.81	101325	0	0.6028	0.0023	0.2908	0.0985	0.0049	0.0000	0.0004	0.0004
22	332.82	101325	0	0.6026	0.0023	0.2903	0.0991	0.0049	0.0000	0.0004	0.0004
23	332.83	101325	0	0.6025	0.0023	0.2895	0.1001	0.0049	0.0000	0.0004	0.0004
24	332.85	101325	0	0.6022	0.0023	0.2882	0.1016	0.0049	0.0000	0.0004	0.0004
25	332.88	101325	0	0.6018	0.0023	0.2863	0.1040	0.0049	0.0000	0.0004	0.0004
26	332.93	101325	0	0.6011	0.0023	0.2832	0.1077	0.0048	0.0000	0.0004	0.0004
27	333.00	101325	0	0.6002	0.0022	0.2783	0.1135	0.0048	0.0000	0.0004	0.0004
28	333.13	101325	0	0.5988	0.0022	0.2707	0.1225	0.0048	0.0000	0.0004	0.0005
29	333.33	101325	0	0.5971	0.0023	0.2585	0.1362	0.0048	0.0000	0.0005	0.0006

Table I-29: Azeotropic column information (continued) for the vapour phase for the recovery of ethanol from a Fischer-Tropsch waste water stream via heterogeneous azeotropic distillation with DIPE as entrainer. The simulation was performed with Aspen using NRTL.

Stage	Temperature K	Pressure N/sqm	Heat duty Watt	Vapour (mole fraction)							
				DIPE	IPA	H2O	ETHANOL	N-PROPAN	ACID	ALDEHYDE	MEK
30	333.65	101325	0	0.5954	0.0023	0.2395	0.1563	0.0049	0.0000	0.0006	0.0009
31	334.14	101325	0	0.5953	0.0025	0.2104	0.1842	0.0051	0.0000	0.0008	0.0017
32	334.82	101325	0	0.5987	0.0027	0.1701	0.2186	0.0054	0.0001	0.0012	0.0032
33	335.62	101325	0	0.6050	0.0030	0.1232	0.2547	0.0058	0.0001	0.0019	0.0062
34	336.40	101325	0	0.6079	0.0034	0.0803	0.2879	0.0062	0.0001	0.0032	0.0111
35	337.15	101325	0	0.5957	0.0040	0.0489	0.3206	0.0066	0.0001	0.0055	0.0187
36	338.27	101325	0	0.5455	0.0052	0.0304	0.3720	0.0077	0.0001	0.0092	0.0298
37	341.53	101325	0	0.4077	0.0087	0.0228	0.4909	0.0120	0.0001	0.0145	0.0433
38	347.32	101325	0	0.1870	0.0156	0.0221	0.6875	0.0245	0.0002	0.0174	0.0456
39	351.16	101325	0	0.0519	0.0230	0.0215	0.8074	0.0481	0.0005	0.0147	0.0329
40	353.45	101325	4907814.06	0.0115	0.0298	0.0189	0.8169	0.0907	0.0021	0.0103	0.0198

Table I-30: Azeotropic column information for the 1st liquid phase phase for the recovery of ethanol from a Fischer-Tropsch waste water stream via heterogeneous azeotropic distillation with DIPE as entrainer. The simulation was performed with Aspen using NRTL.

Stage	Temperature K	Pressure N/sqm	Heat duty Watt	1 st Liquid (mole fraction)							
				DIPE	IPA	H2O	ETHANOL	N-PROPAN	ACID	ALDEHYDE	MEK
1	334.30	101325	-4436190	0.0034	0.0011	0.9078	0.0867	0.0009	0.0000	0.0000	0.0000
2	334.44	101325	0	0.0028	0.0011	0.9247	0.0697	0.0016	0.0000	0.0000	0.0000
3	332.80	101325	0	0.5642	0.0046	0.2738	0.1392	0.0156	0.0008	0.0008	0.0010
4	332.80	101325	0	0.5642	0.0046	0.2738	0.1392	0.0156	0.0008	0.0008	0.0010
5	332.80	101325	0	0.5642	0.0046	0.2738	0.1392	0.0156	0.0008	0.0008	0.0010
6	332.80	101325	0	0.5642	0.0046	0.2738	0.1392	0.0156	0.0008	0.0008	0.0010
7	332.80	101325	0	0.5642	0.0046	0.2738	0.1392	0.0156	0.0008	0.0008	0.0010
8	332.80	101325	0	0.5642	0.0046	0.2738	0.1392	0.0156	0.0008	0.0008	0.0010
9	332.80	101325	0	0.5642	0.0046	0.2738	0.1392	0.0156	0.0008	0.0008	0.0010
10	332.80	101325	0	0.5642	0.0046	0.2738	0.1392	0.0156	0.0008	0.0008	0.0010
11	332.80	101325	0	0.5642	0.0046	0.2738	0.1392	0.0156	0.0008	0.0008	0.0010
12	332.80	101325	0	0.5642	0.0046	0.2738	0.1392	0.0156	0.0008	0.0008	0.0010
13	332.80	101325	0	0.5642	0.0046	0.2738	0.1392	0.0156	0.0008	0.0008	0.0010
14	332.80	101325	0	0.5642	0.0046	0.2738	0.1393	0.0156	0.0008	0.0008	0.0010
15	332.80	101325	0	0.5642	0.0046	0.2737	0.1393	0.0156	0.0008	0.0008	0.0010
16	332.80	101325	0	0.5642	0.0046	0.2737	0.1394	0.0156	0.0008	0.0008	0.0010
17	332.80	101325	0	0.5642	0.0046	0.2736	0.1395	0.0156	0.0008	0.0008	0.0010
18	332.80	101325	0	0.5641	0.0046	0.2735	0.1396	0.0156	0.0008	0.0008	0.0010
19	332.80	101325	0	0.5641	0.0046	0.2733	0.1398	0.0156	0.0008	0.0008	0.0010
20	332.80	101325	0	0.5640	0.0046	0.2730	0.1402	0.0156	0.0008	0.0008	0.0010
21	332.81	101325	0	0.5639	0.0046	0.2725	0.1408	0.0156	0.0008	0.0008	0.0010
22	332.82	101325	0	0.5638	0.0046	0.2718	0.1417	0.0156	0.0008	0.0008	0.0010
23	332.83	101325	0	0.5635	0.0046	0.2706	0.1431	0.0156	0.0008	0.0008	0.0011
24	332.85	101325	0	0.5631	0.0046	0.2688	0.1454	0.0155	0.0008	0.0008	0.0011
25	332.88	101325	0	0.5625	0.0045	0.2659	0.1488	0.0155	0.0008	0.0008	0.0011
26	332.93	101325	0	0.5616	0.0045	0.2614	0.1543	0.0155	0.0008	0.0008	0.0011
27	333.00	101325	0	0.5604	0.0045	0.2542	0.1627	0.0155	0.0008	0.0008	0.0011
28	333.13	101325	0	0.5587	0.0045	0.2428	0.1754	0.0155	0.0008	0.0009	0.0013
29	333.33	101325	0	0.5572	0.0046	0.2250	0.1943	0.0156	0.0008	0.0010	0.0016

Table I-31: Azeotropic column information (continued) for the 1st liquid phase phase for the recovery of ethanol from a Fischer-Tropsch waste water stream via heterogeneous azeotropic distillation with DIPE as entrainer. The simulation was performed with Aspen using NRTL.

Stage	Temperature K	Pressure N/sqm	Heat duty Watt	1 st Liquid (mole fraction)							
				DIPE	IPA	H2O	ETHANOL	N-PROPAN	ACID	ALDEHYDE	MEK
30	333.65	101325	0	0.5571	0.0047	0.1979	0.2203	0.0158	0.0008	0.0012	0.0023
31	334.14	101325	0	0.5604	0.0050	0.1601	0.2525	0.0161	0.0008	0.0015	0.0037
32	334.82	101325	0	0.5663	0.0053	0.1163	0.2863	0.0164	0.0008	0.0022	0.0065
33	335.62	101325	0	0.5688	0.0056	0.0761	0.3174	0.0168	0.0008	0.0034	0.0111
34	336.40	101325	0	0.5569	0.0062	0.0467	0.3484	0.0173	0.0008	0.0055	0.0182
35	337.15	101325	0	0.5092	0.0074	0.0294	0.3970	0.0186	0.0008	0.0091	0.0286
36	338.27	101325	0	0.3796	0.0107	0.0223	0.5085	0.0230	0.0009	0.0140	0.0410
37	341.53	101325	0	0.1738	0.0172	0.0216	0.6917	0.0350	0.0010	0.0167	0.0431
38	347.32	101325	0	0.0483	0.0240	0.0210	0.8030	0.0569	0.0013	0.0141	0.0313
39	351.16	101325	0	0.0108	0.0304	0.0186	0.8118	0.0965	0.0028	0.0100	0.0191
40	353.45	101325	4907814.06	0.0022	0.0376	0.0151	0.7457	0.1707	0.0113	0.0067	0.0107

Table I-32: Azeotropic column information for the 2nd liquid phase phase for the recovery of ethanol from a Fischer-Tropsch waste water stream via heterogeneous azeotropic distillation with DIPE as entrainer. The simulation was performed with Aspen using NRTL.

Stage	Temperature K	Pressure N/sqm	Heat duty Watt	2 nd Liquid (mole fraction)							
				DIPE	IPA	H2O	ETHANOL	N-PROPAN	ACID	ALDEHYDE	MEK
1	334.30	101325	-4436190	0.0034	0.0011	0.9078	0.0867	0.0009	0.0000	0.0000	0.0000
2	334.44	101325	0	0.0028	0.0011	0.9247	0.0697	0.0016	0.0000	0.0000	0.0000
3	332.80	101325	0	0.5642	0.0046	0.2738	0.1392	0.0156	0.0008	0.0008	0.0010
4	332.80	101325	0	0.5642	0.0046	0.2738	0.1392	0.0156	0.0008	0.0008	0.0010
5	332.80	101325	0	0.5642	0.0046	0.2738	0.1392	0.0156	0.0008	0.0008	0.0010
6	332.80	101325	0	0.5642	0.0046	0.2738	0.1392	0.0156	0.0008	0.0008	0.0010
7	332.80	101325	0	0.5642	0.0046	0.2738	0.1392	0.0156	0.0008	0.0008	0.0010
8	332.80	101325	0	0.5642	0.0046	0.2738	0.1392	0.0156	0.0008	0.0008	0.0010
9	332.80	101325	0	0.5642	0.0046	0.2738	0.1392	0.0156	0.0008	0.0008	0.0010
10	332.80	101325	0	0.5642	0.0046	0.2738	0.1392	0.0156	0.0008	0.0008	0.0010
11	332.80	101325	0	0.5642	0.0046	0.2738	0.1392	0.0156	0.0008	0.0008	0.0010
12	332.80	101325	0	0.5642	0.0046	0.2738	0.1392	0.0156	0.0008	0.0008	0.0010
13	332.80	101325	0	0.5642	0.0046	0.2738	0.1392	0.0156	0.0008	0.0008	0.0010
14	332.80	101325	0	0.5642	0.0046	0.2738	0.1393	0.0156	0.0008	0.0008	0.0010
15	332.80	101325	0	0.5642	0.0046	0.2737	0.1393	0.0156	0.0008	0.0008	0.0010
16	332.80	101325	0	0.5642	0.0046	0.2737	0.1394	0.0156	0.0008	0.0008	0.0010
17	332.80	101325	0	0.5642	0.0046	0.2736	0.1395	0.0156	0.0008	0.0008	0.0010
18	332.80	101325	0	0.5641	0.0046	0.2735	0.1396	0.0156	0.0008	0.0008	0.0010
19	332.80	101325	0	0.5641	0.0046	0.2733	0.1398	0.0156	0.0008	0.0008	0.0010
20	332.80	101325	0	0.5640	0.0046	0.2730	0.1402	0.0156	0.0008	0.0008	0.0010
21	332.81	101325	0	0.5639	0.0046	0.2725	0.1408	0.0156	0.0008	0.0008	0.0010
22	332.82	101325	0	0.5638	0.0046	0.2718	0.1417	0.0156	0.0008	0.0008	0.0010
23	332.83	101325	0	0.5635	0.0046	0.2706	0.1431	0.0156	0.0008	0.0008	0.0011
24	332.85	101325	0	0.5631	0.0046	0.2688	0.1454	0.0155	0.0008	0.0008	0.0011
25	332.88	101325	0	0.5625	0.0045	0.2659	0.1488	0.0155	0.0008	0.0008	0.0011
26	332.93	101325	0	0.5616	0.0045	0.2614	0.1543	0.0155	0.0008	0.0008	0.0011
27	333.00	101325	0	0.5604	0.0045	0.2542	0.1627	0.0155	0.0008	0.0008	0.0011
28	333.13	101325	0	0.5587	0.0045	0.2428	0.1754	0.0155	0.0008	0.0009	0.0013
29	333.33	101325	0	0.5572	0.0046	0.2250	0.1943	0.0156	0.0008	0.0010	0.0016

Table I-33: Azeotropic column information (continued) for the 2nd liquid phase phase for the recovery of ethanol from a Fischer-Tropsch waste water stream via heterogeneous azeotropic distillation with DIPE as entrainer. The simulation was performed with Aspen using NRTL.

Stage	Temperature K	Pressure N/sqm	Heat duty Watt	2 nd Liquid (mole fraction)							
				DIPE	IPA	H2O	ETHANOL	N-PROPAN	ACID	ALDEHYDE	MEK
30	333.65	101325	0	0.5571	0.0047	0.1979	0.2203	0.0158	0.0008	0.0012	0.0023
31	334.14	101325	0	0.5604	0.0050	0.1601	0.2525	0.0161	0.0008	0.0015	0.0037
32	334.82	101325	0	0.5663	0.0053	0.1163	0.2863	0.0164	0.0008	0.0022	0.0065
33	335.62	101325	0	0.5688	0.0056	0.0761	0.3174	0.0168	0.0008	0.0034	0.0111
34	336.40	101325	0	0.5569	0.0062	0.0467	0.3484	0.0173	0.0008	0.0055	0.0182
35	337.15	101325	0	0.5092	0.0074	0.0294	0.3970	0.0186	0.0008	0.0091	0.0286
36	338.27	101325	0	0.3796	0.0107	0.0223	0.5085	0.0230	0.0009	0.0140	0.0410
37	341.53	101325	0	0.1738	0.0172	0.0216	0.6917	0.0350	0.0010	0.0167	0.0431
38	347.32	101325	0	0.0483	0.0240	0.0210	0.8030	0.0569	0.0013	0.0141	0.0313
39	351.16	101325	0	0.0108	0.0304	0.0186	0.8118	0.0965	0.0028	0.0100	0.0191
40	353.45	101325	4907814.06	0.0022	0.0376	0.0151	0.7457	0.1707	0.0113	0.0067	0.0107

Table I-34: Recovery column information for the vapour phase phase for the recovery of ethanol from a Fischer-Tropsch waste water stream via heterogeneous azeotropic distillation with DIPE as entrainer. The simulation was performed with Aspen using NRTL.

Stage	Temperature K	Pressure N/sqm	Heat duty Watt	Vapour (mole fraction)							
				DIPE	IPA	H2O	ETHANOL	N-PROPAN	ACID	ALDEHYDE	MEK
1	350.64	101325	-6918573.2	0.0160	0.0069	0.0229	0.9129	0.0001	0.0000	0.0146	0.0267
2	351.12	101325	0	0.0031	0.0086	0.0211	0.9425	0.0001	0.0000	0.0094	0.0151
3	351.29	101325	0	0.0007	0.0103	0.0193	0.9547	0.0003	0.0000	0.0061	0.0086
4	351.38	101325	0	0.0003	0.0122	0.0177	0.9602	0.0005	0.0000	0.0040	0.0051
5	351.44	101325	0	0.0002	0.0143	0.0162	0.9623	0.0009	0.0000	0.0028	0.0033
6	351.49	101325	0	0.0002	0.0168	0.0148	0.9622	0.0017	0.0000	0.0020	0.0023
7	351.55	101325	0	0.0002	0.0195	0.0136	0.9602	0.0031	0.0000	0.0016	0.0018
8	351.64	101325	0	0.0002	0.0226	0.0125	0.9561	0.0057	0.0000	0.0013	0.0015
9	351.78	101325	0	0.0002	0.0262	0.0115	0.9489	0.0104	0.0002	0.0012	0.0014
10	351.83	101325	0	0.0000	0.0301	0.0103	0.9471	0.0107	0.0002	0.0007	0.0008
11	351.88	101325	0	0.0000	0.0347	0.0092	0.9436	0.0114	0.0002	0.0005	0.0004
12	351.94	101325	0	0.0000	0.0403	0.0082	0.9381	0.0128	0.0002	0.0003	0.0002
13	352.05	101325	0	0.0000	0.0469	0.0073	0.9298	0.0156	0.0002	0.0002	0.0001
14	352.24	101325	0	0.0000	0.0549	0.0064	0.9171	0.0212	0.0002	0.0001	0.0001
15	352.58	101325	0	0.0000	0.0645	0.0056	0.8971	0.0325	0.0002	0.0001	0.0000
16	353.22	101325	0	0.0000	0.0763	0.0047	0.8641	0.0547	0.0002	0.0000	0.0000
17	354.43	101325	0	0.0000	0.0905	0.0039	0.8081	0.0974	0.0002	0.0000	0.0000
18	356.51	101325	0	0.0000	0.1064	0.0030	0.7157	0.1745	0.0004	0.0000	0.0000
19	359.54	101325	0	0.0000	0.1201	0.0020	0.5806	0.2958	0.0015	0.0000	0.0000
20	363.29	101325	7000000	0.0000	0.1226	0.0012	0.4220	0.4466	0.0076	0.0000	0.0000

Table I-35: Recovery column information for the liquid phase phase for the recovery of ethanol from a Fischer-Tropsch waste water stream via heterogeneous azeotropic distillation with DIPE as entrainer. The simulation was performed with Aspen using NRTL.

Stage	Temperature K	Pressure N/sqm	Heat duty Watt	Liquid (mole fraction)							
				DIPE	IPA	H2O	ETHANOL	N-PROPAN	ACID	ALDEHYDE	MEK
1	350.64	101325	-6918573.2	0.0031	0.0086	0.0211	0.9425	0.0001	0.0000	0.0094	0.0151
2	351.12	101325	0	0.0006	0.0104	0.0192	0.9552	0.0003	0.0000	0.0059	0.0084
3	351.29	101325	0	0.0001	0.0124	0.0175	0.9610	0.0005	0.0000	0.0038	0.0047
4	351.38	101325	0	0.0000	0.0146	0.0160	0.9632	0.0010	0.0000	0.0025	0.0028
5	351.44	101325	0	0.0000	0.0171	0.0146	0.9630	0.0018	0.0000	0.0017	0.0018
6	351.49	101325	0	0.0000	0.0199	0.0133	0.9610	0.0032	0.0000	0.0012	0.0013
7	351.55	101325	0	0.0000	0.0232	0.0122	0.9567	0.0059	0.0001	0.0010	0.0010
8	351.64	101325	0	0.0000	0.0270	0.0111	0.9492	0.0108	0.0002	0.0008	0.0008
9	351.78	101325	0	0.0000	0.0313	0.0102	0.9364	0.0198	0.0008	0.0007	0.0008
10	351.83	101325	0	0.0000	0.0359	0.0091	0.9329	0.0205	0.0008	0.0005	0.0004
11	351.88	101325	0	0.0000	0.0413	0.0081	0.9274	0.0218	0.0008	0.0003	0.0002
12	351.94	101325	0	0.0000	0.0479	0.0072	0.9193	0.0246	0.0008	0.0002	0.0001
13	352.05	101325	0	0.0000	0.0557	0.0063	0.9068	0.0302	0.0008	0.0001	0.0001
14	352.24	101325	0	0.0000	0.0652	0.0055	0.8872	0.0412	0.0008	0.0001	0.0000
15	352.58	101325	0	0.0000	0.0768	0.0047	0.8546	0.0631	0.0008	0.0000	0.0000
16	353.22	101325	0	0.0000	0.0907	0.0038	0.7995	0.1051	0.0008	0.0000	0.0000
17	354.43	101325	0	0.0000	0.1065	0.0029	0.7086	0.1810	0.0010	0.0000	0.0000
18	356.51	101325	0	0.0000	0.1199	0.0020	0.5757	0.3003	0.0020	0.0000	0.0000
19	359.54	101325	0	0.0000	0.1223	0.0012	0.4196	0.4487	0.0081	0.0000	0.0000
20	363.29	101325	7000000	0.0000	0.1078	0.0006	0.2707	0.5825	0.0384	0.0000	0.0000